

From the
Institute of Pharmacology and Toxicology
of the
Otto-von-Guericke-University Magdeburg
(Department head: Prof. Dr. rer. nat. D. C. Dieterich)



LIN LEIBNIZ-INSTITUT
FÜR NEUROBIOLOGIE
MAGDEBURG

Ageing in a dish - Strategies to rejuvenate neuronal cell cultures and balance protein homoeostasis

DISSERTATION

for the acquirement of the academic degree
doctor rerum naturalium (Dr. rer. nat.)
approved by the Faculty of Natural Sciences
Otto-von-Guericke-University Magdeburg

Submitted by: Julia Abele
born in: Bernburg, 23.10.1988
handed in: 18.07.2018
defended: 13.05.2019

Dean: Prof. Dr. rer. nat. habil. Oliver Speck

First reviewer: Prof. Dr. D. C. Dieterich

Second reviewer: Prof. Dr. Englert

Table of Contents

List of figures	III
List of tables	IV
List of abbreviations	V
1. Summary	1
2. Introduction	4
2.1. Hallmarks of ageing	4
2.1.1. Why do we age? Cellular theories of ageing	5
2.1.2. Neurons and synapses are vulnerable to age-related processes	6
2.2. Finding the right balance - Protein homoeostasis in the ageing brain	7
2.2.1. Techniques to monitor protein homoeostasis	10
2.3. Understanding mechanotransduction and mechanosensing in neuronal cells	12
2.3.1. Synaptogenesis and mechanical signalling	14
2.3.2. The mechanosensor Piezo-1	15
2.3.3. Mechanotransduction in ageing and disease	16
2.4. Ageing in a dish - Stiffness controlled substrates as a model for cellular brain ageing	17
2.5. Objectives	17
3. Methods and Materials	19
3.1. Materials	19
3.1.1. Chemicals	19
3.1.2. Primary antibodies	19
3.1.3. Secondary antibodies	20
3.1.4. Bacterial Strains and Culture Media	21
3.1.5. Animals	21
3.2. Methods	22
3.2.1. Molecular Biology	22
3.2.2. Cell Culture	23
3.2.3. Biochemistry	29
3.2.4. Mass spectrometry	36

3.2.5. Ca ²⁺ Imaging	38
3.2.6. Statistical analysis	39
3.2.7. Software	39
4. Results	40
4.1. Ageing in a dish	40
4.1.1. Long-term culturing of neuronal cells	40
4.1.2. A suitable senescence marker for neuronal cells	41
4.1.3. Deficits in proteostasis in aged neurons	45
4.1.4. Polyamines as an anti-ageing therapy?	50
4.2. Stiffness regulated polyacrylamide gels as a suitable model for brain ageing? .	59
4.2.1. Characterisation of neuronal cells grown on stiffness regulated polyacrylamide gels	59
4.2.2. Protein dynamics are influenced by substrate stiffness in cortical neurons	67
4.2.3. Protein dynamics are influenced by substrate stiffness also in astroglial cells	70
4.2.4. An odd pairing? - Linking protein synthesis dynamics and mechanosensors in cortical neurons	72
4.2.5. Ca ²⁺ transients are influenced by mechanical cues and reflect mechanoreceptor activity	74
4.2.6. Proteomic analysis of neuronal cells grown on stiffness regulated materials revealed new signalling pathways regulated by mechanical cues .	80
4.2.7. Long-term cell culture on stiffness regulated polyacrylamide gels . . .	84
5. Discussion	87
5.1. Ageing in a dish - What long-term neuronal cell cultures can teach us about brain ageing	87
5.1.1. Define old: A senescence marker for neuronal cells	87
5.1.2. The complexity of translational regulation in young and aged systems - many starting points to look for a potential rejuvenation	88
5.1.3. What do Polysome Profiles tell us about translational capacities? . . .	90
5.2. The integration of mechanical signalling into neuronal development and neuronal ageing	91
5.2.1. Polyacrylamide gels are a physiological substrate to study mechnanosignalling in neuronal cell culture	92
5.2.2. New insights in mechanosignalling	93
5.2.3. Ca ²⁺ signalling is modulated by substrate stiffness	94
5.2.4. Proteomic analysis give hints how mechanical signalling encodes and transduces substrates stiffness presented to neuronal cells	95

5.2.5. Are long-term neuronal cultures on stiffness regulated gels a suited model for brain ageing?	100
6. Outlook	103
References	105
A. Appendix	138

List of figures

2.1. Connecting the Theories of Ageing	6
2.2. Proteostasis determinants in the ageing brain	8
2.3. mTor and eEF2 as central regulators of protein translation	10
2.4. Toolbox to study protein homoeostasis	11
2.5. Mechanical properties of brain tissue and how to mimic brain stiffness with polyacrylamide gels	13
4.1. Potential senescence marker γ -H2AX showed no regulation in ageing neuronal cells	42
4.2. Potential senescence marker Lamin B1 showed no decline in ageing primary neuronal cultures	43
4.3. p62-positive protein aggregates formed in ageing neurons	44
4.4. <i>De novo</i> protein synthesis is decreasing in ageing neurons	46
4.5. Protein degradation was slowed down in ageing neurons	47
4.6. Translational capacities declined in aged neuronal cells	49
4.7. Translational capacities declined in aged neuronal cells and are potentially restored by polyamine signaling	51
4.8. Biosynthesis of mature, hypusinated eIF5A	52
4.9. p62-positive protein aggregates were resolved by the polyamine Spermidine	53
4.10. Hypusine and its precursor Spermidine induced <i>de novo</i> protein synthesis and Shank2 expression.	55
4.11. Synaptic vesicle recycling was slowed down in aged neurons and can be increased by Hypusine or Spermidine treatment	56
4.12. Polysome profiles differ between young and old neuronal cultures and short Hypusine application rejuvenates polysome profiles in aged cultures	57
4.13. Comparing laminin coating, neuronal attachment and -outgrowth on polyacrylamide surface and glass.	60
4.14. Dendritic arborisation was regulated by substrate stiffness in neuronal cultures.	61
4.15. Synaptogenesis was influenced by substrate stiffness	63
4.16. Synaptic vesicle recycling was triggered by mechanical cues	64
4.17. Expression of candidate synaptic proteins appeared earlier on soft substrates.	65
4.18. NMDA receptor subunit switch appeared earlier on soft substrates.	66

4.19. <i>De novo</i> protein synthesis was enhanced on soft substrates - Snapshot with Puromycin Assay.	68
4.20. <i>De novo</i> protein synthesis was enhanced on soft substrates - FUNCAT.	69
4.21. Substrate stiffness influenced expression levels of glial marker proteins	71
4.22. Tunable stiffness influenced astroglia shape and <i>de novo</i> protein synthesis	71
4.23. <i>De novo</i> protein synthesis was influenced by pharmacologically manipulation of mechanosensitive channels.	73
4.24. Spontaneous Ca ²⁺ oscillation depend on the stiffness of the substrate in immature cultured cortical neurons.	75
4.25. Spontaneous Ca ²⁺ oscillation was not affected by the stiffness of the substrate in mature cultured cortical neurons.	76
4.26. Yoda-1 stimulation leads to different patterns in Ca ²⁺ spiking related to tunable stiffness Piezo-1 expression varies between stiffness regulated substrates and age <i>in vivo</i>	78
4.27. Overexpression of a mCherry labelled Piezo-1 construct in primary cortical neurons lead to silencing of spontaneous Ca ²⁺ oscillations	79
4.28. Proteomic analysis of the neuronal cells grown on different materials: Mass Spectrometry Analysis was controlled for probe quality	81
4.29. Proteomic analysis of the neuronal cells grown on different materials	83
4.30. FUNCAT experiment with long-term culture of neuronal cells in stiffness regulated polyacrylamide gels.	85
4.31. Less p62-positive protein aggregates accumulated on soft PAA gels in aged neurons	86
5.1. STRING Network analysis of protein cluster 'up-regulated on soft substrates'	97
5.2. STRING Network analysis of protein cluster 'down-regulated on soft substrates'	98

List of tables

3.1. Primary antibodies	19
3.2. Secondary antibodies	20
3.3. Bacteria Media	21
3.4. Shear modulus, acrylamide and bis-acrylamide concentrations of the PAA gels used in this study	24
3.5. Chemical composition of 12 gradient mini tris glycine gels (5 % - 20 %) . . .	31
3.6. Chemical composition of 12 homogeneous mini tris glycine gels (9.5 %) . . .	32
3.7. Chemical composition of 12 homogeneous mini tris glycine gels (15 %) . . .	32
3.8. Chemical composition of 12 gradient tris acetate gels (3.5 % - 8 %)	32
3.9. Software used in this study	39
4.1. Comparing routine cell culture conditions for primary cortical neurons with new established protocol for long-term cell cultures	41

List of abbreviations

Abbreviation	Meaning
4E-BP	eIF4E-binding protein
aa	amino acid
AD	Alzheimer's disease
AFM	atomic force microscopy
AHA	azidohomoalanine
AMPAR	alpha-amino-3-hydroxy-5-methyl-4-isoxazolepropionic acid receptor
ANOVA	analysis of variance
APS	ammonium persulfate
APTMS	(3-aminopropyl) trimethoxysilane
AU	arbitrary units
BONCAT	bio-orthogonal non-canonical amino acid tagging
BSA	bovine serum albumin
C	celsius
Ca	calcium
CaM	calmodulin
cDNA	complementary DNA
chk	chicken
ctrl	control
DHPS	Deoxyhypusinesynthase
DIV	days <i>in vitro</i>
dk	donkey
DMEM	Dulbeccos' modified eagle medium
DMSO	dimethyl sulfoxide
DNA	deoxyribonucleic acid
<i>E. coli</i>	<i>Escherichia coli</i>
ECL	electrochemiluminescence
ECM	extracellular matrix
EDTA	ethylenediaminetetraacetic acid
eEF2	eukaryotic elongation factor 2

eEF2K	eukaryotic elongation factor 2 kinase
e. g.	for example (latin: exempli gratia
EGFP	enhanced green fluorescent protein
elF4E	eukaryotic initiation factor 4E
elF5a	eukaryotic translation initiation factor 5A
FAK	focal adhesion kinase
FBS	fetal bovine serum
fig.	figure
FUNCAT	fluorescent non-canonical amino acid tagging
g	gram
GFP	green fluorescent protein
GFAP	glial fibrillary acid protein
gp	guinea pig
gt	goat
h	hour
HBSS	hanks buffered salt solution
Hek293T	human embryonic kidney 293T cells
HEPES	2-(4-(2-hydroxyethyl)-1-piperanzinyl)-ethansulfon acid
HRP	horse-radish peroxidase
HSP	heat-shock proteins
ICC	immunocytochemistry
IgG	immunoglobulin G
IGF-1	insulin-like growth factor
k	kilo
kDa	kilo dalton
l	liter
Lab	Laboratory
LB-medium	lysogeny broth-medium
LC-MS	liquid chromatography mass spectroscopy
LTD	long term depression
LTP	long term potentiation
mc	monoclonal
M	molar
mA	milli ampere
MAP2	microtubule-associated protein 2
Met	methionine
min	minute
mg	milli gram
Mg	magnesium

mM	milli molare
μ l	micro liter
mRNA	messenger RNA
MS	mass spectrometry
ms	mouse
mtDNA	mitochondrial DNA
mTOR	mechanistic target of rapamycin
NaCl	sodium chloride
NaOH	sodium hydroxide
NMDA	N-methyl-D-aspartate
NMDAR	N-methyl-D-aspartate receptor
NR2A	N-methyl-D-aspartate receptor subunit A
NR2B	N-methyl-D-aspartate receptor subunit B
ns	not significant
Pa	pascal
PAA	polyacrylamide
PBS	phosphate buffered saline
PBS-MC	phosphate buffered saline with MgCl ₂ and MgCl ₂
PBT	phosphate buffer with Triton-X-100
pc	polyclonal
PFA	paraformaldehyd
pH	<i>potentia hydrogenii</i>
PI	protease inhibitor
PKA	protein kinase A
PSD-95	postsynaptic density protein 95
rb	rabbit
RNA	ribonucleic acid
ROS	reactive oxygen species
RT	room temperature
S6K	S6 kinase
SD	standard deviation
SDS	sodium dodecyl sulfate
SDS-PAGE	sodium dodecyl sulfate polyacrylamide gel
SEM	standard error of the mean
SOC medium	super optimal broth with Catabolite repression
SUnSET	surface sensing of translation
Sys	Systems
TAMRA	tetramethylrhodamine
TBS	tris buffered saline

TBS-T	tris buffered saline-Tween20
TECEP	tris[(1-benzyl-1H-1,2,3-triazo-4-yl)methyl]amine)
TEMED	tetramethylethylenediamine
TRIS	tris(hydroxymethyl)aminomethane
v / v	volume per volume
WB	western blot
w / o	without
w / v	weight per volume
x g	gravity

1. Summary

Ageing is a central aspect of life itself. Even after extensive research during the last decades, little is known about this highly complex biological process. In conclusion, the achievement of scientific milestones such as an increased healthspan or the retaining of cognitive functions is still in distant future. Another aspect poorly understood in terms of biochemical signalling pathways is the communication via mechanical cues also termed mechanosensing and -transduction. Both aspects, neuronal ageing and mechanosensing in neuronal cells will be addressed and connected in this thesis.

As central aspect, first we present an *in vitro* model optimised for long-term culturing conditions to define hallmarks of neuronal ageing in more detail. Known as one central hallmark of ageing from mammalian and human research, the focus of investigations was set on the control of proteostasis. With different experimental approaches such as immunocytochemistry, western blotting, FUNCAT and BONCAT, we showed that protein translation and -degradation is indeed decreased in aged neuronal cells, ultimately leading to the formation of protein aggregates. These protein aggregates formed in aged neurons were successfully resolved by applying the polyamine Spermidine. The ability of Spermidine to restore translational capacities to juvenile levels was functionally linked to activation of the translational regulator eIF5A. In the next part, we introduced a new hallmark of the neuronal ageing process: the sensation of mechanical signals and the integration of mechanical cues into biochemical pathways. This thesis underlines that polyacrylamide gels with defined stiffness are a suitable cell culture system to investigate the impact of mechanical cues on neuronal morphology and protein translation. We stated that soft substrates, presenting a stiffness comparable to juvenile brain tissue, promote dendritic complexity and synapse maturation during early development. Further, protein synthesis and spontaneous Ca^{2+} transients were enhanced on soft substrates most likely connected to activation of the mechanosensor Piezo-1. A proteome analysis provides a detailed list of proteins regulated by substrate stiffness during early development mainly from the family of cytoskeleton regulators. This list of differently regulated proteins is a promising starting point for future investigations. Finally, we proved that stiffness regulated substrates are suited also for the growth of long-term neuronal cultures and that soft environment prevented the formation of protein aggregates in aged neurons *in vitro*.

Zusammenfassung

Leben bedeutet auch Altern. Und trotz intensiver Forschung in den letzten Jahrzehnten bleiben viele Aspekte dieses komplexen biologischen Prozesses weiterhin unaufgeklärt. Erstrebenswerte wissenschaftliche Errungenschaften, wie die Verlängerung der Anzahl gesunder Lebensjahre oder die Aufrechterhaltung kognitiver Leistungen, basierend auf der biochemischen Forschung, sind bisher ausgeblieben.

Ein weiterer Bereich, der in Bezug auf biochemische Signalwege wenig erforscht ist, ist die Fähigkeit von Zellen durch mechanische Reize zu kommunizieren, auch "mechanosensing" oder "mechanotransduction" genannt. Beide Aspekte, das Altern von neuronalen Zellen und die Kommunikation mittels mechanischer Reize, werden in dieser Arbeit untersucht und thematisch verbunden.

Als zentraler Ausgangspunkt wurde ein für das Überleben von Langzeit-Zellkulturen optimiertes Zellkultursystem entwickelt, um Merkmale von neuronalem Altern umfangreich zu beschreiben. Wissenschaftliche Arbeiten in diversen Modellorganismen haben gezeigt, dass ein entscheidendes Kennzeichen des Alterungsprozesses die fehlgeschlagene Kontrolle von Proteindynamiken ist. Mit verschiedenen experimentellen Herangehensweisen wie Immunfärbungen, Western Blot, FUNCAT und BONCAT wurde in dieser Arbeit gezeigt, dass Proteinsynthese und Proteinabbau tatsächlich in gealterten neuronalen Zellen verlangsamt sind, was letztendlich zur Bildung von Proteinaggregaten beiträgt. Diese Proteinaggregate konnten erfolgreich durch die Applikation des Polyamines Spermidine aufgelöst werden. Die Fähigkeit von Spermidine Proteintranslation "zu verjüngen" wurde funktionell mit der Aktivierung des Translationsregulators eIF5A in Verbindung gebracht.

Im nächsten Abschnitt dieser Arbeit wird ein neues Kennzeichen von neuronalem Altern vorgestellt: das Wahrnehmen von mechanischen Reizen und die Integration dieser in biochemische Signalwege. Wir bestätigen, dass Polyacrylamide Gele, die eine definierte Steifheit im Zellkultursystem präsentieren, geeignet sind, um den Einfluss von mechanischen Reizen auf Zellmorphologie und Proteintranslation zu untersuchen. Es wurde gezeigt, dass weichere Substrate mit einer Beschaffenheit vergleichbar mit jungem Hirngewebe, die Ausbildung von Dendriten und Synapsenreifung begünstigen. Weiterhin wurde beschrieben, dass spontane Ca^{2+} Signale und Proteinsynthese erhöht sind, wenn Zellen auf weichen Substraten wachsen, was vermutlichen im Zusammenhang mit der Aktivierung des Mechanosensors Piezo-1 steht.

Eine Proteomeanalyse stellte eine detaillierte Zusammenstellung an Proteinen bereit, die durch den Einfluss von mechanischen Reizen in ihrer Expression reguliert werden. Ein Grossteil dieser Proteine stammt aus der Familie der Zytoskelett-Regulatoren und bildet einen

vielversprechenden Ausgangspunkt für weitere Experimente. Abschliessend wurde gezeigt, dass Polyacrylamide Gele mit definierter Steifheit auch für Langzeit-Zellkulturen geeignet sind und dass auf weicherem Untergrund weniger Proteinaggregate in alternden Neuronen gebildet werden.

2. Introduction

2.1. Hallmarks of ageing

Ageing is a complex process with high variability between individuals. Despite being an inevitable part of life, it remains a poorly understood process with respect to its molecular mechanisms.

The science behind ageing has evolved from the treasure hunt for the legendary "fountain of youth" to one of the most delicate research fields [López-Otín et al., 2013]. Thus far, no single theory adequately explains ageing; each theory most likely highlights some fundamental aspect of its complex nature. Today, ageing and age-related diseases are a major challenge both for the individual and for society [Cutler and Mattson, 2006]. Given that ageing is known to be one primary risk factor for cardiovascular diseases, diabetes, cancer, and cognitive degeneration, these challenges (both financial and personal) are likely to increase as more of us are predicted to reach the age of 90 by 2030 [Kontis et al., 2017]. Therefore, learning more about the ageing process will be crucial to improve health care both for the existing elderly population and for our future selves. The idea of an increased health span led to attempts to identify features and intervention strategies to promote successful ageing. The concept of successful ageing depends on three central elements: low probability of disease, high cognitive paired with physical functionality, and active engagement in life [Rowe and Kahn, 1998].

Much research has attempted to answer two fundamental questions: 1) how does a person with healthy brain function differ from those facing early cognitive decline? 2) are there differences in genetics, or do external factors such as nutrition or physical activity play a role?

The ageing research has made remarkable progress in recent years leading to the finding that genetic pathways and biochemical signalling can control the rate of ageing. However, the major human pathologies related to older age remain far from being understood in depth or even cured. For example, over a hundred clinical trials have been conducted in the search for therapeutic intervention for Alzheimer's diseases, but no compound with an actual therapeutic profile was found [Schneider et al., 2014].

For future studies, the known hallmarks of ageing such as DNA damage, telomere loss,

epigenetic drift and defective proteostasis need to be studied with integrative paradigms to face the complex structure of the ageing process.

In this thesis, I will set the focus on the control of proteostasis in ageing neuronal cells. Additionally, I will introduce and define a new hallmark of the ageing process: the sensing and conduction of mechanical signals in neuronal cells.

2.1.1. Why do we age? Cellular theories of ageing

So far, no single, unifying theory of ageing has been proposed that explains the multifaceted aspects an ageing organism faces. With this in mind, the theories of ageing presented here should be viewed in connection to each other and continuously updated with new research findings.

The historically important Telomere Loss Theory explains ageing by the limited capacity of cells to replicate. Cellular senescence was thought to be a result of the shortening of the chromosomal telomeres [Hayflick and Moorhead, 1961], [Castorina et al., 2015]. Whether telomere length is related to longevity is still under debate; mice with high telomerase activity have a high cancer rate and do not live longer [de Magalhães and Toussaint, 2004], suggesting that telomerase, the enzyme elongating telomeres, may not be a suitable anti-ageing target. Another group reported that overexpression of the telomerase gene has led to an increased lifespan around 24 % in mice [Bernardes de Jesus et al., 2012].

The Somatic Mutation Theory couples the rate of ageing to mutations in somatic DNA [Promislow, 1994]. The theory correlates above-average rates of DNA repair with the longevity observed in many long-lived organisms such as the rock fish (140 years), the sturgeon (150 years) and the ocean quahog (220 years) [Finch and Austad, 2001]. On the other hand, mutations causing dysfunctional DNA repair enzymes give rise to phenotypes with accelerated ageing. The spectrum of genetic mutations leading to accelerated ageing is of diverse nature, again highlighting the complexity of ageing but also revealing signalling pathways involved in the regulation of the ageing process. One example of accelerated ageing is the Hutchinson-Gilford progeria syndrome mainly caused by point mutations in the nuclear lamina A protein [Ahmed et al., 2018]. Another condition termed Werner syndrome shows signs of early ageing manifesting during young adolescence and is induced by mutations in a specific ATP-dependent helicase [Lebel and Monnat, 2018]. For both diseases and also for a variety of other conditions causing accelerated ageing, mouse models are available to investigate the ageing process in more detail [Kõks et al., 2016].

The Mitochondrial Theory states that ageing results from functionally impaired mitochondria that give rise to reactive oxygen species (ROS). ROS are extremely harmful to cellular

macromolecules such as DNA, proteins, and lipids [Wallace, 1999]. In addition, with age mutations occur in the mitochondrial DNA (mtDNA) leading to disrupted ATP production and ultimately to a decline in cellular energy levels. Comparing mitochondria isolated from aged rats to those from young rats, showed enhanced ROS production, mitochondrial swelling, and reduced buffering capacities of voltage-gated Ca^{2+} influx [Brown et al., 2004], [Murchison et al., 2004] in the older population.

The last theory of ageing explained here is The Altered Proteins or Waste Accumulation Theories [Cook et al., 2009]. Since my thesis is mainly built on this theory I will give a broad overview and highlight more details in the next section.

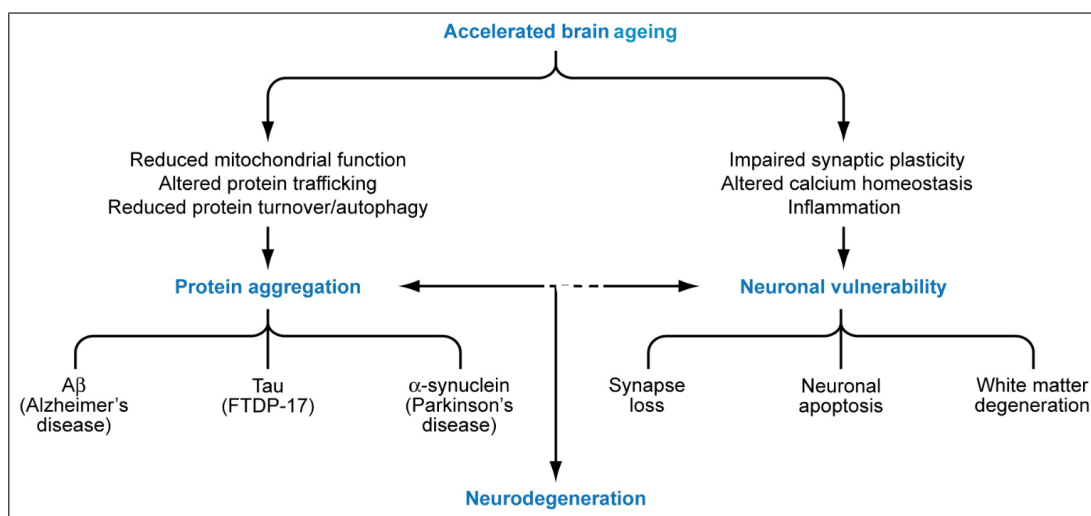


Figure 2.1.: Connecting the Theories of Ageing

In neuronal ageing, different pathological processes are interconnected. Reduced mitochondrial functions and deficits in protein turnover were described as changes occurring early on. Additionally, a reduction in synaptic plasticity and altered Ca^{2+} homoeostasis lead to neuronal vulnerability. Adapted from: [Yankner et al., 2008]

2.1.2. Neurons and synapses are vulnerable to age-related processes

Early studies proposed a mechanism whereby massive neuronal loss in cortical and hippocampal areas during ageing results in cognitive decline [Brody, 1955], [Scheibel et al., 1976]. With the help of advanced methods and equipment, this theory was proven to be a misunderstanding in the mid 2000's [Burke and Barnes, 2006]. Today, the decline in cognitive brain function during ageing is described by unstable synapses [Grillo et al., 2013]. The cortical synapse appears particularly vulnerable to ageing, explained by the complex synaptic architecture and extensive synaptic plasticity in this brain area [Moore et al., 2006], [Lyons-Warren et al., 2004]. It has been postulated that synapses appear less stable with age, determined by an observable change in remodelling and bouton loss. Modern electron microscopy revealed a striking loss of up to 30 % cortical synapses in area 46 in aged pri-

mates [Peters et al., 2008], whereas glutamatergic axospinous synapses are most vulnerable and lost as the major group [Dumitriu et al., 2010]. GABAergic synapse function has also been studied extensively in the context of ageing. In general, the GABAergic system appears to have reduced inhibition in an aged rodent model, whereas in the prefrontal cortex inhibition increases with age [Potier et al., 2006], [Bories et al., 2013].

Electrophysiological studies explained age-related memory-loss with a non-precise long-term potentiation LTP not restricted to the activated synapses [Ris and Godaux, 2007]. Additionally, brain ageing is thought to be accompanied by a shift towards decreased synaptic transmission, proposed to begin at mid-age [Rex et al., 2005]. To explore synaptic ageing in more detail and eventually find connections to reduced cognitive performance inside synaptic networks, current paradigms need to be studied together rather than separately.

2.2. Finding the right balance - Protein homoeostasis in the ageing brain

Several observations from more simple model organisms such as *C. elegans* and *D. melanogaster* have established the hypothesis that protein synthesis and protein degradation are impaired in aged organisms [Syntichaki et al., 2007], [Chiocchetti et al., 2007], [Hussain and Ramaiah, 2007].

Furthermore, irreversible modifications caused by free radicals can damage proteins in various ways, such as the formation of carbonyl groups or unphysiological glycosylation pattern [Baynes, 2001]. Whilst protein turnover capacities differ between cell types and are tissue or organ specific, the trend towards an impaired protein homoeostasis holds true for almost every probe examined during ageing.

Protein repair has its limits and continuous renewal of intracellular proteins is vital. During their lifetime, proteins are physically challenged by folding in a crowded environment, refolding, post-translational modifications, and protein-protein interactions. The imbalance between protein synthesis and degradation of dysfunctional proteins leads to the formation of toxic protein aggregates [Koga et al., 2011] (see Fig. 2.2). Metabolic stress situations in neurons can lead to the formation of proteotoxic aggregates resulting from high intracellular protein concentrations [Zhou et al., 2008]. Aggregation of specific proteins is known to be a major contributor to age-related pathologies such as Alzheimer's-, Parkinson's- or Huntington's disease [Balch et al., 2008]. In addition to neurodegeneration, there is increasing evidence that defective protein homoeostasis is linked to other age-related diseases including type-2 diabetes, cancer, and cardiovascular disease [Balch et al., 2008].

Cells have several mechanisms to handle damaged or unfolded proteins. The main cellular protein degradation pathway occurs via the ubiquitin-proteasome [Bard et al., 2018] and the autophagy-lysosomal system [Kulkarni et al., 2018], [Nakamura and Yoshimori, 2018]. Both degradation systems are known to be deregulated during ageing: proteasomal activity was shown to be reduced in aged human dermal fibroblasts [Hwang et al., 2007] and in *D. melanogaster*, where this was correlated with a 50 % reduction in ATP levels [Vernace et al., 2007].

In addition, genetic studies have associated increased autophagy-lysosomal system activity with longevity [Meléndez et al., 2003], [Tóth et al., 2008]. Pharmacological inducers of autophagy, like the mTOR inhibitor Rapamycin, are of great interest since this compound was shown to increase lifespan in mid-aged mice up to 35 % [Blagosklonny, 2011], [Harrison et al., 2009]. The polyamine Spermidine is another macroautophagy inducer and can increase life span in *C. elegans* and *D. melanogaster* besides various other rejuvenation effects [Eisenberg et al., 2009], [Oliverio et al., 2014], [Gupta et al., 2013]. Since polyamines such as Spermidine can by its nature interact with a huge variety of molecules it is rather difficult to pin down the exact signalling actions leading to the described rejuvenation effects.

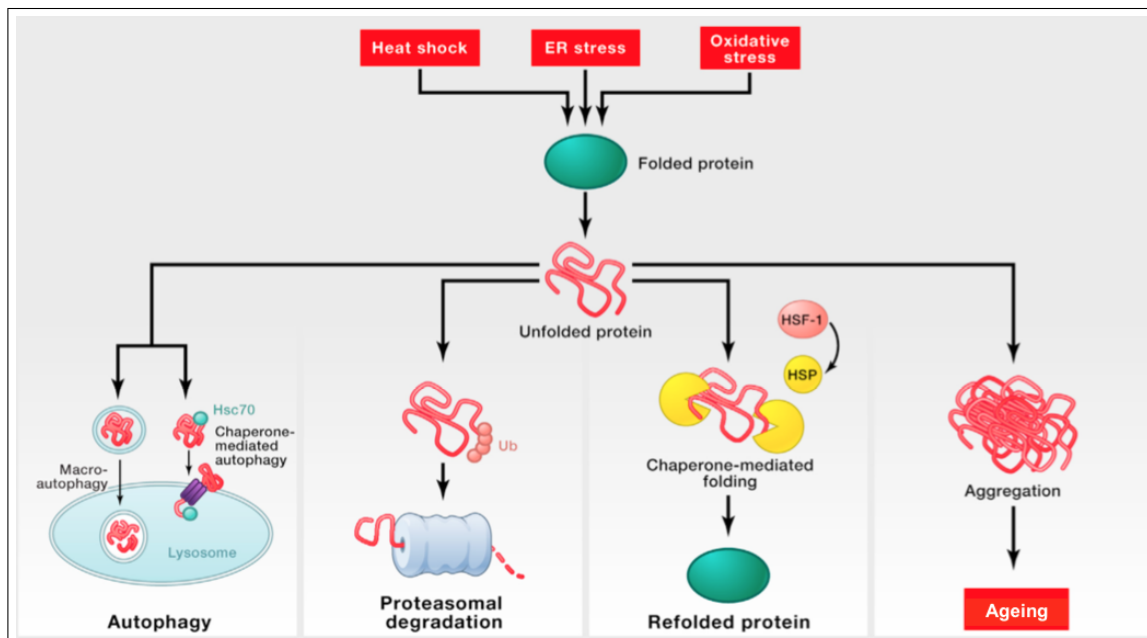


Figure 2.2.: Proteostasis determinants in the ageing brain

Different obstacles such as heat shock, ER stress or oxidative stress impair proper protein folding. Heat-shock proteins (HSP) can refold proteins, or unfolded proteins can be labelled for degradation by the lysosome or the ubiquitin-proteasome pathway. During ageing, unfolded proteins accumulate and aggregate, leading to cytotoxic side effects. Image adapted from: [López-Otín et al., 2013]

Other studies showed that Spermidine also has the potential to reduce inflammation and re-

juvenile lipid metabolism and cell proliferation via central regulation of the MAPK pathway. Additionally, over the last decades, experimental studies investigated the effects of Spermidine on NMDA receptor regulation. So far, results are inconsistent with some studies claiming that Spermidine activates NMDA receptors [Marvizón and Baudry, 1993], [McGurk et al., 1990] while other researchers showed that Spermidine actually blocks this receptor type [Araneda et al., 1999], [Rock and MacDonald, 1992].

From these observations, the question arises whether the ageing process is simply caused by a global collapse in protein homoeostasis. More and more studies point towards the idea that only specific proteins are affected by ageing, and that manipulating certain signalling transduction pathways could control this collapse. However, it remains uncertain whether reduced protein turnover is a consequence of the ageing process (for example, as an adaptation to reduced energy metabolism), or is a risk factor leading to senescence.

Studies designed to investigate how the rate of ageing is regulated by internal signalling networks and whether it is, therefore, open for manipulation [Kenyon, 2005] have attempted to answer this question. One of the first pathways investigated in relation to longevity was the insulin-like growth factor-1 (IGF-1) signalling pathway and its downstream effector mammalian target of Rapamycin (mTOR) [Wullschleger et al., 2006] [Sarbassov et al., 2005]. Through different downstream targets, mTOR controls protein homoeostasis, in particular, protein synthesis. In a variety of model organisms, a reduction in mTOR signalling is associated with an extended lifespan, presumably due to better protein quality control [Kapahi et al., 2010] although this idea remains under debate. In contrast, upregulation of mTOR signalling appears to be beneficial in neurodegenerative disorders [Reiling and Sabatini, 2008], [Ozcan et al., 2008].

The main interaction partners of mTOR through which it acts to regulate protein translation are the eukaryotic initiation factor 4E (eIF4E) and its repressor eIF4E-binding protein (4E-BP), eukaryotic elongation factor 2 (eEF2), and the S6 kinase (S6K) and its target ribosomal protein S6 [Dowling et al., 2010] (for details see Fig. 2.3).

In Alzheimer's brain samples, remarkable changes in mTOR and S6 kinase pathways suggest there is an imbalance in protein synthesis capacities [Li et al., 2005]. However, changes in mTOR signalling have not been studied in the ageing of a healthy brain in any great detail. Another translational regulator associated with ageing is the eukaryotic translation initiation factor 5A (eIF5A), which is unique in that it has the unusual amino acid residue hypusine formed as a posttranslational modification [Chen and Liu, 1997]. Loss of eIF5A function has been described in ageing Purkinje cells [Luchessi et al., 2008] and is associated with ribosomal stalling during translation [Gutierrez et al., 2013].

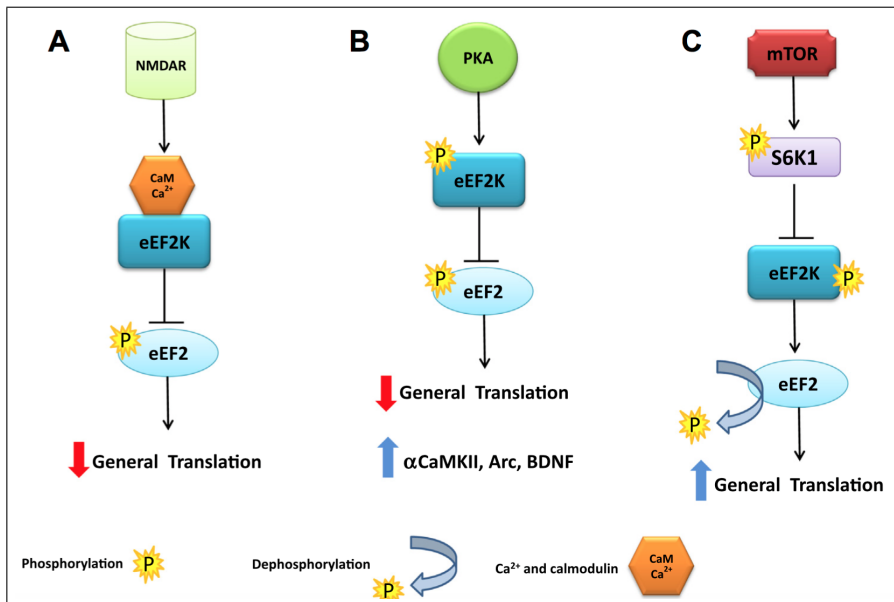


Figure 2.3.: mTor and eEF2 as central regulators of protein translation

(A) Activation of NMDA receptors leads to Ca²⁺ efflux and, together with the co-agonist calmodulin (CaM), activation of elongation factor 2 kinase (eEF2K). This leads to increased phosphorylation (here: inhibition) of the elongation factor 2 (eEF2) and a reduction in overall protein translation rates. (B) eEF2K can also be phosphorylated by protein kinase A (PKA) leading to enhanced activity. Again, eEF2K inhibits eEF2 by phosphorylation resulting in reduced cap-dependent translation, but also in enhanced translation of other proteins such as Arc, BDNF, and CAMKII (C) New insights show that mTOR can regulate eEF2 phosphorylation by phosphorylation of S6K1. This results in reduced eEF2K activity by phosphorylation (at a different site than that phosphorylated by PKA) and decreased phospho-eEF2 levels. This results in increased rates of elongation. Figure adapted from: [Taha et al., 2013].

In summary, the evidence is still increasing that protein translation and -degradation are essential for cellular survival and that during ageing more and more defective signal regulation occurs. Since the control of protein dynamics is highly complex and some details still remain unknown a therapeutic approach focusing on rejuvenating cells by reprogramming translational capacities has not been developed so far. Interestingly, one recent study showed that health benefits seen in physically active seniors are mainly due to enhanced levels of protein translation [Robinson et al., 2017], highlighting the significance to connect the two research topics: ageing and translational regulation.

2.2.1. Techniques to monitor protein homoeostasis

In general, global deficits in protein homoeostasis have been described for aged cells. Every cell type relies on stable and functional proteomes and a robust quality control mechanism is essential to prevent the formation of protein aggregates.

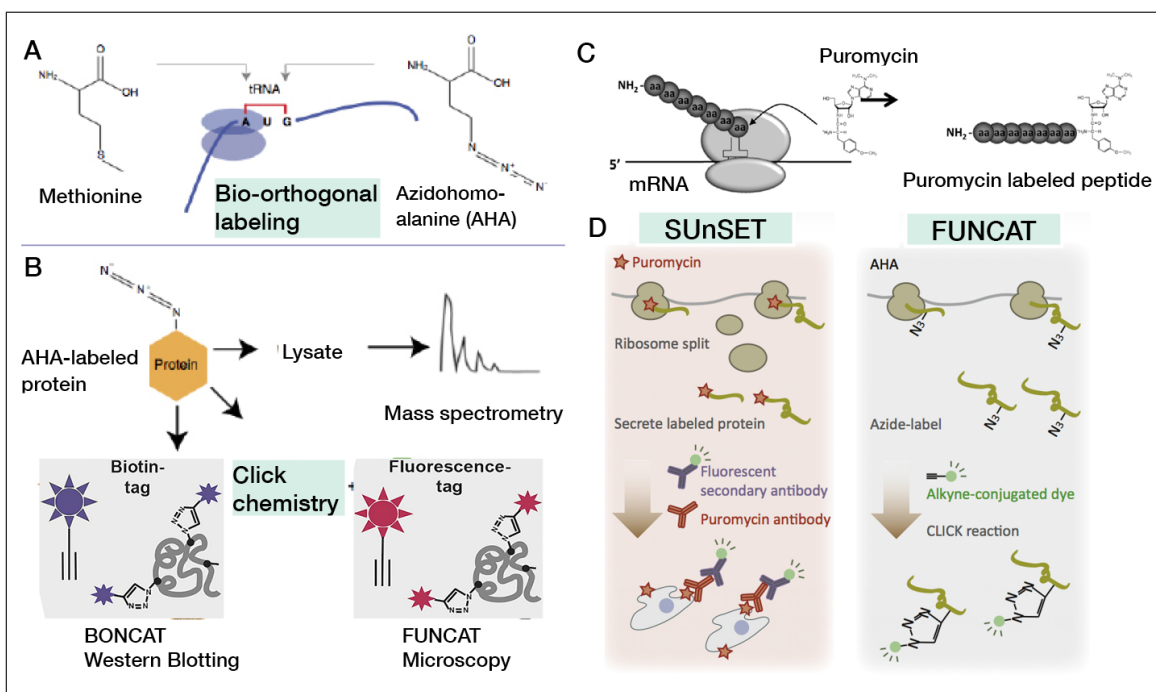


Figure 2.4.: Toolbox to study protein homeostasis

(A) Bio-orthogonal labelling is based on the ability of the methionyl-tRNA synthetase to incorporate Azidohomoalanine (AHA) instead of Methionine into the nascent polypeptide chain. (B) AHA-labelled proteins can be lysed and analysed using Mass Spectrometry or tagged with a Biotin-tag and further purified or analysed by Western Blotting. In a cellular network, AHA-labelled proteins can be visualised using a fluorescent tag and imaged with basic microscopy. Images adapted from: [Müller et al., 2015], [Ullrich et al., 2014] (C) The antibiotic Puromycin functions as an analogue of aminoacyl tRNAs, and is incorporated into the C-terminal end of a nascent peptide chain producing a termination of the translational process. In this manner, Puromycin functions as a tag for newly synthesized proteins and can be visualised with an anti-Puromycin antibody. This labelling technique is termed "Surface sensing of translation" (SUnSET). Image adapted from: [Goodman and Hornberger, 2013] (D) Graphic illustration comparing the protein labelling approach SUnSET and FUNCAT. SUnSET is based on Puromycin incorporation and visualisation by antibody binding, whereas in FUNCAT the non-canonical amino acid AHA is incorporated and visualized by "click reaction" and subsequent immunostaining. Both techniques have different advantages: high speed for puromycin labelling and longer time labelling for FUNCAT thus resulting in functional, non-terminated proteins. Images adapted from: [Iwasaki and Ingolia, 2017]

To study cellular proteomes in more detail, a variety of different labelling approaches have been used including isotope-coded affinity tags [Gygi et al., 1999], isobaric tags for relative and absolute quantification [Ross et al., 2004], or stable isotope labelling by amino acids in cell culture [Andersen et al., 2005].

In this thesis I will use non-canonical amino acids such as azidohomoalanine (AHA) in combination with click chemistry to describe age-related changes in protein synthesis and degradation [Link et al., 2003], [Beatty et al., 2006], [Dieterich et al., 2006], [Dieterich et al., 2010]

(see Fig. 2.4, A, B). In short, the non-canonical amino acid azidohomoalanine (AHA) is incorporation in the nascent peptide chain instead of methionine and can, later on, be detected by conjugating with a specific tag (fluorescent particle or biotin) via copper-based catalyzed azid-alkyne cycloaddition also termed *click reaction* [Nwe and Brechbiel, 2009]. With this methodology, protein turnover can be assessed for the cell soma or even specialized compartments like the synapse.

Another concept to study translational capacities is termed "Surface sensing of translation" (SUnSET) utilizing the antibiotic and translational inhibitor Puromycin [Nathans, 1964] (Fig. 2.4, C, D). As an analogue of aminoacyl tRNAs, Puromycin is added to the nascent peptide chain and terminates elongation. Thereby a shorter, truncated protein is released from the ribosome, which is puromycylated. The Puromycin-tag is subsequently used to identify newly synthesized proteins. Here, a specific anti-Puromycin antibody is incubated during immunocytochemistry (see 3.2.2.11) and detected by fluorescence microscopy. The staining intensity correlates with translational activity at a given time point.

2.3. Understanding mechanotransduction and mechanosensing in neuronal cells

It is generally believed that neuronal cells respond to a multitude of chemical and electrical cues [Lovinger, 2008]. Research of the last decades has identified a variety of chemical signalling pathways regulating gene expression and translation. Nevertheless, the evidence is increasing that communication strategies of neuronal cells are even more complex and that neuronal cells are able to share information by sending and responding to mechanical cues. This phenomenon is intensively investigated in the rather young field termed "neuromechanics".

In the field of neuromechanics, cells are considered as viscoelastic material and their response to forces can be determined as solid-like or fluid-like material with a frequency-dependent response. In addition to this, there is increasing evidence that neuronal cells also respond to mechanical cues [Flanagan et al., 2002], [Bernick et al., 2011], [Lu et al., 2006]. However, the mechanism of how individual cells can sense these mechanical signals and translate them into changes in intracellular biochemistry and gene expression, a process termed mechanotransduction, remains unclear. In more detail, the process of mechanotransduction is defined by three phases: signal transduction, signal propagation, and finally a cellular response. The mechanisms underlying mechanotransduction are of scientific interest since mechanical based signal propagation is thought to be six orders of magnitude faster than chemical diffusion or receptor-based signal transfer [Wang et al., 2009]. The translation of external mechanical forces into a biochemical signal includes force transmission, mechanosensing, transduction, and signalling transmission and each step is executed by a high number of

molecular components, many of them still being unknown.

Research focusing on mechanotransduction has expanded our view on cellular communication and it has been shown that mechanical forces are able to regulate cellular properties such as morphology [Brunetti et al., 2010], [Blumenthal et al., 2014], differentiation [Georges et al., 2006], [Young and Engler, 2011], and gene expression [Wang et al., 2009].

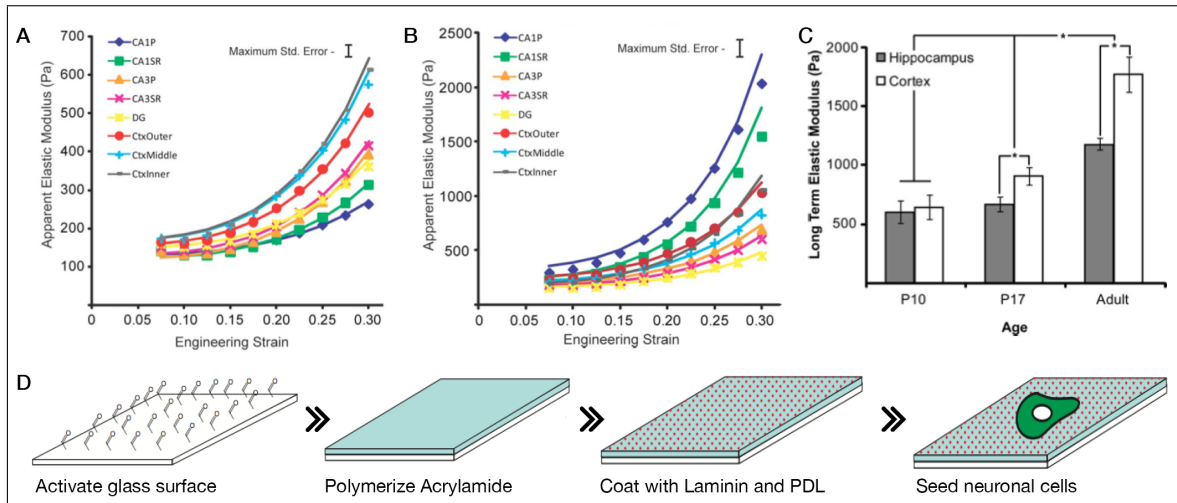


Figure 2.5.: Mechanical properties of brain tissue and how to mimic brain stiffness with polyacrylamide gels

(A) Non-linear apparent elastic modulus measured with atomic force microscopy (AFM) describing different degrees of brain stiffness in cortical and hippocampal regions at time point P10 in rats. (B) AFM measurements were repeated for mature animals. The elastic modulus increases as brain tissue matures. (C) Graph summarizing the increasing brain stiffness from P10 to adulthood. Note that the stiffening process is more prominent in cortical regions. (D) Manufacturing polyacrylamide gels: Glass coverslips are activated and acrylamide is polymerized on top. Gels are coated with Laminin and Poly-D-Lysine to ensure optimal conditions for neuronal cell seeding. Images adapted from: [Elkin et al., 2010] (A - C) and [Fischer et al., 2012] (D).

Advances in technology over the past 15 years have enabled scientists to measure several mechanical properties [Pravincumar et al., 2012], [Kirmizis and Logothetidis, 2010], [Celedon et al., 2011], including global and local viscoelastic properties, the cellular response to externally applied forces or growth cone motility. This thesis focuses on substrate elasticity and mechanosensing - the capacity of neuronal cells to actively measure the stiffness of their surroundings and to respond to this information. These two aspects of mechanosignalling were chosen since especially neuronal cells are challenged by changes in their environmental stiffness during their lifetime and secondly because methodological advances now allow combining neuronal cell biology and non-toxic stiffness regulated cell culture substrates.

In mechanics, the elasticity of a substrate is defined as the resistance of a material to deformation by an applied force [Buxboim et al., 2010]. The ratio of stress to strain is defined

by a modulus and describes the stiffness of a given material. For most biological substances, such as tissues or cells, the response to mechanical stress is in part elastic and viscous, defining biological samples as viscoelastic [Burstein and Frankel, 1968]. In particular, brain tissue has complex viscoelastic properties and is one of the softest tissues in the body. Different studies focusing on brain stiffness reported an elastic modulus ranging from 0.04 kPa to 20 kPa, with variations arising from the study design and methods of measurement. In order to compare these different elastic moduli, they were remodelled to low-strain shear moduli and plotted in relation to the time-scale by which the stiffness was measured. To summarize, brain regions differ in their elastic modulus: cortical regions appear to be between 0.15 and 0.5 kPa [Moeendarbary et al., 2017] compared to an elastic modulus of over 2 kPa in the hippocampus (see Fig. 2.5 A - C).

The response to viscoelastic properties is cell-type specific and seems to occur in defined patterns correlated to the native surrounding of a cell [Yeung et al., 2005], [Koser et al., 2016].

To allow proper signal transduction and ultimately brain function, neuronal cells have to be in contact with each other [Garzón-Muvdi and Quiñones-Hinojosa, 2009]. Physical contact is initiated by neurite outgrow - a highly regulated process. Several studies have examined the effects of substrate stiffness on neurite formation and outgrowth in primary neuronal cultures. It appears that primary neurons prefer softer substrates that more closely mimic the native elastic properties found throughout development, forming more neurites and branches on such substrates [Flanagan et al., 2002], [Balgude et al., 2001]. In contrast, astrocytes increase their growth area and overall complexity on stiffer substrates. In general, glia cells are stated to be more compliant compared to neurons [Lu et al., 2006].

Axonal stiffness can also vary between different cell types such as dorsal root ganglion cells and cortical neurons [Dennerll et al., 1989], [Chada et al., 1997], whereas cortical neurons have an elastic modulus ranging from 0.1 - 2 kPa with an average at 0.2 kPa and root ganglion cells appear stiffer with a average elastic modulus of 0.9 kPa [Spedden et al., 2012], [Athamneh and Suter, 2015]. Even dendritic spines show a broad variation in their viscoelastic properties based on the density of soluble proteins they are containing. An underlying pattern was described correlating dendritic stiffness with morphological features and the ability to be stimulated by glutamatergic signalling [Smith et al., 2007], [Chen and Sabatini, 2012].

2.3.1. Synaptogenesis and mechanical signalling

Neuronal cells are highly sophisticated in their communication strategies and use trillions of synapses to enable sufficient information transfer between cells. Synapses are specialized structures built of a dense network of proteins compartmentalized into the presynapse, synaptic cleft and postsynapse [Laßek et al., 2015], [Rosenmund et al., 2003]. During development, the process of neuronal differentiation is tightly coupled to initial synapse formation. The

release of neurotransmitters has been studied in great detail and revealed an orchestrated chemical signalling cascade [Südhof, 2013], [Kavalali, 2015].

Very recently, studies have indicated mechano-chemical crosstalk occurring at the synapse. A large amount of energy is needed to induce curvature of the vesicular membrane [Sackmann, 1994], [Rangamani et al., 2014], [Jarsch et al., 2016]. Considering this theoretical perspective, substantial mechanical forces must be developed to form and release vesicles. So far, testing this hypothesis *in vivo* has proven to be challenging, since the process is executed in a matter of milliseconds. Today, integrated theoretical models are used to better understand the mechano-chemical feedback loop during vesicle formation [Liu et al., 2010].

Another approach is to study the neuromuscular presynaptic terminal in embryonic *Drosophila*. Here, it was shown that clustering and release of neurotransmitters at the synaptic cleft are associated with membrane tension inside the axon [Siechen et al., 2009]. Consequently, the correct assembly of all protein partners at the synapse is not sufficient to trigger signalling - axonal tension is also needed. The tension itself is thought to be produced by the actomyosin machinery, in which myosin is in parallel contact with F-Actin [Heinrich and Sackmann, 2006]. Cell adhesion molecules such as integrins [Chen and Grinnell, 1995] or Ca^{2+} influx through stretch-sensitive ion channels [Glogauer et al., 1997], is thought to convert force into a biochemical signal. The linking role of Ca^{2+} influx between chemical- and mechanical signalling will be investigated in more detail in this thesis.

2.3.2. The mechanosensor Piezo-1

How do neuronal cells sense mechanical cues? There are several potential candidates, with mechano-sensitive ion channels being one prominent example. Having one of the highest turnover rates [O'Leary et al., 2013], mechano-sensitive ion channels enable a rapid cellular response. In this study, I am particularly interested in the mechanosensor Piezo-1. The evolutionarily conserved family of Piezo proteins was recently discovered [Coste et al., 2010] and since then it has been demonstrated that Piezo proteins play an essential role in a multitude of mechanical signalling processes including gentle touch sensation [Ranade et al., 2014b] and vascular development [Li et al., 2014]. Further, Piezo-1 has been described to regulate cell migration and differentiation in the nervous system, highlighting the importance of mechanotransduction during brain development and maturation [Pathak et al., 2014].

With approximately 2,500 amino acids and 24 transmembrane regions, Piezo-1 is a huge transmembrane protein, which assembles into a tetramer with no other proteins needed for its full activation state. This structural complexity, and an absence of sequence homology with any other known classes of ion channels makes Piezo-1 a challenging protein to study.

Very recently, the architecture, gating mechanism and central ion-conducting pore of mammalian Piezo-1 channels were described [Zhao et al., 2016], [Xu, 2016], [Ge et al., 2015]. For pharmacological manipulation of Piezo-1, two compounds are commercially available so far. The first is the unspecific extracellular inhibitor peptide GsMTx4, which inhibits Piezo-1 [Bae et al., 2011] but also various other mechanical-sensitive and stretch-activated channels such as NaV1.7 channel or TRCP1 [Gnanasambandam et al., 2017]. Interestingly, GsMTx4 is a naturally occurring compound extracted from spider venom [Chen and Chung, 2013]. The second is the chemical activator Yoda-1 [Syeda et al., 2015] especially designed for specific Piezo-1 interaction.

2.3.3. Mechanotransduction in ageing and disease

A myriad of studies has shown that changes in stiffness within a cellular microdomain can interfere with physiological functions [Ingber, 2003]. One prominent example where the mechanical properties of the brain tissue undergo changes is indeed during the process of ageing, where the stiffness of the neuronal tissue increases with age [Gefen et al., 2003], [Sack et al., 2009], [Elkin et al., 2010]. Why brain stiffness is higher in aged tissue is not known. The link between mechanobiology and ageing has been better characterised in other tissue and age-dependent mechanical changes in cellular microenvironments are associated with impaired wound healing [Guo and Dipietro, 2010], cancer progression [Gilkes et al., 2014], and cardiovascular disease [López-Otín et al., 2013]. Despite this, the connection between neuronal ageing and mechanosignalling has not been investigated in detail; fMRI and AFM studies reflect global changes in brain mechanics, but cellular heterogeneity cannot be taken into account.

Besides global stiffening, the aged brain also has to deal with mechanosensory disturbances arising from protein aggregates and fibrils. Technical advances in nano-mechanics enabled the measurement of the mechanical parameters of alpha-synuclein, revealing an elastic modulus within the range of 1.3 to 2.1 GPa [Sweers et al., 2011]. Another protein prone to aggregate in neurodegenerative diseases is beta-amyloid [Condello and Stöehr, 2018]. For structural biologists, amyloids are appealing biopolymers that are made up of non-covalently bound aggregates of misfolded polypeptides, resulting in insoluble protein aggregates [vandenAkker et al., 2011]. Welland and his group showed that amyloid fibrils have an elastic modulus ranging from 2 to 14 GPa, predominantly defined by intermolecular interactions [Knowles et al., 2007], [Paparcone et al., 2010]. It is easy to imagine that these extremely stiff fibrils lead to local perturbations in mechanosensing and -transduction. It is of great interest to further illustrate the intracellular signalling pathways related to this and integrate these finding with the common understanding of neurodegenerative diseases.

2.4. Ageing in a dish - Stiffness controlled substrates as a model for cellular brain ageing

In ageing and degenerative research, mainly less complex model organisms have been used in most experimental studies. One advantage of this strategy is that it is more convenient to investigate the multifaceted and long ranging ageing process in a less complicated model and additionally *D. melanogaster* and *C. elegans* already show an aged phenotype after 20 days of adulthood [Piper and Partridge, 2016], [Talboom et al., 2015]. Nevertheless, the signalling pathways found to regulate the ageing process in these model organisms have to be transferred to the mammalian system. Here, *in vitro* models such as primary cell culture preparations are an elegant way to investigate signalling cascades in more details. Further, primary cell cultures can be manipulated efficiently either by pharmacological or genetic tools and subsequent analysis can be run a rather short time range [Lopes et al., 2017], [Hollenbeck and Bamburg, 2003], [Oberpichler-Schwenk and Kriegstein, 1994].

To examine the potential relation between brain stiffening and cognitive decline during ageing in a cell culture model, stiffness controlled substrates can be used [Moshayedi et al., 2010], [Fischer et al., 2012]. Studies focusing on neuronal cell types worked with three main synthetic materials: poly(ethylene glycol) (PEG)-based hydrogels, poly(dimethyl siloxane) (PDMS) or polyacrylamide gels [Nemir and West, 2010]. In this study, I used polyacrylamide (PAA) gels that can be altered in their stiffness by changing the degree of cross-linkers in the gel [Pelham and Wang, 1997], while defining constant chemical properties for all substrates. The porosity of polyacrylamide also makes it practical for cell growth (see Fig. 2.5, D). In general, the pore sizes of the PAA gels are compatible with cell growth: measurements of the nanotopic surface structure revealed that the pore size is ranging from 15 nm to 5.8 nm when the gel stiffness is raised from 2 kPa to 10 kPa [Yang et al., 2017].

PAA gels were manufactured in the lower and upper range of *in vivo* brain stiffness (0.1 kPa, 1 kPa and 10 kPa) and set in contrast to conventional glass coverslips. This allowed the elastic modulus of both a young brain (0.1 kPa) and an aged brain (>2 kPa) to be mimicked in a manner suitable for cell culture (see 3.2.3.2). Throughout this study, primary cortical cultures or cortex lysates were examined, since the prefrontal cortex is thought to be the most vulnerable to ageing [Herndon et al., 1997], [Voytko, 1999].

2.5. Objectives

The previous introduction summarized that ageing research brought up several theories trying to explain the complex ageing process. Nevertheless, so far no fully comprehensive theoretical concept on how and why we age exists. In this thesis, I will concentrate on neuronal ageing

processes especially in cortical areas since this brain part is vulnerable to ageing and mostly associated with cognitive decline [Robinson et al., 2018], [Folke et al., 2018].

To decode complex biological processes one needs a simple, yet sophisticated research model. Primary cortical cultures display ageing processes but the current cell culture systems do not allow survival of neurons up to old age. One main objective of this thesis is therefore to introduce a long-term cell culture system which promotes neuronal survival up to 80 days *in vitro* in a reproducible manner. As one hallmark of ageing, the main experimental focus of this thesis will be on protein homoeostasis and the control of protein synthesis and -degradation. Different techniques to monitor protein homoeostasis such as BONCAT [Dieterich et al., 2006], [Landgraf et al., 2015], FUNCAT [Hinz et al., 2013] and SUNSET will be used to describe how young and aged neurons differently regulate protein dynamics. As one central pathway in translational control, the mTOR and S6 kinase pathway will be investigated. The idea to restore translational capacities and rejuvenate aged neurons by "anti-ageing" compounds is still present in modern ageing research. In this thesis, the effects of the polyamine Spermidine in relation to protein translation and clearing of protein aggregates will be investigated and linked to translational regulators.

Next, this thesis will introduce and characterise a new hallmark of ageing: sensing and conduction of mechanical cues. As introduced, the mechanical integrity of brain tissue itself is changing from a young age to adulthood. At old age, degenerative diseases are, besides various other pathological processes, characterized by an extreme increase in brain stiffness inside cellular microdomains. Therefore, it is of great interest to learn more about how mechanosignalling is connected to cellular metabolism. As an experimental cell culture model, stiffness regulated polyacrylamide gels will be used to present different but still physiological degrees of stiffness to neuronal cells. The knowledge about mechanosensors has increased in the last years but it is still ill-defined which second messengers link mechanical cues to intracellular, chemical or electrical pathways. As one main second messenger, the influx of Ca^{2+} ions will be investigated due to the fact that most mechanochannels are at least partly permeable to Ca^{2+} ions. More details about potential downstream regulator proteins will be revealed by a proteome study and subsequent network analysis. To bring both main aspects of this thesis, neuronal ageing and mechanosensing, to a conclusion, long-term cortical cultures will be grown and investigated using stiffness regulated polyacrylamide gels as cell culture substrate.

3. Methods and Materials

3.1. Materials

3.1.1. Chemicals

All chemicals were obtained from Roth, Sigma Aldrich, Roche, Thermo Scientific, Invitrogen, and Merck in *pro analysis* or molecular-biology grade. For protein biochemical experiments molecular biology-graded water (Roth) was used. For buffers ddH₂O (Milli-Q System, Millipore) was used. Special chemicals and solutions are mentioned at the beginning of each corresponding methods section. The amino acid Azidohomoalanine (AHA) was synthesized by Prof. Dr. Daniela C. Dieterich or by Dr. Peter Landgraf as described by [Link et al., 2007].

3.1.2. Primary antibodies

Table 3.1.: Primary antibodies

Antibody	Species	Dilution	Supplier
anti-ATG8	rb, pc	ICC 1:100	Abcam, ab4753
anti-Bassoon	gp, pc	ICC 1:200/WB 1:1000	Synaptic Sys. 141004
anti-Biotin	gt, pc	WB 1:5000	Bethyl Lab. A150111A
anti-eEF2	rb, pc	ICC 1:100/WB 1:500	Cell Signaling 2332
anti-phospho-eEF2 (Thr56)	rb, pc	ICC 1:100/WB 1:1000	Cell Signaling 2331
anti-eEF2 K.	rb, mc	WB 1:1000	Sigma Aldrich 100652
anti-phospho-eEF2K (Ser366)	rb, pc	WB 1:1000	Cell Signaling 3691
anti-eIF4E	rb, pc	WB 1:1000	Cell Signaling 9742
anti-GFAP	chk, pc	ICC 1:1000/WB 1:5000	Abcam ab4674
anti-GFAP	rb, pc	ICC 1:1000	Synaptic Sys. 173002
anti-GluR1	rb, mc	WB 1:500	Cell Signaling 13185
anti- γ -H2AX	rb, mc	ICC 1:250	Bethyl Lab. A132187
anti-Homer-1	rb, pc	ICC 1:200/WB 1:1000	Synaptic Sys. 160003
anti-Hypusine	rb, pc	ICC 1:500	Millipore ABS1064
anti-Iba-1	gt, pc	WB 1:5000	Abcam ab5076
anti-Lamin-B1	rb, pc	ICC 1:500	Abcam ab16048
anti-Laminin	rb, pc	ICC 1:1000	Cell Signaling ab11575

anti-MAP2	gp, pc	ICC 1:2000	Synaptic Sys. 188004
anti-MAP2	ms, mc	ICC 1:2000/WB 1:1000	Sigma Aldrich M1406
anti-MAP2	rb, pc	ICC 1:2000/WB 1:3000	Abcam ab32454
anti-NeuN	ms, mc	ICC 1:200/WB 1:1000	Millipore MAB377
anti-NMDAR1	rb, mc	WB 1:1000	Cell Signaling 5704
anti-NMDAR2A	rb, mc	WB 1:200	Alomone Labs AGC-002
anti-NMDAR2B	rb, mc	WB 1:200	Alomone Labs AGC-003
anti-p62/SQSTM1	ms, mc	ICC 1:50	Abcam ab56416
anti-p62/SQSTM1	rb, pc	WB 1:500	Cell Signaling 5114
anti-phospho-p62 (Ser349)	rb, pc	WB 1:500	Cell Signaling 95697
anti-Piezo-1	rb, pc	WB 1:500, ICC 1:100	Alomone labs APC-087
anti-Puromycin	ms, mc	ICC 1:250	Millipore MABE343
anti-PDS-95	ms, mc	ICC 1:200	Synaptic Sys. 124011
anti-Rpl10a	ms, mc	ICC 1:200/WB 1:1000	Abcam ab55544
anti-S6K1	rb, mc	WB 1:1000	Abcam ab42357
anti-phospho-S6K1 (S424)	rb, mc	WB 1:1000	Abcam ab47379
anti-S6 Rib. Protein	rb, pc	WB 1:1000	Cell Signaling 2217
anti-Shank-2	ms, mc	ICC 1:500/WB 1:1000	Neuromab 75-088
anti-Synaptophysin1	gp, pc	ICC 1:1000/WB 1:2000	Synaptic Sys. 101004

3.1.3. Secondary antibodies

Table 3.2.: Secondary antibodies

Antibody	Species	Dilution	Supplier
anti-rb IgG, HRP conjugated	gt	WB 1:7500	Jackson Immuno 711-035-152
anti-gp IgG, HRP conjugated	dk	WB 1:7500	Jackson Immuno 706-035-148
anti-ms IgG, HRP conjugated	gt	WB 1:7500	Jackson Immuno 115-035-146
anti-gt IgG, HRP conjugated	dk	WB 1:7500	Jackson Immuno 705-035-147
anti-chk IgG, HRP conjugated	gt	WB 1:7500	Jackson Immuno 103-035-155
anti-rat IgG, HRP conjugated	dk	WB 1:7500	Jackson Immuno 112-035-003
anti-rb IgG, Alexa 405 TM conjugated	dk	ICC 1:1000	Abcam ab175648
anti-rb IgG, Alexa 488 TM conjugated	gt	ICC 1:2000	Invitrogen A21206
anti-rb IgG, Cy3 conjugated	chk	ICC 1:2000	Invitrogen 711-165-152
anti-rb IgG, Alexa 647 TM conjugated	dk	ICC 1:1000	Abcam ab150083
anti-ms IgG, Alexa 405 TM conjugated	dk	ICC 1:1000	Abcam ab175661
anti-ms IgG, Alexa 488 TM conjugated	gt	ICC 1:2000	Invitrogen ab150117
anti-ms IgG, Alexa 555 TM conjugated	dk	ICC 1:1000	Abcam ab150110

anti-ms IgG, Alexa 647 TM conjugated	dk	ICC 1:1000	Abcam ab 150087
anti-gp IgG, Cy3 conjugated	dk	ICC 1:2000	Invitrogen 706-165-148
anti-gp IgG, Cy5 conjugated	dk	ICC 1:2000	Invitrogen 706-175-148
anti-chk IgG, Alexa 488 TM conjugated	gt	ICC 1:2000	Invitrogen ab175675
anti-chk IgG Alexa 647 TM conjugated	dk	ICC 1:1000	Abcam 703-605-155
DAPI (1 mg/ml)	-	ICC 1:10000	Sigma

3.1.4. Bacterial Strains and Culture Media

For transformations and preparations of plasmid DNA from bacteria, the bacterial strain XL10-GOLD with the genotype *endA1 glnV44 recA1 thi-1 gyrA96 relA1 lac Hte (mcrA)183 (mcrCB-hsdSMRmrr)173 tetR FproAB lacIqZM15 Tn10(TetR Amy CmR)* (Stratagene) was used.

Table 3.3.: Bacteria Media

Medium	Ingredients
LB-medium	5 g/l yeast-extract, 10 g/l bacto-tryptone, 5 g/l NaCl
LB-plates	1000 ml LB-medium, 15 g agar
SOC-medium	20 g/l bacto-tryptone, 5 g/l yeast-extract, 10 mM NaCl, 2.5 mM KCl, 10 mM MgSO ₄ , 10 mM MgCl ₂ , 20 mM glucose

3.1.5. Animals

In this study, Wistar rats and C57BL/6J mice from the animal facility of the Institute of Pharmacology and Toxicology (Magdeburg, Germany) were used. Cultures were obtained from E18 rats or E15 mice. Adult rats and mice were housed in groups of 5-6 animals, at constant temperature (22 ± 2 °C) and relative humidity (50 %) under a regular 12 h light-dark schedule (lights on 6 AM-6 PM) with food and water available *ad libitum*. Adult rats or mice were deeply anaesthetized with Isofluran Baxter (Baxter GmbH) prior decapitation using an animal guillotine. Embryos and pups were decapitated without prior treatment using decapitation scissors. In previous and present studies, animal care and procedures were approved and conducted under established standards of the German federal state of Sachsen-Anhalt (Institutional Animal Care and Use Committee: Landesverwaltungsamt Sachsen-Anhalt; License No. 42505-2-1172 UniMD Germany in accordance with the European Communities Council Directive; 86/609/EEC).

3.2. Methods

3.2.1. Molecular Biology

In this study, primarily standard molecular procedures were used. They followed established protocols as described in "Molecular Cloning: A Laboratory Manual" (Green and Sambrook, 2012). Therefore, all protocols are described briefly unless they were significantly altered.

3.2.1.1. Transformation of Chemically Competent Bacteria

For the transformation of *E.coli* XL10-GOLD, 1 or 2 μ l ligation sample DNA was added to 100 μ l of bacteria and incubated on ice for 10 min. After a 45 s heat shock at 42 °C, the samples were put on ice for 2 min before they were transferred to 1 ml preheated SOC medium. The bacteria were incubated at 37 °C for 50 min with constant shaking and then plated on LB-agar plates with respective antibiotics. Plates were incubated overnight at 37 °C and then stored at 4 °C for further experiments.

3.2.1.2. Preparation of Plasmid DNA (Mini and Midi preparations)

- Antibiotics: Ampicillin 100 μ g / ml, Chloramphenicol 25 μ g / ml, Kanamycin 10 μ g / ml
- Buffer P1: 50 mM Tris-HCl (pH 8.0), 10 mM EDTA, 100 μ g/ml RNase A
- Buffer P2: 200 mM NaOH, 1 % (w/v) SDS
- Buffer P3: 3M potassium acetate (pH 5.5)
- Midi preparation: NucleoBond Xtra Midi, Macherey-Nagel

To look for positive clones after transformation, picked colonies were cultivated in 2 ml LB-medium containing the respective antibiotics at 37 °C overnight. The preparation protocol was modified from [Birnboim and Doly, 1979]. Bacteria were pelleted by centrifugation at full speed and resuspended with 300 μ l P1. Cells were lysed with 300 μ l P2 for 5 min, neutralized with 300 μ l P3, and then incubated on ice for 5 min. Precipitated proteins were removed by centrifugation at 20.000 x g for 10 min. The DNA in the supernatant was precipitated with isopropanol. Plasmid DNA was collected by centrifugation at 20000 x g, for 10 min and washed with 70 % ethanol. After drying, the pellet was resuspended in 25 μ l ddH₂O. Large quantities of plasmid DNA with high purity were prepared from 250 ml overnight cultures using the NucleoBond Xtra Midi Kit according to manufacturer's instructions. The DNA pellet was reconstituted in 30 μ l ddH₂O and the DNA concentration was measured using the Nanodrop lite spectrophotometer (Thermo Scientific).

3.2.1.3. Sequencing and Sequence Analysis

Sequencing was done by the company SeqLab. The program Standard Nucleotide Blast by NCBI was used for sequence analysis.

3.2.1.4. Transfection using Ca²⁺-Phosphate

- Solution A: 500 mM CaCl₂
- Solution B: 140 mM NaCl, 50mM HEPES, 1.5 mM Na₂PO₄
- Plating Medium: DMEM, 10 % (v/v) FBS, 100 U/ml Penicillin, 100 µg/ml Streptomycin, 2 mM L-glutamine (all Gibco)

One day before transfection, Hek293T cells in a dilution of 1:12 were seeded into a 24 well plate. Next, 25 µl Solution A was mixed thoroughly with 1 µg DNA. To this mixture, 25 µl of Solution B was added and incubated for exactly 1 min at room temperature (RT). Drop per drop 50 µl of the formed precipitate was added to the cells per well. The cells were incubated for 4 h at 37 °C and 5 % CO₂, then the media was aspirated and 0,5 ml fresh pre-warmed media was added. Subsequently, Hek293T cells were fixed for immunofluorescence staining 24 - 72 h post transfection.

3.2.1.5. Transfection using Electroporation

- Plating Medium: DMEM, 10 % (v/v) FBS, 100 U/ml Penicillin, 100 µg/ml Streptomycin, 2 mM L-glutamine (all Gibco)
- Nucleofector Kit (Lonza)

To prepare the electroporation, 0.5 ml plating medium was added to 2.25 ml Nucleofector solution and pre-warmed to 37 °C. The well plates used for cell seeding were pre-incubated in a humidified 37 °C / 5 % CO₂ incubator filled with a sufficient volume of plating medium. Prepared primary neuronal cells as described under 3.2.4.3 and 5 x 10⁶ cells were centrifuged at 90 x g at RT for 10 min. The supernatant was discarded so that no residual medium was covering the cell pellet. The cell pellet was resuspended in 1.5 ml Nucleofector solution and mixed with 2 µg / 100 µl DNA of interest. The sample was transferred to an amaxa cuvette and a pre-installed Nucleofector program designed for primary neuronal cells was performed. After electroporation, 500 µl pre-warmed plating medium was added to the cells and the suspension was transferred to previously pre-warmed plates in an appropriate cell dilution. For a detectable gene expression, cells were incubated in a humidified 37 °C / 5 % CO₂ incubator for at least 24 h.

3.2.2. Cell Culture

3.2.2.1. Cultivation of HEK293T cells

- Culture medium: DMEM, 10 % (v/v) FBS, 100 U/ml Penicillin, 100 µg/ml Streptomycin, 2 mM L-glutamine (all Gibco)
- TrypLE Express: 1 x Gibco
- Wash Buffer: HBSS with Phenolred (Gibco)

- Culture dishes: TPP
- Poly-D-lysine: 100 mg/l in 0.15 M boric acid, pH 8.4 (Sigma)

The human embryonic kidney cell line (HEK293T) was used for overexpression of protein constructs. Maintenance of cells was done in cell incubators (Heraeus or Thermo Scientific) at 37 °C, 5 % CO₂ and 95 % humidity and confluent cultures were passaged twice a week. For this, the cells were washed twice with 37 °C warm HBSS containing 1 x TrypLE for 3 min and one-tenth was transferred into new culture medium. For immunocytochemistry, Hek293T cells were cultured in 24-well plates on poly-D-lysine treated coverslips. In preparation for a transfection, cells were split to achieve 80 % confluence within 24 h.

3.2.2.2. Fabrication of polyacrylamide (PAA) gels

- Coverslips: Menzel (15, 18, 28, 30 mm)
- Glutaraldehyde (Sigma)
- (3- aminopropyl) trimethoxysilane (APTMS) (Sigma)
- Rain-X solution (Shell Car Care International Ltd, UK)
- 40 % (w/v) acrylamide solution (Sigma)
- 2 % (w/v) bis-acrylamide solution (Fisher Scientific)
- Poly-D-lysine: 100 mg/l in 0.15 M boric acid, pH 8.4 (Sigma)
- Laminin: 211 or 521 (BioLamina)

PAA gels were fabricated on conventional glass coverslips as described previously [Pelham and Wang, 1997]. Briefly, 18 or 30 mm round glass coverslips (Menzel) (referred to as 'bottom coverslips') were treated with 200 µl APTMS and washed thoroughly with distilled water after 3 min incubation. After drying, 400 µl of 0.5 % glutaraldehyde solution was added to the bottom coverslips, which were washed and dried after 30 min. Round glass coverslips of 15 or 28 mm diameter ('top coverslips') were coated with Rain-X solution for 30 min and dried afterwards. In order to create a range of PAA gel elasticities, PAA premixes were prepared from volumes of 1x PBS, 40 % acrylamide solution, and 2 % bis-acrylamide solution according to the following table:

Table 3.4.: Shear modulus, acrylamide and bis-acrylamide concentrations of the PAA gels used in this study

Stiffness (Shear modulus G')(kPa)	acrylamide (%)	bis-Acrylamide (%)
~ 0.1	5	0.04
~ 1	7.5	0.06
~ 10	12	0.21

To initiate polymerization, 1 % ammonium persulfate (APS) and 0.3 % tetramethylethylenediamine (TEMED, ThermoFisher) were applied to the PAA premixes. Subsequently, 7 or 12 μ l of the solution was put in the middle of the bottom coverslip and quickly covered with a top coverslip. After 15 min, gel and coverslips were soaked in PBS for 20 min to facilitate the removal of the top coverslip. The exposed gel was washed in sterile 1x PBS three times. For sterilisation, gels were kept under UV-light for 2 h. Then the gels were treated with poly-D-lysine solution overnight at 4 °C and washed three times with sterile H₂O. Finally, the gels were coated with Laminin-211 (for long-term cultures) or Laminin-521 (1:100) for 2h at 37 °C and 5 % CO₂. The gels were ready for cell seeding.

3.2.2.3. Preparation and cultivation of Cortical Primary Cells from Rat

- Plating Medium: DMEM, 10 % (v/v) FBS, 100 U/ml Penicillin, 100 μ g/ml Streptomycin, 2 mM L-glutamine (all Gibco)
- Culture Medium: NeurobasalTM, 1 x B27, 0.8 mM L-glutamine (all Gibco)
- Culture dishes: TPP
- Coverslips: Menzel
- Wash Buffer: HBSS with Phenolred (Gibco)
- Trypsin: 10 x Trypsin (-EDTA), (Gibco)
- DNase I: 0,1 % (200U) in HBSS, 2.4 mM MgSO₄ (Sigma)
- Poly-d-Lysine: 100 mg/l in 0.15 M boric acid, pH 8.4 (Sigma)

The preparation of primary neuronal cultures from rat was performed according to Kaech and Banker [Kaech and Banker, 2006] with slight modifications. Rat embryos were decapitated at E18 and the brain was laid open. The cortices were separated from the rest of the brain in HBSS and the tissue was trypsinized for 15 min at 37 °C. Afterwards the tissue was washed three times in HBSS to remove residual trypsin. The cortex tissue was dissociated by repeatedly pipetting through syringes (0.9 mm and 0.45 mm, Brandt) and the addition of 0,1 % DNase. After filtration through a 0.45 μ m membrane the cells were diluted in plating medium and the cell density was determined. Then neuronal cells were seeded onto poly-D-lysine treated coverslips or culture dishes. For immunocytochemical experiments, *low-density* cultures (40.000 cells per 12 mm coverslip) or *high-density* cultures (100.000 cells per 12 mm coverslip, for long-term experiments) were used. Biochemical experiments were performed with cortical cells in 6-well plates (300.000 cells per well) or 75 cm² flasks. Conventional glass coverslips or PAA gels were used (see 3.2.3.2). Neuronal cells were kept at 37 °C and 5 % CO₂. One day after the cell preparation the plating medium was exchanged to culture medium. Once a week the cortical cultures were fed with a tenth of their culture medium.

3.2.2.4. Stimulation of Cortical Primary Cells

- Spermidine: 25 μ M or 50 μ M for 3 h or 24 h
- Hypusine: 10 μ M or 25 μ M for 3 h or 24 h
- Yoda-1: 0.1 μ M or 10 μ M for 15 min
- GsMTx4: 1 μ M or 10 μ M for 15 min
- Wash Buffer: HBSS (Gibco)

For the pharmacological manipulation of primary cortical cells, the corresponding substance was pipetted directly into the culture media to a final concentration mentioned above. As a control condition, the corresponding solvent such as 1x PBS (for Spermidine, Hypsusine) 1x HBSS (for GsMTx4) or DMSO (for Yoda-1) for each stimulant was applied alone. After the incubation time, cells were washed once with prewarmed HBSS (Gibco) and fixed for further analysis.

3.2.2.5. Cultivation of Primary Glia Cells from Rat

- Plating Medium: DMEM, 10 % (v/v) FBS, 100 U/ml Penicillin, 100 μ g/ml Streptomycin, 2 mM L-glutamine (all Gibco)
- Wash Buffer: HBSS with Phenolred (Gibco)
- Trypsin: 10 x Trypsin (-EDTA), (Gibco)

Preparation of glia cells was performed as described by [Guizzetti and Costa, 1996]. In brief, pups (P2 - P4) from Wistar rats were decapitated and both hemispheres were isolated and cleaned from meninges in ice cold wash buffer. After three washing steps with ice cold wash buffer, 10 x trypsin was added and incubated for 20 min at 37 °C. The hemispheres were washed three times with wash buffer and dissociated in 1 ml plating medium by using two types of syringes (G21 and G25). Cells were plated in 10 ml plating medium in 75 cm² flasks and kept in the incubator at 37 °C and 5 % CO₂. The media was changed the following day and then every 4 - 5 days. Microglia were patted off twice a week during media change. Glia cells were seeded onto 12 mm coverslips with conventional glass surfaces or coated with PAA gels (see 3.2.3.2) for ICC.

3.2.2.6. Stimulation of Primary Glia Cell

- Yoda-1: 0.1 μ M for 15 min
- GsMTx4: 1 μ M for 30 min

For the pharmacological manipulation of primary glial cells, the corresponding stimulant was applied directly into the culture media to a final concentration mentioned above. As control condition, the corresponding solvent such as 1x HBSS (for GsMTx4) or DMSO (for Yoda-1) was applied alone. After incubation the time, cells were washed once with prewarmed HBSS (Gibco), fixed and stored for further analysis.

3.2.2.7. Incorporation of non-canonical amino acids in neuronal cells

- HBSS: 1 x HBSS (Gibco)
- L-Methionine: 200 mM (Sigma) in ddH₂O
- Azidohomoalanine: 200 mM (synthesized by D.C. Dieterich or P. Landgraf) in ddH₂O
- Hibernate: see recipe in [Brewer and Price, 1996] (Sigma, Roth, Serva)
- PBS-MC: 1 x PBS pH 7.8, 0.1 mM CaCl₂, 1 mM MgCl₂
- 4 % PFA (w/v), 1x PBS pH 7.4

To incorporate non-canonical amino acids in primary neuronal cells, the cultures were washed once with warm HBSS and incubated for 30 min at 37 °C and 5 % CO₂ with Hibernate medium (without methionine) to deplete the methionine stores inside the cell. Subsequent labelling with AHA (or methionine as control) was performed for 2 - 4 h at a final concentration of 4 mM in Hibernate medium. Neuronal cells were washed with ice cold PBS-MC and lysed for BONCAT reaction (see 3.2.2.1) or were fixed with 4 % PFA for FUNCAT (see 3.2.4.8).

3.2.2.8. FUNCAT

- 4 % PFA (w/v), 1x PBS pH 7.4
- B-block: 10 % (w/v) Horse Serum (Gibco), 5 % (w/v) Sucrose, 2 % (w/v) BSA in 1 x PBS pH 7.4
- TAMRA-alkyne tag: 200 mM in DMSO (Invitrogen)
- Coppersulfate: 200 mM (Sigma) in ultra pure H₂O (Roth)
- Triazol-ligand (Tris[(1-benzyl-1H-1,2,3-triazol-4-yl)methyl]amine): 200mM in DMSO (Sigma)
- TCEP: Tris(2-carboxyethyl)phosphine hydrochloride, 500 mM in ultrapure H₂O (Roth)
- FUNCAT wash buffer: 0.5 mM EDTA, 1 % (v/v) Tween-20 in 1x PBS pH 7.8
- Mowiol: 10 % (w/v) Mowiol, 25 % (v/v) Glycerol, 100 mM Tris-HCl pH 8.5, 2.5 % (w/v) DABCO

After incorporation of non-canonical amino acids neuronal cells were fixed for 7 min at RT with 4 % PFA. Cells were washed three times with 1 x PBS pH 7.4, blocked with B-block for 1.5 h under gentle agitation and subsequently washed three times with 1 x PBS pH 7.8 at RT. The click reaction mix was prepared by first adding the triazol-ligand (1:1000) to 1 x PBS pH 7.8 and mixed by strong vortexing. Next, TCEP (1:1000) was added to the click reaction mix and vortexed for 10 s followed by the TAMRA-tag (1:10000) and mixing for again 10 s. After adding the coppersulfate solution (1:1000) and mixing for 30 s the reaction solution was transferred to a 24-well plate (400 µl per well). The coverslips were placed on top of small paraffin dots with cells facing down to prevent accumulation of precipitates and incubation was performed overnight at RT under gentle agitation. To stop the click reaction,

cells were washed two times with FUNCAT wash buffer and three times with 1 x PBS pH 7.4 for 10 min each. Afterwards, immunocytochemistry was performed to counter-stain for different proteins of interest as described under 3.2.3.10, starting with the primary antibody incubation step.

3.2.2.9. Puromycin assay

- Puromycin dihydrochloride (Sigma, stock 100 mM in water, 1 μ M final)
- HBSS: 1 x HBSS (Gibco)
- B-block: 10 % (w/v) Horse Serum (Gibco), 5 % (w/v) Sucrose, 2 % (w/v) BSA in 1 x PBS pH 7.4
- PLP fixative: 0.2 M Lysine-HCl (Sigma), 0.05 Sodium Phosphate (Roth), 0.1 M Sodium Periodate (Sigma), 4 % (w/v) PFA (Thermo Scientific) [McLean and Nakane, 1974]

The antibiotic Puromycin was used to monitor protein synthesis. Primary cortical cultures were incubated with pre-warmed 1x HBSS (Gibco) containing 10 μ g/ml Puromycin for 1 min. Puromycin labelling was stopped by washing with 1 x HBSS once and fixed with PLP fixative. Puromycin incorporation was visualized by immunocytochemistry (see 3.2.3.10) using a specific antibody against Puromycin and combined with antibodies for specific proteins of interest.

3.2.2.10. Synaptotagmin uptake assay

To study presynaptic activity an antibody against the luminal domain of synaptotagmin-1 coupled with a fluorophore (Synaptic Systems) was added in a concentration 1:100 directly to the Neurobasal medium of neuronal cultures *in vivo* for 30 min at 37 °C and 5 % CO₂. When synapses fuse their neurotransmitter vesicles during this time period, the luminal part of synaptotagmin-1 gets exposed so that the antibody can bind. The fluorescence intensity of this antibody reflects the active state on a single synapse level. For quantification of co-localisations the Puncta Analyzer plug-in (under ImageJ software) from the Eroglu Lab was used [Ippolito and Eroglu, 2010].

3.2.2.11. Immunocytochemistry

- 4 % PFA (w/v), 1x PBS pH 7.4
- B-block: 10 % (w/v) Horse Serum (Gibco), 5 % (w/v) Sucrose, 2 % (w/v) BSA in 1 x PBS pH 7.4
- 1x PBS pH 7.4, 0,3 % (v/v) Triton-X-100
- Mowiol: 10 % (w/v) Mowiol, 25 % (v/v) Glycerol, 100 mM Tris-HCl pH 8.5, 2.5 % (w/v) DABCO

Cells were grown on 12 mm coverslips and fixed with 4 % PFA in 1 x PBS for 10 min at RT. Coverslips were washed three times with 1 x PBS to remove residual PFA. Cells were blocked for 1 h with blocking solution and subsequent incubation with primary antibodies diluted in blocking solution was performed for 1.5 h at RT or overnight at 4°C. After thorough washing, cells were incubated with secondary antibodies diluted in blocking solution for 1 h at RT. Then, cells were washed four times with PBS, rinsed briefly in twofold distilled water and mounted onto microscope slides in 7 to 14 μ l Mowiol.

3.2.2.12. Sholl Analysis

To quantify for dendrite complexity, DIV 7 cortical neurons were stained using ICC as described above. Images were acquired with a 20x objective and 2x camera binning to improve visualization of dendrites with LSM 800 systems (Zeiss, Germany). Soma and dendrites of neurons were traced along MAP2 positive dendrites using Adobe Photoshop (Adobe Systems, San Jose, USA). The trace copy of the neuron was subjected to Sholl analysis (Sholl Analysis Plugin for ImageJ, public domain, imagej.nih.gov/ij/) with the following parameters:

- Starting radius: 0 μ m
- Ending radius: 200 μ m
- Radius step size: 5 μ m
- Radius Span: 0
- Span Type: Median

3.2.3. Biochemistry

3.2.3.1. Cell lysis and protein extraction

- 1 x PBS pH 7.4: 37 mM NaCl, 2.7 mM KCl, 4.3 mM Na₂HPO₄ x 7 H₂O, 1.4 mM KH₂PO₄
- PBS-MC: 1 x PBS pH 7.8, 0.1 mM MgCl₂, 1 mM MgCl₂
- Protease Inhibitor (PI): Complete EDTA-free Protease Inhibitor cocktail tablets (Roche)
- PhosSTOPTM (Roche)
- 4 x SDS sample buffer: 250 mM Tris, 1 % (w/v) SDS, 40 % (v/v) glycerol, 20 % (v/v) β -Mercaptoethanol, 62.5 mM Tris pH 6.8, 0.001 % (w/v) Bromophenol Blue
- Benzonase: Benzonase Nuclease 250 U/ μ l (Sigma Aldrich)
- 1 x PBS pH 7.8 + PI w/o EDTA (Roche): 137 mM NaCl, 2.7 mM KCl, 4.3 mM Na₂HPO₄ x 7 H₂O, 1.4 mM KH₂PO₄

Primary cortical cells were washed once with ice-cold PBS-MC and scraped off on ice in 1 ml 1 x PBS pH 7.4 + PI + PhosSTOPTM. The cell suspension was spun down at 3.000 x g for 5 min at 4 °C (Eppendorf centrifuge 5810R). The cell pellets were frozen at -20 °C at least overnight or longer for storage. For a protein extract, cell pellets were thawed completely on

ice and 1 x PBS pH 7.8 + PI, 125 U Benzonase and 0.2 % SDS were added. The cell lysate was incubated at 95 °C for 5 min with gentle agitation, afterwards 0.2 % Triton-X-100 and PBS pH 7.8 + PI were added to attain a SDS concentration of 0.1 %. The lysis volume was 500 µl for one 75 cm² flask or 200 µl for a 6-well cell culture plate. Finally, the corresponding volume of 4 x SDS sample buffer was added for a 1 x concentration.

3.2.3.2. BONCAT

- Biotin alkyne tag: 25 mM in 1x PBS pH 7,8 (Syntheses: Dr. Peter Landgraf as described in [Szychowski et al., 2010])
- Copper(I)bromid suspension: 10 mg/ml in ultrapure H₂O (Roth)
- Triazol ligand: (Tris(1-benzyl-1H-1,2,3-triazo-4-yl)methylamine) 200 mM in DMSO (Sigma)

The BONCAT procedure was described by [Dieterich et al., 2007] and detection of AHA-labelled proteins was performed in accordance to this publication. Protein lysates containing AHA-labelled proteins were tagged by addition of Triazol ligand (200 µM), Biotin alkyne tag (25 µM) and copper(I)bromide suspension (100 µg/ml). The samples were incubated in a spinning wheel for 90 min at RT. Precipitates were removed by centrifugation at 3,000 x g for 5 min at 4 °C. The resulting supernatant was mixed with 4 x SDS sample buffer for a final 1 x concentration and stored at -20 °C for further analysis by SDS-Page and Western Blotting.

3.2.3.3. Determination of protein concentration with amido black assay

- Washing solution: methanol-acetic acid solution: 90 % (v/v) methanol, 10 % (v/v) acetic acid
- Staining solution: 1.44 % (w/v) amido black in methanol-acetic acid solution
- Standard: 0.5 mg/ml BSA solution
- 0.1 M NaOH

To determine the protein concentration of a certain lysate the amido black assay according to [Badin and Herve, 1965] was executed. Standard BSA samples and sample of protein probes were prepared as triplets in a 96 well plate (see table 3.4). For protein samples, 10 µl protein probe was mixed with 90 µl ddH₂O. To all samples, 200 µl amido black solution was added and incubated for 10 min at RT. After centrifugation at 3.220 x g for 10 min (Eppendorf centrifuge 5810R) the supernatant was decanted and the pellet was washed with 300 µl methanol-acetic acid. Subsequent centrifugation was performed at 3.220 x g for 10 min. This washing step was repeated once more. The protein pellet was air-dried at RT and dissolved in 300 µl 0.1 M NaOH under gentle agitation. The extinction was measured at 620 nm (absorption of amido black die) in a photometer (ASYS ExpertPlus). The extinction was then compared to a BSA standard to deduce the protein concentration in the samples.

3.2.3.4. Coomassie Brilliant Blue R250 staining

- Coomassie Brilliant Blue staining solution: 0.125 % (w/v) Coomassie Brilliant Blue R250, 50 % (v/v) methanol, 10 % (v/v) acetic acid
- Destaining solution: 7 % (v/v) acetic acid
- Conservation solution: 50 % (v/v) methanol, 5 % (v/v) glycerol

SDS-Gels were stained with Coomassie Brilliant Blue R250 staining solution overnight at RT and destained with Destaining solution after gently heating in the microwave. The unbound staining solution was collected with a tissue and the gels were destained until protein bands were clearly visible. For digitalisation the stained gels were scanned with an Artix Scan F2 (Microtek) scanner. A quantitative analysis was performed with ImageJ. For conservation, gels were incubated in Conservation solution for 5 min and spanned in a frame between two cellophane sheets (Roth) to dry.

3.2.3.5. Sodium dodecyl sulphate polyacrylamide gel electrophoresis (SDS-PAGE) and Western Blot

Tris glycine gels:

- 4 x separating gel buffer: 1.5 M Tris-HCl pH 8.8
- 4 x stacking gel buffer: 0.5 M Tris-HCl, pH 6.8
- acrylamide: Rotiphorese Gel 40 (19:1) T=40 %, C= 5 % (Roth)
- 30 % acrylamide/Bis solution (37,5:1) T= 30.8 %, C=2.6 % (Biorad Laboratories)

Table 3.5.: Chemical composition of 12 gradient mini tris glycine gels (5 % - 20 %)

Compound	Separating gel 5 %	Separating gel 20 %	Stacking gel 5 %
4x buffer	6.84 ml	6.84 ml	6 ml
87 % glycerol	1.8 ml	7.2 ml	5.52 ml
acrylamide 40 %	4.056 ml	16.2 ml	-
acrylamide 30 %	-	-	3.84 ml
0.2 M EDTA	316.8 μ l	316.8 μ l	240 μ l
10 % SDS	316.8 μ l	316.8 μ l	240 μ l
TEMED (Sigma)	21.6 μ l	21.6 μ l	18.2 μ l
10 % APS (Sigma)	115.2 μ l	72 μ l	148.2 μ l
0,5 % bromophenol blue	-	48 μ l	-
0,2 % phenolred	-	-	12 μ l
ddH ₂ O	18.94 ml	1.392 ml	7.95 ml

Table 3.6.: Chemical composition of 12 homogeneous mini tris glycine gels (9.5 %)

Compound	Separating gel 9.5 %	Stacking gel 5 %
4x buffer	17.5 ml	7 ml
87 % glycerol	5.25 ml	6.4 ml
acrylamide 30 %	22.2 ml	4.6 ml
TEMED (Sigma)	46.6 μ l	40 μ l
10 % APS (Sigma)	466.7 μ l	160 μ l
0,5 % bromophenol blue	29.2 μ l	-
0,2 % phenolred	-	103.5 μ l
ddH ₂ O	24.5 ml	9.8 ml

Table 3.7.: Chemical composition of 12 homogeneous mini tris glycine gels (15 %)

Compound	Separating gel 9.5 %	Stacking gel 5 %
4x buffer	17.5 ml	7 ml
87 % glycerol	5.26 ml	6.4 ml
acrylamide 30 %	35 ml	4.6 ml
TEMED (Sigma)	46.68 μ l	40 μ l
10 % APS (Sigma)	466.7 μ l	160 μ l
0,5 % bromophenol blue	29.2 μ l	-
0,2 % phenolred	-	103.5 μ l
ddH ₂ O	11.67 ml	9.8 ml

Tris acetate gels:

- 4 x gel buffer: 0.5 M Tris-HCl pH 7.0
- 30 % acrylamide/bis solution (37,5:1) T= 30.8 %, C=2.6 % (Biorad Laboratories)

Table 3.8.: Chemical composition of 12 gradient tris acetate gels (3.5 % - 8 %)

Compound	Separating gel 3.5 %	Separating gel 8 %	Stacking gel 3 %
4x buffer	7.8 ml	7.8 ml	6 ml
87 % glycerol	1.8 ml	7.2 ml	5.52 ml
Acrylamide 30 %	3.65 ml	8.33 ml	2.4 ml
TEMED (Sigma)	24 μ l	24 μ l	24 μ l
10 % APS (Sigma)	120 μ l	120 μ l	144 μ l
0,5 % bromophenol blue	-	48 μ l	-
0,2 % phenolred	-	-	12 μ l
ddH ₂ O	17.952 ml	7.872 ml	10.08 ml

- 1 x Electrophoresis buffer: 25 mM Tris pH 8.3, 192 mM glycine, 0.1 % (w/v) SDS

- 1 x SDS buffer: 1x SDS buffer: 0.25 % (w/v) SDS, 10 % (v/v) Glycerol, 5 % (v/v) β -mercaptoethanol, 62.5 mM Tris pH 6.8, 0.001 % (w/v) Bromophenol blue
- Marker: prestained Protein Ladder, Page Ruler (Fermentas), Page Ruler Plus (Fermentas)
- 1 x Western Blot buffer: 25 mM Tris-Base, 192 mM Glycine, 0.02 % (w/v) SDS
- 1 x TBS: 20 mM Tris-Base, 0.8 % (w/v) NaCl
- 1 x TBS-T: 20 mM Tris-Base, 0.8 % (w/v) NaCl, 0.1 % (v/v) Tween-20
- 1 x TBS-A: 20 mM Tris-Base, 0.8 % (w/v) NaCl, 0.02 % (w/v) Na-Azide
- 5 % (w/v) dry milk in TBS-T
- 5 % (w/v) BSA in TBS-T
- Nitrocellulose membrane (Protran BA85, 0.45 μ m, Whatman)
- Nitrocellulose membrane (Protran BA85, 0.20 μ m, Licor)
- PonceauS staining solution: 5 % (w/v) PonceauS, 3 % (v/v) acetic acid

SDS-PAGE was performed according to the standards described by Laemmli [Laemmli, 1970]. Protein mixtures were separated by size with gradient- (5 % - 20 %), homogeneous tris glycine mini gels (9.5 %), homogeneous tris glycine mini gels (15 %) or gradient tris acetate (3.5 % - 8 %) mini gels in a Hoefer Mighty Small System SE250 (Amersham Biosciences) with a constant current of 10 mA per gel. The separation was terminated when the bromophenol blue front left the separating gel. Subsequently, the separated proteins were either stained with Coomassie brilliant blue staining solution (as described in 3.2.2.4) or transferred onto a nitrocellulose membrane (Protan BA85, 0.45 μ m, Whatman, Protan BA85, 0.22 μ m, Licor) at 200 mA for 1.5 h (for tris-acetate gels: 4 h) to perform Western Blot Analysis. To avoid unspecific binding of the primary antibody solved in TBS-A, the membrane was blocked with 5 % dry milk or 5 % BSA in TBS-T for 1.5 h at RT. Incubation with a primary antibody was performed overnight at 4 °C under permanent agitation. The next day, the membrane was washed two times for 10 min with TBS and TBS-T and two times for 5 min with TBS-T and TBS. Then the horseradish peroxidase-conjugated secondary antibody in 5 % dry milk in TBS-T, was added and incubated for 1.5 h at RT under permanent agitation. Again the membrane was washed as described above and the protein bands were developed with the ECL detection system (Pierce). For visualisation an Odyssey Fc scanner (Licor) was used, utilizing the chemiluminescence properties of the secondary antibody.

To ensure equal loading concentrations, an amido black assay (3.2.4) was performed. Subsequently, 10 μ g, 15 μ g, 20 μ g or 40 μ g, depending on experimental design, of protein lysates were loaded on an SDS-gel and stained with Coomassie staining solution. The Coomassie staining, representing the total protein amount of a given sample, was used as Loading Control unless stated otherwise. Since primary neuronal cells investigated in this thesis were characterized during different developmental stages or even at aged time points, conventional loading controls such as Actin or beta-Tubulin were not well suited because the cytoskeleton

itself is most likely regulated. Also recent studies suggest that total protein amount visualized by Coomassie is a more robust and reliable loading control [Welinder and Ekblad, 2011], [Eaton et al., 2013], [Faden et al., 2016], [Nie et al., 2017]. The cell cultures grown on stiffness regulated substrates were also quantified using a total protein staining since the different conditions compared presumably also differ in their cytoskeleton [Vishavkarma et al., 2014], [Gupta et al., 2016].

Signal intensities for each protein lane were quantified using ImageJ and the loading volume of the samples was normalized to ensure equal protein concentrations in all samples. In all Western Blots presented in this thesis, a Coomassie staining was used as loading control. If Western Blots were also semi-quantitatively analysed, the Coomassie Loading control was also used for normalization in the statistical analysis.

3.2.3.6. Synaptoneurosome Preparation

- HOM-Buffer: 20 mM HEPES (Roth), pH 7.4, 0.32 M Sucrose (Roth), 2mM MgCl₂, 1 x complete Protease Inhibitor Mix (Roche)
- Ficoll 400 (Pharmacia) solution: 5 % (w/v), 13 % (w/v) and 16 % (w/v), prepared in HOM buffer, used as step gradient
- Azidohomoalanine (AHA): 200 mM (synthesized by D.C. Dieterich or P. Landgraf) in ddH₂O
- Hypusine (Hyp): 50 µm in ddH₂O (Sigma)
- Preincubation buffer: 20 mM HEPES, pH 7.4, 20 mM Glucose, 3.5 mM KCl, 1.2 mM Na₂HPO₄, 2 mM MgCl₂, 129 mM NaCl (all Roth)
- Incubation buffer: 25 mM HEPES, pH 7.4, 20 mM Glucose, 3.5 mM KCl, 1.8 mM CaCl₂, 1.2 mM Na₂HPO₄, 1 mM MgCl₂, 129 mM NaCl (All Roth)

For the preparation of synaptoneurosomes, brains from mice aged 3, 18 or 26 months were dissected and homogenized in 3 ml HOM-buffer using a teflon homogenizer (12 strokes at 1000 rpm). To remove cell debris and nuclei the lysate was centrifuged for 5 min at 1000 x g, 4 °C (Centrifuge 5810R, Eppendorf), yielding the pellet P1 and supernatant S1. The S1 fraction was placed into a new tube and if too many tissue pieces remained in the supernatant it was homogenised again with 6 strokes at 1000 rpm. Subsequently, the S1 fraction was centrifuged for 5 min at 1300 x g, 4 °C, leading to pellet P2 and supernatant S2. S2 was carefully removed from the pellet P2 and spun down for 20 min at 14000 x g, 4 °C (Optima XPN-80, Ultracentrifuge, Beckman). In parallel, the Ficoll 400 step gradient was prepared using 4 ml of each concentration (5 %, 13 %, 16 %) into an ultracentrifugation tube, starting with 5 % and layering to higher concentrations from beneath. The supernatant S3 was discarded while the crude membrane pellet P3 was resuspended in 3 ml HOM-buffer and loaded on top of the prepared Ficoll 400 step gradient. Centrifugation was performed for 50 min, at 40000 xg and 4 °C. In between, the non-canonical amino acid AHA was solved for later incorporation into

newly synthesized proteins instead of methionine. After centrifugation, synaptoneuroosomes (SNS) are visible as third densely white band between 13 % and 16 % ficoll 400. The SNS fraction was isolated from the rest of the gradient and resuspended in 6 ml pre incubation buffer. Next, the SNS fraction was divided into two and each probe is added to the prepared AHA solutions (4 mM final concentration). One group was additionally stimulated with 50 μ M Hypusine [Huang et al., 2007]; one is kept as control. For labelling with AHA, SNS fractions were incubated for 2 h at 37 °C, 5 % CO₂ and 95 % humidity in a cell culture incubator [Landgraf et al., 2015]. Afterwards, each probe was collected and spun down for 5 min, 4 °C at 3200 x g and the pellet was stored for further experiments (see BONCAT 3.2.2.1 or SDS-Page 3.2.2.5) at - 80 °C.

3.2.3.7. Polysome Profiling

- Lysis Buffer: 10 mM NaCl, 10 mM MgCl₂, 30 mM Tris pH 7.4, 0.1 mg/ml cycloheximide (Sigma), 6.6 mM DTT, 1 x cCompleteTM Protease Inhibitor Mix (Roche), 1 x PhosphoSTOPP, 1000 U RNaseinhibitor (Promega), H₂O (RNase-free, Qiagen)
- sucrose gradient: 70% (w/v) Sucrose, 10 mM NaCl, 10 mM MgCl₂, 30 mM Tris pH 7.4, 6.6 mM DTT, 125 U RNaseinhibitor (Promega), H₂O (RNase-free, Qiagen)
- 0,1 mg/ml Cycloheximide (Sigma)
- HBSS: 1 x HBSS (Gibco)
- 1% (v/v) Triton X-100, 2 % (v/v) Tween-20, 1% (v/v) desoxycholat
- 4 x SDS sample buffer: 250 mM Tris, 1 % (w/v) SDS, 40 % (v/v) glycerol, 20 % (v/v) β -mercaptoethanol, 62.5 mM Tris pH 6.8, 0.001 % (w/v) bromophenol blue

During Polysome Profiling, all attempts were made to work RNase-free.

A 20 % to 60 % sucrose gradient (in 10 % steps) was prepared one day in advance to ensure a continuous distribution of the different sucrose concentrations inside the gradient and kept overnight at 4 °C. The next day, 20 million primary cortical cells (5 million per 75 cm² flasks) were pooled for each experimental condition. Two time points were investigated: DIV 20 reflecting mature but young cells and their aged counterpart at DIV 60. One experimental cell group was incubated with 10 mM Cycloheximid for 20 min. Afterwards, all cells were washed once with 1 x HBSS (supplemented with 10 mM cycloheximid or not) and scraped off in 400 μ l lysis buffer. This lysis buffer containing cells from the first flask was also used to harvest the other four flasks since a small lysis volume is critical.

After harvesting, cells were kept on ice and mechanically disrupted by repeatedly pipetting through syringes (0.9 mm and 0.45 mm, Brandt). Triton X-100, Tween-20 and deoxycholate were added to the cell suspension and vortexed five times for one minute to further destroy cell integrity. The cell lysate was spun down at 5000 x g for 10 min at 4 °C and the supernatant

was loaded on top of the sucrose gradient. Now ultracentrifugation at 35000 x g was performed for 2 h at 4 °C with the lowest acceleration- and deceleration rate. To fractionate the gradient the Biocomp Gradient Station (Biocomp) was used. The ultracentrifugation tube was placed inside the holder and 15 fractions of the same volume (around 450 µl) were collected. In parallel, the RNA profile was measured by a photometer at 260 nm and drawn live. All fractions were supplemented with 4 x SDS sample buffer and heated to 95 ° for 5 min. Probes were stored at -20 ° for SDS-Page and Western Blot analysis.

3.2.4. Mass spectrometry

All mass spectrometry experiments were performed in cooperation with Robert Ahrends and Chi Nyugen from the ISAS Dortmund.

3.2.4.1. Proteomics Sample Preparation

- Lysis buffer: 1 % (w/v) SDS, 150 mM NaCl, 50 mM Tris-HCl pH 7.8, 1 x cOmpleteTM (1 tablet per 50 ml, Mini Protease Inhibitor Cocktail, Roche)
- SDS buffer: 1 % (w/v) SDS, 150 mM NaCl, 50 mM Tris-HCl pH 7.8
- Tris(2-carboxyethyl)phosphine hydrochloride (TCEP, Sigma-Aldrich)
- Iodoacetamide (IAA, Sigma-Aldrich)
- Benzonase: Benzonase Nuclease 250 U/µl (Sigma Aldrich)
- Urea buffer: 8 M Urea in 100 mM Tris-HCl pH 8.5
- Trypsin: Trypsin Gold, Promega
- Digestion buffer: 0.2 M Guanidine-HCl, 2 mM CaCl₂, 50 mM NH₄HCO₃ pH 7.8

For each condition (compliant 0.1 kPa, intermediate 1 kPa, stiff 10 kPa and glass), three biological replicates were carried out. The cell pellets were thawed on ice and lysed in 50 - 200 µl lysis buffer depending on the pellet size. Subsequently, 1 µl Benzonase Nuclease (Merck KGaA) per 300 µl and the same volume of 1 M MgCl₂ were added to the cell lysates. After incubation at 37 °C for 30 min, the cell lysates were clarified by centrifugation for 30 min at 18.000 g and 4 °C and the supernatant was used for further steps. To remove gel residues in cell lysates, a two-step protein precipitation method was used. First, 9 volumes of ice cold ethanol was added to the cell lysates and they were incubated at -20 °C for 4 h. The protein pellets were collected by centrifugation (18.000 g, 30 min, 4 °C) and dissolved in 40 µl of SDS-buffer. Then, 500 µl ice cold acetone was added to the cell lysates for the second round of protein precipitation. After incubation (-20 °C, overnight) and centrifugation (18.000 g, 30 min, 4 °C), they were dissolved in 40 µl of SDS-buffer. The disulfide bonds were reduced with 10 mM TCEP at 56 °C for 30 min. The free sulphydryl groups were alkylated with 30 mM Iodoacetamide at 25 °C, protected from light and for 30 min. Sample cleanup and proteolytic digestion were done using filter-aided sample preparation protocol (FASP). The protein samples dissolved in SDS buffer were diluted to less than 0.2 % SDS

with freshly prepared Urea buffer and loaded onto a centrifugal device (PALL Nanosep, 30 kDa molecular weight cutoff) with a filter membrane equilibrated twice with 100 μ l Urea buffer. The centrifugation at 13.500 g and 25 °C was applied for all centrifugation steps with this device. After centrifugation for 30 min, the filter membrane was washed four times with 100 μ l Urea buffer to remove SDS and gel residues, followed by washing three times with 100 μ l 50 mM NH₄HCO₃ (pH 7.8). Trypsin was used at a ratio of 1 : 25 (w / w, protease to substrate) for the enzymatic digestion in 100 μ l digestion buffer. The digestion was performed for maximum 15 hours at 37 °C. The tryptic peptides were collected by centrifugation in 25 mM NH₄HCO₃ (pH 7.8) at a final volume of 200 μ l and acidified with 10 μ l 10 % trifluoroacetic acid (TFA). The digestion efficiency was checked by monolithic reverse phase separation [Burkhart et al., 2012] and stored at -80 °C for further analysis.

3.2.4.2. LC-MS / MS analysis

- trapping-column (Acclaim C18 PepMap100, 100 μ m 2 cm, Thermo Scientific)
- 0.1 % (w/v) TFA (Roth)
- reverse phase main-column (Acclaim C18 PepMap100, 75 μ m 50 cm, Thermo Scientific)
- binary gradient solution (A): 0.1 % (v/v) formic acid (FA)
- binary gradient solution (B): 84 % (v/v) acetonitrile, 0.1 % (v/v) FA

The peptide samples were separated on an Ultimate 3000 Rapid Separation Liquid Chromatography (RSLC) nano system coupled to a Q Exactive HF mass spectrometer (both Thermo Scientific). On the nano liquid chromatography (nanoLC) system, peptides were concentrated on a trapping-column (Acclaim C18 PepMap100, 100 μ m 2 cm, Thermo Scientific) using 0.1 % TFA at a flow rate of 20 μ l / min and subsequently separated on a reverse phase main-column (Acclaim C18 PepMap100, 75 μ m 50 cm, Thermo Scientific) using a binary gradient consisted of A: 0.1 % formic acid (FA) and B: 84 % acetonitrile, 0.1 % FA at a flow rate of 250 nl / min. The gradient increased linearly from 3 % A to 42 % B over 90 min. Three washing steps at 95 % of organic solvent B at the end of the gradient were applied to prevent carry-over effect from run to run. For the mass spectrometry (MS) analysis, full MS scans were acquired at a resolution of 60.000 full width at half maximum (FWHM), target value of 1 x 106, maximum injection time of 120 ms and scan range from 300 to 1500 mass-to-charge (m / z). Data dependent MS scans were acquired using high-energy collisional dissociation (HCD) on 15 most abundant ions (top15) at normalized collision energy of 27 %, resolution of 15.000 FWHM, isolation window of 1.6 m / z, target value of 1 x 106 and maximum injection time of 250 ms. Only precursor ions with charge states between 2 and 4 will be fragmented.

3.2.4.3. Label-free data analysis

For the label-free data analysis, Progenesis QI for Proteomics software (version 3.0 NonLinear Dynamics) was used. The exported peak lists were imported in SearchGUI version 2.5.0 [Vaudel et al., 2011] for the peptide identification with X!Tandem [Craig and Beavis, 2004]. The identification was also done with Mascot 2.4 (Matrix Science). The Uniprot human database downloaded on 22nd of July 2015 was used for the search with trypsin as protease (maximum two miss cleavages), carbamidomethylation at cysteine as fixed modification, oxidation of methionine as variable modifications, 10 ppm as precursor mass tolerance and 0.02 Da as fragment mass tolerance. PeptideShaker [Vaudel et al., 2015] was used to combine search results from X!Tandem and Mascot and filtered at a false discovery rate of 1 %. Only proteins identified with at least two unique peptides were used for further analysis. The average of normalized abundances of the three biological replicates was calculated and the ratio (fold change) between three conditions (compliant 0.1 kPa, intermediate 1 kPa and stiff 10 kPa) to control condition glass was determined. The significance (P-value) was calculated using Student's t-test, two-sided, true variance equality, confidence level at 0.95. Proteins were considered to be differentially regulated, if their P-value was below 0.05 and the fold change was greater than the median fold change value plus twice the standard deviation (up-regulated) or less than the median fold change value minus twice the standard deviation (down-regulated). To generate a heatmap of fold change and the clustering pattern, the R package 'gplots' (version 3.0.1) and the hierarchical clustering function was used.

3.2.5. Ca²⁺ Imaging

- Neurobasal medium
- Fluo-4 AM: 1 μ M
- Wash Buffer: HBSS (Gibco)

All Ca²⁺ imaging experiments were performed in cooperation with Dr. Camilla Fusi (Research Group "Neuroplasticity", Michael Kreutz, LIN Magdeburg). For Ca²⁺ imaging the SP5 CLSM systems (Leica-Microsystems, Germany) equipped with Diode (405 nm), Argon (458, 476, 488, 496, 514 nm laser lines), Diode Pumped Solid State (DPSS, 561nm) and HeNe (633nm) lasers and acousto-optic tunable filters (AOTF) for selection and intensity adaptation of laser lines using LAS AF (Leica Application Suite Advanced Fluorescence) imaging software was used. The Quick Change Chamber 18 mm Low Profile RC-41LP (Warner Instruments) was used for mounting coverslips with living cells in Neurobasal medium on the microscope stage.

Cells were loaded with 1 μ M Fluo-4 AM in NB for 10 min at 37 °C and subsequently imaged. Quantification of spontaneous Ca²⁺ transients was completed using ImageJ software (NIH, <http://rsb.info.nih.gov/ij/>). Fluorescence signals were reported as a ratio ($\Delta F / F_0$)

of the change in fluorescence (ΔF) in a region of interest relative to the baseline fluorescence (F_0). Given a stack of images containing time-lapse images of Ca^{2+} fluorescence and delineate neurons from background, first a fluorescence versus time trace was calculated for each neuron of interest. Neurons of interest were defined as pyramidal neurons and selected morphologically [Csicsvari et al., 1998]. This normalized fluorescence trace ($\Delta F / F_0$) was characterized by a baseline that was periodically interrupted by Ca^{2+} transients of varying amplitude and duration. Since individual transients may have different amplitudes, different durations, occur at irregular intervals, and may be buried in significant noise, for peak detection in a time series, transients with amplitude $< 2 \times$ standard deviation of F_0 were discarded as noise. Detection of peaks, quantified for each ROIs in the time frame between 50 and 250 s, was performed using the ImageJ Find Peaks plug-in.

3.2.6. Statistical analysis

Data are presented as mean \pm standard error of the mean (SEM) for data displaying Gaussian distribution or median values alone. ANOVA tests, one-way analysis of variance and Bonferroni's multiple comparison and Tukey post-test were employed for testing for significant differences. Statistical analysis was performed with Prism version 6 (GraphPad Software, USA). p values, as indicated in detail in the figure legend in the results section, of $p < 0.05$ were considered statistically significant with * : $p < 0.05$; ** : $p < 0.01$; *** : $p < 0.001$.

3.2.7. Software

Table 3.9.: Software used in this study

Used for	programm and software producer
Analysis of grey values and Blot Quantification	Li-Cor ImageStudio Lite Ver. 5.0 ImageJ version 1.48v
Tables and calculations for image analysis	Fiji version 2.0.0-rc-43 / 1.50e
Statistics	Microsoft Excel 2011 for Mac
Image composition	GraphPad Prism version 5.0b
Literature	Adobe InDesign, Adobe Illustrator
Writing	BibDesk version 1.6.11 TeXstudio version 5.6.2

4. Results

4.1. Ageing in a dish

In cell biology, the production and culturing of primary neuronal cells have long been stated as "royal discipline". With the help of well established protocols [Banker and Cowan, 1977], [Cáceres et al., 1986], [Sciarretta and Minichiello, 2010], [Pacifici and Peruzzi, 2012], neuronal cell cultures are now a powerful tool to study and manipulate living neurons. Due to the fact that neurons in a dish are less entangled compared to the intact brain, they can be used to study the dynamics and subcellular localization of proteins.

4.1.1. Long-term culturing of neuronal cells

Routinely, neuronal cells are kept in culture until they reach a mature state, mostly defined around DIV 20, and are then used for a variety of experiments. In most labs, cell culture conditions were optimised to maintain neuronal cells vitality up to this time point and more and more cell death is observed as neuronal cultures get older. In our hands, primary neuronal cultures consisting of neurons and glial cells (mainly astrocytes) survived up to 40 days *in vitro* and displayed a rather two-dimensional cellular ultrastructure using the established protocols mentioned before. Further, glial growth was dominating in the limited space of a coverslip and ultimately neurons were overgrown [Piret et al., 2015].

One main aim of this thesis was to keep neuronal cells alive up to 80 days without the addition of antibiotics and investigate their physiological ageing process. Since this was more complicated than first imagined and could not be achieved by waiting passively for 80 days, cell culture conditions had to be adjusted. After each step-wise adaptation to the culturing protocol, the survival of neuronal cells was inspected visually and signs of cell detachment and cell death were noted.

First, the feeding procedure with 10% media volume was increased from once to twice a week, since evaporation of NB media and the lack of nutrients could be one possible explanation for cell death. Another critical step was to reduce contaminations from microorganisms since infected cells had to be trashed immediately and could not be used for experiments. To prevent contaminations and ensure stable temperature, humidity and CO₂ percentage, neuronal long term cultures were stored in a separate incubator with antimicrobial copper

inlay. Lastly, it is known from the literature that for survival, a dense cellular network is crucial [Pfisterer and Khodosevich, 2017], [Cullen et al., 2010]. In light of this, cell density was increased from 40 K to 100 K neuronal cells for a 12-well plate.

Table 4.1.: Comparing routine cell culture conditions for primary cortical neurons with new established protocol for long-term cell cultures

Routine cell culture conditions	Long-term cell culture conditions
Feeding 1x a week with 10% media vol.	Feeding 2xa week with 10 % media vol.
One incubator for all cell culture users	Incubator solely for long-term cultures
40 K cell density on 12 well plate	100 K cell density on 12 well plate

4.1.2. A suitable senescence marker for neuronal cells

Once cell culture conditions were adjusted to the needs of a long-term neuronal culture, the actual ageing process had to be confirmed using senescent markers known from literature [Sharpless and Sherr, 2015], [Muñoz-Espín and Serrano, 2014]. It is known that finding a specific senescence marker for post-mitotic neurons is especially challenging since most senescence markers are related to cell-cycle arrest, DNA damage or replicative exhaustion [Campisi and d'Adda di Fagagna, 2007], i.e. are indeed suited for actively dividing cells and not for post-mitotic cells such as neurons.

First, γ -H2AX was tested as a biomarker for DNA double-strand breaks, a known hallmark of ageing and senescence [Kuo and Yang, 2008]. Known as a sensitive indicator of double-strand breaks from cancer research and experiments using irradiation to induce DNA damage [Rogakou et al., 2000], increased γ -H2AX expression is expected with age [Xia et al., 2017]. To investigate expression levels of γ -H2AX in ageing neuronal cells, cells were cultured in NB media (see 3.2.4.3) and fixed with 4 % PFA at DIV 20, 40, 60 or 80. Immunostainings of γ -H2AX revealed no distinct increase in expression levels in neurons (MAP2-positive cells) or astroglia (GFAP-positive cells). Since γ -H2AX showed no promising results in neuronal cell culture, the expression of the nuclear lamina protein Lamin B1 was tested next.

Experimental studies pointed out that Lamin B1 decline is a general senescence marker *in vitro* and *in vivo*, whereas expression levels of Lamin A, C and B2 are stable after induced DNA damage in primary human fibroblasts [Freund et al., 2012]. In this study, no decline in Lamin B1 expression could be detected for ageing neuronal cells (Fig. 4.2), leading to the assumption that also Lamin B1 is not a suitable senescence marker for the cell culture system used here or that cells had not reached a senescent phenotype, yet.

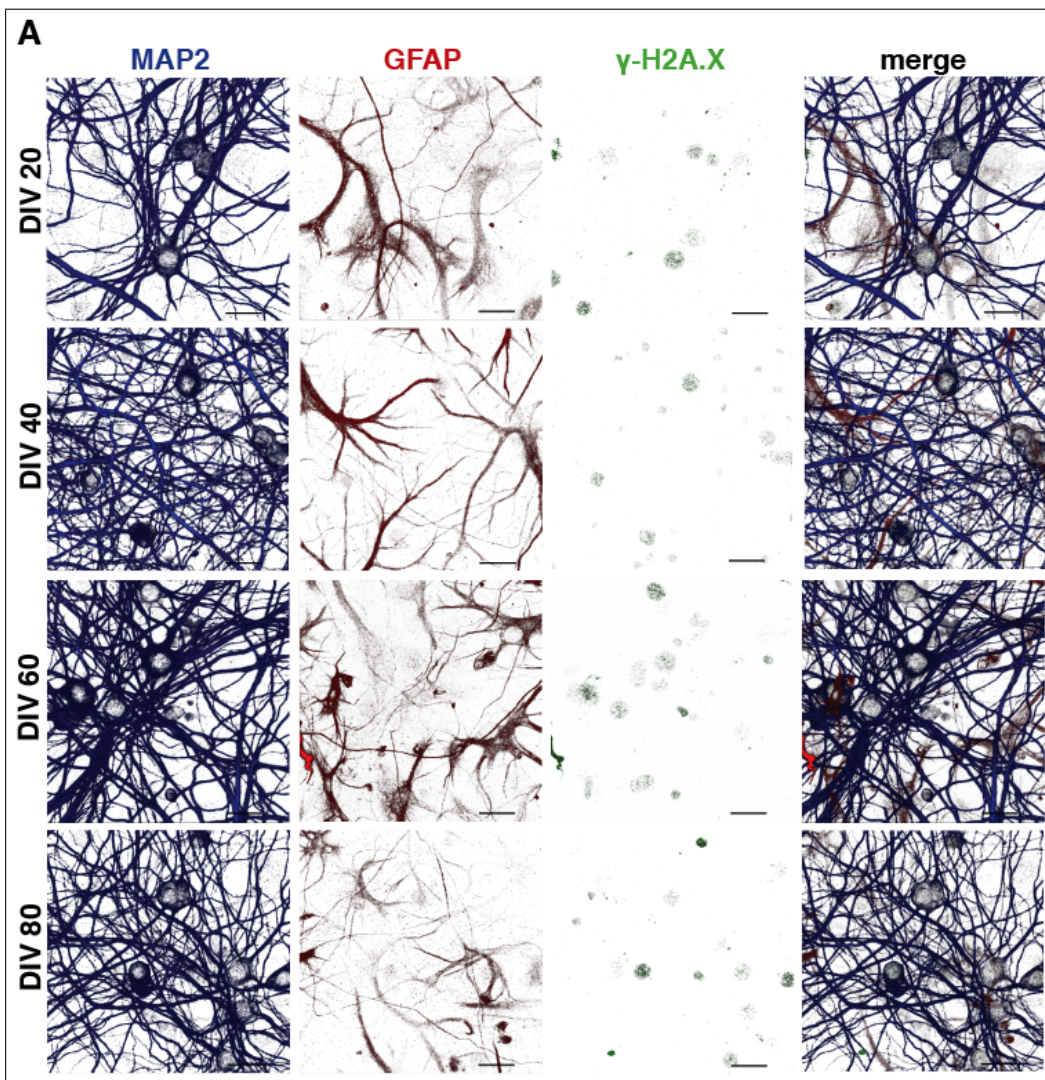


Figure 4.1.: Potential senescence marker γ -H2AX showed no regulation in ageing neuronal cells

(A) Immunostainings were performed at DIV 20, 40, 60 and 80 to monitor the expression of the potential senescence marker γ -H2AX in neurons (MAP2-positive) and astroglia cells (GFAP-positive) during ageing. No remarkable differences in γ -H2AX expression were detected over time. Scale bar: 20 μ m.

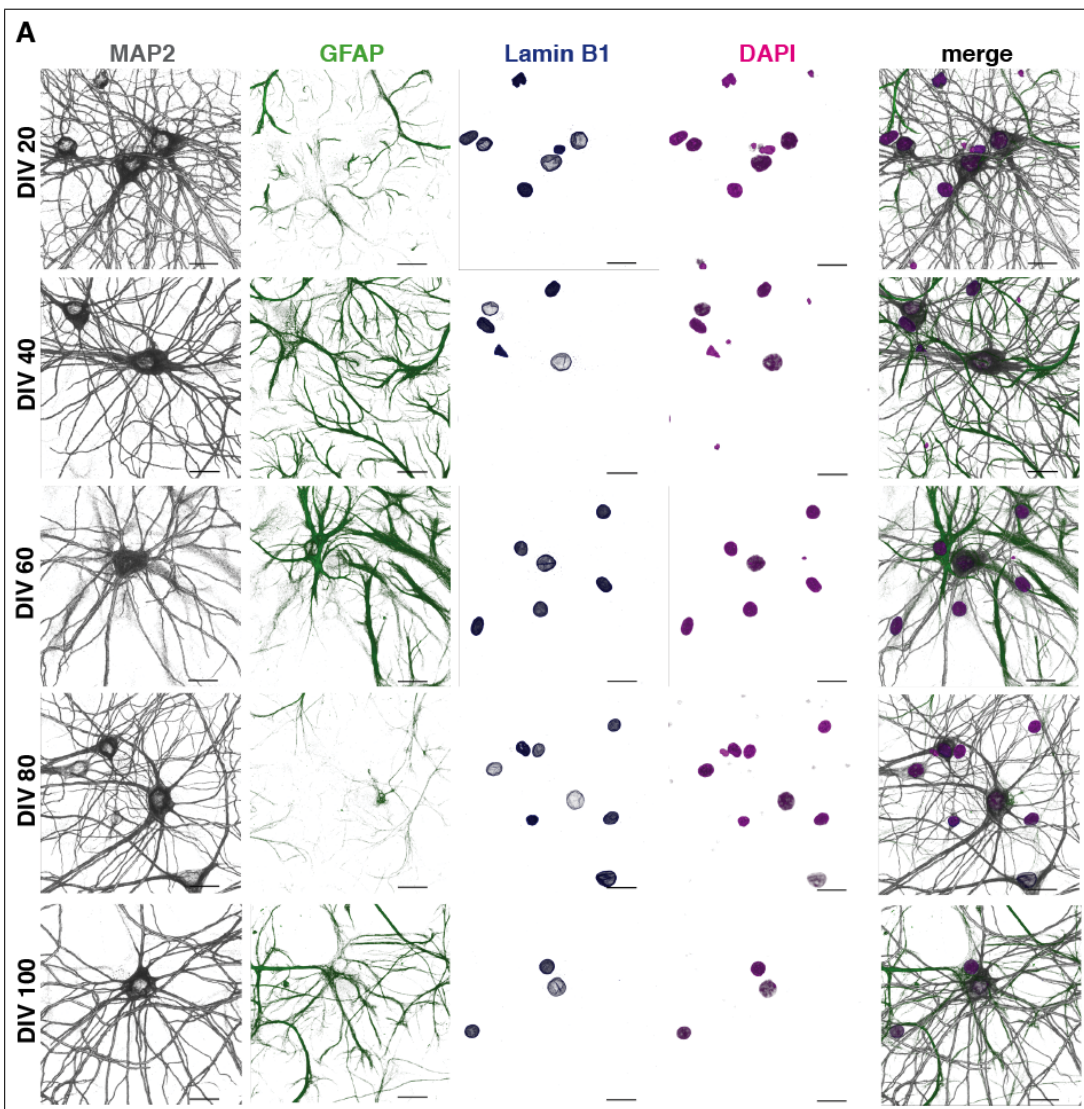


Figure 4.2.: Potential senescence marker Lamin B1 showed no decline in ageing primary neuronal cultures

(A) Immunostainings were used to show the expression levels of the potential senescence marker Lamin B1 in neurons and astroglia cells at DIV 20, 40, 60, 80 and 100. DAPI staining showed cellular nuclei. No remarkable decline in Lamin B1 expression was seen as cell age. Note that clear cut nuclear lamina outlines were shown. Scale bar: 20 μ m.

As described in the Introduction (2.1.1.), disturbed protein homoeostasis is one factor of the ageing process. Following this idea, SQSTM1 / p62, an autophagosome cargo protein that marks proteins for autophagy, was tested as a potential senescence marker. Numerous studies showed that p62 co-localizes with ubiquitin-positive protein complexes and facilitates protein degradation by binding to autophagy regulators [Bjørkøy et al., 2006], [Knaevelsrød and Simonsen, 2010]. Here, p62 was used as marker for intracellular protein aggregates since it binds proteins that are tagged for degradation [Sakuma et al., 2015],

[Bitto et al., 2014]. It is known that neurons are among the most vulnerable cell types in age-related aggregate formation [Lim and Yue, 2015], presumably because of their complex structure including fine protrusions and the fact that they are post-mitotic cells and can not be replaced, especially as a large, functionally integrated population [Valiente-Gabioud et al., 2016]. When autophagy is disturbed, p62-containing aggregates become bigger and ultimately proteotoxic stress is harmful to neurons [Komatsu et al., 2007], [Lim et al., 2015]).

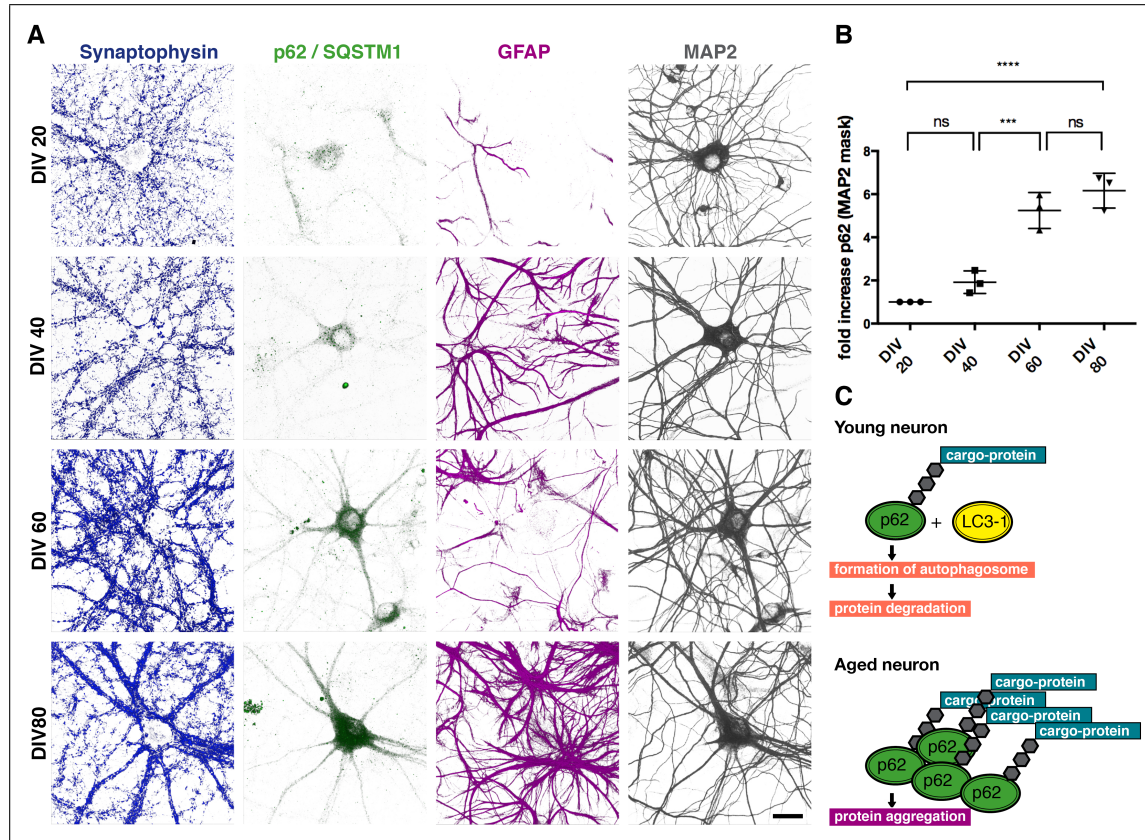


Figure 4.3.: p62-positive protein aggregates formed in ageing neurons

(A) Investigating neuronal cell cultures from DIV 20 to 80, a clear increase in p62-positive protein aggregates was visualised using immunocytochemistry. Especially in neurons, the cell soma and protrusions were filled with protein aggregates at later time point investigated, whereas astroglia cells appear less prone to protein aggregation. For visualisation of the presynapse, Synaptophysin was used. Scale bar: 20 μ m. (B) Quantification of p62-positive puncta inside a MAP2 mask revealed a gradual and up to 6-fold increase of protein aggregates comparing young and old cells. N = 3 independent experiments, with 10 neurons per group, assessed by one-way ANOVA with Tukey post-test. (C) The Illustration shows schematically how autophagosome formation and protein degradation is handled in a young neuron, whereas aged neurons are vulnerable to the formation of protein aggregates.

In our experiments, neuronal cells were again cultured up to DIV 80 in NB medium and probed for p62-positive protein aggregates at DIV 20, 40, 60 and 80 by immunocytochemistry. A clear, significant and gradual increase in p62-positive protein aggregates was detected in neurons ageing from DIV 20 to DIV 80. Whereas at DIV 20 only a small portion of intracel-

lular proteins is marked for degradation, already at DIV 40 p62-positive aggregates increase.

At DIV 80 the whole soma and a remarkable part of dendritic protrusions are crowded with p62-labelled, misfolded or dysfunctional proteins. Note that astroglial cells were less prone to build up p62-positive aggregates and MAP2 signal intensity, as well as Synaptophysin expression, appears stable for all time points tested (Fig 4.3, A). Quantification of the p62-immunopositive area was performed inside a MAP2 mask to outline the neuronal structure. A gradual increase in p62-immunopositive area was revealed ranging from 2-fold at DIV 40, 5-fold at DIV 60 and to up to 6-fold at DIV 80 compared to mature neurons at DIV 20, suggesting a mechanistic link between ageing and protein aggregation (Fig 4.3, B). A schematic drawing helps to understand the link between p62-accumulation and protein aggregation: in a young neuron, a protein is marked for degradation (cargo-protein) by p62-binding and together with LC3-1 and other effector proteins the formation of the autophagosome is initiated (Fig 4.3, C). In an aged neuron deficit in autophagosome formation and other degradation pathways lead to the accumulation of p62-marked proteins and overtime to increase protein aggregation. Concluding from these results and literature findings, p62 was used as a senescence marker for ongoing experiments and DIV 80, or at some points, DIV 100 was used as the latest time point of investigations.

4.1.3. Deficits in proteostasis in aged neurons

In light of the described defects in proteostasis, *de novo* protein synthesis capacities were investigated next in neurons at different ages. To visualize newly synthesised proteins, the FUNCAT method was used (see 3.2.3.8). In short, the non-canonical amino acid AHA was incorporated as a surrogate for methionine into the nascent polypeptide chain of newly synthesised proteins. Utilizing click chemistry, the azide group of AHA was subsequently tagged with the TAMRA fluorophore of the alkyne tag to visualize protein synthesis capacities. The fluorescent signal of the TAMRA tag can be detected with conventional microscopy and cellular or even synaptic structures were detected by immunocytochemistry and appropriate synaptic and dendritic markers.

In this experimental setup, cortical neuronal cultures of different ages (DIV 20, 40, 60, 80) were labelled with AHA for 3 h in methionine-free medium (Hibernate) and fixated directly afterwards. Immunostaining was performed to outline the neuronal structure (MAP2) and the presynapse (Synaptophysin).

As demonstrated by the decrease in TAMRA signal intensity, *de novo* protein synthesis is reduced as neurons age. In young neurons, a high quantity of newly built proteins is visualised in the soma and even in distal dendrites. In contrast, as neurons age, fewer proteins were produced during the investigated time frame in dendrite and soma (Fig 4.4, A). To have a better visualisation of the described effect, dendrites were straightened (Fig 4.4, B).

Quantification of TAMRA signal intensity inside a MAP2 mask demonstrates a significant decrease in protein synthesis activity in aged neurons (Fig 4.4, C).

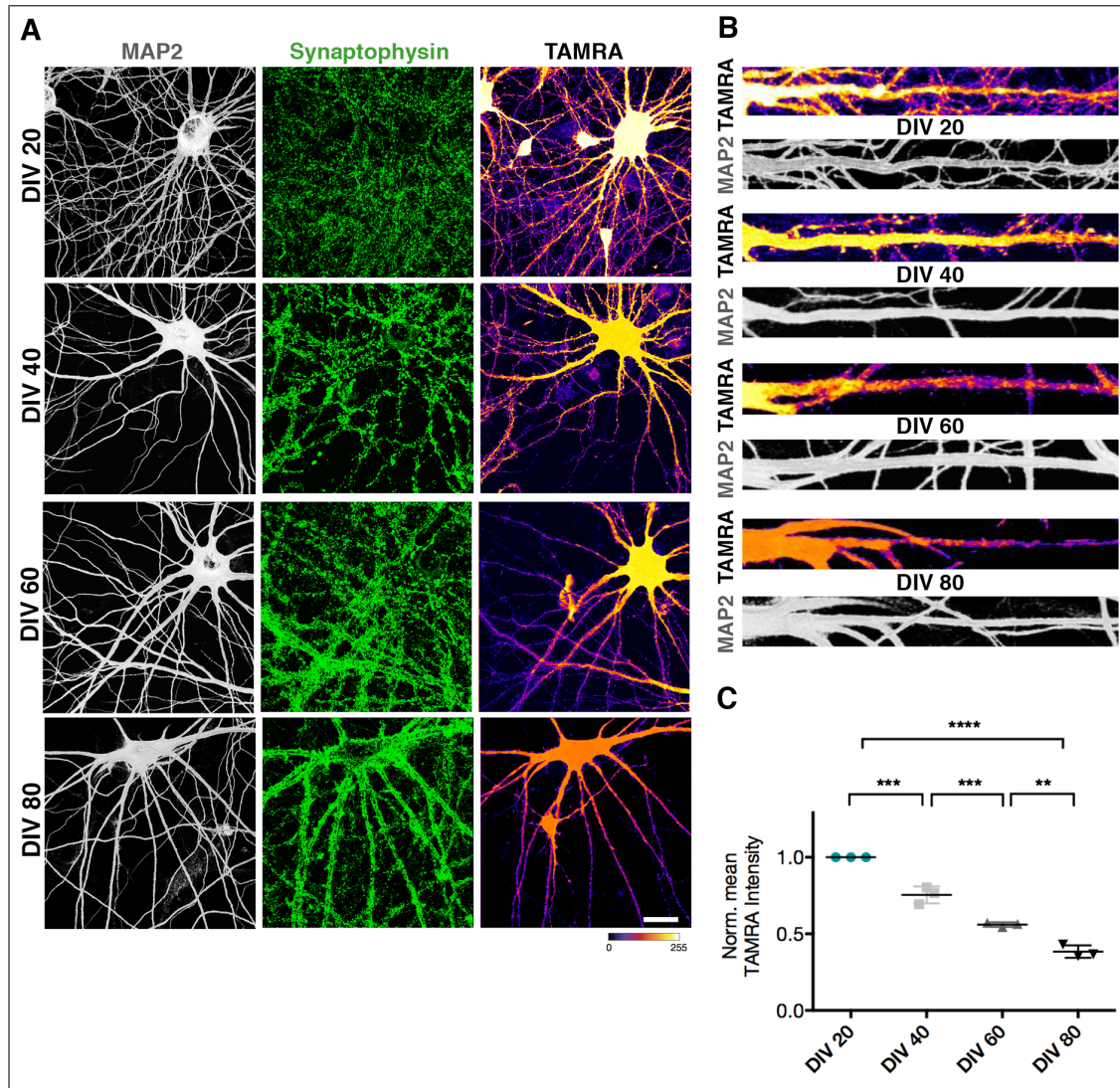


Figure 4.4.: *De novo* protein synthesis is decreasing in ageing neurons

(A) Primary cortical neurons were labelled with the non-canonical amino acid AHA for 3 h in Hibernation medium at different time points in their development (DIV 20, 40, 60 or 80). Proteins, newly synthesised during this 3 h time period, were visualised via click-chemistry using the FUNCAT technique (see TAMRA signal). The neuronal structure was stained using immunocytochemistry against MAP2 and the presynapse was visualised analogously with Synaptophysin. Scale bar: 20 μ m. (B) The main dendrite of single neurons was straightened to visualize the distribution of newly synthesised proteins in more detail. MAP2 is shown to outline the neuronal structure. (C) Quantification of normalised TAMRA signal states a significant decrease in *de novo* protein synthesis as neurons age. MAP2 is used as a mask for neuronal structure. (N = 3 independent experiments, with 10 neurons per group, F = 169.9, ****P < 0,0001, ***P = 0,0006, **P = 0,0012, assessed by one-way ANOVA with Tukey post-test.)

Besides *de novo* protein synthesis, FUNCAT can be also used to measure protein degradation inspired by classical pulse-chase experiments [Takahashi and Ono, 2003], [Cohen et al., 2013]. Here, AHA incorporation was performed for 3 h in Hibernate medium without methionine and subsequently neuronal cultures were incubated with their previously-used NB medium containing methionine and no AHA.

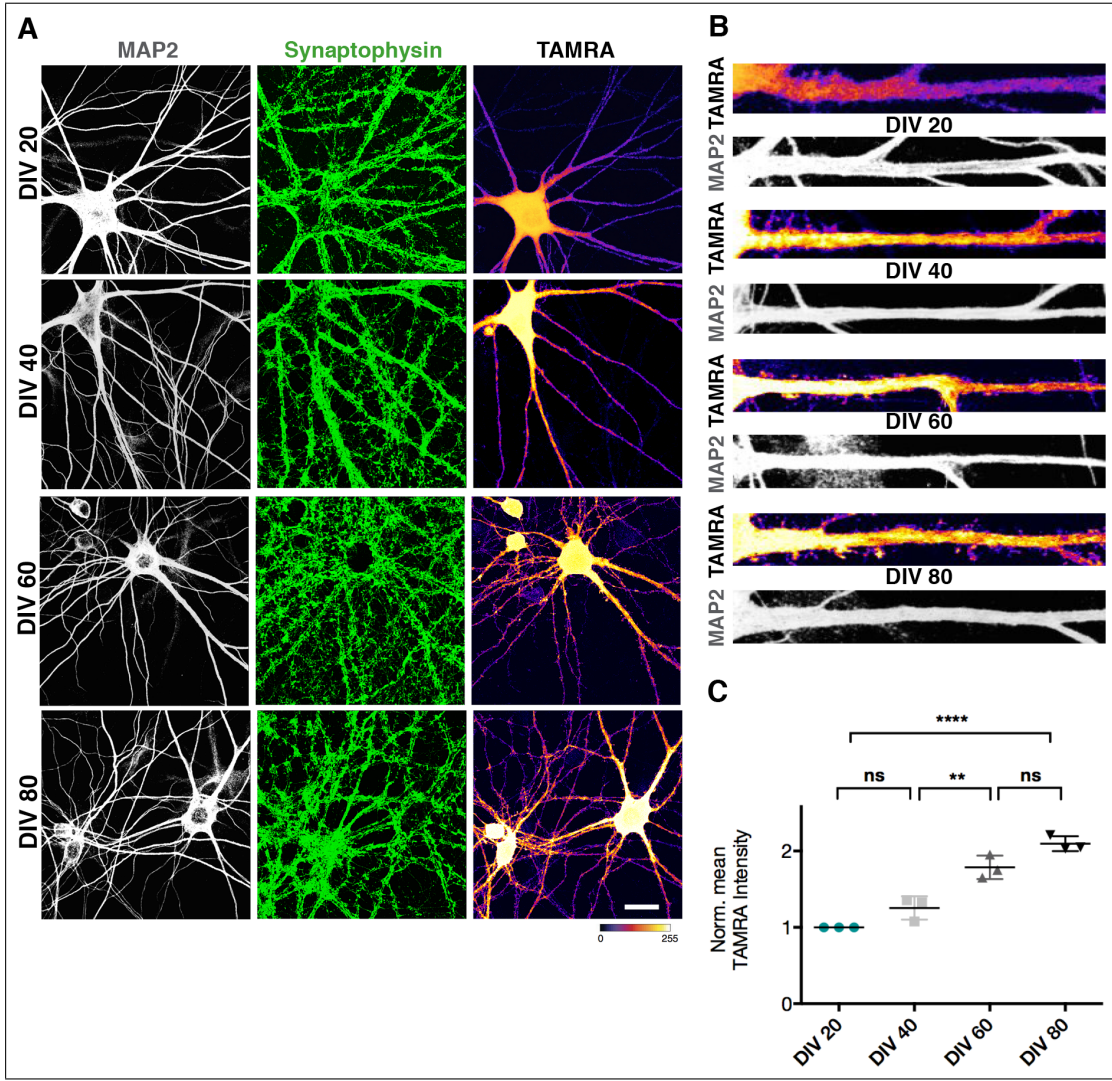


Figure 4.5.: Protein degradation was slowed down in ageing neurons

(A) Primary cortical neurons were labelled for 3 h with AHA and subsequently chased with Methionine containing medium for 3 h. This experimental setup allows to monitor the degradation of AHA-containing proteins at different time points (DIV 20 to DIV 80, see TAMRA signal). To assess neuronal and synaptic shape, immunocytochemistry for MAP2 and Synaptophysin was performed. Scale bar: 20 μ m. (B) To show the location of non-degraded AHA-positive proteins, the main neuronal dendrites were straightened. (C) Quantification of normalised TAMRA signal shows a lack of reduction of AHA labelled proteins with increasing age compared to control conditions at DIV 20. ($N = 3$ independent experiments, with 10 neurons per group, $F = 52,61$, **** $P < 0,0001$, *** $P = 0,0002 / 0,0001$, ** $P = 0,0026$, assessed by one-way ANOVA with Tukey post-test.)

This approach allows to monitor how many AHA-labelled proteins remain over a defined time point (chase time: 3 h) and insights into degradation dynamics are given. Again cells were investigated at the age of DIV 20 to DIV 80 and immunostained for MAP2 and Synaptophysin. For young neurons, AHA-labelled proteins were visualised inside the cell soma and in nearby dendritic areas, whereas with increasing age also the intensity of TAMRA-positive probes increases in all cellular compartments (Fig 4.5, A). For better illustration, dendrites were straightened and also here the signal intensities of AHA-labelled proteins were increased inside the soma and at distal dendrites in aged neurons (Fig 4.5, B). A significant increase in TAMRA signal was revealed by quantification (Fig 4.5, C).

Another way to study the dynamics of protein translation is the BONCAT technique (see 3.2.2.2). Similar to the FUNCAT method, a Biotin tag is linked to incorporated AHA by click chemistry. In this experimental pulse-chase setup, primary neuronal cultures ageing from DIV 20 to DIV 60 were labelled for 3 h with the non-canonical amino acid AHA in Hibernate medium to tag newly synthesised proteins. Subsequently, cells were harvested directly after 3 h labelling time (= chase 0 h). Analogous to the FUNCAT experiment in Fig 4.5, one group of cells were incubated with Methionine containing medium for 6 h or 24 h and degradation of AHA-containing proteins was investigated. For each probe, protein amounts were adjusted to 10 µg prior to loading. For better quantification of biotin signal intensity, a Dot Blot analysis of the same probes was performed. As first result, a reduction in protein synthesis capacities was shown in aged cells (see: chase 0 h, Fig 4.6, A, DIV 50, 60), visualised by a weaker biotin signal compared to mature controls (DIV 20). At later time points (DIV 50 or 60), additionally a slowed protein degradation rate is seen, fitting to previous results (see: chase 6 h, 24 h, Fig 4.6, A).

Taken together, we can conclude that protein turnover is slowed down in ageing neurons like it was reported before in literature with other experimental approaches [Mitra et al., 2009], [Toyama and Hetzer, 2013]. With the sister methods FUNCAT and BONCAT we were able to directly visualize the decline in protein synthesis and -degradation in a cellular context and on Western Blot level.

To further clarify a potential dysregulation of translational pathways in neuronal ageing, the expression profile of key regulator proteins was probed in lysates of primary cortical cells using Western Blot. For this, primary cortical cells were harvested at different ages (DIV 20 to DIV 60) and protein lysates were analysed with respect to proteins involved in S6 kinase / eEF2 pathway. As loading control a total protein Coomassie staining was used as explained under 3.2.3.5.

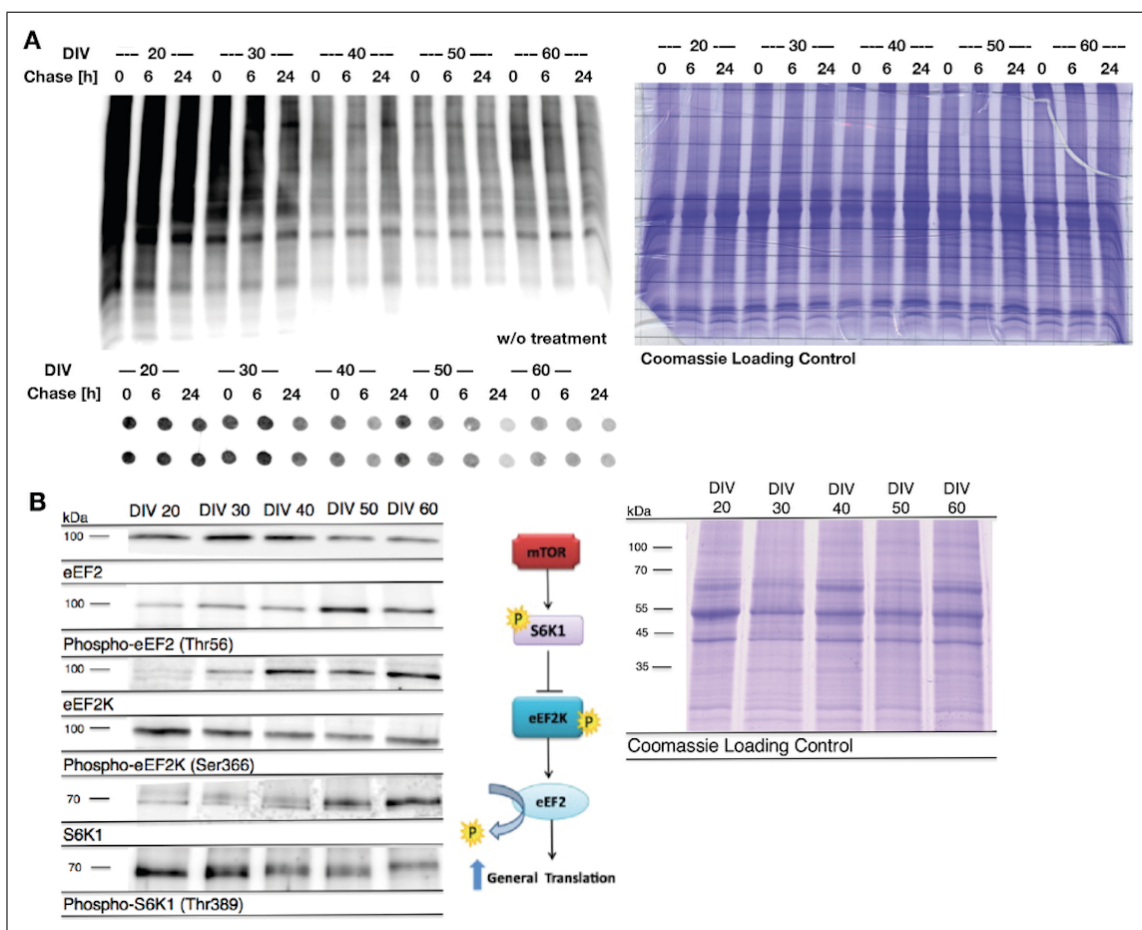


Figure 4.6.: Translational capacities declined in aged neuronal cells

(A) BONCAT pulse-chase experiments with 0 h, 6 h or 24 h chase time. Neuronal cultures were labelled for 3 h with AHA at different age (DIV 20 to DIV 60) and further coupled to biotin tag via click reaction. A reduction in protein synthesis and -degradation is seen in aged cells. 10 µg of protein lysates were loaded for Dot blot for evaluation of the biotin signal. Coomassie Loading control representing the total protein amount for each sample analysed. Coomassie Loading control was used for normalisation and to load equal protein amounts for each sample, since recent studies suggest that total protein amount visualized by Coomassie is a more robust and reliable loading control [Welinder and Ekblad, 2011], [Eaton et al., 2013], [Faden et al., 2016], [Nie et al., 2017]. The signal intensity for each protein lane was quantified using ImageJ. The signal intensities were normalized and a new loading volume for each sample was calculated based on these results. The cross-pattern in background of the Coomassie gel is caused by the checked paper of the lab book. (B) Phosphorylation pattern of key regulators in the S6 kinase / eEF2 pathway is shifted to less translational activity in aged neuronal cells analysed by Western Blot. Graphical illustration of S6 kinase / eEF2 pathway adapted from: [Taha et al., 2013]. Again, a Coomassie Loading control representing the total protein amount for each sample was used as loading control to ensure that the same amount of protein concentration is loaded.

Originating from the mTOR signalling pathway, S6 kinase is one of the most conserved modulators of ageing and essential for translational regulation. The S6 kinase is activated by a complex multi phosphorylation pattern. Here, we concentrate on the phosphorylation site

at Thr389 activated by mTOR since it is most critical for kinase function [Moser et al., 1997], [Pullen and Thomas, 1997].

As cells age from DIV 20 to DIV 60, a clear reduction of phospho-S6 kinase (Thr389) was revealed, whereas the expression of unphosphorylated S6 kinase is increasing (Fig. 4.6, B). From the four known targets of S6 kinase, eEF2K was highlighted to control protein translation and cellular lifespan [Richardson et al., 2004], [Hernández et al., 2004]. When phosphorylated at Ser366, eEF2K is inactivated [Wang et al., 2001], which in turn promotes the dephosphorylation of eEF2, and thus accelerates translation. In our experiments, less phospho-eEF2K (Ser366) was seen at aged state and in line with this, also the inactive phospho-eEF2 (Thr56) accumulates. Taken together, this complex pathway is shifted towards a general decline in translational activity, supporting previous results presented here.

4.1.4. Polyamines as an anti-ageing therapy?

As a next goal, potential anti-ageing reagents known from literature [de Cabo et al., 2014], [Longo et al., 2015] were tested in their capability to restore protein synthesis and -degradation rates to a juvenile level. This testing was done as a subproject in cooperation with Eric Hoehne and was summarized in his Bachelors Thesis. From the group of reagents we tested, the polyamine Spermidine showed the most promising effects in preliminary experiments not mentioned here and was thereby chosen to be investigated in more detail. Spermidine was applied for 3 h at a concentration of 50 μ M to mature (DIV 20) or aged (DIV 60) neuronal cells. After incubation with Spermidine, cells were washed once with HBSS, harvested and protein lysates for subsequent Western Blot analysis were prepared.

Applying Spermidine for 3 h restored the expression levels of the translational effectors eEF2 and eIF5A in aged cultures back to those observed in young cultures. (Fig 4.7, A). Also, the ribosomal protein Rpl10a showed an increased expression in old cultures after treatment with Spermidine. Following the hypothesis that the pro-translational effects of Spermidine were partly a result of the relation to the Eukaryotic Translation Initiation Factor 5A (eIF5A), the same Western Blot analysis was repeated with Hypusine treatment, a metabolite of Spermidine, essential for eIF5A function. For a better understanding of this rather unknown biosynthesis pathway, the following graphic will illustrate how Spermidine is added to eIF5A and thereby converted to the amino acid Hypusine (see Fig. 4.8). This process takes place as a post-translational modification at Lysine 50 of eIF5A [Martinez-Rocha et al., 2016].

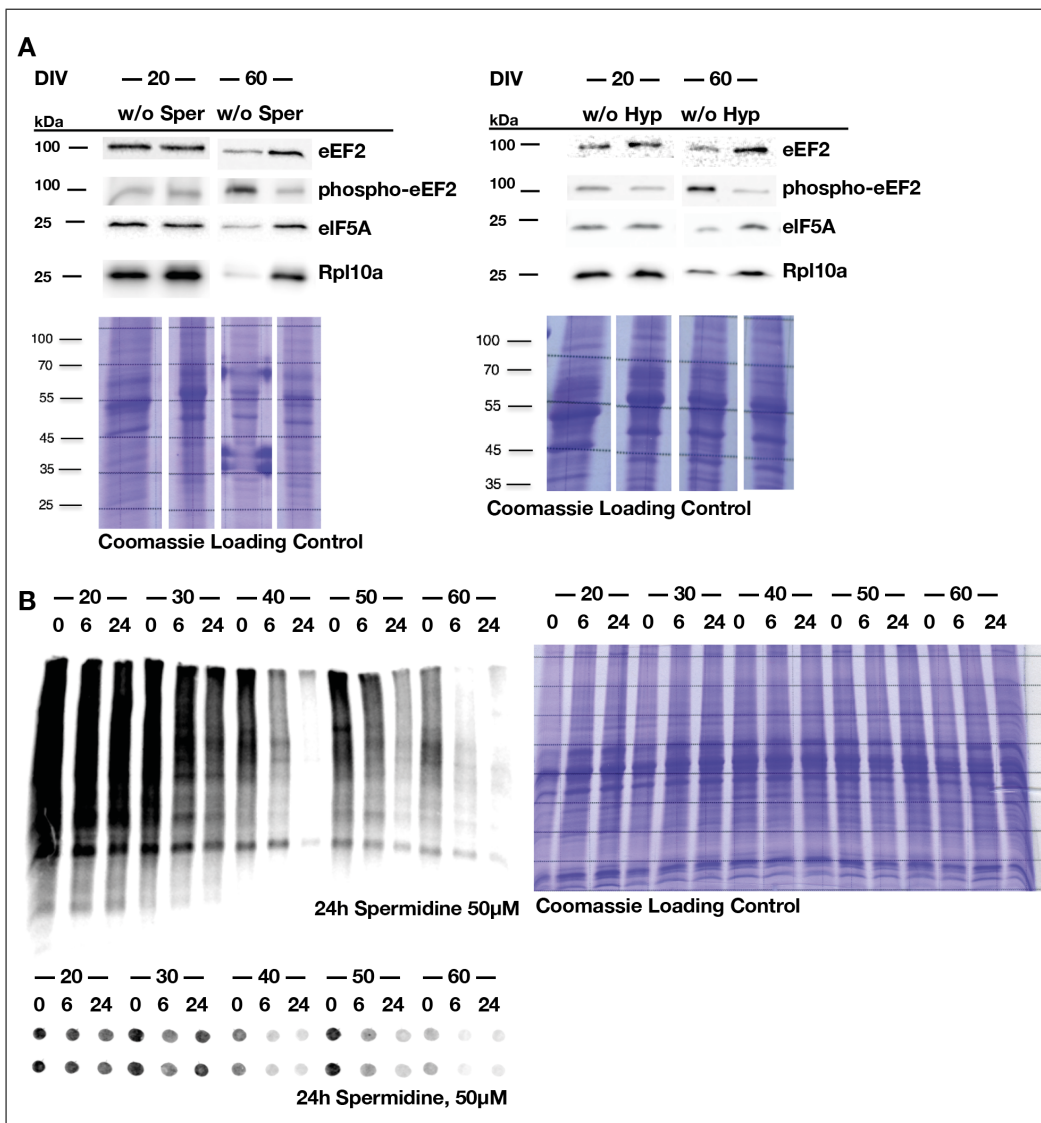


Figure 4.7.: Translational capacities declined in aged neuronal cells and are potentially restored by polyamine signaling

(A) Expression levels of activators of protein translation such as eEF2, eIF5A and Rpl10a were replenished after 3h Spermidine or Hypusine application. In contrast, the expression of the translational repressor phospho-eEF2 was reduced after Spermidine and Hypusine treatment to levels seen in young but mature cells. Coomassie Loading control representing the total protein amount for each sample analysed. For both experiments, Coomassie Loading control was used for normalisation and to load equal protein amounts for each sample, since recent studies suggest that total protein amount visualized by Coomassie is a more robust and reliable loading control [Welinder and Ekblad, 2011], [Eaton et al., 2013], [Faden et al., 2016], [Nie et al., 2017]. The signal intensity for each protein lane was quantified using ImageJ. The signal intensities were normalized and a new loading volume for each sample was calculated based on these results. Due to technical replication, the lanes of the Coomassie staining have a different order than the presented Western Blots. The cross-pattern in background of the Coomassie gel is caused by the checked paper of the lab book. (B) Spermidine treatment 24 h before BONCAT pulse-chase experiment with 0 h, 6 h, or 24 h chase time accelerates protein degradation in aged neuronal cells. Coomassie Loading control representing the total protein amount for each sample analysed. Also here, Coomassie Loading control was used for normalisation and to load equal protein amounts for each sample. The cross-pattern in background of the Coomassie gel is caused by the checked paper of the lab book.

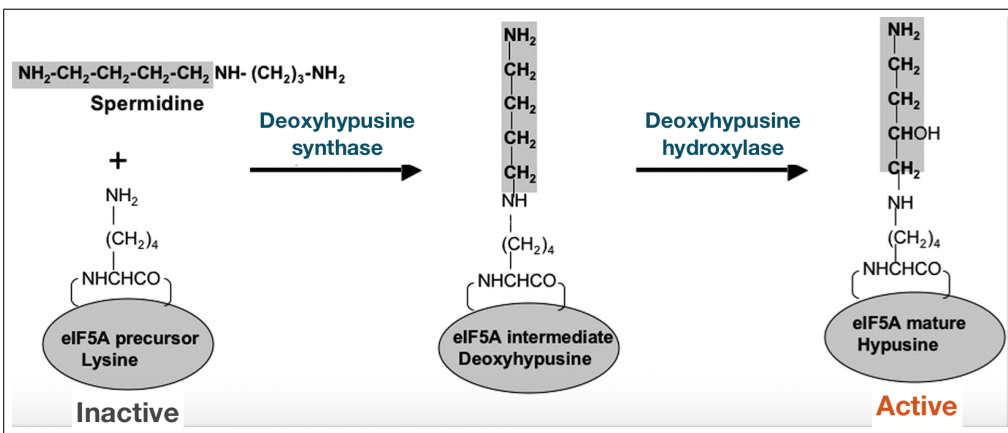


Figure 4.8.: Biosynthesis of mature, hypusinated eIF5A

Besides various functions in cellular survival, Spermidine serves as donor for the unique hypusine modification of eIF5A. The process of modification is divided into two parts: First, Deoxyhypusine synthase covalently attaches Spermidine to a lysine residue of eIF5A to form the intermediate eIF5A Deoxyhypusine. In a second step, deoxyhypusine hydroxylase modifies the intermediate to the functionally active, hypusinated eIF5A. Figure adapted from: [Chattopadhyay et al., 2008].

As a result, the same tendency towards a translational activation described for short-term Spermidine application was seen after Hypusine treatment in aged neuronal cells (Fig 4.7, A). The expression levels of eEF2, eIF5A and Rpl10a in aged cells were restored after Hypusine treatment to levels seen in mature, but not aged neuronal cultures, pointing to pro-translational effects of the unusual amino acid Hypusine [Saini et al., 2009]. To verify that Spermidine application results also in accelerated protein turnover capacities in aged cells, the BONCAT experimental setup from Fig. 4.6 A was repeated with 24 h Spermidine treatment ($50 \mu\text{M}$) *a priori* AHA incubation. Compared to a control situation in Fig. 4.6 A, a clear increase in protein degradation is seen in probes with 6, 24 h chase time at aged time points (DIV 50 and DIV 60, Fig 4.7, B).

As discussed in Fig. 4.3, p62-positive protein aggregates built up in ageing neurons probably due to deficits in protein degradation. Therefore, we checked whether Spermidine is capable to resolve those aggregates in mammalian neurons by activation of autophagy. These effect of Spermidine is known from studies in *Drosophila* [Gupta et al., 2013]. As a marker for autophagic vesicles we used antibodies against LC3 A / B and p62 / SQSTM1 [Pankiv et al., 2007]. For a better understanding of the processes in autophagic degradation of proteins, a graphic illustration is provided (Fig 4.9, C), depicting the interaction between LC3 and the adaptor protein p62 in autophagosome formation [Tyedmers et al., 2010]. LC3 shares structural features with ubiquitin and is essential in autophagy substrate selection and regulates membrane fusion of the autophagosomes. The exact temporal coordination of these complex events during autophagy remains unknown.

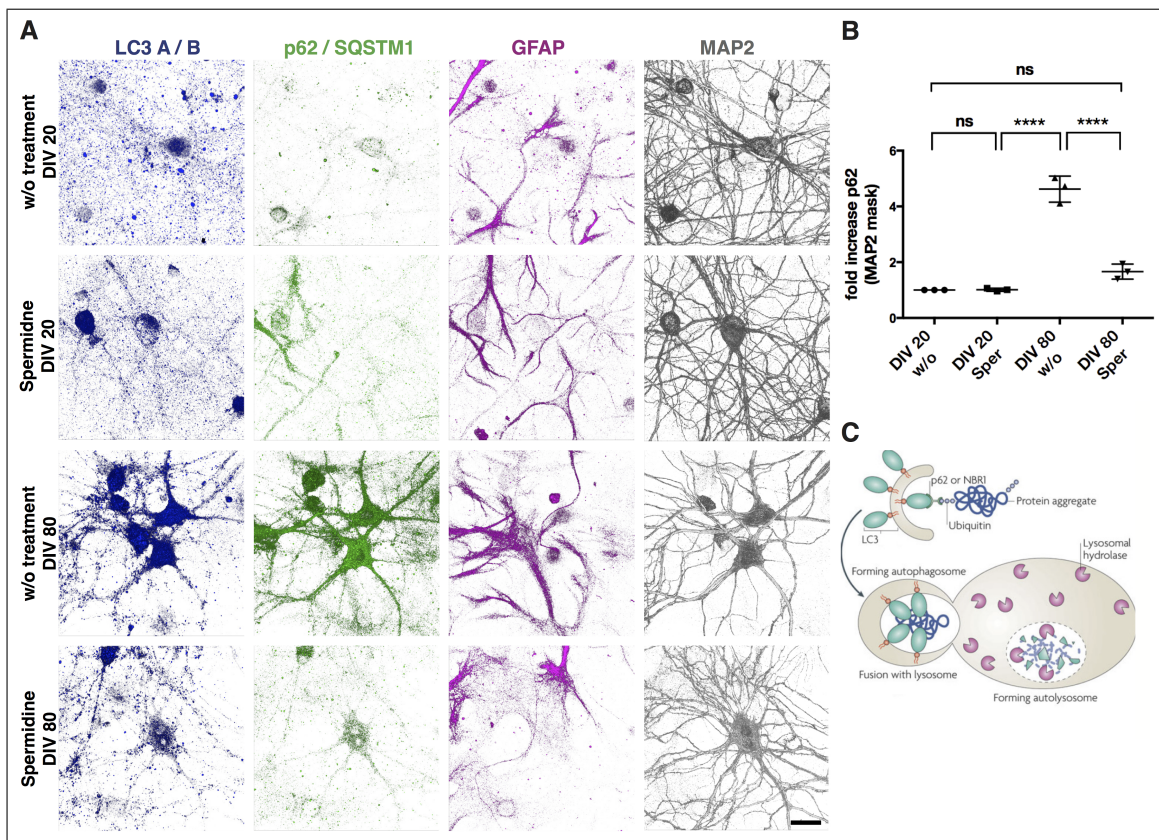


Figure 4.9.: p62-positive protein aggregates were resolved by the polyamine Spermidine (A) Immunostaining of the autophagic effector protein LC3 A/B, p62/SQSTM1 and the cell type marker GFAP and MAP2 revealed an increase in p62-positive area co-localised with neurons. Treatment with 50 μ M Spermidine for 24 h reduced p62-positive protein aggregate load at DIV 80, whereas no effects were seen in young cultures (DIV 20). Scale bar: 20 μ m. (B) Quantification highlights an up to 5 fold increase of p62-positive protein aggregates inside a MAP2 mask. Spermidine application reduces p62 area to juvenile levels. (N = 3 independent experiments, with 10 neurons per group, assessed by one-way ANOVA with Tukey post-test, F = 121.8, ***P < 0,0001, ns = not significant (C) Illustration explaining the interaction between LC3 A/B and p62 and their role in autophagic vesicle formation. Adapted from: [Tyedmers et al., 2010])

In our experiments indeed, both LC3 A / B and p62-positive puncta increase in aged neurons (for p62 also shown in Fig 4.3) and 24 h treatment with Spermidine was sufficient to resolve around 50 % of p62-positive protein aggregates accumulated in aged neurons (DIV 80, Fig 4.9, A, B). Note, that Spermidine application had no significant effect on young neurons (DIV 20). For all conditions tested neuronal- and glia structure appears intact. Quantification of the p62-positive area inside neurons revealed again an up to 5-fold increase from DIV 20 to DIV 80, whereas Spermidine application reduced p62 levels to a juvenile state.

To further analyse whether Hypusine or its precursor Spermidine is also able to change dynamics in protein translation a FUNCAT experiment with subsequent immunostaining was

performed in aged cortical cells. Cells were treated with Hypusine (50 μ M) or Spermidine (25 μ M) for 24 h prior to 3h labelling with AHA and compared to control conditions without pharmacological treatment. In control conditions, the solvent of the responding compound was applied solely. Neuronal morphology (MAP2), hypusinated eIF5A levels, and Shank2 expression were visualised by immunostaining (Fig 4.10, A) and analysed as described above. Hypusinated eIF5A levels were increased around 2 fold after treatment with Hypusine or Spermidine, compared to control conditions. Also, a rise in TAMRA signal intensity around 2-fold was detected after Hypusine or Spermidine treatment, pointing to an increased protein translation rate (Fig 4.10, C). For a more detailed visualisation straightened dendrites (Fig 4.10, E) showing newly synthesised proteins also located in dendritic spines for neurons treated with Hypusine or Spermidine.

To prove that Hypusine and its precursor Spermidine act upon eIF5A activity, we used the Spermidine analogue GC7 (10 μ M), which competitively and reversibly inhibits deoxyhypusine synthetase and thereby the hypusination of mature eIF5A [Oliverio et al., 2014]. When incubating with Spermidine (25 μ M) and the DHS blocker GC7, Hypusine levels remain at a basal level, underlining the inhibition of hypusination (Fig 4.10, B). Note, that GC7 treatment diminishes the described increase in TAMRA signal intensity under Spermidine treatment, suggesting a link between hypusination and protein synthesis capacities. Further, increased expression of the postsynaptic density protein Shank2 was revealed in DIV 80 neurons after Hypusine or Spermidine treatment, highlighting the structural and functional plasticity inside the synaptic organization even at an aged phenotype (Fig 4.10, D). Looking into more detailed molecular properties, the scaffolding protein Shank2 harbours multiple proline-enriched stretches and is indeed considered to be a proline-rich protein [Raab et al., 2010]. Interestingly, the translation factor eIF5A was described to promote the translation of such polyproline motifs [Gutierrez et al., 2013]. In general, Shank2 is known as a postsynaptic scaffold protein, coordinating the spatial arrangement of metabotropic glutamate- and NMDA receptors [Boeckers et al., 2002].

Connecting the hypothesis that reduced synthesis of proline-rich proteins leads to deficits in synaptic function during ageing, we wondered whether also synaptic function and especially synaptic vesicle recycling can be rejuvenated by Hypusine or Spermidine treatment. So the same pharmacological treatment from Fig 4.8 was used to perform a Synaptotagmin uptake (see 3.2.4.10) experiment in DIV 80 neuronal cells. Live staining was performed with a fluorescent antibody against the luminal domain of Synaptotagmin, and once taken up by endocytosis, indicating sites of active vesicle recycling in subsequent image analysis. Furthermore, presynapses and neuronal shape were visualised with Synaptophysin and MAP2 immunostaining, respectively. Clearly, Synaptotagmin-positive puncta increase in number and brightness when cells were treated for 24 h with Hypusine or its precursor Spermidine.

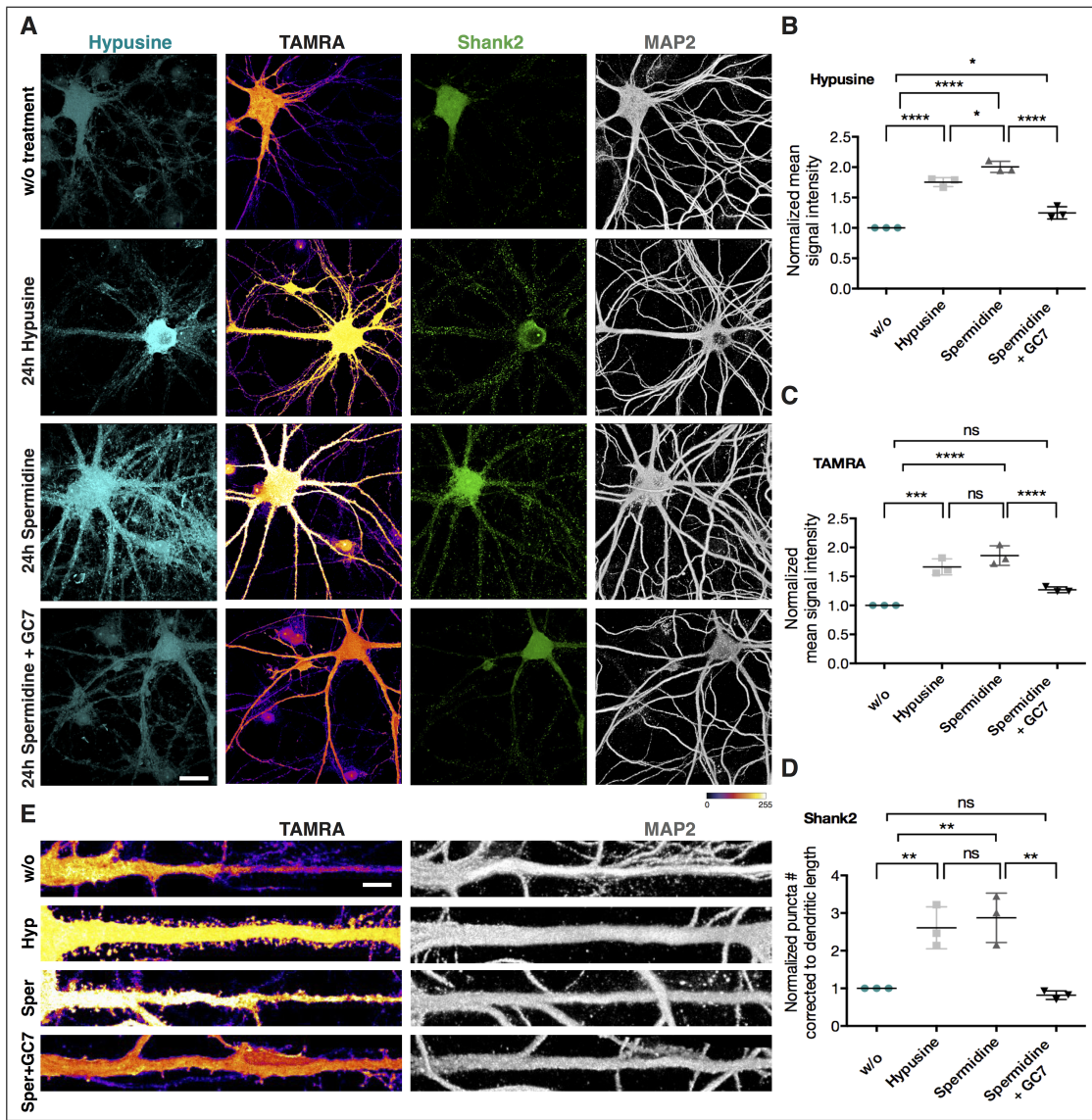


Figure 4.10.: Hypusine and its precursor Spermidine induced *de novo* protein synthesis and Shank2 expression.

(A) Rat primary cortical neurons (DIV 80) were treated with Hypusine (50 μ M), Spermidine (25 μ M) or Spermidine (25 μ M) + the DHS synthase inhibitor GC7 (10 μ M) for 24 h. Hypusine modification, Shank2 expression, and neuronal structure (MAP2) were visualised using immunocytochemistry. The rate of newly synthesised proteins is monitored via FUNCAT (3 h labelling time, see TAMRA signal). Identical confocal settings were used for acquisition of all images, and representative images are shown, scale bar: 20 μ m. (B) Quantification of Hypusine signal depicts significant increase in normalized mean signal intensity in Hypusine and Spermidine treated samples compared to controls. MAP2 is used as mask for neuronal structure. (N = 3 independent experiments, with 10 neurons per group, F = 105.8, ***P < 0,0001, *P = 0,0174 / 0,0186. Data is represented as median, upper / lower quantile and Minimum / Maximum.) (C) Quantification of TAMRA signal depicts significant increase in normalized mean signal intensity in Hypusine and Spermidine treated samples. MAP2 is used as mask for neuronal structure. (F = 35.96, ***P < 0,0001, ***P = 0,0004). (D) Quantification of Shank2 positive puncta depicts significant increase in normalized mean signal intensity in Hypusine and Spermidine treated samples. Corrected for dendritic length. (F = 18.12, **P = 0,0033 / 0,0084 assessed by one-way ANOVA with Tukey post-test). (E) FUNCAT signal of representative straightened dendrites of neurons treated with Hypusine, Spermidine or Spermidine + GC7 for 24 h. Scale bar: 5 μ m.

Blocking the conversion of Spermidine to Hypusine with GC7 brought Synaptotagmin puncta back to a level comparable to control conditions in aged neurons (Fig 4.11, A, C). Note that Synaptophysin expression appears alike between all conditions tested, pointing to structural stable synapses with a slowed down vesicle release probability [Kober et al., 2016].

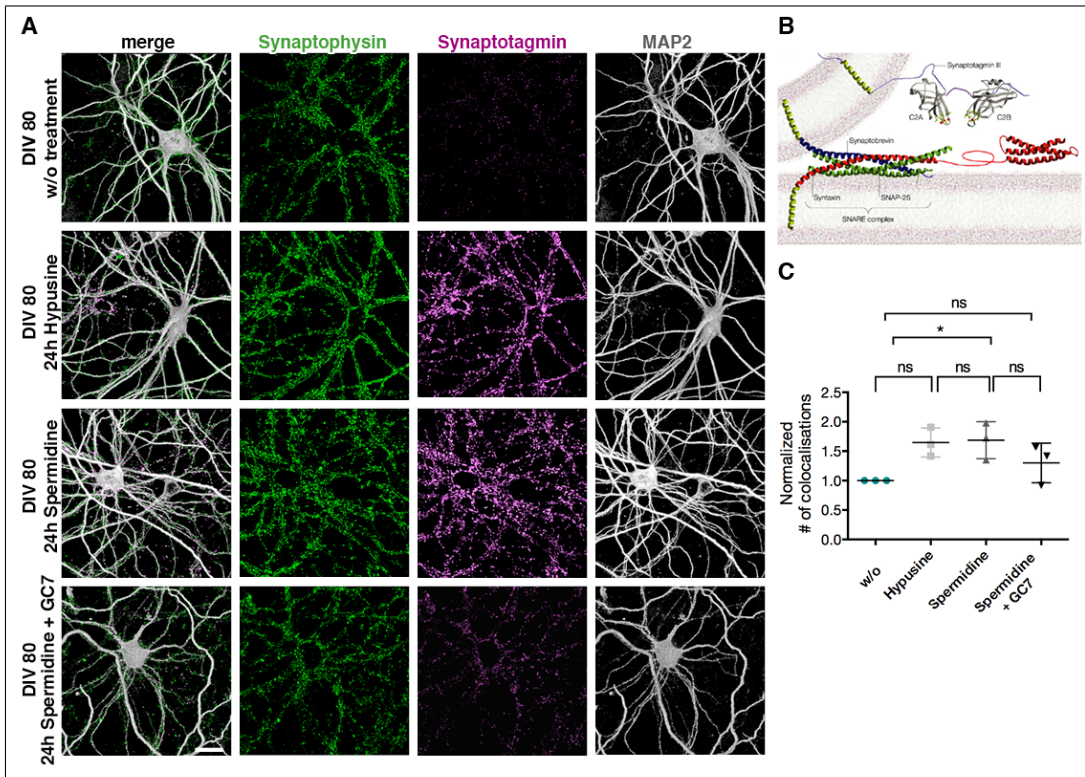


Figure 4.11.: Synaptic vesicle recycling was slowed down in aged neurons and can be increased by Hypusine or Spermidine treatment

(A) Live staining with an antibody against the luminal domain of Synaptotagmin-1 coupled to Alexa488 was performed in neuronal cultures *in vivo* for 30 min with subsequent immunostaining for the presynapse (Synaptophysin) and the neuronal structure (MAP2). Note the increase in immunopositive puncta for Synaptotagmin when aged cells were treated with Hypusine or Spermidine for 24h prior to the live labelling with Synaptotagmin-1 antibody, whereas blocking the conversion from Spermidine to Hypusine showed no effect compared to control conditions. Expression of Synaptophysin appears stable across all conditions tested. (B) Graphic illustration of the synaptic vesicle release machinery depicting the binding site of the luminal Synaptotagmin-1 antibody [Chapman, 2002]. (C) Quantification of Synaptophysin and Synaptotagmin colocalisation showed a significant increase in Synaptotagmin-positive released vesicles when aged neurons were treated with Spermidine. ($F = 4.576$, $*P < 0.0490$, ns = not significant, assessed by one-way ANOVA with Tukey post-test)

To further prove that Hypusine application increases eIF5A activity and thereby global translational elongation and termination [Schuller et al., 2017], a polysome profiling experiment was performed together with Dr. Felix Mertin [Hanebuth et al., 2016]. In general, polysome profiling is a technique to describe the translational status of a cellular population at a specific time point and thereby quantify the subset of actively translated mRNAs. To

identify, whether ageing as an effect on the proportion of polysomes, representing the actively translating complex, primary cortical cells were grown until DIV 60 and compared to young control cells (DIV20).

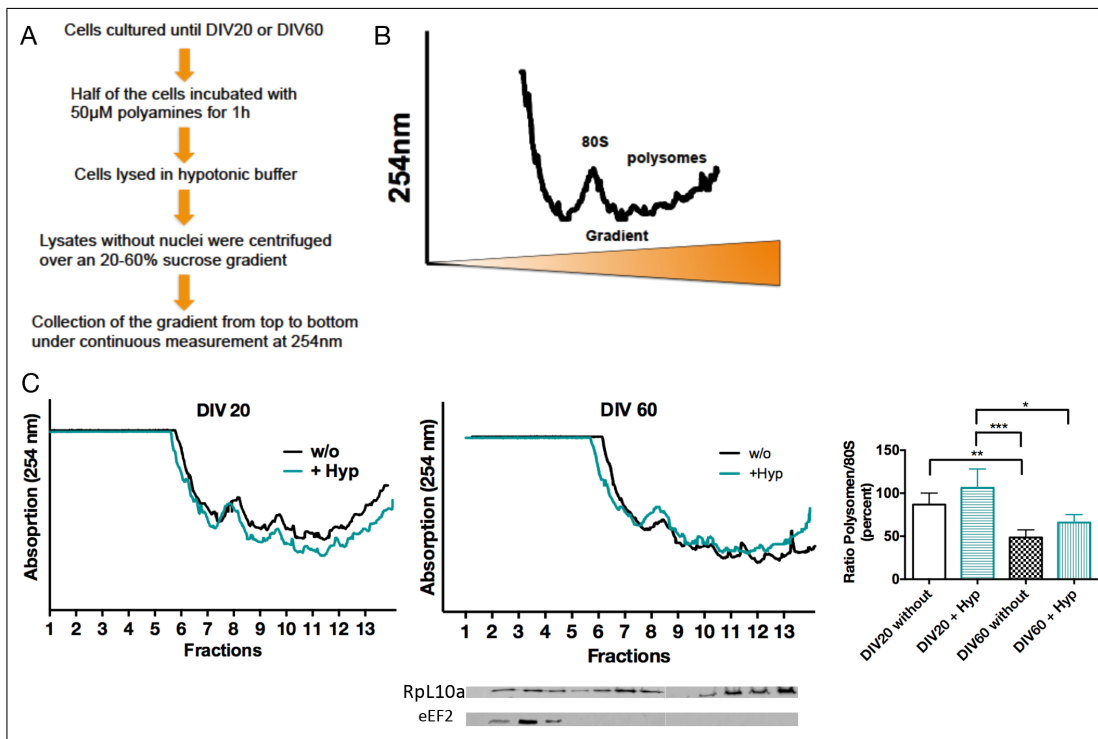


Figure 4.12.: Polysome profiles differ between young and old neuronal cultures and short Hypusine application rejuvenates polysome profiles in aged cultures

(A) Workflow of polysome profiling especially optimised for primary neuronal cells. Note the hypotonic conditions applied. (B) Example polysome profile is depicted for better understandability of the experimental results: After cell lysates were fractionated over 20 to 60 % sucrose gradient, amount of mRNA was measured at 254 nm and a characteristic profile is revealed. (C) Polysome profiles measured at 254 nm from primary cortical cultures harvested at DIV 20 or DIV 60, respectively. Besides control conditions (black graph), one set of cells was treated with 50 µM Hypusine for 3 h before profiling experiment (see green graph). Polysome profiles were quantified by comparing the area under the curve (AUC) for the polysome peaks relative to the 80 S peak. A significant reduction in polysome abundance was recorded for aged neuronal cultures. This trend was rescued by Hypusine treatment and an increase in the number of polysomes was seen. Western Blot analysis of translational markers revealed a characteristic distribution of the ribosomal protein Rpl10a and the translational regulator eEF2 along the separated fractions. Rpl10a is enriched at ribosomal peak and at polysome fractions, whereas eEF2 is mainly detected insoluble fractions [Hanebuth et al., 2016]. ($F = 11.47$, * $P < 0.0465$, ** $P < 0.0024$, *** $P = 0.0001$, assessed by one-way ANOVA with Bartlett's test and Bonferroni's Multiple Comparison Test, $n = 6$)

For both time points, one sample was treated for 3 h with Hypusine (50 µ M) and the second sample was handled as a control condition. Cells were lysed in a specifically designed hypotonic buffer to restore the integrity of polysomes (see 3.2.2.7). Lysates were loaded onto

a 20 - 60 % sucrose gradient and after centrifugation, the gradient samples of 400 μ l containing ribosomes and polysomes were analysed continuously at 254 nm to quantify their mRNA content (Fig 4.12, A & B). Comparing these polysome profiles of young and aged neuronal cells, a significant drop in the number of polysomes, i.e. actively translating ribosomes, in aged samples was detected. This finding agrees with the reduced protein synthesis capacities described before and points towards a lack of translating polyribosomes as one potential explanation or even consequence of aged cells. Note that at a young age (DIV 20), Hypusine treatment did not change the characteristic peak pattern of the polysome profile (Fig 4.12, C).

The aged cultures treated with Hypusine showed a significant increase in the level of polysomes, again highlighting its rejuvenation effects. These findings give a hint that indeed Hypusine directly increases eIF5A activity and thereby promotes active translation via polysomes [Henderson and Hershey, 2011]. As a reference for a successful fractionation of soluble and ribosome-bound proteins, example Western Blots for the ribosomal protein Rpl10a and the translational regulator eEF2 for all 13 separated fractions are shown. As expected, eEF2 shows the strongest appearance in fraction 2 - 4, known as fractions where soluble proteins appear. In contrast, Rpl10a is clearly enhanced in fractions associated with ribosomal peaks and appears most prominently on polysomal fractions 11 to 13.

In conclusion, this chapter introduced p62 / SQSTM1 as a senescence marker for protein aggregates and a clear increase in p62-positive aggregates was visualised in aged neurons. Further, deficits in protein *de novo* synthesis and -degradation could be demonstrated courtesy of the FUNCAT and BONCAT methods, and the S6 kinase / eEF2 pathway was described as one potential signalling cascade related to this ageing phenotype. Finally, the rejuvenation effects of Hypusine and its precursor Spermidine were shown in regard to the induction of autophagy, translational capacities and synaptic vesicle recycling. We provide first hints that polyamines are capable via activation of eIF5A to boost the amount of actively translating polysomes back to levels normally found in young neurons.

In the next chapter, a novel cell culture model with an emphasis on mechanosignalling will be introduced and its potential to mimic the neuronal ageing process will be investigated.

4.2. Stiffness regulated polyacrylamide gels as a suitable model for brain ageing?

Up to now, several attempts were made to study the ageing of the nervous system in diverse cell culture systems including dissociated cultures or organotypic slices [Humpel, 2015], [Jang et al., 2018]. Most studies concentrated on a stress-induced model of cellular ageing linked to increases in reactive oxygen species (ROS) [Dong et al., 2017], [Campos et al., 2014] or mitochondrial dysfunction [Dong et al., 2011]. In this experimental thesis, we aim to connect neuronal ageing with mechanosignalling and investigate how changes in tissue mechanics affect neuronal cells during their ageing process. Conventional cultures conditions use glass coverslips with Poly-D- or L-Lysine coating, however, over the last decade a variety of different substrates with tunable stiffness have been described [Ross et al., 2012]. In this study, we choose to use polyacrylamide (PAA) gels since they are non-toxic to neuronal cells and can be produced in a fairly uncomplicated manner. In the course of this thesis, polyacrylamide (PAA) gels were prepared in the lower and upper range of *in vivo* brain stiffness, i.e. ranging from 0.1 kPa and 1 kPa to 10 kPa to bridge towards the infinite stiffness of conventional glass coverslips generally used in the majority of cellular and molecular neuroscience labs. This allows the elastic modulus of both a young brain (around 0.1 kPa) and a more mature brain ($> 1 \text{ kPa}$) to be mimicked in a manner suitable for cell culture [Moeendarbary et al., 2017]. Further, we used these stiffness regulated cell culture substrates to mimic the mechanical properties of the ageing brain (beyond 1 kPa). Hereby, this set-up allows us to study neurons in a mechanically changing environment and to characterising their formation of dendritic protrusions, synapses and mechanisms of protein synthesis.

4.2.1. Characterisation of neuronal cells grown on stiffness regulated polyacrylamide gels

To first characterize these four different substrates and prove that they are indeed suitable to seed and grow neuronal cells, Laminin coating and overall cell attachment were investigated. Laminin was coated onto all substrates tested and coating efficiency was visualised using a specific antibody against Laminin with subsequent immunocytochemistry before any cells were seeded. We detected no difference in coating pattern or -intensity between all stiffness grades concluding that the attachment of Laminin is similar between the conditions tested and, hence, does not depend on substrate stiffness (Fig 4.13, A). Next, primary cortical cells were seeded onto the different substrates with tunable stiffness or conventional glass coverslips and fixed at a young age (DIV 7).

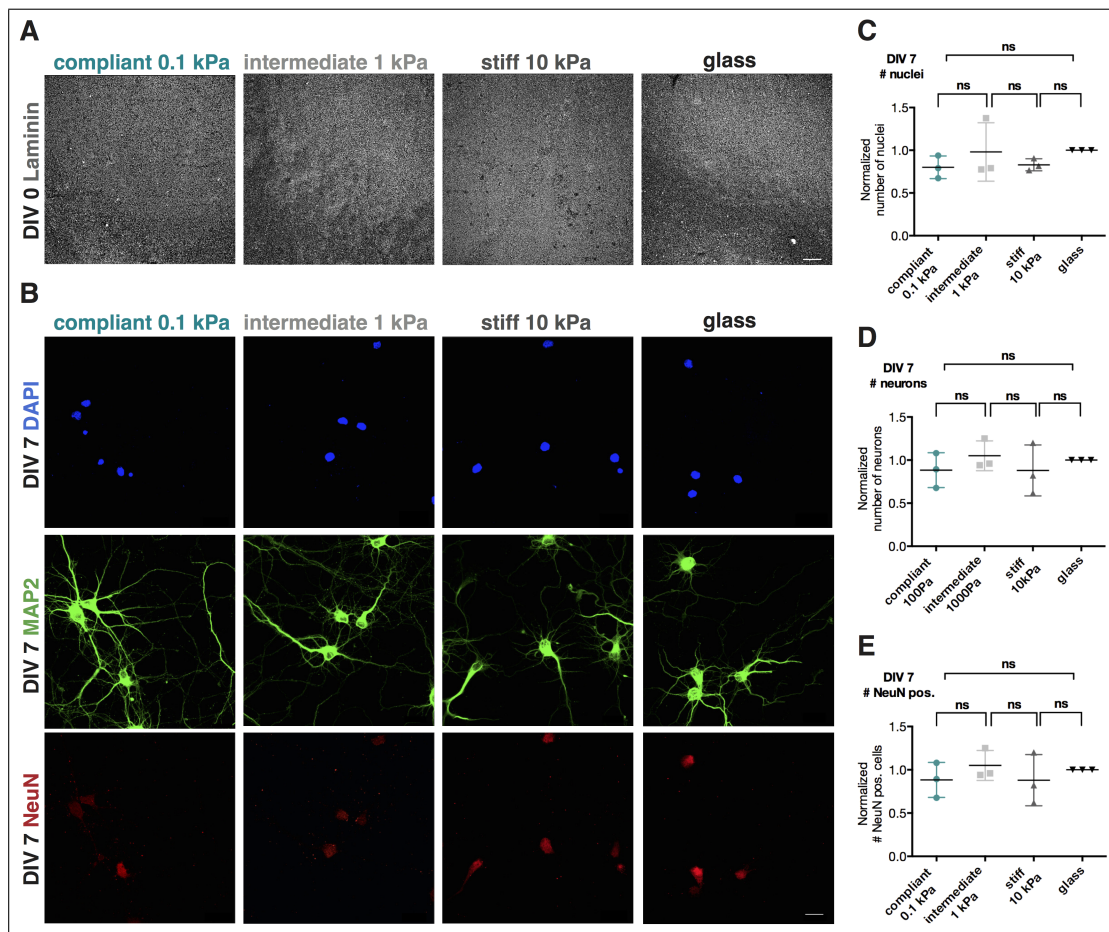


Figure 4.13.: Comparing laminin coating, neuronal attachment and -outgrowth on polyacrylamide surface and glass.

(A) Polyacrylamide (PAA) substrates and glass coverslips showed a comparable pattern and density of Laminin coating. (B) Neuronal attachment was compared between PAA substrates with different stiffness and glass by visualising overall cellular nuclei (DAPI), neuronal dendrites (MAP2) and mature neuronal nuclei (NeuN) using immunocytochemistry at DIV 7. For each cell culture substrate, a similar cell attachment is seen. Scale bar: 20 μ m. (C - E) Quantification of neuronal attachment at DIV 7. No significant difference was described for the number of nuclei (C), neuronal cells (D) or mature neuronal nuclei (E) for the different substrates tested here. In general, no difference in cellular attachment was seen for the cell culture substrates used. ($N = 3$ independent experiments, with 10 neurons per group each, ns = not significant, assessed by one-way ANOVA with Tukey post-test.)

To test whether cell attachment was similar between all substrates and to exclude that PAA gels had a toxic effect on neuronal cells, immunostainings were performed for neural nuclei (DAPI; i.e. neurons and glia cells), neuronal morphology and arborization (MAP2), and mature neuronal nuclei (NeuN) to quantify total neuronal cell number. Subsequent quantification revealed a similar amount of neuronal and glial nuclei, neuronal cell bodies, and neuronal nuclei when comparing the different substrates with each other (Fig 4.13, B - E).

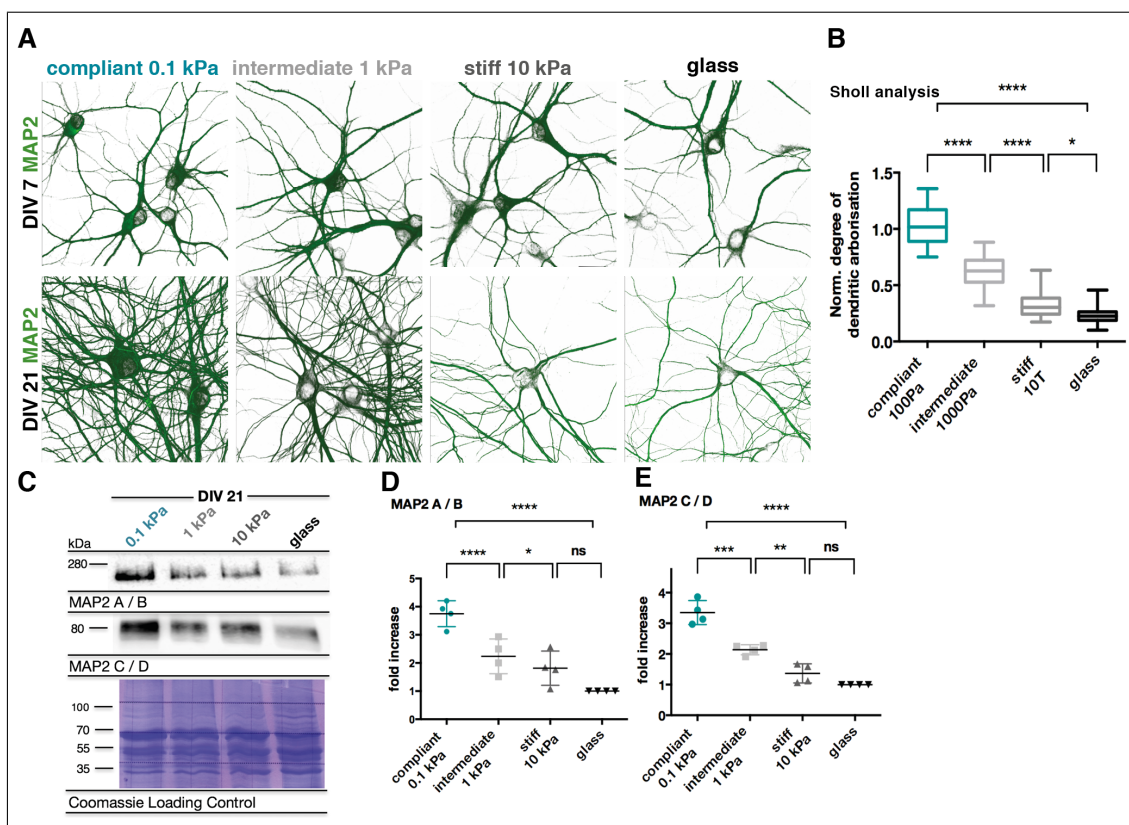


Figure 4.14.: Dendritic arborisation was regulated by substrate stiffness in neuronal cultures. (A) Rat primary cortical cultures grown on stiffness regulated PAA substrates or glass show a similar dendritic arborisation pattern and morphology at immature state (DIV 7). Clear differences in neuronal morphology and in the degree of dendritic arborisation are seen at a mature state (DIV 21). Scale bar: 20 μ m. (B) Quantification of dendritic complexity at DIV 21 by Sholl analysis, depicting number of dendritic crossings per 200 μ m radial distance from the soma. The degree of dendritic arborisation is most complex on compliant substrates (0.1 kPa) and decreases with higher stiffness ($N = 3$ independent experiments, with 10 neurons per group, $F = 287.6$, ****P < 0,0001, *P = 0,03). (C) Quantitative Western Blot reveals a reduction of MAP2 A/B and C/D of mature cultures (DIV 21) with increasing stiffness of PAA gels. Coomassie Loading control representing the total protein amount for each sample analysed. Coomassie Loading control was used for normalisation and to load equal protein amounts for each sample, since recent studies suggest that total protein amount visualized by Coomassie is a more robust and reliable loading control [Welinder and Ekblad, 2011], [Eaton et al., 2013], [Faden et al., 2016], [Nie et al., 2017]. The signal intensity for each protein lane was quantified using ImageJ. The signal intensities were normalized and a new loading volume for each sample was calculated based on these results. The cross-pattern in background of the Coomassie gel is caused by the checked paper of the lab book. (D & E) Quantification of MAP2 expression levels normalized to total lane density (Coomassie Loading control). Signal intensity of MAP2 bands was measured using ImageJ and measured values were normalized to corresponding Coomassie loading control. Normalized values were analyzed with one-way ANOVA with Tukey post-test ($n = 3$ technical replicates from 4 independent biological replicates, for MAP2 A / B, $F = 22.12$, ****P < 0.0001, *P = 0,02, for MAP2 C/D, $F = 62,32$, ***P = 0.0001, **P = 0.006 assessed by one-way ANOVA with Tukey post-test)

This initial experiment ensures that neuronal cells are similarly likely to attach and grow on PAA gels with different stiffness or glass coverslips. Note, that basic neuronal health can be assumed when cells attach to the substrate and survive for 7 days in culture. In conclusion, this cell culture system is suited to study mechanosignalling from neuronal development to aged conditions. To perform a more detailed and functional characterisation of these primary cortical neurons cultured on stiffness regulated substrates, dendritic outgrow and arborisation were examined first. Dendritic shape was visualised with a specific antibody against the microtubular protein MAP2 at early development (DIV 7) and at a mature state (DIV 21). By eye, dendritic shape appears similar on the different substrates used at DIV 7. In contrast, at the mature time point, a clear increase in dendritic arborisation can be observed when cells were cultured on soft substrates (Fig 4.14, A). This finding was verified using Sholl analysis as a quantitative method to characterize the dendritic morphology of the imaged neurons [SHOLL, 1953], [Schoenen, 1982]. Here, the degree of dendritic arborisation was significantly enhanced on soft substrates, i.e. with increasing stiffness the dendritic complexity significantly decreases (Fig 4.14, B). As an alternative method, a semi-quantitative Western Blot probing for MAP2 (subunit A / B and C / D) was used to further underline the findings described. Again, the overall MAP2 expression is highest on the softest substrates used and decreases on a stiffer underground (Fig 4.14, C - E).

Dendritic outgrowth is intimately linked to synaptogenesis [McAllister, 2000]. Synaptic sites are established after or in parallel to dendritic development and slight changes in the extracellular milieu of the neuronal network can cause either a formation or breakdown of a synaptic connection [Cline, 2001], [Wong et al., 2018]. To quantify the overall number of synapses at developmental and mature state the presynaptic protein Bassoon and the postsynaptic marker Homer-1 were visualised via immunostaining (Fig 4.15, A). Where presynaptic and postsynaptic puncta colocalise the structure for a functional synapse can be assumed [Geissler et al., 2013], [Ippolito and Eroglu, 2010]. Indeed, colocalisation of Basson and Homer-1 is increased on soft substrates compared to conventional glass coverslips at early time points in synaptic development (DIV10, Fig 4.15, B). Interestingly, at mature state (DIV 21) the number of synaptic sites is equally distributed over all substrate types studied (Fig 4.15 C, D), pointing towards the importance of mechanic cues especially during synaptic development and for the formation of functionally active synapses. Furthermore and critically, alterations in substrate stiffness do not lead to excess in synaptic connection at a mature state underlining the physiological suitability of this cell culture model.

Besides the expression of key pre- and postsynaptic proteins, synaptic maturation is accomplished by synaptic vesicles release to ensure cellular communication. To analyse the distribution of active synaptic vesicle recycling sites we used the uptake of an antibody against the luminal domain of Synaptotagmin-1.

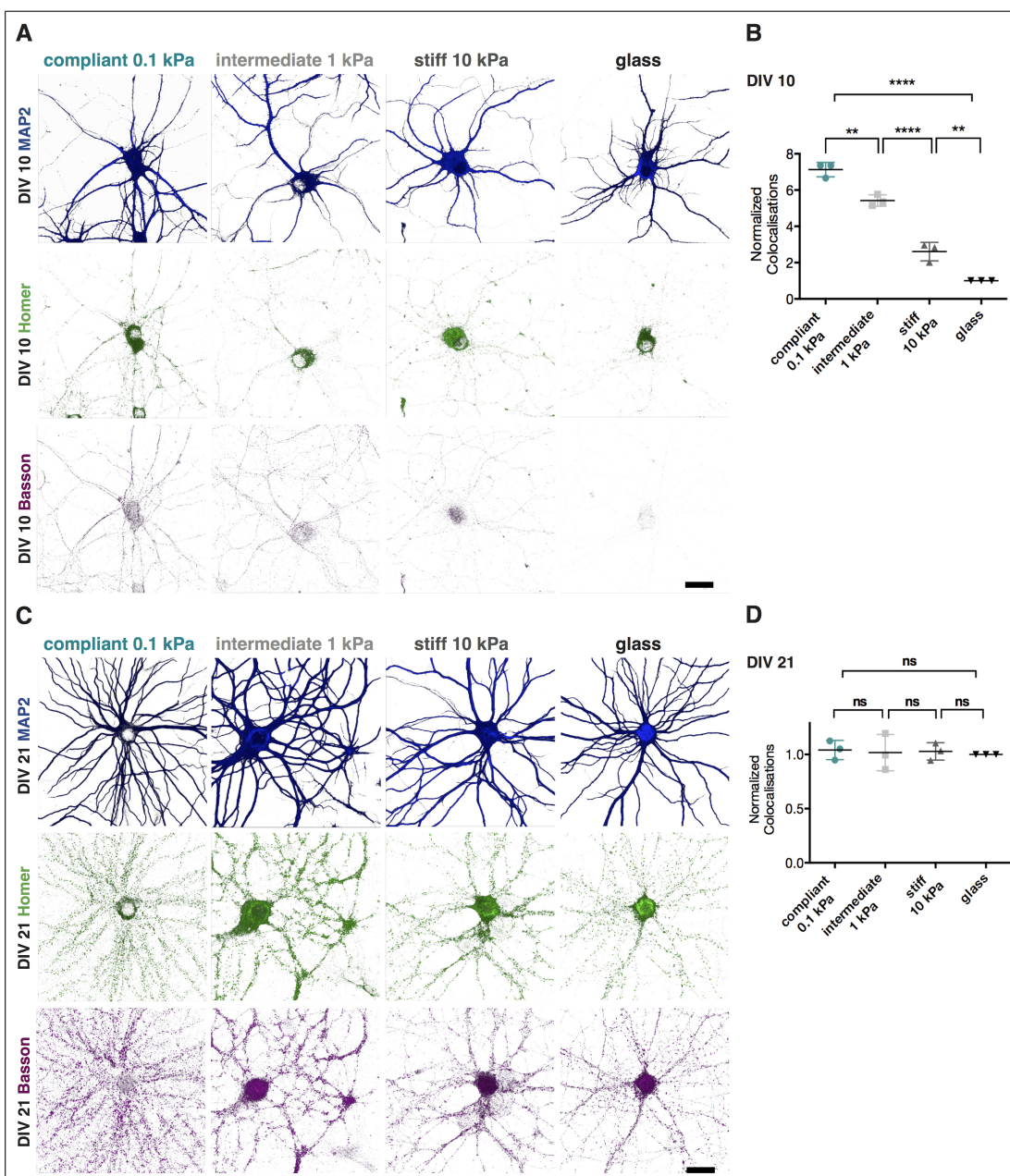


Figure 4.15.: Synaptogenesis was influenced by substrate stiffness

(A) Rat cortical cultures grown on compliant (0.1 kPa) PAA substrates show an up to 7-fold higher co-localisation of the presynaptic Bassoon and postsynaptic Homer-1 at DIV 10. The number of co-localisations decreases gradually as the substrate becomes stiffer. (B) For quantification of co-localisations the Puncta Analyzer plug-in (under ImageJ analysis software) was used. For each experimental condition, three independent experiments analysing each 10 individual neurons were performed resulting in minimally 30 values for statistical analysis (One-way ANOVA with Tukey post-test, $F = 176.5$, $**P < 0.0026$, $****P < 0.0001$). (C) At DIV 21 Homer-1 and Basson immune-positive puncta appear uniformly distributed among all stiffness degrees. (D) Statistical quantification of Homer-1 and Basson co-localisations showed no significant difference between substrates. (One-way ANOVA with Tukey post-test, ns = not significant, Scale bar: 20 μm .)

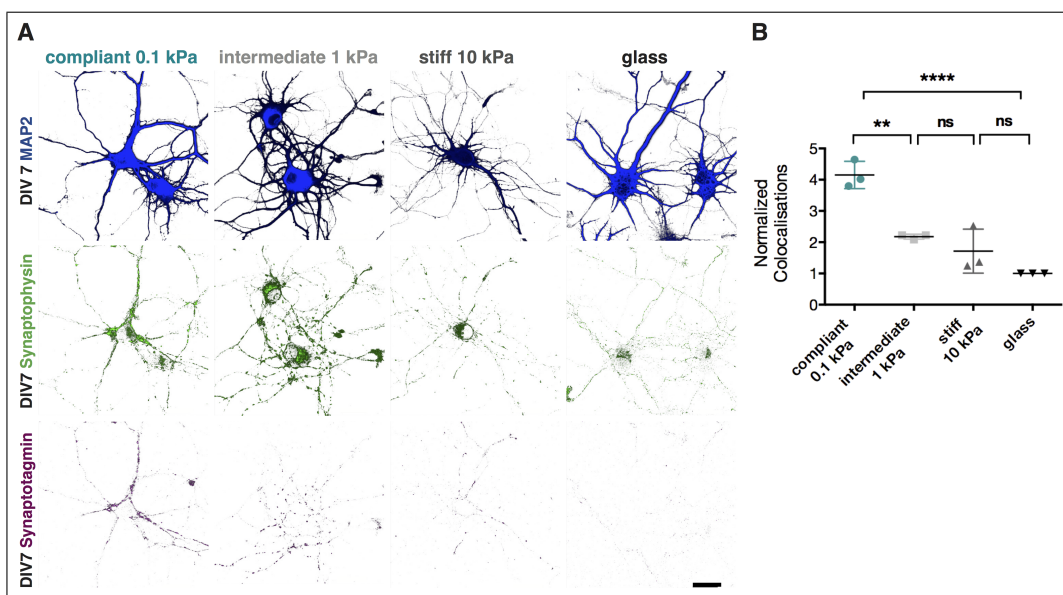


Figure 4.16.: Synaptic vesicle recycling was triggered by mechanical cues

(A) Cortical cultures grown on soft PAA substrates show early synaptic vesicle recycling depicted by live staining using a luminal Synaptotagmin-1 antibody. Active sites of recycling defined by co-localisation of Synaptotagmin-1 and Synaptophysin are up to 4-fold increased compared to conventional glass coverslips at DIV 7. Note that co-localisations are reduced gradually as the substrates stiffness increases. (B) To quantify the co-localisations between Synaptophysin and Synaptotagmin-1 the Puncta Analyzer plug-in (under ImageJ analysis software) from the Eroglu Lab was used. (One-way ANOVA Tukey post-test, $F = 31,41$, **** $P < 0,0001$, ** $P = 0,0018$). Scale bar: $20 \mu\text{m}$.

During life staining, the Synaptotagmin-1 antibody is taken up by endocytosis and thereby indicates sites of active vesicle recycling when co-localised with Synaptophysin. The total number of presynaptic sites was identified using the synaptic vesicle protein Synaptophysin and the neuronal structures is presented by MAP2 immunostaining (Fig 4.16, A). Co-localisations between Synaptotagmin-1 and Synaptophysin were quantified at DIV 7 with the automated Puncta Analyzer plug-in for ImageJ and analysis revealed an increase in co-localisations up to 4-fold on soft substrates mimicking the mechanical cues of juvenile brain tissue (Fig 4.16 B).

To see whether soft substrates increase the number of synapses or even shift synaptic development to an earlier time point, an experiment for a more detailed temporal analysis of the expression of the synaptic proteins was designed. Semi-quantitative Western Blots and subsequent quantification were performed to monitor the expression of synaptic proteins Homer-1, Synaptophysin, and PSD-95 at three time points that comprise the critical phase of synapse maturation in cell culture: DIV 10, 12, 14 [Craig et al., 2006], [McKellar and Shatz, 2009]. As loading control and for normalisation, a Coomassie staining representing the total protein amount was used, since cytoskeletal proteins such as Actin or Tubulin, which are usually used as loading control, are likely to be also regulated by substrate stiffness. Again, an early in-

crease in expression of all above mentioned synaptic proteins was shown for neurons cultured on soft substrates (Fig 4.17 A & B, see DIV 10). For Homer-1, expression appear similar at DIV 12 for all substrates tested, whereas at DIV 14 a significant increase in expression is seen on soft substrates (see Fig 4.17 for quantification).

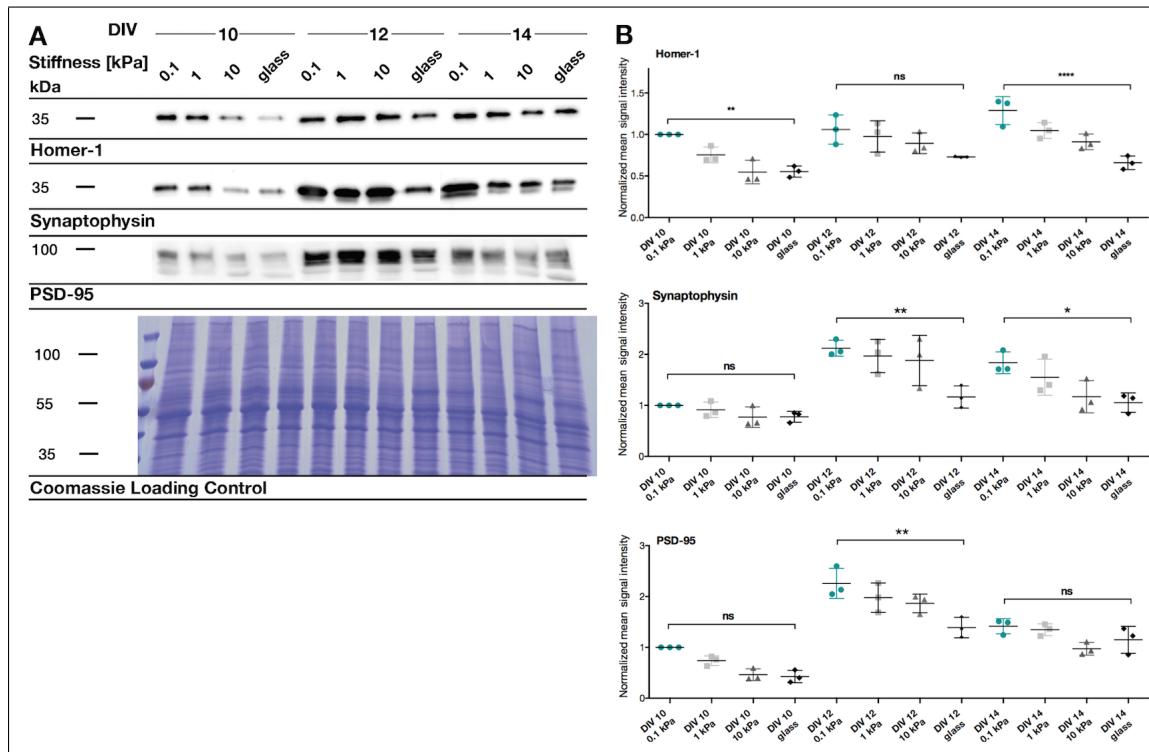


Figure 4.17.: Expression of candidate synaptic proteins appeared earlier on soft substrates. (A) Western Blots of protein lysates collected from neuronal cultures grown on stiffness regulated PAA substrates or glass on three time points of synaptic development (DIV 10,12, 14). The synaptic proteins Homer-1, Synaptophysin and PSD-95 were probed. Coomassie Loading control was used for normalisation and to load equal protein amounts for each sample, since recent studies suggest that total protein amount visualized by Coomassie is a more robust and reliable loading control [Welinder and Ekblad, 2011], [Eaton et al., 2013], [Faden et al., 2016], [Nie et al., 2017]. The signal intensity for each protein lane was quantified using ImageJ. The signal intensities were normalized and a new loading volume for each sample was calculated based on these results. (B) Quantification of Western Blots for synaptic proteins normalized to total lane density (Coomassie Loading control). At DIV 10 significantly higher amounts of Homer-1 are expressed on soft substrates compared to glass coverslips. The synaptic proteins Synaptophysin and PSD-95 show a similar tendency, whereas these candidates are significantly up regulated on soft substrates at DIV 12. At DIV 14 increased expression of Homer-1 and Synaptophysin is described on soft substrates. A total protein Coomassie staining is used as loading control. Signal intensity of synaptic proteins analyzed here was measured using ImageJ and measured values were normalized to corresponding Coomassie loading control. Normalized values were compared by one-way ANOVA with Tukey post-test (One-way ANOVA Tukey post-test; Homer-1: $F = 10,73$, ***P < 0,0001, **P = 0,0050; Synaptophysin: F = 10,86, **P = 0,0050, *P = 0,00408; PSD 95: F = 30,03, ***P = 0,0003)

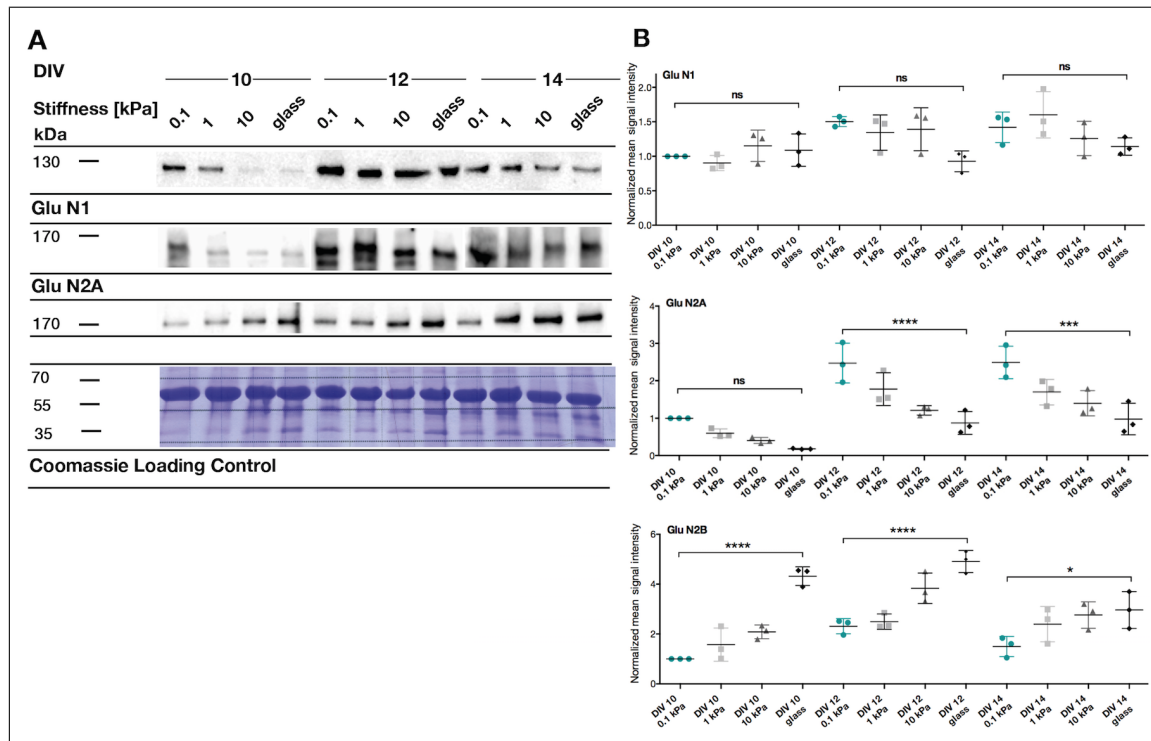


Figure 4.18.: NMDA receptor subunit switch appeared earlier on soft substrates.

(A) Semi-quantitative Western Blot analysis probing for expression levels of GluN subunits 1, 2A and 2B. Coomassie Loading control was used for normalisation and to load equal protein amounts for each sample, since recent studies suggest that total protein amount visualized by Coomassie is a more robust and reliable loading control [Welinder and Ekblad, 2011], [Eaton et al., 2013], [Faden et al., 2016], [Nie et al., 2017]. The signal intensity for each protein lane was quantified using ImageJ. The signal intensities were normalized and a new loading volume for each sample was calculated based on these results. (B) Analysing the GluN receptor subunit 1, no significant changes in expression levels were seen at all time points investigated. Interestingly, the mature subunit 2A is earlier expressed on soft substrates whereas juvenile form 2B shows the opposite tendency. This finding points towards earlier functionally mature GluN receptors on soft substrates and is in line with previous described accelerated synaptogenesis on mechanical environment similar to juvenile brain tissue. A total protein Coomassie staining is used as loading control. Signal intensity of GluN subunits analyzed here was measured using ImageJ and measured values were normalized to corresponding Coomassie loading control. The cross-pattern in background of the Coomassie gel is caused by the checked paper of the lab book. Normalized values were compared by one-way ANOVA with Tukey post-test (One-way ANOVA Tukey post-test; GluN 1: $F = 3,430$, ns = not significant; GluN 2A: $F = 16,65$, ****P < 0,0001, ***P = 0,0003; GluN 2B: $F = 13,88$, ****P < 0,0001, ***P = 0,0002)

Also for Synaptophysin, quantification revealed the highest expression on soft substrates for DIV 12 and DIV 14 and signal intensities gradually decrease as substrates become stiffer. For the postsynaptic protein PSD-95 a comparable regulation pattern was described. This temporal shift in synaptogenesis leads to the conclusion that mechanical cues trigger the orchestrated building and -maturation of synapses. On soft material, synaptic development starts earlier compared to stiffer materials.

In order to underline the hypothesis that a rather soft cellular environment supports synaptic maturation, we further analysed the expression of GluN subunits. It is known from various experiments that during synaptic development GluN subunit composition changes from receptors carrying a 2B- to a 2A unit [Salussolia et al., 2011], [Riou et al., 2012]. Again, a semi-quantitative Western Blot analysis followed by quantification was conducted to explore the expression levels of Glu N1, Glu N2A and Glu N2B subunits. The described developmental switch [Williams et al., 1993] of GluN subunits from 2B to 2A appeared gradually earlier on soft substrates, suggesting a slight acceleration in synaptic maturation on soft substrates (Fig 4.18 A & B). In contrast, the expression pattern of GluN1, a subunit not related to developmental processes, showed no significant regulations when neuronal cells were cultured on substrates tunable in their stiffness.

Taken together, the obtained results describe that substrate stiffness indeed influences synaptic development and vesicle release. This idea can be brought in relation to the deficits in synaptic vesicle recycling seen in aged cultures (Fig 4.11): tissue stiffness increases as the brain ages and eventually these changes in mechanical properties slow down synaptic vesicle recycling or this highly sophisticated process does simply not function as well surrounded by a rather stiff micro-domain.

4.2.2. Protein dynamics are influenced by substrate stiffness in cortical neurons

The general characterisation of cortical neuronal cultures grown on stiffness regulated PAA substrates discussed before, revealed that on soft underground neurons form more complex dendritic networks at mature state and synaptogenesis appears 2 to 3 days earlier compared to conventional glass coverslips. As a next step, we wanted to have a look at even more elaborated cellular signalling processes. We first took a look at protein translation and -synthesis. A high local translation rate in neuronal dendrites represents ongoing activity and reflects a high metabolic status [Perry and Fainzilber, 2014], [Sotelo-Silveira et al., 2006], while as discussed in section 2.2 disturbed protein homoeostasis can be observed in ageing cultures (see Fig 4.4 - 4.6). Therefore, we hypothesized that mechanical signalling might be a novel regulator of protein dynamics and, hence, synaptic function.

In order to monitor fast kinetics of *de novo* protein synthesis in neuronal dendrites we used the SUNSET approach based on Puromycin incorporation into nascent proteins and subsequent Puromycin immunocytochemistry [Schmidt et al., 2009], [Goodman and Hornberger, 2013] (see 3.2.3.9.) Using DIV 7 and DIV 20 cells and substrates of all four different stiffness, Puromycin was added for 1 min labelling time, cells were subsequently washed, fixed and monoclonal antibodies against Puromycin were used to locate newly synthesised proteins in soma and dendrites of neurons. On soft substrates with a comparable stiffness to juvenile brain tissue, protein synthesis was clearly enhanced in soma and dendrites (Fig 4.19 A).

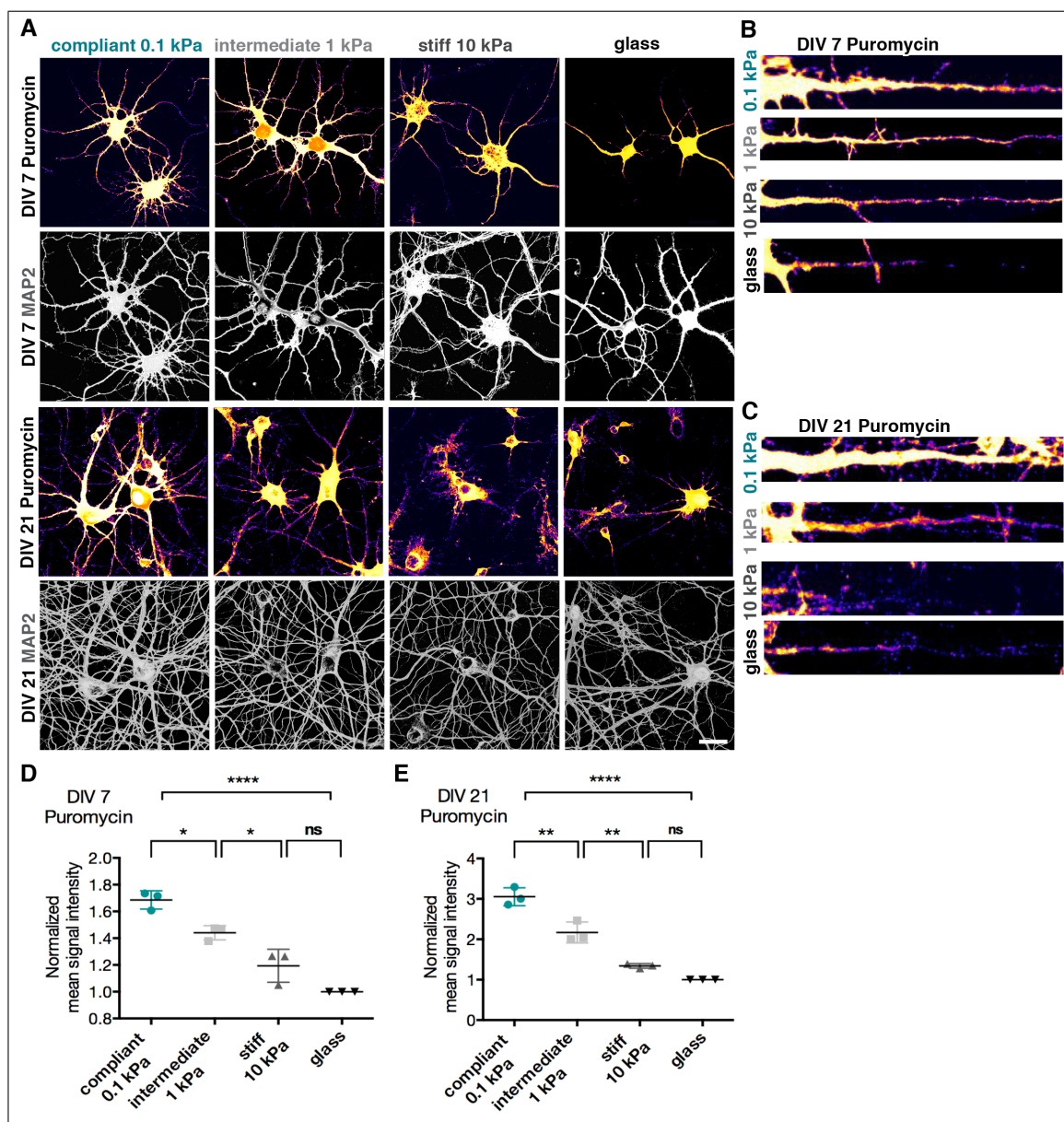


Figure 4.19.: *De novo* protein synthesis was enhanced on soft substrates - Snapshot with Puromycin Assay.

(A) A snapshot of newly synthesised proteins is taken using the Puromycin Assay (1 min labelling time) for rat primary cortical cultures grown on stiffness regulated substrates. A significant increase in protein synthesis is seen for neuronal cultures grown on soft substrates (0.1 and 1 kPa) in young (DIV 7) and mature cultures (DIV 21). N = 3 independent experiments. Scale bar: 20 μ m. (B) Puromycin labelled dendrites were straightened for better visualization of newly synthesised proteins at early development and at mature state (C). (D, E) Quantification of normalized mean intensity of Puromycin signal inside a pre-defined MAP2 mask to outline neuronal structure. For both time points investigated more newly synthesised proteins were detected on soft substrates and the translational capacities decline with increasing substrate stiffness. For each experimental condition, three independent experiments analysing each 10 individual neurons were performed resulting in minimally 30 values for statistical analysis (One-way ANOVA Tukey post-test, F (DIV 7 / 21) = 46,76 / 84,44, ***P < 0,0001, **P = 0.0017 / 0.0011, *P = 0.0171 / 0.0165).

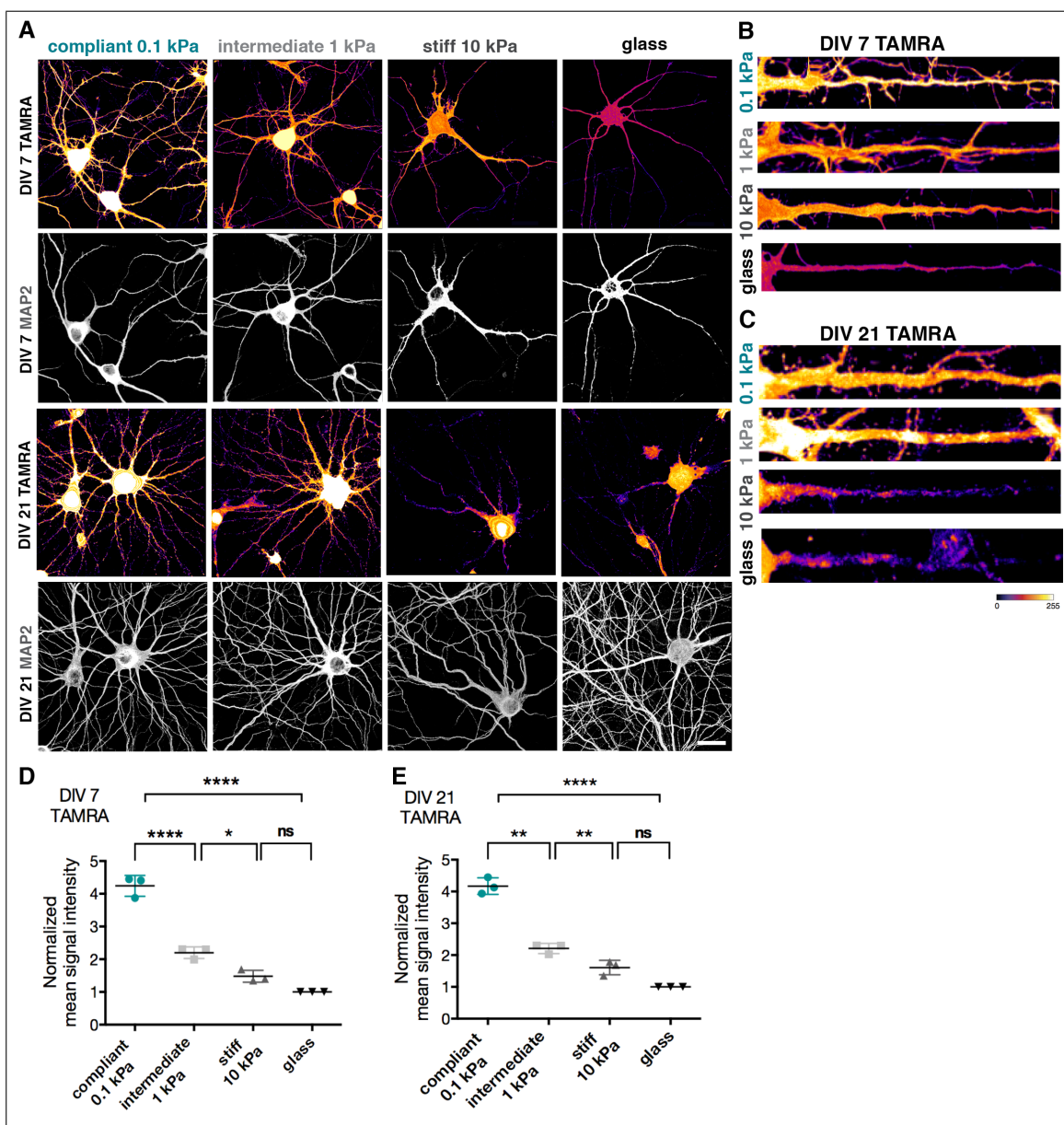


Figure 4.20.: *De novo* protein synthesis was enhanced on soft substrates - FUNCAT.

(A) The rate of newly synthesised proteins was monitored via FUNCAT (3 h labelling time) for rat primary cortical cultures grown on stiffness regulated PAA substrates. An increase in synthesis rate is visualised during development (DIV 7) and at mature state (DIV 21) for neuronal cultures grown on soft substrates (0.1 and 1 kPa) seen by an increase in TAMRA signal. The increase in protein synthesis rate is seen in the soma, dendritic branches and spines (see straightened dendrites in B & C). Identical confocal settings were used for acquisition of all images, and representative images are shown. N = 3 independent experiments. Scale bar: 20 μ m. (D) Quantification of TAMRA signal intensity inside a MAP2 mask revealed up to 4-fold increase of protein synthesis capacities on soft substrates compared to glass coverslips at juvenile state. (E) The same tendency is seen at mature state. (One-way ANOVA Tukey post-test; TAMRA DIV 21: F = 118,83, ****P < 0,0001, *P = 0,0817; TAMRA DIV 7: F = 147,04, ****P < 0,0001, *P = 0,0109)

Note, the location of newly synthesised proteins also in fine, distal dendrites, whereas on conventional glass coverslips protein synthesis is mainly restricted to the soma for both immature (DIV 7) and mature neurons (DIV 21) (Fig 4.19 B & C). Since the labelling time with Puromycin was restricted to 1 min before fixation, transport of labelled proteins can be excluded. This suggests that even the complex process of local protein synthesis is influenced by mechanical cues. Quantification revealed a significant up to 1.6 fold increase in the amount of newly synthesised proteins on compliant substrates (DIV 7) and a 3-fold increase for mature age (DIV 21).

FUNCAT (see 3.2.3.8.) was used as an additional method to visualise *de novo* protein synthesis in temporal and spatial resolution. Here, a longer labelling time (3 h) was used to tag overall translation rates. In line with the Puromycin labelling experiment, also here a significant increase in *de novo* protein synthesis rates is seen in neurons cultured on soft substrates at developmental and mature time points (Fig 4.20, A - C). A significant increase in protein synthesis capacities on more compliant materials was shown by quantification of TAMRA signal inside a MAP2 mask. With increasing stiffness also protein synthesis is down-regulated suggesting a link between mechanical cues and protein translation.

4.2.3. Protein dynamics are influenced by substrate stiffness also in astroglial cells

Besides neurons, mechanical cues are also known to influence astroglia, especially in their morphology and the expression of inflammatory proteins, well characterised by these two studies [Moshayedi et al., 2014], [Chen et al., 2016]. To test, if in our hands the astroglia kept in mono-culture behave similarly, we conducted a Western Blot experiment using a coomassie staining, representing the total protein amount of a sample, as loading control. Cell culture lysates obtained from glia cells grown on substrates with different stiffness were probed for the expression of GFAP as marker protein for astroglia and Iba1 as marker for microglia [Borges et al., 2012]. First results confirmed that expression for both glial protein, Iba1 and GFAP, is highest on conventional glass coverslips, presenting a stiff environment to the cells. These results are in line with previous studies [Moshayedi et al., 2010], [Moshayedi et al., 2014], [Kim et al., 2014]. In a wider sense, Iba1 and GFAP are also associated with inflammation and are often used to describe a status of activated or reactive glial cells [Romero-Sandoval et al., 2008], [Shinozaki et al., 2017].

A soft cellular environment thereby might counteract the formation of reactive glial cells. Also one has to keep in mind, that glial cells do not attach as good on soft substrates compared to stiffer materials, resulting in a lower overall cell number to be investigated.

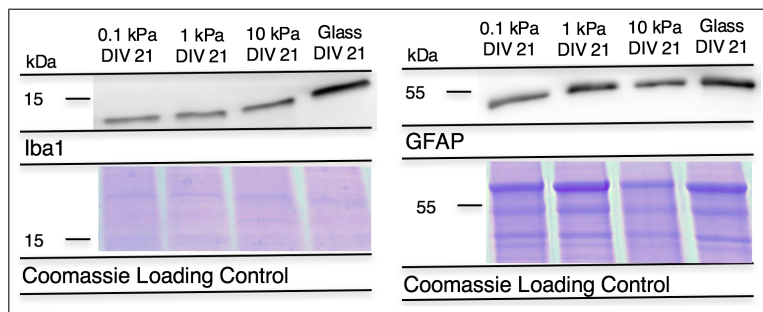


Figure 4.21.: Substrate stiffness influenced expression levels of glial marker proteins. Western Blotting was used to examine the expression levels of the glial protein Iba1 and GFAP. Both proteins show the highest expression levels when glial cultures were grown on conventional glass coverslips, whereas on soft substrates less of these marker proteins were expressed. As loading control, a total protein Coomassie staining was used. Experiments: n = 2, 10 µg total protein were loaded.

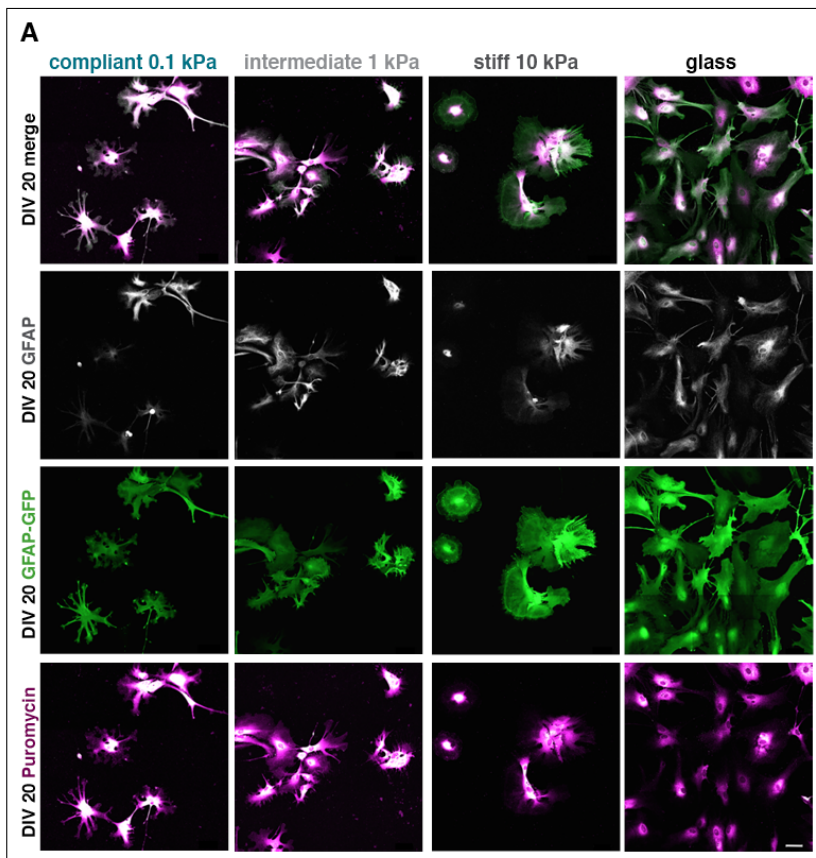


Figure 4.22.: Tunable stiffness influenced astroglia shape and *de novo* protein synthesis (A) Rat glia monocultures were seeded on stiffness regulated polyacrylamide substrates or glass coverslips. The cells were infected with pGfaABC1DEGFP lentivirus to label the cellular area of astrocytes. Before fixation, Puromycin was added for 1min (10 µg / ml) to label growing peptide chains at active translation sites. Using immunocytochemistry this Puromycin label and GFP were visualised. Note the tendency towards formation of fine processes on the soft substrate (0.1 kPa) and a reduced ongoing protein translation on glass compared to cells on soft substrates. Experiments: n= 1.

Next, we wanted to probe whether protein synthesis rates can also be influenced by mechanical stimuli in an astroglia monoculture and performed a corresponding pilot experiment. Astroglia cells were infected with pGfaABS1DEGFP lentivirus to label cell-type specific expression of GFP also in fine protrusions with GFP. Next, the antibiotic Puromycin was incorporated for 1 min and monoclonal antibodies against Puromycin were used to detect newly synthesised proteins. GFAP expression was additionally detected by immunostaining. Astroglia shape and cell attachment were clearly regulated by the stiffness of the substrates used (Fig. 4.22). On soft materials, indeed fewer astroglia cells attach and here the cells show their typical star-like shape with fine protrusions and well defined endpoints. As stiffness increases the astroglia shape changes from ramified to round and flat with the typical "fried egg shape" described in many studies as an activated or inflammatory state [Steiner et al., 2007], [Sharif and Prevot, 2017]. This finding leads to the assumption that a stiff environment alone is sufficient to push astrocytes into a reactive state.

4.2.4. An odd pairing? - Linking protein synthesis dynamics and mechanosensors in cortical neurons

As next step, we wanted to clarify if mechanosensors are involved in regulation of protein synthesis. To this end, we initially choose to pharmacologically manipulate mechanosensitive channels with two compounds: the extracellular mechanosensitive channel inhibitor peptide GsMTx4 [Ostrow et al., 2003] for unspecific blockage of mechanochannels and the chemical activator of Piezo-1, Yoda-1 (Syeda et al., 2015).

Young cortical cultures (DIV 7) were treated with GsMTx4 (25 μ M) or Yoda-1 (10 μ M) for 10 min and medium was changed to Hibernate including 4 mM AHA for 2 h to monitor protein translation. After fixation, newly synthesised proteins were detected via click reaction and an immunostaining was performed for MAP2, the ribosomal protein Rpl10a, and the translational activator eEF2. Interestingly, application of GsMTx4 and blockage of extracellular mechanosensitive channels prior to FUNCAT labelling lead to a significant reduction in the rate of protein synthesis on soft substrates. Soft substrates were chosen as the cell culture substrate of choice since on this surface neurons showed the highest protein synthesis rates (Fig 4.18 and 4.19).

In line with this finding, the ribosomal protein Rpl10a and the translation factor eEF2 showed a decreased expression, pointing to a global reduction in protein synthesis (Fig 4.23, A, B) depending on mechanosignalling. Note that the neuronal structure was not disturbed by GsMTx4 application. The opposite effect in translational dynamics was seen when we activated Piezo-1 channels with 10 μ M Yoda-1 (again for 10 min before 2 h FUNCAT labelling) on stiff substrates. Here, more newly synthesised proteins were detected, especially in the cell soma. Additionally, Rpl10a, as well as eEF2 expression, showed a slight increase, both in somata and dendrites.

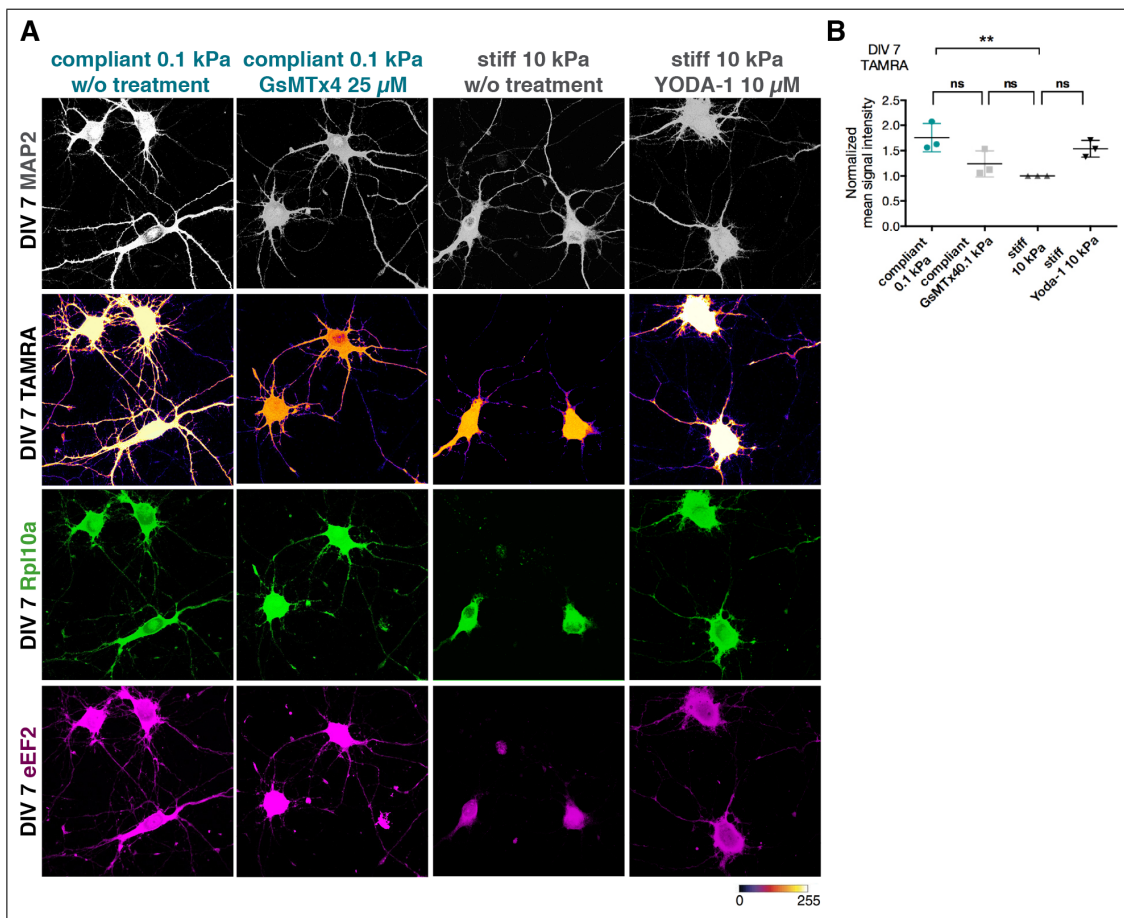


Figure 4.23.: *De novo* protein synthesis was influenced by pharmacologically manipulation of mechanosensitive channels.

(A) The rate of newly synthesised proteins is monitored via FUNCAT (2 h labelling time) for cells grown on stiffness regulated PAA gels or conventional glass coverslips. An increase in synthesis rate is visualised during development (DIV 7) when neurons are grown on soft substrates (0.1 kPa) compared to stiff substrates (10 kPa). Applying the TRP channel inhibitor GsMTx4 (25 μ M) for 10 min before FUNCAT labelling diminishes this effect. Vice versa, the Piezo-1 agonist Yoda-1 (10 μ M, again for 10 min before FUNCAT labelling) was able to increase the protein synthesis rate on stiff substrates (10 kPa). The signal intensity for the translational factor eEF2 and the ribosomal protein Rpl10a follows this described trend (B). Quantification revealed a significant increase in protein synthesis rates when cells were cultured on soft materials. Identical confocal settings were used for acquisition of all images, and representative images are shown. N = 3 independent experiments. Scale bar: 20 μ m. (One-way ANOVA Tukey post-test, F = 7,612 , **P < 0,0093).

In summary, these experiments highlight that mechanical stimuli presented as substrate stiffness are powerful enough to trigger translation of new proteins and that this signalling pathway is initiated by activating mechanosensors such as Piezo-1.

4.2.5. **Ca²⁺ transients are influenced by mechanical cues and reflect mechanoreceptor activity**

Since stiffness-mediated mechanical cues presented to neuronal cells had an impact on cell morphology, synaptic development, and protein synthesis dynamics, it was investigated whether cells grown on different stiffness functionally differ in their Ca²⁺ transients, since Ca²⁺ is one important second messenger in neuronal cells [Brini et al., 2014]. Mechanical tissue properties are sensed by mechanosensitive cation channels *in vivo* and activations of these channels result in Ca²⁺ influx (Ranade et al., 2015) leading to the activation of a wide range of biochemical signalling cascades.

All Ca²⁺ imaging experiments were performed in collaboration with Dr. Michael Kreutz and Dr. Camilla Fusi from the Research Group Neuroplasticity (Leibniz Institute for Neurobiology). In short, young and mature primary neuronal cultures were loaded with 1 μ M of the Ca²⁺ sensor Fluo-4 AM [Hong et al., 2010] in NB for 10 min at 37 °C and then imaged. Quantification of spontaneous Ca²⁺ transients was performed using ImageJ software and fluorescence signals were reported as a ratio ($\Delta F / F_0$) of t change in fluorescence (ΔF) relative to the baseline fluorescence (F_0).

Indeed, monitoring spontaneous Ca²⁺ transients of neurons grown on stiffness regulated substrates revealed a significant increase in the number of spontaneous Ca²⁺ transients at early developmental stages (DIV 10) on compliant substrates (Fig. 4.24, A). On stiffer substrates and glass coverslips the number of Ca²⁺ events per second were significantly lower at this early stage in development. In panel C of Fig. 4.24 temporal traces are shown for each substrate tested. Here, clearly, the most Ca²⁺ transients in the time frame of 250 s were seen on compliant substrates presenting a softness of 0.1 kPa to the cortical neurons.

Having established the interdependency of spontaneous Ca²⁺ transients and substrate stiffness, we next blocked IP3 receptors with the selective antagonist 2-APB (10 μ M) during live recording in order to clarify if Ca²⁺ is entering from outside the cell or released from stores inside the ER. Application of 2-APB [Maruyama et al., 1997] diminished the effect of Ca²⁺ oscillation frequency but only on compliant substrates (Fig. 4.24, B), suggesting that Ca²⁺ is properly released from the ER as shown in Fig 4.24, by representative time courses of spontaneous Ca²⁺ oscillations for all conditions tested (250 s). For each trace also the corresponding neuron loaded with Fluo-4 AM is depicted (Fig 4.24, C).

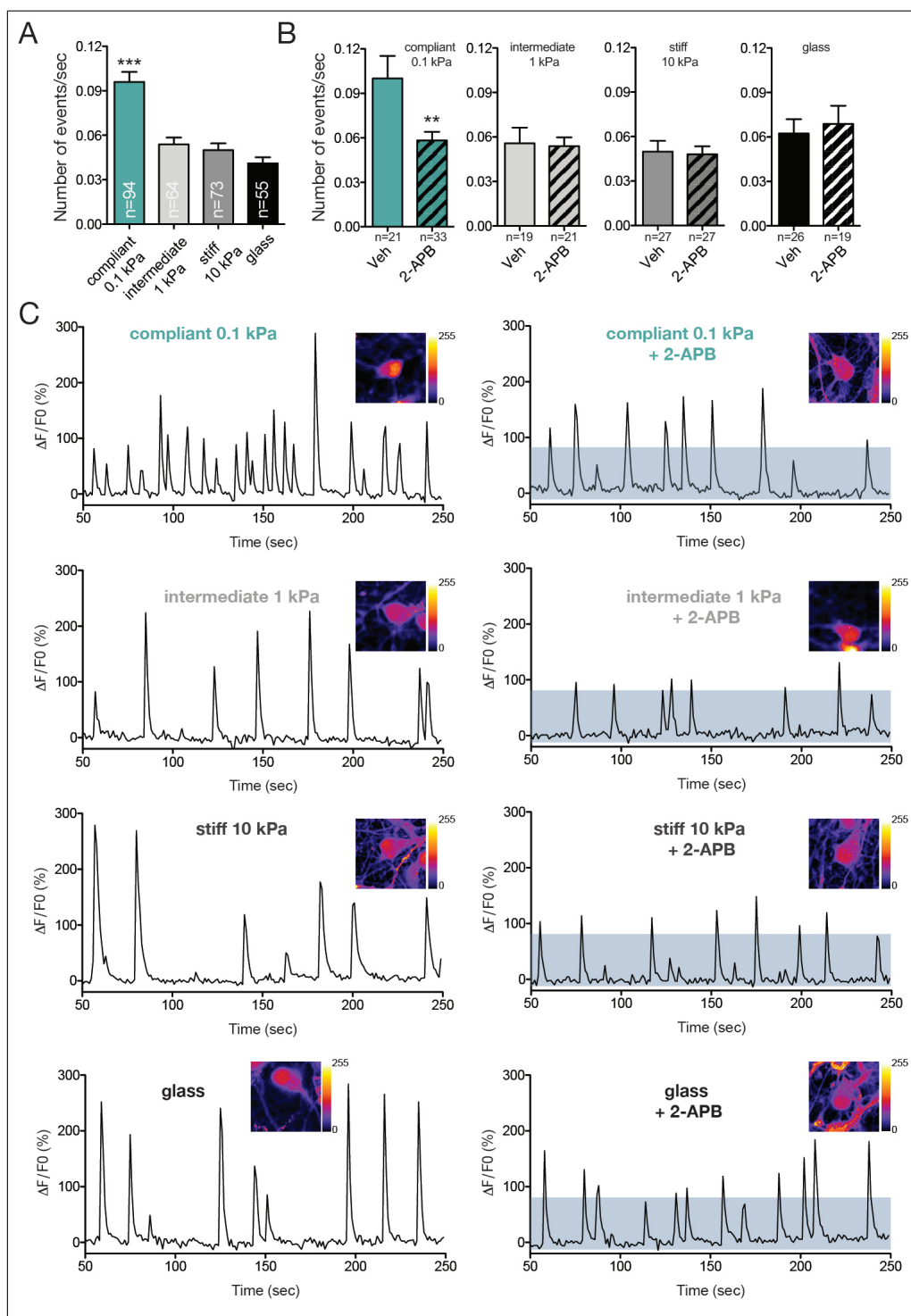


Figure 4.24.: Spontaneous Ca^{2+} oscillation depend on the stiffness of the substrate in immature cultured cortical neurons.

(A) 10 DIV rat cortical neurons were loaded with Fluo-4 AM dye and Ca^{2+} transients were measured. Neurons grown on soft substrate (0.1 kPa), but not on intermediate (1 kPa), stiff substrate (10 kPa) or glass, show an increase in Ca^{2+} oscillation frequency. (B) This increase in Ca^{2+} oscillation is reduced by blocking IP₃ receptors with the selective antagonist 2-APB, 10 μM . Treatment with 2-APB does not affect Ca^{2+} oscillations of cells grown on 1 kPa, 10 kPa or glass substrates. (C) Representative time courses of spontaneous Ca^{2+} oscillations of neurons grown on 0.1 kPa, 1 kPa, 10 kPa and glass substrates with or without 2-APB. Error bars indicate SEM. One-way ANOVA Tukey post-test.

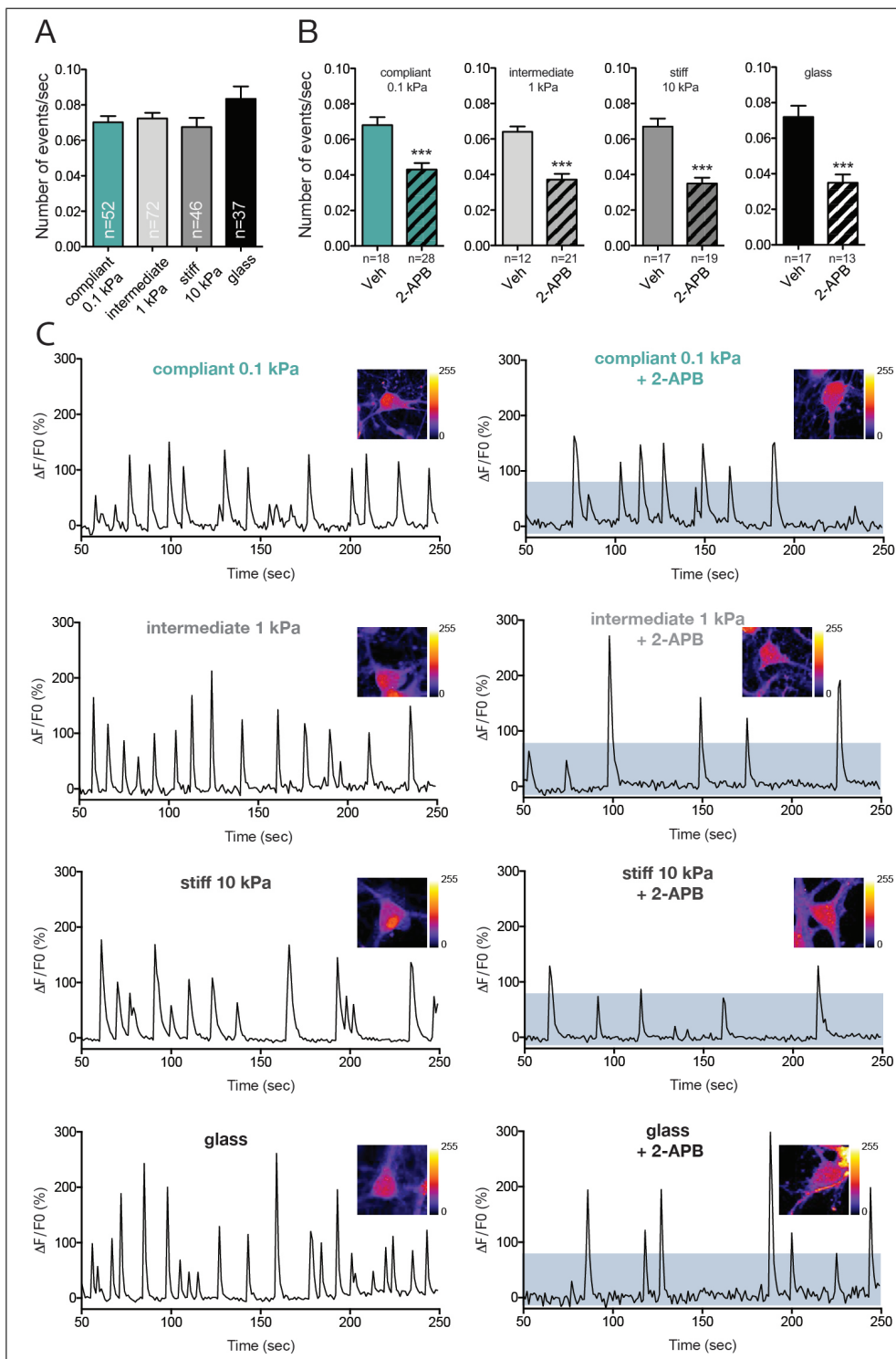


Figure 4.25.: Spontaneous Ca^{2+} oscillation was not affected by the stiffness of the substrate in mature cultured cortical neurons.

(A) At mature state (21 DIV), rat cortical neurons grown on soft substrate (0.1 kPa), intermediate (1 kPa) or stiff substrate (10 kPa) show no difference in Ca^{2+} oscillation frequency. (B) Spontaneous Ca^{2+} oscillations were reduced by blocking IP₃ receptors with the selective antagonist 2-APB, 10 μM , for all substrates tested (C) Representative time courses of spontaneous Ca^{2+} oscillations of neurons grown on 0.1 kPa, 1 kPa and 10 kPa substrates with or without 2-APB. Error bars indicate SEM. One-way ANOVA Tukey post-test.

Interestingly, at mature stage (DIV 21), spontaneous Ca^{2+} spiking showed no differences between the four different substrates investigated (Fig. 4.25, A). For each stiffness tested, the number of events per second was around 0.07, revealed by quantification. At mature conditions, a significant reduction in oscillation frequency by 2-APB ($10 \mu\text{M}$) treatment is found for all substrates tested (Fig. 4.25, B), pointing towards Ca^{2+} release from the ER. The reduction on spike events after 2-APB treatment appeared in a similar range for all stiffness degrees, eventually reflecting a universal mechanism of Ca^{2+} release for mature cortical neurons. Representative time courses and the cellular integrity of the neurons analysed are presented (Fig 4.25, C). In conclusion, the pattern of 'higher activity' on soft substrates at a young age accompanied by a similar level of events at an mature state, reflects the pattern in synaptogenesis observed beforehand. These findings underline the importance of mechanical signalling, especially during developmental processes.

In order to better describe the increase of spontaneous Ca^{2+} transients triggered by soft substrates we concentrated on the recently discovered mechanosensor Piezo-1 and stimulated this channel with its chemical agonist Yoda-1. This stimulation resulted in a characteristic increase in Ca^{2+} influx followed by a unique spiking pattern for each substrate tested: whereas on glass an increase in spontaneous Ca^{2+} spikes is seen, on intermediate stiff substrates a Ca^{2+} burst was visualised (Fig 4.26, A). For stiff substrates (10 kPa), a low burst followed by few spikes was measured. One potential explanation for these phenomena is that the expression of the Piezo-1 receptor itself is regulated by mechanical cues. Therefore we tested the expression levels of Piezo-1 by immunoblotting. Indeed we found that expression of Piezo-1 was regulated by substrate stiffness and, therefore, the increase in spontaneous Ca^{2+} transients might be a result of increased receptor levels (Fig 4.26, B).

Revealed by semi-quantitative Western Blot analysis, on soft substrates significantly higher amounts of Piezo-1 were expressed at young and mature time points compared to stiffer substrates. As introduced under 2.3.3, mechanical stiffness of brain tissue increases during ageing *in vivo* [Gefen et al., 2003] in rats. Again, to test whether our model for neuronal ageing is comparable with the *in vivo* situation, we used lysates of cortical brain homogenates from young (8 weeks), mature (24 weeks) and aged (104 weeks) mice and probed for Piezo-1 expression (Fig 4.26, C). Actin was used as loading control and to normalize the subsequent quantification. As mice were ageing, we saw the amount of cortical Piezo-1 expression decreasing. Comparing 8 weeks and 104 weeks old mice, an approximately 40 % reduction in Piezo-1 protein expression was revealed by Western Blot analysis. Due to the promising, previously presented results describing that Piezo-1 activation- and also expression patterns depend on mechanical cues such as substrate or tissue stiffness, we choose to investigate the role of Piezo-1 in mechanosensing in more detail. The idea was to over express Piezo-1 with a labelled construct and re-investigate spontaneous Ca^{2+} influx of cortical cells grown on stiffness regulated substrates in a pilot experiment.

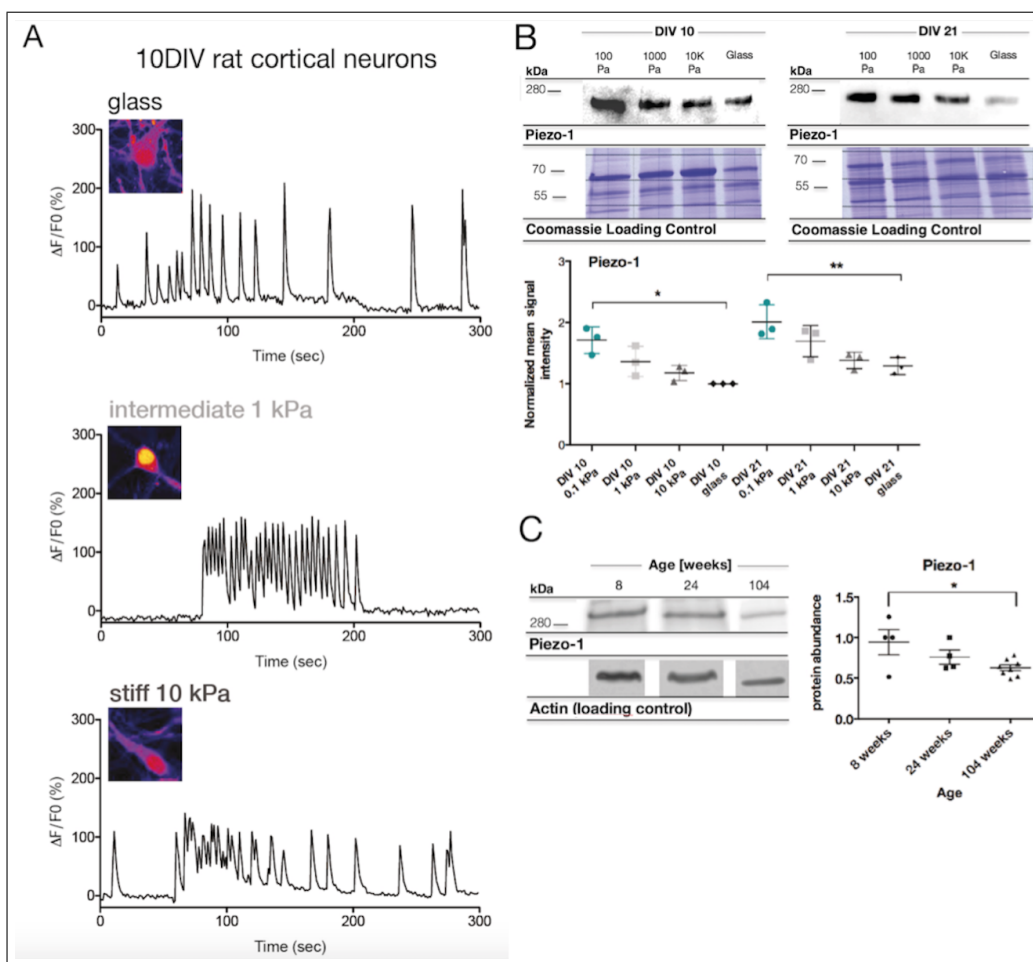


Figure 4.26.: Yoda-1 stimulation leads to different patterns in Ca^{2+} spiking related to tunable stiffness Piezo-1 expression varies between stiffness regulated substrates and age *in vivo*

(A) Cortical neurons grown on substrates with tunable stiffness were exposed to Yoda-1 ($1 \mu\text{M}$), a chemical activator of Piezo-1 channels at DIV 10. Depending on stiffness presented, frequency and duration of Ca^{2+} influx varies, resulting in a characteristic activation profile. $n = 8-10$ traces measured for each substrate. (B) Piezo-1 expression was examined by semi-quantitative Western Blot and a significant increased in protein expression was revealed on soft substrates at young and mature time points. Coomassie Loading control was used for normalisation and to load equal protein amounts for each sample, since recent studies suggest that total protein amount visualized by Coomassie is a more robust and reliable loading control [Welinder and Ekblad, 2011], [Eaton et al., 2013], [Faden et al., 2016], [Nie et al., 2017]. The signal intensity for each protein lane was quantified using ImageJ. Signal intensity of Piezo-1 bands was measured using ImageJ and measured values were normalized to corresponding Coomassie loading control. Normalized values were analysed by one-way ANOVA with Tukey post-test. The cross-pattern in background of the Coomassie gel is caused by the checked paper of the lab book. ($n = 4$, $F = 8.565$, $**P < 0.0063$, $*P = 0.0197$, assessed by one-way ANOVA with Tukey post-test). (C) Probing cortex homogenates from mice with different age (8, 24 and 104 weeks) for Piezo-1 expression, we showed a decrease in expression levels with increasing age. Actin was used as loading control and to normalize subsequent quantification of Piezo-1 bands. Ordinary one-way ANOVA was used for statistical analysis, $F = 3.901$, $*P = 0.0154$. Cortex homogenates provided by Dr. Peter Landgraf and Western Blot experiments performed by Felix Mertin. $n = 4-6$ independent probes for each time point.

The Martinac lab provided us with the Piezo-1-mCherry (1591) construct [Cox et al., 2016]. After that electroporation was used to transfect this construct into freshly prepared cortical cells at DIV 0 (see 3.2.1.5). Then cells were cultured for 10 days *in vitro* first on intermediate stiff substrates (1 kPa) to get a first idea if the transfection is working.

As visualised in Fig. 4.27 A, the transfection sufficiency was around 30 %. This was an encouraging result, especially for such a large construct (9.6 kb) and a cell type that is difficult to transfect.

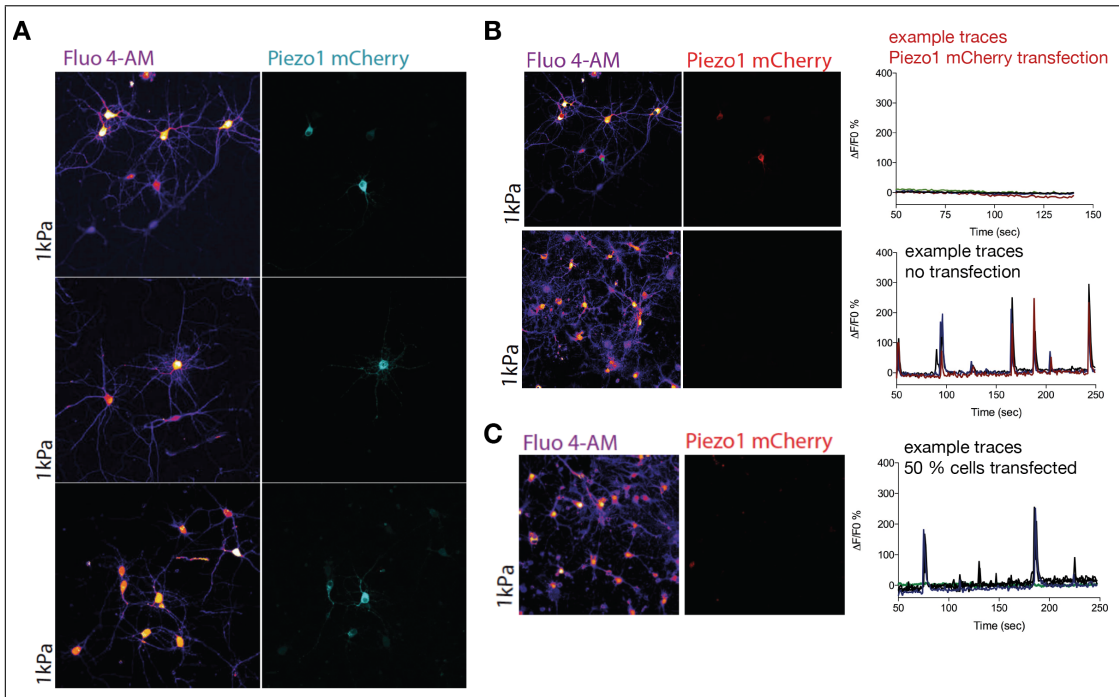


Figure 4.27.: Overexpression of a mCherry labelled Piezo-1 construct in primary cortical neurons lead to silencing of spontaneous Ca^{2+} oscillations

(A) Directly after preparation, primary cortical cells were transfected with the Piezo-1-mCherry (1591) construct by electroporation. Cells were seeded onto intermediate 1 kPa substrates and cultured for 10 DIV before live imaging. Here, examples of the transfection efficiency are shown (around 30 %). Note that glial cells are missing in this preparation. (B) Live recordings of Ca^{2+} influx revealed that transfected neurons appear silent compared with an untransfected control group which should have similar spiking as described beforehand (Fig. 4.24). (C) Mixing cells transfected with the Piezo-1-mCherry (1591) with untransfected cells in a 1:1 ratio, few spontaneous Ca^{2+} oscillations were recorded but also transfected efficiency dropped to 10 %. Scale bar: 50 μm , n = 1.

Also, note that besides the cell soma the Piezo-1-mCherry construct is expressed also in fine neuronal protrusions. Another phenomenon that was encountered by us, was that the neuronal cultures appeared almost free of glial cells; determined by looking at cellular morphology. Next, we monitored spontaneous Ca^{2+} spiking by live imaging of transfected cells and used cell cultures without the Piezo-1-mCherry construct as a control group. As a strik-

ing result, neurons carrying the Piezo-1-mCherry construct and also their direct neighbours appear silent and showed not spiking behaviour at all, compared to control cells without transfection (Fig 27, B). This lack of spontaneous Ca^{2+} spiking can have several reasons, one being that cellular integrity was missing without the involvement of glial cells. In the untransfected control, glial cells were visualised and eventually supported communication and Ca^{2+} signalling. Nevertheless, this result leads to slight changes in experimental strategy and we seeded a mixture of Piezo-1-mCherry transfected and untransfected cells (1:1 ratio) onto 1 kPa substrates and imaged again at DIV 10 for 250 s. In this cell mix, the transfected efficiency was reduced to about 10 %, as expected (Fig 4.27, C). But in this condition, glial cells were present and also few Ca^{2+} spikes were recorded from neighbouring cells but not from neurons carrying the Piezo-1-mCherry construct.

Combining the overexpression of Piezo-1-mCherry with the recording of Ca^{2+} transients gives new ideas about the key role of Piezo-1 in mechanosensing and Ca^{2+} homoeostasis. Also, either Piezo-1-mCherry overexpression or electroporation appears lethal to glial cells. Due to temporal restrictions, these experiments were not further optimised, nevertheless, the preliminary data is interesting and therefore presented here.

4.2.6. Proteomic analysis of neuronal cells grown on stiffness regulated materials revealed new signalling pathways regulated by mechanical cues

As it was shown above and from literature, the evidence is increasing that neuronal cells use not only electrical and chemical but also mechanical cues for signalling and intracellular communication. However, the exact details and signalling pathways responsible for mechanotransduction have not been addressed in much detail yet. To characterise neuronal proteome dynamics and seek for potential signalling pathways regulated in response to substrate stiffness a proteomic analysis utilizing mass spectrometer technology was performed. Again, primary cortical neurons were grown on polyacrylamide gels mimicking the upper and lower bounds of *in vivo* brain tissue stiffness during development, maturation or even at aged time points. All experiments in regard to Proteomic analysis were performed in cooperation with Dr. L.C. Nguyen and Dr. Robert Ahrends from the Research Group Lipidomics based at the Leibniz-Institut für Analytische Wissenschaften-ISAS-e.V, Dortmund. For proteomic profiling neuronal cultures were harvested at DIV 10 from all substrate types introduced before since this time point is described as a phase of late dendritic outgrowth and early synaptogenesis. Cell lysates were proteolytically digested and separated by nano liquid chromatography coupled to a Q Exactive HF mass spectrometer for analysis. In total 1613 proteins are identified with at least 2 unique peptides in all four conditions (compliant 0.1 kPa, intermediate 1 kPa, stiff 10 kPa and glass). The averaged relative protein abundances spread through five orders of magnitude on a negative and positive scale (-5-fold to +5-fold).

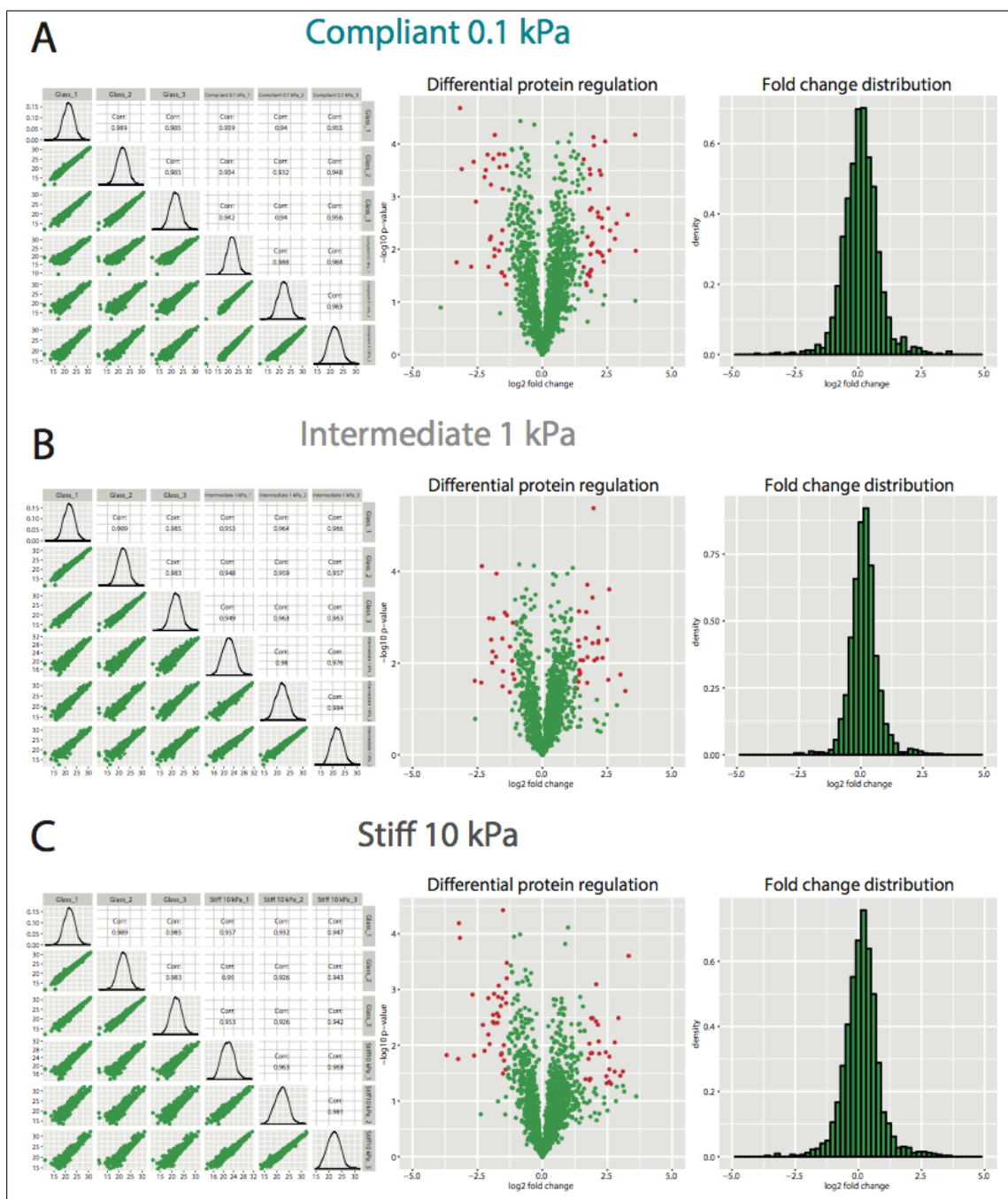


Figure 4.28.: Proteomic analysis of the neuronal cells grown on different materials: Mass Spectrometry Analysis was controlled for probe quality

Proteomic analysis of the neuronal cells grown on different materials: compliant 0.1 kPa (A), intermediate 1 kPa (B), stiff 10 kPa (C) compared to glass. From left to right: Pairwise correlation between the biological replicates of the treated and control conditions: The protein abundances at log 2 scale are plotted for all samples. The Pearson correlation coefficient (Corr) is calculated for each pairwise comparison. Volcano plot of the differential regulation of the identified proteins: The P-value and fold change are calculated for each of the identified proteins in all samples. Proteins are considered to be differentially regulated (red dots), if their P-value is below 0.05 and the fold change is greater than the upper limit (median of log2 fold change + 2 x STD) or less than the lower limit (median of log2 fold change - 2 x STD). Distribution of the fold change: The distribution of the fold change at log 2 scale is presented for all the identified proteins.

Plotting the protein abundances at log 2 scale for all samples and calculating the Pearson correlation coefficient showed a good correlation between biological replicates. For better visualisation, identified differentially regulated proteins were illustrated by volcano plots and the distribution of the fold change for all identified proteins was presented (Fig. 4.28).

To unravel potential proteome dynamics related to mechanical cues the fold change between the three physiological conditions (compliant 0.1 kPa, intermediate 1 kPa and stiff 10 kPa) were compared to the control condition where neuronal cells were cultured on conventional glass coverslips. The differentially regulated proteins (P -value < 0.05 and \log_2 fold change $>$ or $<$ median of \log_2 fold change + or - twice the STD) were clustered into two groups: gradually up-regulated on soft substrate or down-regulated on soft substrates and display using a heat map (Fig. 4.28). For the up-regulated cluster we chose GRAP1, EVL, SHLB2 and MARCS as candidate proteins since their function can be integrated into putative mechanosignalling pathways. The GRIP-associated protein-1 (GRASP-1) as a neuron-specific exchange factor for Rab4 and regulates recycling endosome maturation inside dendrites ([Hoogenraad and van der Sluijs, 2010, Hoogenraad et al., 2010]). Additionally, GRASP-1 is essential for GRIP/AMPA receptor complex formation, spine morphology and synaptic plasticity [Ye et al., 2000]. The Ena/VASP-like protein (EVL) belongs to the Ena/VASP family known as actin regulators involved in cytoskeleton remodelling during neuronal migration and axon guidance [Sechi and Wehland, 2004]. Two other regulators of the neuronal cytoskeleton and especially F-actin are Endophilin B2 (SHLB2) and Myristoylated alanine-rich C-kinase substrate (MARCKS). Current models described SHLB as connecting element between the spine cytoskeleton and endocytic protein complexes specifically in glutamatergic synapses [Loebrich et al., 2016]. MARCKS regulates cell shape and -motility in neuronal development by interacting with F-actin, calmodulin and synapsin [Hartwig et al., 1992], [Zolessi et al., 2006].

In the cluster of down-regulated proteins on soft substrates we highlighted EZRI, MOES, NEST and CALR. The linker proteins Ezrin (EZRI) and Moesin (MOES) of the evolutionarily conserved ezrin/radixin/moesin (ERM) family connect membrane proteins with actin cytoskeleton once activated by phosphorylation. Phosphorylated Ezrin and Moesin are essential for the extension of filopodia and are possibly involved in presynaptic trafficking [Kim et al., 2010]. The next candidate protein Nestin (NEST) is a known neural progenitor marker, expressed in undifferentiated neuronal cells during development. Functionally, Nestin belongs to the class of intermediate filament proteins [Hendrickson et al., 2011]. The endoplasmic reticulum (ER) chaperone protein Calreticulin (CALR) catches misfolded proteins and targets them for degradation before they are exported from the ER. In conditions of cellular stress like inflammation, Calreticulin is up regulated to improve quality control in protein folding [Lee et al., 2003], [Ní Fhlathartaigh et al., 2013].

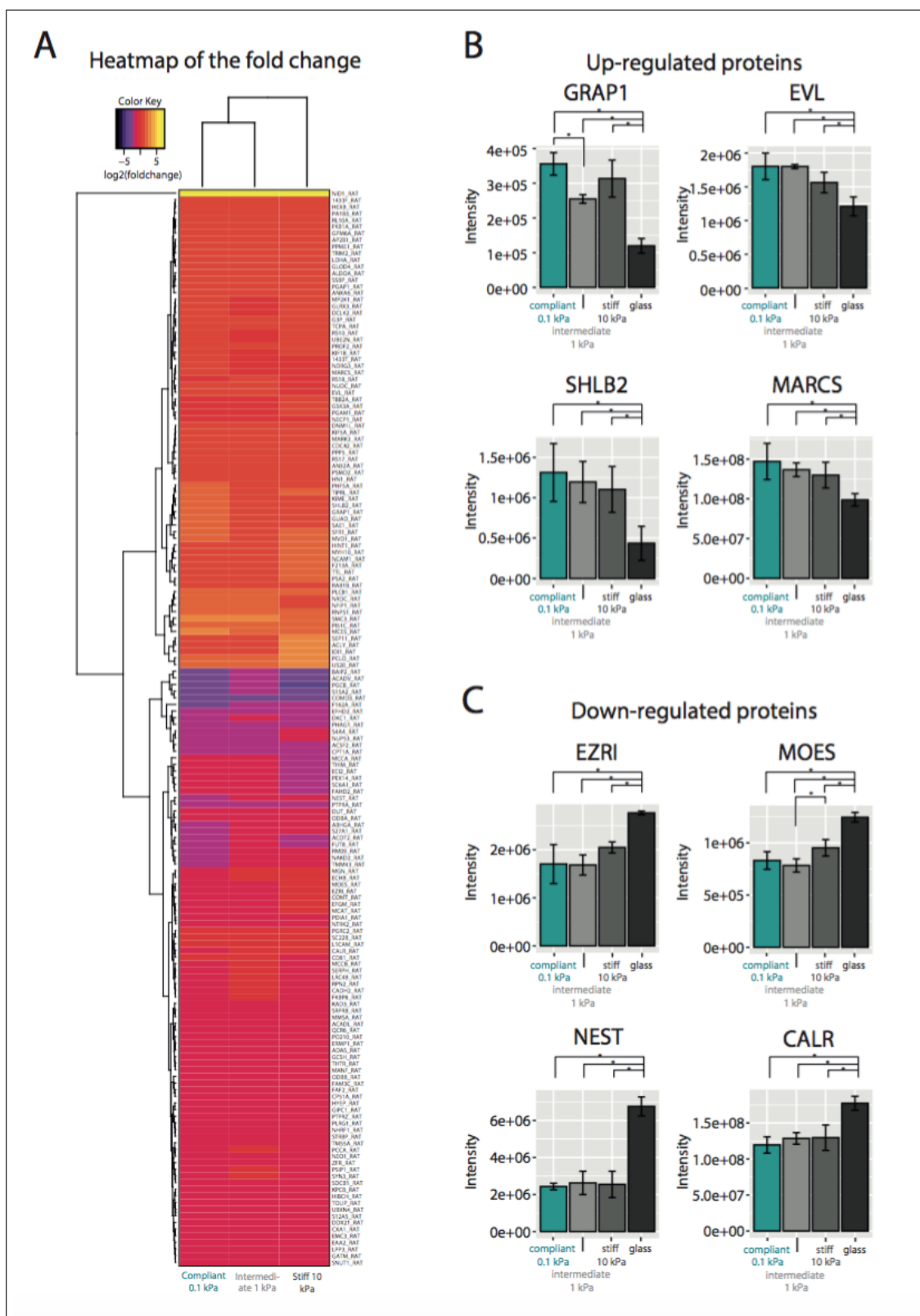


Figure 4.29.: Proteomic analysis of the neuronal cells grown on different materials
 (A) Heat map of the fold change of regulated proteins: In total 1613 proteins are identified with at least 2 unique peptides in all four conditions (compliant 0.1 kPa, intermediate 1 kPa, stiff 10 kPa and glass). The fold change between three conditions (compliant 0.1 kPa, intermediate 1 kPa and stiff 10 kPa) to control condition glass is presented.

Only the differentially regulated proteins (P-value < 0.05 and log₂ fold change > or < median of log₂ fold change + or - twice the STD) are used to generate the heat map. The clustering pattern is generated using hierarchical clustering function. (B & C): Regulation levels of up-regulated proteins (GRAP1, EVL, SHLB2, MARCS) and down-regulated proteins (ERZI, MOES, NEST, CALR): A subset of regulated proteins are presented. * represents the significantly differentiation between two conditions (P-value < 0.05).

With these findings, we finalize our experiments focused on the characterisation of neuronal cells grown on stiffness regulated PAA gels during development and maturation and address the experimental question whether tunable PAA gels are a suitable model for brain ageing.

4.2.7. Long-term cell culture on stiffness regulated polyacrylamide gels

In the previous sections, the behaviour of primary cortical cells during developmental processes such as dendritic outgrowth, expression of pre- and postsynaptic proteins and synaptic vesicle recycling was described. We pointed out that mechanical cues like substrate stiffness influenced neuronal development and maturation. Soft substrates providing the same stiffness as juvenile brain tissue, promoted synaptogenesis (Fig 4.15 - 4.17), *de novo* protein synthesis (Fig 4.19 - 4.21) and increased spontaneous Ca²⁺ oscillations (Fig 4.24 and 4.25).

The final goal of our experiments was to investigate whether neuronal cells age differently on stiffness regulated substrates and connect this cell culture model to the findings from section 4.1 describing age-related deficits in proteostasis. To ensure the long-term vitality of neuronal cells grown on stiffness regulated substrates cell culture conditions described under 4.1.1 were followed. Additionally, a special Laminin coating was used: Laminin-521 provided by BioLamina [Rodin et al., 2014] to prevent detachment of cells from the rather flexible polyacrylamide surface.

Once all conditions for a long-term culture were met, primary cortical neurons were cultured on stiffness regulated polyacrylamide gels or glass coverslips up to DIV 80. At this age, cells were labelled for 3 h with AHA in Hibernate Medium lacking Methionine to initiate a FUNCAT reaction and investigate how proteins are newly synthesised and located under these cell culture conditions.

Again, immunocytochemical stainings were performed to illustrate the neuronal structure (MAP2) and postsynaptic sites (Shank2). As result, neuronal structure and distribution of post synaptic sites appears alike between substrates tested here and no neuronal health was ensured even at old age (Fig 4.30). The intensity of the TAMRA signal reflects the amount of newly synthesised proteins and on soft gels a tendency for higher translational activity was shown. Note that with increasing stiffness TAMRA signal intensity is becoming less as described for young and mature age at Fig 4.20. This observation underlines our findings that protein translation is influenced by mechanical cues such as substrate stiffness, even for aged

neurons. In conclusion, increased brain stiffness found as in aged tissue [Elkin et al., 2010] could be one cause or consequence for less efficient protein synthesis.

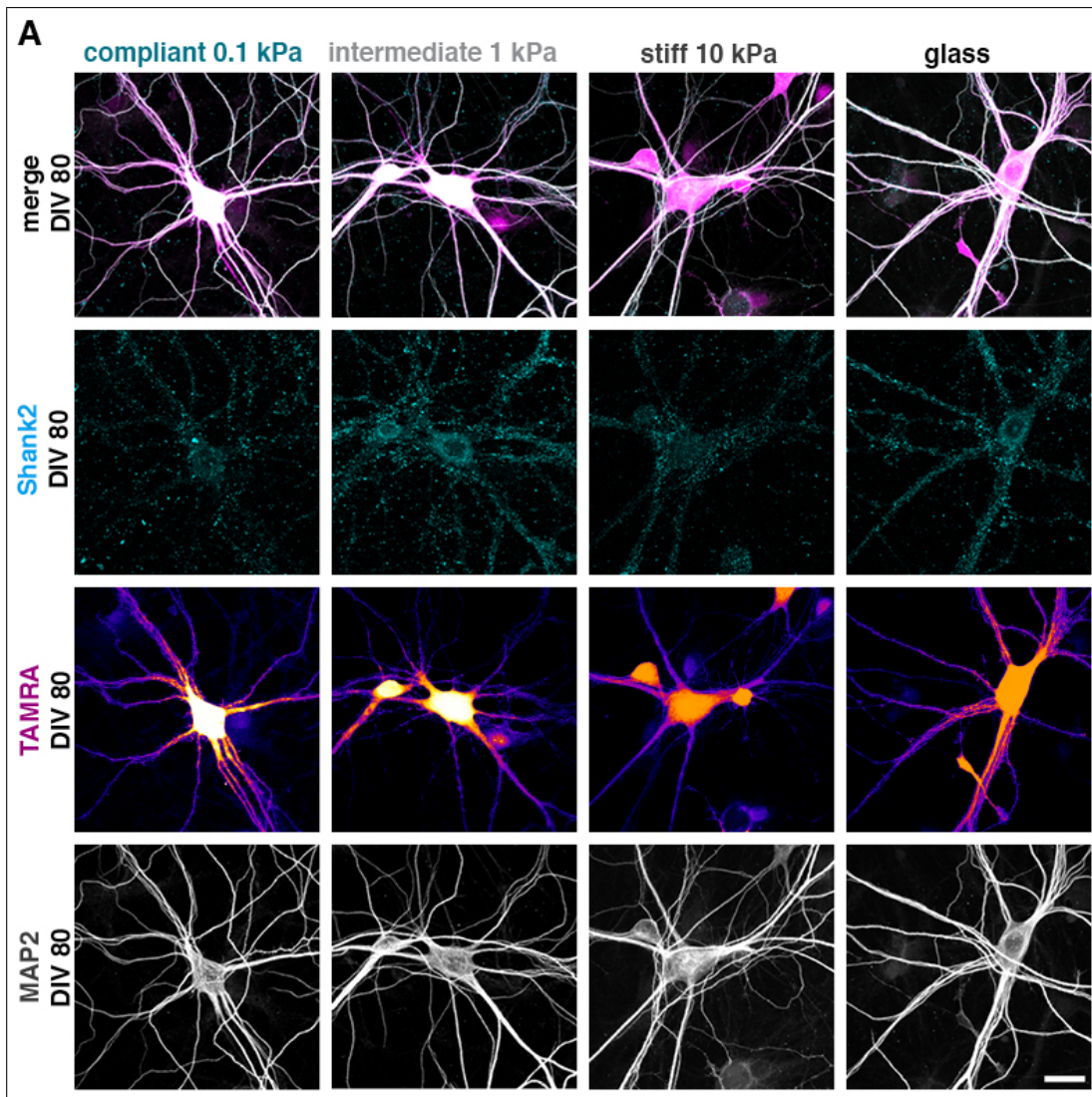


Figure 4.30.: FUNCAT experiment with long-term culture of neuronal cells in stiffness regulated polyacrylamide gels.

(A) Primary neuronal cultures were grown on stiffness regulated polyacrylamide gels or glass coverslips for 80 days. At DIV 80, cells were labelled for 3 h with the non-canonical amino acid AHA and subsequently newly synthesised proteins were visualised by click-reaction. On soft substrates a higher TAMRA signal is seen compared to stiffer underground in soma and neuronal dendrites. Neuronal structure was stained with MAP2 and postsynaptic sites are depicted by Shank2-positive puncta and signals appear similar between all substrates tested. n = 2 independent experiments, Scale bar: 20 μ m.

In this thesis, we defined p62-positive protein aggregates as one hallmark of neuronal ageing and viewed the accumulation of misfolded or dysfunctional proteins as senescence marker (see Fig 4.3). To test how protein aggregation occurs during ageing on stiffness regulated

substrates, we again cultured primary neuronal cells up to DIV 80 and stained for neuronal structure (MAP2), p62-positive protein aggregates and presynaptic sites (Synaptophysin).

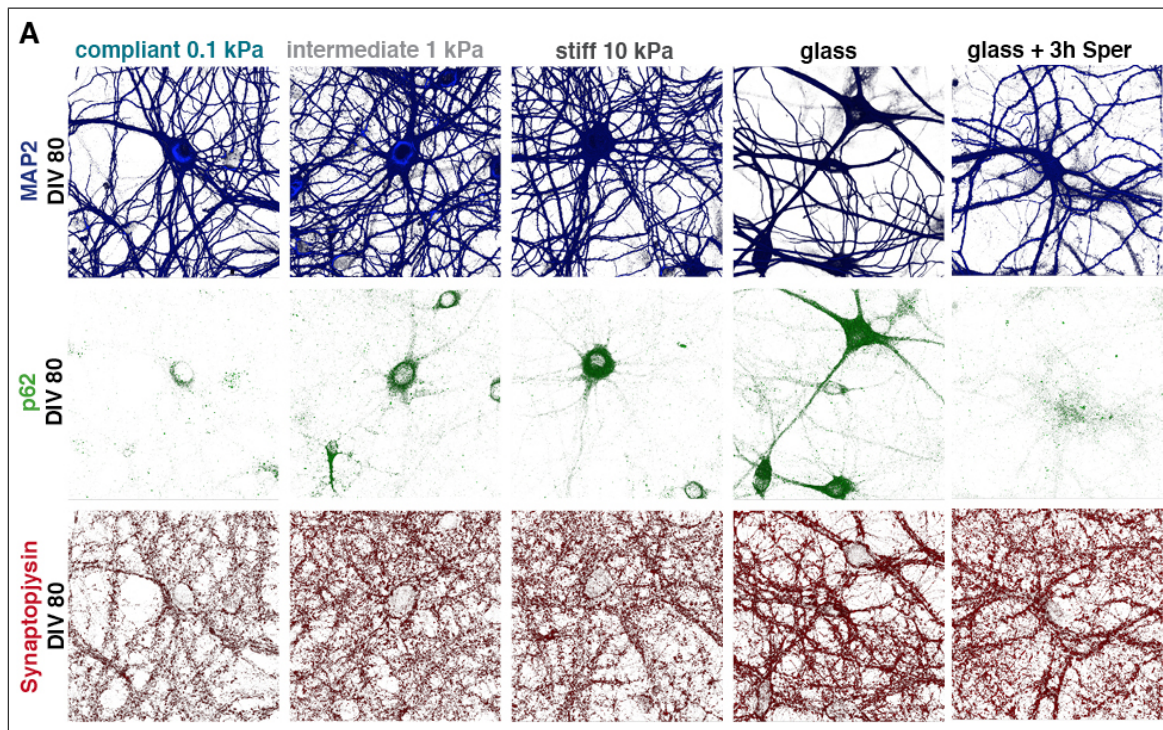


Figure 4.31.: Less p62-positive protein aggregates accumulated on soft PAA gels in aged neurons

(A) Immunostaining for p62 revealed less protein aggregates tagged for degradation on soft PAA gels compared to stiffer substrates at DIV 80. Note that neuronal structure shown by MAP2 staining and presynaptic structure (Synaptophysin) appears alike for all substrates tested. Treatment with the Polyamine Spermidine for 2 h was sufficient to clear p62-positive protein aggregates in aged cells cultured on glass coverslips. n = 2 independent experiments, Scale bar: 20 μ m.

In one experimental condition, cells grown on glass coverslips were treated with the polyamine Spermidine (25 μ M) for 3 h before fixation. For all substrates tested, neuronal structure and presynaptic sites looked similar. Interestingly, on soft substrates, reflecting the mechanical properties of juvenile brain tissue, less p62-positive protein aggregates inside neurons were detected, compared to stiffer substrates or glass coverslips. As a control experiment, again Spermidine application was sufficient to clear most of the p62-positive protein aggregates (Fig 4.31).

In summary, these experiments show that it is possible to grow long-term neuronal cultures (up to DIV 80) on stiffness regulated PAA gels. Also, we give a first hint that indeed the mechanics of the cellular environment contribute to neuronal ageing and open the way for future experiments to clarify the underlying molecular mechanisms.

5. Discussion

5.1. Ageing in a dish - What long-term neuronal cell cultures can teach us about brain ageing

When it comes to life expectancy, the amount of humans over 60 years is estimated to double between 2010 and 2050 [Bomsdorf, 2004]. Facing the needs of our ageing society, it is important to learn more about the ageing process and especially brain ageing itself. Focusing on the mammalian organism, ageing studies need a lot of time and are cost-intensive since mice or rats have to be kept for up to three years to investigate an aged phenotype. Because of the fact that ageing is a multifaceted process, the survival rate of the animals is relatively low, tumours occur with a higher frequency, and, therefore, it is particularly hard to distinguish healthy brain function from deficits in other organs.

Although, *in vitro* cultures have been investigated and modified towards the enablement of the ageing process cell culture conditions need still to be optimized and many open questions about the ageing process remain as well [Sebben et al., 1990]. For primary hippocampal cultures, an increase in amyloidal aggregates and protein oxidation has been shown when neurons were cultured up to DIV 60 [Bertrand et al., 2011], [Aksenova et al., 1999], proving that long-term cultures are a suitable model for certain aspects of neuronal ageing. We choose to work with primary cortical cells since cortical neurons are known to be vulnerable in neurodegenerative diseases and play an important role in a variety of cognitive processes declining with age.

5.1.1. Define old: A senescence marker for neuronal cells

Although a remarkable breakthrough was achieved in characterising and even clearing out senescent cells over the last decade, still no defining feature such as a specific surface marker was found to label senescent cells from different tissues or organs [Scudellari, 2017]. Nevertheless, the field of senolytic drugs, i.e. uniting drugs with the ability to identify and eliminate a specific type of senescent cell, is one of the fastest growing group in drug discovery. Moreover, treatment of different age-related diseases such as chronic kidney disease or atherosclerosis is already entering clinical trials. However, for brain cells, no specific senescence marker was defined so far and clearing senescent cells from the brain is a goal which likely will not be

achieved in near future [Soto-Gamez and Demaria, 2017].

In basic research, most known senescence markers have been described and characterized for dividing cells, so additional investigations are necessary to verify whether neurons show actually the same senescence markers like proliferating cells. Indeed, few studies claimed that neurons have a senescent phenotype including DNA breaks, increased oxidative damage, activated p38 / MAPkinase and deficits in p21 function [Jurk et al., 2012]. One study further described increased levels of γ -H2AX in ageing cortical neurons already at DIV 27 [Bigagli et al., 2016]. This observation we were not able to replicate in the course of our own investigations (see Fig 4.1). One potential explanation for this difference is that the cortical neurons prepared and cultured in our group have an increased health span and do not display increased double-strand breaks marked by γ -H2AX even at DIV 80. So we changed strategy and looked for a new class of senescent marker related to translational regulation, a known hallmark of ageing.

5.1.2. The complexity of translational regulation in young and aged systems - many starting points to look for a potential rejuvenation

The maintenance of a functional proteome is vital throughout all life stages and requires a tight temporal and spatial regulation [Chen et al., 2010], [Narayan et al., 2016]. Altogether, the process defined as proteostasis involves a synthesis of new proteins, folding, post-translational modifications, transport, and also degradation of old and/or non-functional proteins. More and more errors occur in all of these interconnected steps while the organism is ageing [Tosato et al., 2007], [Press et al., 2018]. Especially, a reduction in the amount of newly synthesized proteins has been reported for every aged cell, tissue, organ or even organism investigated [López-Otín et al., 2013]. Thus, it has also been shown that the total protein concentration of a cell is increasing due to the accumulation of dysfunctional proteins. In our investigations using aged cell cultures, we proved both of these findings by describing a decline in translational capacities for neuronal cells (Fig 4.4 - 4.7, 4.12) and protein aggregation as consequences of ageing (Fig 4.3, 4.9). Further, we underlined that also protein degradation is slowed down in aged neuronal cells (Fig. 4.6, 4.7), which is known from various studies [Rattan, 1996], [Kononenko, 2017].

On the bright side, the complex regulation of protein translation, requiring more than 200 molecules to translate one single mRNA, offers many signalling nodes for a potential regulation of translational capacities or even the development of anti-ageing therapies. We were especially interested in the S6 kinase / eEF2 pathway because of its direct connection to the mTOR signalling pathway, as one of the first identified anti-ageing regulators [Kennedy and Lamming, 2016]. In summary, we were able to show that the detected decline in general translation is partly a result of regulating the S6 kinase / eEF2 pathway towards

a reduction in translational activation (see Fig 4.6).

We hypothesized that with age the phosphorylation pattern of eEF2 is shifting towards its inactive form, probably due to increased phosphorylation of Thr56 by the eEF2 kinase. In the literature, conflicting studies about eEF2 expression during ageing are reported [Takahashi et al., 1985], [Riis et al., 1990] and no study focused on healthy brain tissue so far. In general, the activity of eEF2 is regulated by a distinct phosphorylation pattern, with phosphorylation of threonine 56 by eEF2K being most critical [Redpath et al., 1996]. In conditions of increased cellular stress, eEF2 is known to be down-regulated, especially under conditions of ER stress or nutrient deprivation. Further, eEF2 expression can be regulated by the nutrient-sensing kinase AMPK [Browne and Proud, 2004], [Browne et al., 2004], which is associated with lifespan extension [Stenesen et al., 2013], [Ulgherait et al., 2014]. In the case of AD, a clear decrease in eEF2 expression was reported compared to control brains [Li et al., 2005].

Further, we demonstrate that the upstream effector S6 kinase is differently phosphorylated when comparing young and old cells pointing towards reduced translational capacities in aged samples. Phosphorylation of Thr389 is vital for the enzymes kinase function [Weng et al., 1998] and a reduction of this isoform is linked to a general decline in translation in aged cells. But it is important to keep in mind that regulation of the S6 kinase activity is much more complicated since it possesses multiple phosphorylation sites, additional regulators elements, a high number of activator kinases, and strongly depends on growth factors [Dufner and Thomas, 1999]. Nevertheless, the S6 kinase will remain an important regulator of translational control and cellular ageing and a better understanding of the multiple functions will provide a basis for potential anti-ageing drugs such as Rapamycin [Aliper et al., 2017] or even new strategies in drug development.

Next, we asked whether the deficiency in proteostasis could be rescued by restoring polyamine concentrations. Previous studies reported that mice with a high polyamine diet had prolonged life spans and less age-related pathologies [Soda et al., 2009]. The increased life expectancy after spermidine supplementation also holds true for *C. elegans* and *Drosophila* [Eisenberg et al., 2009], [Gupta et al., 2013], presumably due to enhanced autophagy. In a wider context, autophagy is linked to cellular energy metabolism and ultimately to protein translation [Hands et al., 2009], [Lindqvist et al., 2017]: a connection we aimed to investigate in more detail. Since polyamines such as spermidine are a natural compound in the human diet and no side effects are known, it is of special interest to explore the anti-ageing actions of polyamines, too. We indeed could show that Spermidine application restores the activity of the translational factor eEF2 and upregulates expression levels of the elongation factor eIF5A and the ribosomal protein Rpl10a. In line with previous results [Madeo et al., 2018], protein

turnover was promoted by Spermidine in aged cultures presumably by enhanced autophagy as shown by Madeo and colleagues [Eisenberg et al., 2009]. We also probed for the effects of the hypusine on translational regulation since Spermidine is metabolized to this unusual amino acid. Here, we observed the same tendencies towards translational activation pointing towards Spermidine function via eIF5A (Fig 4.7). Looking into more detail, Spermidine is slightly more efficient in its rejuvenation capacities mainly because its cellular uptake is regulated more precise by amino acid transporters [Uemura and Gerner, 2011] and its proposed function as a NMDAR ligand [Williams et al., 1991]. In Fig 4.9 we showed a staining for hypusine with higher intensity levels after treatment with Spermidine than for pure hypusine, raising also the question whether hypusine is more unstable as a free amino acid and prone for degradation when not directly linked to its co-factor eIF5A.

Besides their effect on proteostasis and autophagy-induction, polyamines are proposed to facilitate higher cognitive functions such as learning and memory [Guerra et al., 2016] and protect against age-related memory decline and loss of motor functions [Gupta et al., 2013], [Minois et al., 2014]. Since the molecular basis for this phenomenon are unknown, we conducted an experiment to investigate synaptic vesicle recycling in aged cortical cultures and highlighted that both spermidine and hypusine are capable to restore vesicle recycling (Fig 4.10) to juvenile levels. Our results are in agreement with studies which proved that spermidine application has the power to rejuvenate memory deficits in old mice [Kibe et al., 2014] or even in a mouse model of Huntington's disease [Velloso et al., 2009]. These are just a few studies explaining the effects of polyamines and especially spermidine in ageing and disease (see [Madeo et al., 2018] for a recent review) and future investigations will further characterise its positive effects on the nervous system.

5.1.3. What do Polysome Profiles tell us about translational capacities?

Polysome profiling is a widely used and reliable method to investigate the translational status of a given cell type under native conditions or in response to a chemical stimulation [Chassé et al., 2017]. Due to technical advances, other methods have been developed to study translating mRNAs, such as ribosome profiling and translating ribosome affinity purification (TRAP) [King and Gerber, 2016]. In this study, we used a classical polysome profiling built on sucrose-gradient separation as we were mainly interested in the global aspects of ribosomal activity and not primarily in the identity of actively translating mRNAs. Comparing young and aged primary cortical cells, we identified a significant reduction in the number of polysomes for the aged group. This finding is in agreement with previous studies showing a decline in polysome abundance with stable levels of total RNA in ageing *C. elegans* cells [Kirstein-Miles et al., 2013]. Second, we highlighted the rejuvenating potential of the amino acid hypusine in aged cultures reflected by an increase in polysome levels (Fig. 4.14). These findings are the first hints at how hypusine and its precursor Spermidine affect ageing by

controlling translational capacities in a rather complex cellular system such as primary mammalian neuronal cells.

The unusual amino acid hypusine [Park et al., 1981] is solely found as a posttranslational modification of the elongation factor eIF5A, proven by experiments wherein the presence of radioactive-labelled spermidine yeast cells were cultured and eIF5A was the only protein to be found labelled [Murphrey and Gerner, 1987]. Because of its uniqueness, previous studies were already interested to point out the importance of the posttranslational hypusination. Especially in conditions of cellular stress such as oxidative stress or starvation, hypusine-eIF5A promoted translation elongation [Li et al., 2010], [Melnikov et al., 2016]. Studies in yeast defined eIF5A and its binding capacities to the rotated form of the 80S ribosome as the third vital translation elongation factor next to eEF1A and eEF2 [Saini et al., 2009], [Melnikov et al., 2016].

More recent studies described that eIF5A especially facilitates peptide bond formation of proline-rich proteins [Rossi et al., 2016]. As a consequence, depletion of eIF5A leads to translational arrest of polyproline-rich proteins and finally to ribosome stalling, underlining the importance of eIF5A for translating long stretches of proline. Our finding that hypusine restores polysome levels in aged cells could be explained by its stimulating effects in proline peptide bond formation, followed by the release of stalled ribosomes which are again free to start new translational processes or form polyribosomal complexes.

5.2. The integration of mechanical signalling into neuronal development and neuronal ageing

The experiments described in the second part of this thesis (chapter 4.2) connect neuronal cell biology and mechanical signalling for a better understanding of the highly sophisticated communication strategies in neuronal cells. We choose to investigate mechanosensing and -signalling in young, mature, and even aged neurons in more detail since still little is known about these processes. We describe how mechanical properties, such as substrate stiffness, influence central processes in cortical neuronal development including dendritic outgrowth and synaptic maturation and might also impact neuronal function in ageing. Further, for the first time to our knowledge, mechanical cues are shown to influence complex cellular processes including alterations in protein translation and Ca^{2+} signalling being reflected by changes in the neural proteome.

5.2.1. Polyacrylamide gels are a physiological substrate to study mechanosignalling in neuronal cell culture

So far, cell culture studies focusing on neuronal development were performed on glass coverslips. The integration of these experimental findings led to the theoretical concept of how we explain axonal path finding, synaptogenesis and vesicle recycling today. In contrast, it has been proven that the mammalian cortex presents stiffness gradients to neuronal cells dependent on region and developmental stage [Iwashita et al., 2014]. Picking up on the concept, that mechanical forces drive developmental processes, we show the tremendous effects how mimicking *in vivo* brain stiffness can influence developmental processes like dendritic outgrowth and synaptogenesis. We confirm the idea that mechanical signalling plays an important part in neuronal development and should be investigated in more detail.

As an initial experiment, we tested whether Laminin coating, neuronal attachment and cellular growth is similar between cell culture substrates with tunable stiffness and traditionally used glass coverslips. We proved that the different surfaces overall had the same density in Laminin coating and probability of neuronal attachment, opening the path for further investigations. Our results are in line with previous studies utilizing fluorescent coating proteins and stating that protein binding is not influenced by the stiffness of the polyacrylamide gels [Engler et al., 2006], [Leach et al., 2007].

One limitation of our experimental set-up was due to the fact that we had no equipment to directly measure the elastic modulus of the polyacrylamide gels we manufactured. Instead, we had to rely on previous calculations [Pelham and Wang, 1997], [Moshayedi et al., 2010], which defined concentrations of acrylamide and bis-acrylamide to produce gels with a defined stiffness. For future studies, a more detailed control of the actual substrate stiffness would be beneficial to ensure high quality and minimize variations of elastic moduli. Further, the idea arose to manufacture gels with a stiffness gradient but due to temporal limitations, this idea was no further pursued. A central study already pointed out that gradients in substrate stiffness regulate growth direction of *Xenopus* retinal ganglion cell axons [Koser et al., 2016]. These mechanisms probably also hold true for the mammalian system, since we could show that the complexity of dendritic arborisation is determined by substrate stiffness (Fig 4.14). In line with our results, Koser and colleagues showed that soft substrates with a shear modulus of 0.1 kPa, as used by us, promoted spreading of axons which is essential to find their target cell and start synapse formation. This outgrowth pattern also holds true for spinal cord neurons which display a more complex branching pattern on compliant materials [Flanagan et al., 2002].

Additionally, the fact that soft materials similar to the juvenile *in vivo* brain stiffness promote neuronal over glial growth in mixed cortical cultures [Georges et al., 2006] underlines

the idea that as material, glass provides an unphysiological environment for neuronal cells presenting only one defined stiffness throughout lifespan. From early development to maturation brain stiffness increases [Elkin et al., 2010] and this shift in compliance could be one temporal trigger for growth and integration of glia cells into the neuronal network, due to the fact that glial cells prefer a stiffer microdomain than neurons. In general, it is of great importance to study the effect of substrate stiffness or other mechanical cues on glial morphology and metabolism. We demonstrated that substrate stiffness modulates glial shape as described by other authors [Moshayedi et al., 2014], [Lu et al., 2006]. Looking into more detail, stiff substrates had been shown to facilitate glial differentiation in mixed cultures and glia cells are in general softer than neurons (around 0.4 kPa). In combination, these are interesting hints how neuron-glia interaction is also provided via mechanical features and it has been postulated that glia cells provided a soft substrate for neurons to support plasticity [Lu et al., 2006].

5.2.2. New insights in mechanosignalling

Clarifying how mechanotransduction works in detail and which proteins are involved, remains a central question in mechanobiology. Especially during tissue growth and cellular development, individual cells are constantly pushed, pulled, and exposed to physical forces such as shear forces, compression and osmotic pressure. The process how cells sense these forces is termed mechanotransduction. So far, it is known that forces are generated inside cells by the cytoskeleton with actomyosin being one central component. The actomyosin cytoskeleton builds up clusters at the outer membrane known as focal adhesions and connects through transmembrane integrin receptors to the ECM. Whenever a structural deformation appears at the ECM, the whole complex will be structurally reorganized including the position of the ER or even free ribosomes [Wang et al., 1993]. Interestingly, when cells are mechanically stretched, a process occurring frequently during cell growth and development *in vivo*, quaternary domain structures inside protein complexes can be opened [Krammer et al., 1999], proteins like talin or p130cas are being unfolded [del Rio et al., 2009], [Sawada et al., 2006] and even cryptic signalling sites such as hidden cysteine are unmasked for downstream signalling [Johnson et al., 2007]. Taken together, re-localisation of the ER or free ribosomes and structural changes inside protein complexes could be one underlying cause for the difference in protein translation capacities we observed when presenting different mechanical cues to neurons (Fig 4.19, 4.20, 4.23, 4.29). Anyway, the fact that mechanical properties influence protein translation has been described here for the first time and more detailed studies will explain this phenomenon more closely.

A more elaborately studied element in mechanotransduction are stretch-gated ion channels [Lansman et al., 1987] such as channels from the TRP- and ENaC/Dec super family or the recently discovered Piezo family [Coste et al., 2012]. The downstream signalling cas-

cades are mostly speculated on but surely effector kinases and small GTPases are activated for signal amplification and propagation [Ranade et al., 2015]. A number of studies showed that stretch-gated ion channels open with a higher frequency when presented to stiff environments [Zhang et al., 2014], [Pathak et al., 2014]. Because of this, one central point in characterizing neuronal behavior on stiffness regulated gels was to investigate Ca^{2+} signals utilizing established Ca^{2+} indicators such as Fluo-4 AM in live cell imaging [Sato et al., 2007], [Paredes et al., 2008].

5.2.3. Ca^{2+} signalling is modulated by substrate stiffness

In our results, we showed that the number of Ca^{2+} releases per second was significantly increased on compliant gels compared to stiffer substrates or glass coverslips at DIV 10 (Fig 4.24). These results give a hint that developmental Ca^{2+} signalling is indeed influenced by substrate stiffness and that communication via Ca^{2+} flux is essential to build a functional neuronal network. The effect of increased Ca^{2+} oscillations on soft substrates was diminished by applying the widely used IP3 receptor antagonist 2-APB during live recording. In contrast, in a mature cell culture system, Ca^{2+} oscillations were distributed equally between all substrates tested and were again reduced by 2-APB treatment (Fig 4.25). This finding highlights that an established network Ca^{2+} signalling is no longer modulated by mechanical cues such as substrate stiffness. Overall, our findings are a first hint in the rather young field combining Ca^{2+} - and mechanosignalling.

To gather more information about the Ca^{2+} source, we used 2-APB to block Ca^{2+} release from intracellular stores like the ER. More recent studies have shown that 2-APB is a rather unspecific modulator of Ca^{2+} signals since it also modifies TRP channel activity.

In more detail, 2-APB blocks the cation channel TRPM2 [Togashi et al., 2008] and TRPC5 [Xu et al., 2005] and on the other hand stimulates the thermosensitive TRPV1 channel [Mamatova and Kang, 2013]. Since the family of TRP channels are a key player in mechanosensation, the unspecific effects of 2-APB are especially serious in our studies focusing on mechanical signalling. In conclusion, the results of the 2-APB application have to be viewed critically and should not be seen as a definite explanation of the Ca^{2+} source. In future studies, Xestospongin C [Gafni et al., 1997] could be used to block IP3-dependent Ca^{2+} release more specifically and, thus, clarify whether intracellular Ca^{2+} stores are responsible for the oscillations reported here. Another idea is to block ryanodine receptors since they are the second family responsible for Ca^{2+} release from internal stores [Berridge, 1998] or concentrate on Ca^{2+} permeable mechano channels of the TRP- or Piezo family.

We showed that expression levels of the mechanosensor Piezo1 are highest in cells cultured on soft substrates and that the expression of Piezo1 is declining in wild-type mice with age (Fig. 4.26). To our best knowledge, these are the first results depicting that expression of

a mechanoreceptor is regulated by mechanical cues such as substrates stiffness, pointing towards a feedback loop connecting sensing of surface stiffness and activation of transcription factors known as mechanoreciprocity [DuFort et al., 2011]. In turn, the observed differences in Piezo1 expression can be linked to the increased Ca^{2+} oscillations on soft substrates. A recent study described that Piezo1 channel activity modulates human neurogenesis and stimulated neuronal- over glial differentiation through the YAP-kinase of the Hippo pathway [Pathak et al., 2014]. In conclusion, the Piezo family is a promising candidate to concentrate future studies on since evidence increase that this mechanosensor connects central signalling hubs in mechanobiology.

In the past years, several research groups investigated the effect of substrate stiffness on Ca^{2+} signalling. A prominent cellular model system to study the effects of elastic tissue properties are cardiomyocytes since their physiological survival depends highly on the mechanical properties of the surrounding myocardial tissue [Jacot et al., 2010]. The group of Jeffrey Jacot found that soft substrates (soft is defined as 8 kPa for cardiovascular tissue) mimicking the same elastic features as juvenile cardiovascular tissue increased maximum Ca^{2+} currents and action potential duration in neonatal rat ventricular myocytes [Jacot et al., 2008], [Boothe et al., 2016]. Also in human mesenchymal stem cells Ca^{2+} oscillations were highest on soft substrates and that these effects are probably regulated by the RhoA / ROCK pathway [Kim et al., 2009]. For neuronal cells only one study was published this far revealing that Ca^{2+} oscillations are more frequent on stiff substrates in primary hippocampal neurons or PC12 cells [Zhang et al., 2014]. That we reported the opposite effects for cortical neurons is not surprising since cortex and hippocampus differ in their cellular composition and mechanical tissue properties.

Free Ca^{2+} ions are central signalling molecules in biological systems and control complex functions such as vesicle release, synaptic plasticity and even gene transcription in neurons [Lohmann and Bonhoeffer, 2008]. It is well described that Ca^{2+} influx controls neurotransmitter release via the Ca^{2+} sensor Synaptotagmin-1 (for review see [Südhof, 2012]). We described an increased synaptic vesicle recycling for neurons cultured on compliant gels. This effect can be related to the higher frequency of spontaneous Ca^{2+} oscillations on compliant gels suggesting that differences in Ca^{2+} signalling are the main source connecting our observations of how substrate stiffness modulates neuronal development.

5.2.4. Proteomic analysis give hints how mechanical signalling encodes and transduces substrates stiffness presented to neuronal cells

To spot molecules involved in cellular signalling pathways, mainly genomic methods or biochemical assays have been used traditionally. Nowadays, the technical progress made in the field of nano liquid chromatography coupled to mass spectrometric analysis, let this tech-

nique become a common tool to discover and study previously unknown signalling pathways [Pandey et al., 2000], [Ho et al., 2002]. To this point, three studies investigated how mechanical cues influence protein expression and rates of protein synthesis by analysing cells grown on stiffness regulated substrates with mass spectrometry. One study concentrated on tumor cells and presented soft and stiff microenvironments. They were able to show that over 1200 cellular proteins were regulated by these growth conditions such as proteins essential for cytoskeletal structures (tubulins) and proteins known as regulators of the NAD salvage pathway [Tilghman et al., 2012]. The team of Viljar Jaks investigated ECM composition of liver tissue after damage and showed stiffness dependent changes in ECM structural components including elastin, fibronectin and collagens I, IV, V [Klaas et al., 2016]. As last cell type, mesenchymal stem cells grown on gelatinous gels with tunable stiffness were examined by proteomic analysis and the abundance of cytoskeletal proteins such as vimentin, tubulin, beta-actin and alpha-tubulin were significantly different between soft and stiff substrates [Kuboki et al., 2012]. So far, a proteomic study investigating how substrate stiffness influences protein expression in neuronal cells, especially during development, is missing and for that reason, we conducted such an experiment.

We identified 1613 proteins with at least 2 unique peptides for all four substrates tested and compared the three gel conditions (compliant 0.1 kPa, intermediate 1 kPa and stiff 10 kPa) with control conditions (conventional glass coverslips). We were especially interested in proteins that showed a gradual expression pattern between the different stiffness conditions tested: either highest expression on soft substrates with decreasing abundance as stiffness increases or highest expression on stiff substrates with decreasing abundance as stiffness is reduced (see heat map Fig. 4.28). For the 'up-regulated on soft substrates' cluster we selected GRAP1 (GRASP-1), EVL (Ena/VASP-like protein), SHLB2 (Endophilin B2) and MARCS (Myristoylated alanine-rich C-kinase substrate) as candidate proteins since their cellular function can be related to the effects mechanical cues had on dendritic outgrowth and synaptic maturation described in Fig 4.14 to 4.18.

The increased expression level of the recycling endosome protein GRASP-1 detected on soft substrates is in line with the accelerated vesicle recycling and early expression of synaptic proteins we described beforehand (Fig. 4.15, 4.17, 4.18). Recent studies further link GRASP-1 to glutamatergic synapse function and animal learning behaviour [Chiu et al., 2017]. Interestingly, point mutations detected in the GRASP1 gene we associated with forms of intellectual disability in human patients. In conclusion, a sufficient GRASP-1 expression is essential for proper AMPAR-dependent synaptic function and pathophysiological increases in brain tissue stiffness could be harmful. The finding that expression levels of the actin regulator EVL are regulated by substrate stiffness gives a hint that the Ena/VASP family is involved in mechanical signal transduction and that the observed morphological differences in neurite outgrowth

(Fig. 4.15) could be associated with this signalling cascade. In cortical development, the rearrangement of the actin cytoskeleton during neurite growth and retraction is essentially regulated by Ena/VASP proteins since knock-out mice lacking all three murine Ena/VASP proteins show severe defects in axon formation and neuritogenesis [Kwiatkowski et al., 2007]. We showed that the abundance of EVL is regulated by substrate stiffness and axons use mechanical signals during path finding [Koser et al., 2016], the Ena/VASP family could be an essential link between mechanical cues presented to cells in their natural environment, the actin cytoskeleton and neuritogenesis [Lin et al., 2007].

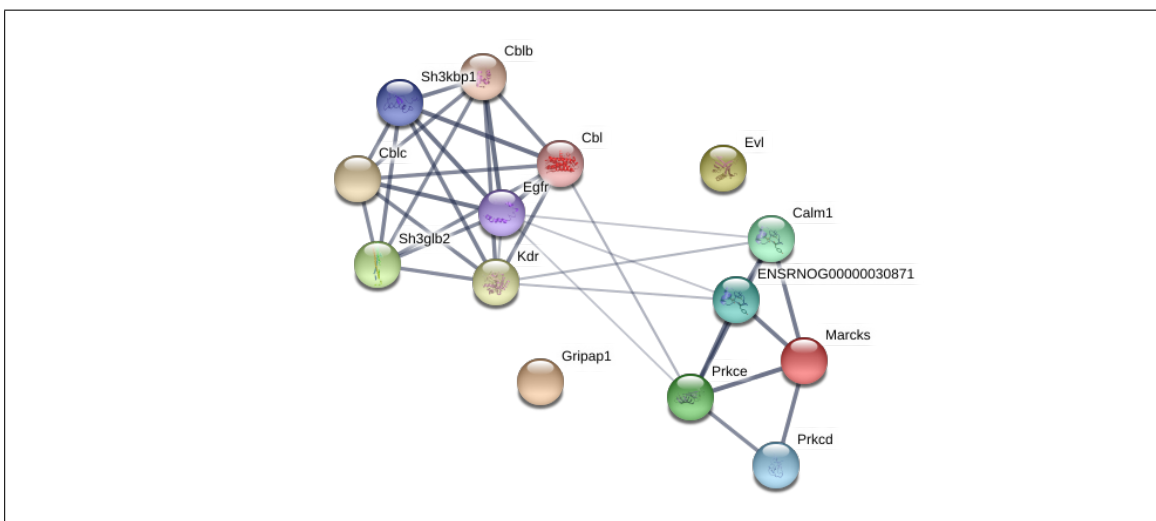


Figure 5.1.: STRING Network analysis of protein cluster 'up-regulated on soft substrates' Predicted protein-protein interactions for candidate proteins 'up-regulated on soft substrates': GRAP1 (GRASP-1), EVL (Ena/VASP-like protein), SHLB2 (Endophilin B2) and MARCS (Myristoylated alanine-rich C-kinase substrate) calculated with STRING database. Abbreviations: Marcks = Myristoylated alanine-rich C-kinase substrate, Gripap1 = GRIP1-associated protein 1, Sh3glb2 = SH3-domain GRB2-like endophilin B2, Prkce = Protein kinase C epsilon type, Calm1 = Calmodulin, Prkcd = Protein kinase C delta type, Sh3kbp1 = SH3 domain-containing kinase-binding protein 1, Egfr = Epidermal growth factor receptor precursor, Cbl = Protein Cbl, Cblb = E3 ubiquitin-protein ligase CBL-B, Cblc = Cas-Br-M, Kdr = Vascular endothelial growth factor receptor 2 precursor.

For Endophilin B2, different functions have been proposed. One study claims that endophilin B2 regulates endocytic vesicle trafficking and promotes maturation of autophagosomes to late endosomes or lysosomes [Serfass et al., 2017]. Another research group showed that endophilin B2 facilitates inner mitochondrial membrane degradation [Wang et al., 2016]. Due to the uncertainty of endophilin B2 function, especially in neuronal cells, I will withhold potential explanations for the detected upregulation on soft substrates. The significant upregulation of MARCKS on soft substrates mimicking developmental brain tissue underlines its importance in regulating actin dynamics in juvenile neurons [Stumpo et al., 1995]. In more detail, MARCKS is claimed to stabilize growth cone adhesions in its non-phosphorylated form and via phosphorylation destabilises growth cone dynamics to facilitate directional changes

and turning of the growth cone during pathfinding [Gatlin et al., 2006].

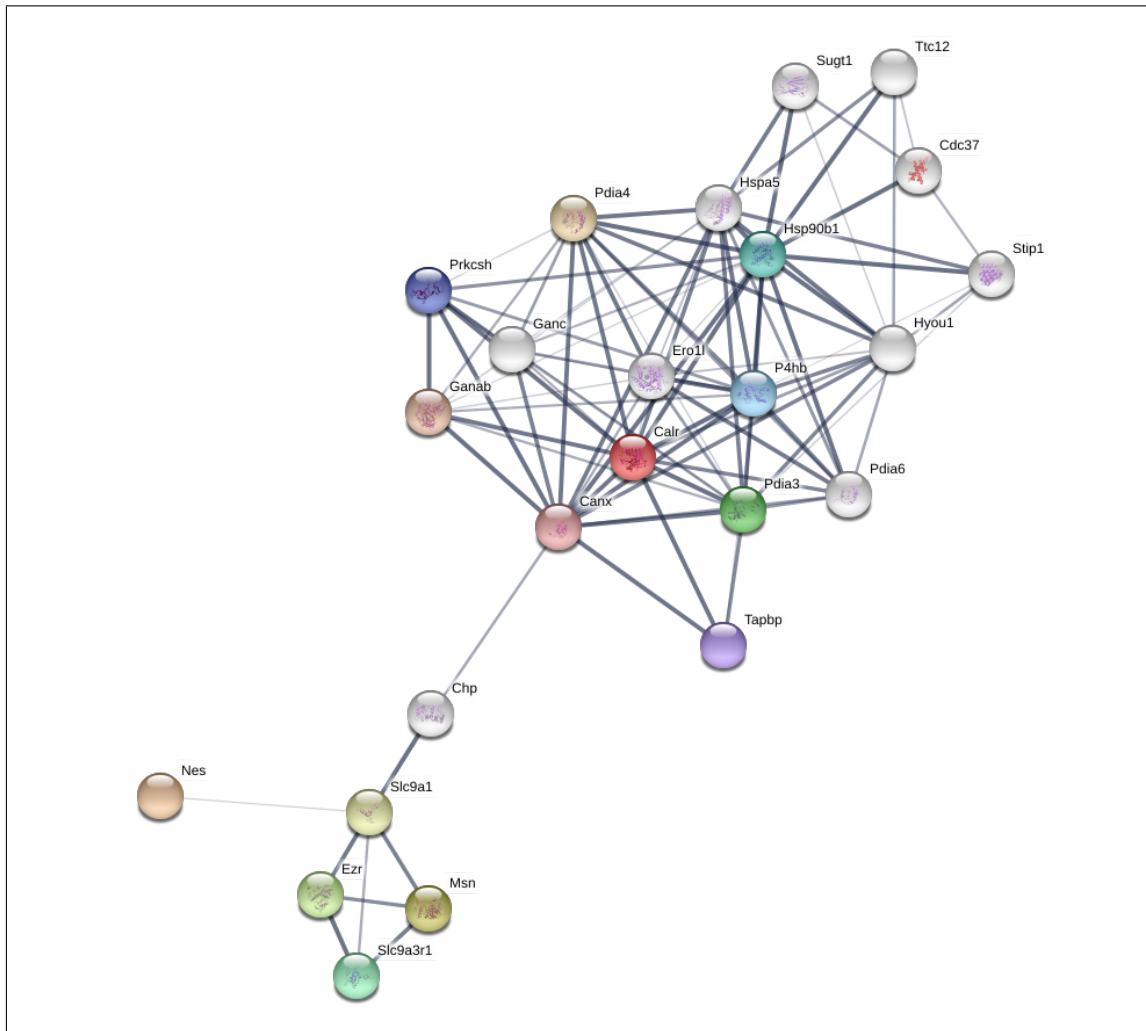


Figure 5.2.: STRING Network analysis of protein cluster 'down-regulated on soft substrates' Predicted protein-protein interactions for candidate proteins 'down-regulated on soft substrates': EZRI (Ezrin), MOES (Moesin), NEST (Nestin) and CALR (Calreticulin) provided by STRING database. Abbreviations: Calr = Calreticulin, Nes = Nestin, Msn = Moesin, Ezr = Ezrin, Pdia3 = Protein disulfide-isomerase A3, Slc9a3r1= Na(+) / H(+) exchange regulatory cofactor NHE-RF1, Hsp90b1 = Endoplasmic, P4hb = Protein disulfide-isomerase, Prkcs = Glucosidase 2 subunit beta precursor, Tapbp = TAP-binding protein precursor, Canx = Calnexin, Ganab = Neutral alpha-glucosidase AB, Pdia4 = Protein disulfide-isomerase A4 precursor, Slc9a1 = Sodium Hydrogen exchanger 1.

How these four candidate proteins are interconnected is depicted by a STRING network analysis identifying protein-protein interactions and presented here for a better illustration (Fig 5.1).

For the second cluster, 'down-regulated on soft substrates', EZRI (Ezrin), MOES (Moesin),

NEST (Nestin) and CALR (Calreticulin) have been identified as candidate proteins. The gradual increase in the expression of Ezrin and Moesin with higher stiffness can be viewed as compensatory mechanism to provide functional growth cone motility and neurite extension even on stiff substrates. The family of Ezrin / Radixin / Moesin proteins is known to be activated by Rho kinase and to mediate their function after phosphorylation [Haas et al., 2007]. Our mass spec analysis does not give information about the phosphorylation status of Ezrin and Moesin, so increased protein expression may not reflect a higher activation.

The reduced expression of Nestin in cells grown on soft substrates clearly reinforces the accelerated developmental processes described before (see Fig. 4.14 - 4.18 and 4.24). As a structural intermediate filament protein, Nestin is described to be found exclusively in neural progenitor cells or in unique neurons inside a small niche in the adult brain, and is replaced by GFAP in glia cells or neurofilaments in neurons as they mature into their differentiated state [Hendrickson et al., 2011]. Our finding that Nestin is less expressed in neuronal cells grown on soft substrates could reflect the promotion of cell maturation by mechanical cues presented by soft substrates [Mousavi and Doweidar, 2015], [Lourenço et al., 2016] and is of special interest for the field of neuronal stem cell research. The increased Calreticulin expression in neuronal cells grown on stiffer substrates may reflect a stress response triggered by the not-physiological mechanical properties presented to the cells. Further, it is known that stiff substrates trigger inflammatory processes in glia cells [Moshayedi et al., 2014], so culturing primary neuronal cells on substrates reflecting actual *in vivo* brain stiffness could be beneficial to reduce cellular stress and inflammatory processes. Again, a STRING network analysis was performed to illustrate protein-protein interactions between these four candidate proteins (Fig 5.2) and connect potential signalling pathways.

Since we only identified 1613 proteins from a rather complex cell culture sample, ideas arose on how to improve future proteomic analysis. One approach is to simply increase the protein concentration of a given protein mixture by pooling more cell culture sample from a 6-well plate. Another option would be to use harsher deattachment conditions to increase harvesting efficiency, but chemical detergents again interfere with mass spec based protein identification so a mechanical separation suits better. One limitation was also to build a large surface area with defined elastic properties to increase the volume of cellular material. This technical limitation could be solved in collaboration with a department specialized in nano fabrication of hydrogels. Anyway, our identified candidates and also the whole data set can be viewed as an information platform for future studies interested in pathways of mechanotransduction. Especially the actin regulator EVL and the corresponding protein network, known to be involved in path finding and axonal outgrow, is a promising candidate for further investigations.

Very recently, a proteomic study was released focusing on mechanotransduction in PC12

cells in response to variations in nanotopographic features [Schulte et al., 2017]. The group of Gabriella Tedeschi was able to show that ECM-like nano roughness [Chen et al., 2014], [Dalby et al., 2014], another key mechanical cue presented to neuronal cells besides substrate stiffness, promotes neuronal differentiation similar to biochemical signals such as NGF stimulation. Since the signalling pathways of mechanotransduction are mainly unknown they used a shotgun mass spectrometry approach with label free quantification, similar to our proteomic analysis of primary cortical neurons. Their proteomic experiment revealed a complex signalling hub with many proteins regulated including key modulators of actomyosin organisation, ECM and integrin activation and cell-cell adhesion. Consistent with our results, they also pointed out that mechanotransduction is associated with the mTOR signalling pathway and Ca^{2+} oscillations [Maffioli et al., 2017].

5.2.5. Are long-term neuronal cultures on stiffness regulated gels a suited model for brain ageing?

Ageing is a multifaceted and highly individual process accompanied by declining functionality of almost every organ and miscommunication inside various cellular networks, ultimately leading to degenerative processes. Changes in brain elastic moduli have been related to a variety of age-related neurological diseases such as multiple sclerosis [Streitberger et al., 2012], brain tumours and neurodegenerative diseases [Murphy et al., 2011]. Additionally, it has been demonstrated that with increasing age tissue and different cell types such as fibroblasts [Schulze et al., 2010] and myocytes [Lieber et al., 2004] show an impaired response to mechanical forces, whereas studies focusing on neuronal cells are missing so far [Wu et al., 2011]. Due to these observations, it is of pivotal interest to determine the mechanic features and details in mechanotransduction for specific brain regions and cell populations throughout the live span in health and disease.

In this study, we were the first to show that long-term neuronal cultures survive on stiffness regulated polyacrylamide gels. Further, the tunable elastic properties presented to neuronal cells had a functional relevance. On soft substrates with similar stiffness than juvenile brain tissue, higher rates in *de novo* protein synthesis were visualized compared to stiffer substrates (Fig 4.30). Interestingly, the formation of p62-positive protein aggregates was promoted by stiff substrates during ageing and neurons grown on soft gels were almost free of proteins tagged for degradation (Fig 4.31). This observation suggests that mechanoreciprocity is involved in protein homoeostasis and that *in vivo* brain stiffness is a potential regulator of protein aggregation. These findings underline the relevance of mechanical signalling in age-related deficits in proteostasis and future studies are needed to explain this observation in more detail.

There are different methods to measure elastic properties of brain tissue. So far, studies

conducted in rodents and human show conflicting results considering tissue elasticity during brain ageing. Elkin and colleagues showed that rat cortical tissue stiffens from P10 to adulthood measured by atomic force microscopy [Elkin et al., 2010]. In this study, the age-span 'adult' remains undefined and also more aged time points would be of interest. Another interesting study postulates that induced adult hippocampal neurogenesis is responsible for enhanced brain stiffness in a mouse model for dopaminergic neurodegeneration [Klein et al., 2014], again linking mechanical cues and cellular actions.

For the human brain a decrease in elastic modulus was measured by non-invasive magnetic resonance elastography in two studies [Arani et al., 2015], [Sack et al., 2009]. In conclusion, it can be stated that ageing has an influence on elastic brain properties but the trends remain unclear. Eventually, the human and rodent brain behaves differently or the two methods cannot be compared. One additional study could investigate rodent brain stiffness using magnetic resonance elastography as performed by Murphy and colleagues [Murphy et al., 2012] who showed a decline in rodent brain stiffness in a mouse model of AD. Additionally, the participants in human studies could be diagnosed for potential early signs of mild cognitive decline to ensure a group actually representing physiological ageing. Another idea is that brain tissue presents complex stiffness gradients in defined microdomains and measuring overall stiffness is just too superficial to make a conclusion towards an intrinsic mechanism. This concept is in line with findings that during ageing axonal viscosity is increasing and this process was associated with a lack of axonal regeneration in adult sensory axons [Lamoureux et al., 2010].

Given the increasing prevalence of AD and rising life expectancies worldwide, also the mechanical aspects of neurodegenerative disease are of interest and could explain the progression in more detail. As mentioned before, the nanomechanical properties of alpha-synuclein- and amyloid fibrils were measured with harmonic force microscopy [Sweers et al., 2011]. Once the soluble amyloid and alpha-synuclein proteins form fibrillar nano structures their elastic moduli increase up to the GPa range [Paparcone et al., 2010]. The detection of these ultra-stiff fibrils using magnetic resonance elastography has the potential to be an early diagnostic tool for degenerative diseases. Since changes in brain elasticity can also be measured non-invasive by ultrasound hyperechogenicity even in deep areas like the substantia nigra, revealing decreased brain stiffness in this area is already used as a detection method for Parkinson's disease even before motor problems occur [Berg, 2011].

In summary, the rather young field of neuromechanics is not able to give defined answers to central questions in mechanobiology, yet. More studies need to be conducted and repeated to find out more details on how the elastic properties of brain tissue and neuronal cells itself contribute to the ageing process. Anyway, stiffness regulated gels are a great tool to present mechanical cues to neuronal cells and study cellular development, maturation and ageing

since they model actually *in vivo* brain stiffness.

6. Outlook

Certainly, the crosstalk between chemical- and mechanical signalling is even more complex than described in this dissertation. In this short outlook, I will present further ideas to learn more about the connection between mechanical cues and brain function.

Utilizing the stiffness regulated cell culture substrates presented and characterised in this thesis, future experiments regarding mechanobiology in neuronal cells can be conducted. It will be of special interest to investigate disease states known to interfere with mechanical properties and integrity of the nervous tissue. Here, especially glial cells with their inherent ability to proliferate at high numbers even at adult age [Jäkel and Dimou, 2017] are known to contribute to alterations in brains stiffness [Moeendarbary et al., 2017] such as glial scar formation after injury or glial activation during inflammation. As one potential experimental concept to explore potential mechanosensitive pathways in glial activation, primary neuronal cultures or glial monocultures grown on stiffness regulated substrates could be challenged by viral infection or incubation with soluble cytokines such as interferon-gamma. Building on that, it would be of great interest to analyse cell morphology and different signalling cascade related to protein translation or inflammation processes. The results obtained would be compared between the different degrees of substrate stiffness presented to the cells. Finally, these future approaches should guide improvements in regenerative medicine and facilitate brain recovery after injuries of a different kind.

Also the formation of insoluble protein aggregates, tangles and fibrils during neurodegenerative diseases such as AD or Parkinson's disease cause disturbances inside the mechanical environment. Aggregated forms of alpha-synuclein or beta-amyloid share an elastic modulus in GPa range and this extreme stiffness could be an additional reason why the cellular protein degradation systems are unable to handle these aggregates. In consequence, it is of significant importance to integrate the concepts of mechanobiology into neurodegenerative research.

A high diversity of electrophysiological studies could be performed by experts in this fields. The results would lead to a more detailed characterisation of electrical signalling and receptor properties of neuronal cells cultured on stiffness regulated gels. Different mechanical receptors could be silenced by introducing shRNA constructs via transfection using electroporation or even lentiviral expression if longer culturing periods are necessary.

We were able to characterize one mechano receptor and showed that the mechanosensor Piezo-1 is a central element in translating mechanical forced into chemical, intracellular signals. One way to investigate Piezo-1 function in the brain in more details would be the generation of a neuron-specific, conditional knock-out mouse line [Wang et al., 2010], potentially using CRISPR / Cas gene editing[Horii et al., 2017], [Miura et al., 2018]. Since Piezo-1 is vital during organ formation and a complete knock-out leads to mostly lethal offspring [Ranade et al., 2014a], [Zhao et al., 2017].

Taken together, the experimental approaches and results described in this dissertation build a solid foundation for future investigations. Based on this foundation a profound and deeper gain of knowledge in the fields of ageing research and neuromechanics will be enabled.

Bibliography

- [Ahmed et al., 2018] Ahmed, M. S., Ikram, S., Bibi, N., and Mir, A. (2018). Hutchinson-gilford progeria syndrome: A premature aging disease. *Mol Neurobiol*, 55(5):4417–4427.
- [Aksenova et al., 1999] Aksenova, M. V., Aksenov, M. Y., Markesberry, W. R., and Butterfield, D. A. (1999). Aging in a dish: age-dependent changes of neuronal survival, protein oxidation, and creatine kinase bb expression in long-term hippocampal cell culture. *J Neurosci Res*, 58(2):308–17.
- [Aliper et al., 2017] Aliper, A., Jellen, L., Cortese, F., Artemov, A., Karpinsky-Semper, D., Moskalev, A., Swick, A. G., and Zhavoronkov, A. (2017). Towards natural mimetics of metformin and rapamycin. *Aging (Albany NY)*, 9(11):2245–2268.
- [Andersen et al., 2005] Andersen, J. S., Lam, Y. W., Leung, A. K. L., Ong, S.-E., Lyon, C. E., Lamond, A. I., and Mann, M. (2005). Nucleolar proteome dynamics. *Nature*, 433(7021):77–83.
- [Araneda et al., 1999] Araneda, R. C., Lan, J. Y., Zheng, X., Zukin, R. S., and Bennett, M. V. (1999). Spermine and arcaine block and permeate n-methyl-d-aspartate receptor channels. *Biophys J*, 76(6):2899–911.
- [Arani et al., 2015] Arani, A., Murphy, M. C., Glaser, K. J., Manduca, A., Lake, D. S., Kruse, S. A., Jack, Jr, C. R., Ehman, R. L., and Huston, 3rd, J. (2015). Measuring the effects of aging and sex on regional brain stiffness with mr elastography in healthy older adults. *Neuroimage*, 111:59–64.
- [Athamneh and Suter, 2015] Athamneh, A. I. M. and Suter, D. M. (2015). Quantifying mechanical force in axonal growth and guidance. *Front Cell Neurosci*, 9:359.
- [Badin and Herve, 1965] Badin, J. and Herve, B. (1965). [protein precipitation by amidoschwarz and its application to the microdetermination of blood proteins]. *Ann Biol Clin (Paris)*, 23:321–32.
- [Bae et al., 2011] Bae, C., Sachs, F., and Gottlieb, P. A. (2011). The mechanosensitive ion channel piezo1 is inhibited by the peptide gsmtx4. *Biochemistry*, 50(29):6295–300.
- [Balch et al., 2008] Balch, W. E., Morimoto, R. I., Dillin, A., and Kelly, J. W. (2008). Adapting proteostasis for disease intervention. *Science*, 319(5865):916–9.

- [Balgude et al., 2001] Balgude, A. P., Yu, X., Szymanski, A., and Bellamkonda, R. V. (2001). Agarose gel stiffness determines rate of drg neurite extension in 3d cultures. *Biomaterials*, 22(10):1077–84.
- [Banker and Cowan, 1977] Banker, G. A. and Cowan, W. M. (1977). Rat hippocampal neurons in dispersed cell culture. *Brain Res*, 126(3):397–42.
- [Bard et al., 2018] Bard, J. A. M., Goodall, E. A., Greene, E. R., Jonsson, E., Dong, K. C., and Martin, A. (2018). Structure and function of the 26s proteasome. *Annu Rev Biochem*.
- [Baynes, 2001] Baynes, J. W. (2001). The role of ages in aging: causation or correlation. *Exp Gerontol*, 36(9):1527–37.
- [Beatty et al., 2006] Beatty, K. E., Liu, J. C., Xie, F., Dieterich, D. C., Schuman, E. M., Wang, Q., and Tirrell, D. A. (2006). Fluorescence visualization of newly synthesized proteins in mammalian cells. *Angew Chem Int Ed Engl*, 45(44):7364–7.
- [Berg, 2011] Berg, D. (2011). Hyperechogenicity of the substantia nigra: pitfalls in assessment and specificity for parkinson’s disease. *J Neural Transm (Vienna)*, 118(3):453–61.
- [Bernardes de Jesus et al., 2012] Bernardes de Jesus, B., Vera, E., Schneeberger, K., Tejera, A. M., Ayuso, E., Bosch, F., and Blasco, M. A. (2012). Telomerase gene therapy in adult and old mice delays aging and increases longevity without increasing cancer. *EMBO Mol Med*, 4(8):691–704.
- [Bernick et al., 2011] Bernick, K. B., Prevost, T. P., Suresh, S., and Socrate, S. (2011). Biomechanics of single cortical neurons. *Acta Biomater*, 7(3):1210–9.
- [Berridge, 1998] Berridge, M. J. (1998). Neuronal calcium signaling. *Neuron*, 21(1):13–26.
- [Bertrand et al., 2011] Bertrand, S. J., Aksenova, M. V., Aksenov, M. Y., Mactutus, C. F., and Booze, R. M. (2011). Endogenous amyloidogenesis in long-term rat hippocampal cell cultures. *BMC Neurosci*, 12:38.
- [Bigagli et al., 2016] Bigagli, E., Luceri, C., Scartabelli, T., Dolara, P., Casamenti, F., Pellegrini-Giampietro, D. E., and Giovannelli, L. (2016). Long-term neuroglial cocultures as a brain aging model: Hallmarks of senescence, microRNA expression profiles, and comparison with in vivo models. *J Gerontol A Biol Sci Med Sci*, 71(1):50–60.
- [Birnboim and Doly, 1979] Birnboim, H. C. and Doly, J. (1979). A rapid alkaline extraction procedure for screening recombinant plasmid dna. *Nucleic Acids Res*, 7(6):1513–23.
- [Bitto et al., 2014] Bitto, A., Lerner, C. A., Nacarelli, T., Crowe, E., Torres, C., and Sell, C. (2014). P62/sqstm1 at the interface of aging, autophagy, and disease. *Age (Dordr)*, 36(3):9626.

- [Bjørkøy et al., 2006] Bjørkøy, G., Lamark, T., and Johansen, T. (2006). p62/sqstm1: a missing link between protein aggregates and the autophagy machinery. *Autophagy*, 2(2):138–9.
- [Blagosklonny, 2011] Blagosklonny, M. V. (2011). Rapamycin-induced glucose intolerance: hunger or starvation diabetes. *Cell Cycle*, 10(24):4217–24.
- [Blumenthal et al., 2014] Blumenthal, N. R., Hermanson, O., Heimrich, B., and Shastri, V. P. (2014). Stochastic nanoroughness modulates neuron-astrocyte interactions and function via mechanosensing cation channels. *Proc Natl Acad Sci U S A*, 111(45):16124–9.
- [Boeckers et al., 2002] Boeckers, T. M., Bockmann, J., Kreutz, M. R., and Gundelfinger, E. D. (2002). Prosap/shank proteins - a family of higher order organizing molecules of the postsynaptic density with an emerging role in human neurological disease. *J Neurochem*, 81(5):903–10.
- [Bomsdorf, 2004] Bomsdorf, E. (2004). Life expectancy in germany until 2050. *Exp Gerontol*, 39(2):159–63.
- [Boothe et al., 2016] Boothe, S. D., Myers, J. D., Pok, S., Sun, J., Xi, Y., Nieto, R. M., Cheng, J., and Jacot, J. G. (2016). The effect of substrate stiffness on cardiomyocyte action potentials. *Cell Biochem Biophys*, 74(4):527–535.
- [Borges et al., 2012] Borges, B. C., Rorato, R., Antunes-Rodrigues, J., and Elias, L. L. K. (2012). Glial cell activity is maintained during prolonged inflammatory challenge in rats. *Braz J Med Biol Res*, 45(8):784–91.
- [Bories et al., 2013] Bories, C., Husson, Z., Guitton, M. J., and De Koninck, Y. (2013). Differential balance of prefrontal synaptic activity in successful versus unsuccessful cognitive aging. *J Neurosci*, 33(4):1344–56.
- [Brewer and Price, 1996] Brewer, G. J. and Price, P. J. (1996). Viable cultured neurons in ambient carbon dioxide and hibernation storage for a month. *Neuroreport*, 7(9):1509–12.
- [Brini et al., 2014] Brini, M., Calì, T., Ottolini, D., and Carafoli, E. (2014). Neuronal calcium signaling: function and dysfunction. *Cell Mol Life Sci*, 71(15):2787–814.
- [Brody, 1955] Brody, H. (1955). Organization of the cerebral cortex. iii. a study of aging in the human cerebral cortex. *J Comp Neurol*, 102(2):511–6.
- [Brown et al., 2004] Brown, M. R., Geddes, J. W., and Sullivan, P. G. (2004). Brain region-specific, age-related, alterations in mitochondrial responses to elevated calcium. *J Bioenerg Biomembr*, 36(4):401–6.
- [Browne et al., 2004] Browne, G. J., Finn, S. G., and Proud, C. G. (2004). Stimulation of the amp-activated protein kinase leads to activation of eukaryotic elongation factor 2 kinase and to its phosphorylation at a novel site, serine 398. *J Biol Chem*, 279(13):12220–31.

- [Browne and Proud, 2004] Browne, G. J. and Proud, C. G. (2004). A novel mtor-regulated phosphorylation site in elongation factor 2 kinase modulates the activity of the kinase and its binding to calmodulin. *Mol Cell Biol*, 24(7):2986–97.
- [Brunetti et al., 2010] Brunetti, V., Maiorano, G., Rizzello, L., Sorce, B., Sabella, S., Cingolani, R., and Pompa, P. P. (2010). Neurons sense nanoscale roughness with nanometer sensitivity. *Proc Natl Acad Sci U S A*, 107(14):6264–9.
- [Burke and Barnes, 2006] Burke, S. N. and Barnes, C. A. (2006). Neural plasticity in the ageing brain. *Nat Rev Neurosci*, 7(1):30–40.
- [Burkhart et al., 2012] Burkhart, J. M., Schumbrutzki, C., Wortelkamp, S., Sickmann, A., and Zahedi, R. P. (2012). Systematic and quantitative comparison of digest efficiency and specificity reveals the impact of trypsin quality on ms-based proteomics. *J Proteomics*, 75(4):1454–62.
- [Burstein and Frankel, 1968] Burstein, A. H. and Frankel, V. H. (1968). The viscoelastic properties of some biological materials. *Ann N Y Acad Sci*, 146(1):158–65.
- [Buxboim et al., 2010] Buxboim, A., Ivanovska, I. L., and Discher, D. E. (2010). Matrix elasticity, cytoskeletal forces and physics of the nucleus: how deeply do cells 'feel' outside and in? *J Cell Sci*, 123(Pt 3):297–308.
- [Cáceres et al., 1986] Cáceres, A., Banker, G. A., and Binder, L. (1986). Immunocytochemical localization of tubulin and microtubule-associated protein 2 during the development of hippocampal neurons in culture. *J Neurosci*, 6(3):714–22.
- [Campisi and d’Adda di Fagagna, 2007] Campisi, J. and d’Adda di Fagagna, F. (2007). Cellular senescence: when bad things happen to good cells. *Nat Rev Mol Cell Biol*, 8(9):729–40.
- [Campos et al., 2014] Campos, P. B., Paulsen, B. S., and Rehen, S. K. (2014). Accelerating neuronal aging in in vitro model brain disorders: a focus on reactive oxygen species. *Front Aging Neurosci*, 6:292.
- [Castorina et al., 2015] Castorina, A., Szychlinska, M. A., Marzagalli, R., and Musumeci, G. (2015). Mesenchymal stem cells-based therapy as a potential treatment in neurodegenerative disorders: is the escape from senescence an answer? *Neural Regen Res*, 10(6):850–8.
- [Celedon et al., 2011] Celedon, A., Hale, C. M., and Wirtz, D. (2011). Magnetic manipulation of nanorods in the nucleus of living cells. *Biophys J*, 101(8):1880–6.
- [Chada et al., 1997] Chada, S., Lamoureux, P., Buxbaum, R. E., and Heidemann, S. R. (1997). Cytomechanics of neurite outgrowth from chick brain neurons. *J Cell Sci*, 110 (Pt 10):1179–86.

- [Chapman, 2002] Chapman, E. R. (2002). Synaptotagmin: a Ca^{2+} sensor that triggers exocytosis? *Nat Rev Mol Cell Biol*, 3(7):498–508.
- [Chassé et al., 2017] Chassé, H., Boulben, S., Costache, V., Cormier, P., and Morales, J. (2017). Analysis of translation using polysome profiling. *Nucleic Acids Res*, 45(3):e15.
- [Chattopadhyay et al., 2008] Chattopadhyay, M. K., Park, M. H., and Tabor, H. (2008). Hypusine modification for growth is the major function of spermidine in *Saccharomyces cerevisiae* polyamine auxotrophs grown in limiting spermidine. *Proc Natl Acad Sci U S A*, 105(18):6554–9.
- [Chen and Grinnell, 1995] Chen, B. M. and Grinnell, A. D. (1995). Integrins and modulation of transmitter release from motor nerve terminals by stretch. *Science*, 269(5230):1578–80.
- [Chen and Liu, 1997] Chen, K. Y. and Liu, A. Y. (1997). Biochemistry and function of hypusine formation on eukaryotic initiation factor 5a. *Biol Signals*, 6(3):105–9.
- [Chen et al., 2016] Chen, L., Li, W., Maybeck, V., Offenhäusser, A., and Krause, H.-J. (2016). Statistical study of biomechanics of living brain cells during growth and maturation on artificial substrates. *Biomaterials*, 106:240–9.
- [Chen et al., 2010] Chen, Q.-R., Song, Y. K., Yu, L.-R., Wei, J. S., Chung, J.-Y., Hewitt, S. M., Veenstra, T. D., and Khan, J. (2010). Global genomic and proteomic analysis identifies biological pathways related to high-risk neuroblastoma. *J Proteome Res*, 9(1):373–82.
- [Chen and Chung, 2013] Chen, R. and Chung, S.-H. (2013). Effect of gating modifier toxins on membrane thickness: implications for toxin effect on gramicidin and mechanosensitive channels. *Toxins (Basel)*, 5(2):456–71.
- [Chen et al., 2014] Chen, W., Shao, Y., Li, X., Zhao, G., and Fu, J. (2014). Nanotopographical surfaces for stem cell fate control: Engineering mechanobiology from the bottom. *Nano Today*, 9(6):759–784.
- [Chen and Sabatini, 2012] Chen, Y. and Sabatini, B. L. (2012). Signaling in dendritic spines and spine microdomains. *Curr Opin Neurobiol*, 22(3):389–96.
- [Chiocchetti et al., 2007] Chiocchetti, A., Zhou, J., Zhu, H., Karl, T., Haubenreisser, O., Rinnerthaler, M., Heeren, G., Oender, K., Bauer, J., Hintner, H., Breitenbach, M., and Breitenbach-Koller, L. (2007). Ribosomal proteins rpl10 and rps6 are potent regulators of yeast replicative life span. *Exp Gerontol*, 42(4):275–86.
- [Chiu et al., 2017] Chiu, S.-L., Diering, G. H., Ye, B., Takamiya, K., Chen, C.-M., Jiang, Y., Niranjan, T., Schwartz, C. E., Wang, T., and Huganir, R. L. (2017). Grasp1 regulates synaptic plasticity and learning through endosomal recycling of AMPA receptors. *Neuron*, 93(6):1405–1419.e8.

- [Cline, 2001] Cline, H. T. (2001). Dendritic arbor development and synaptogenesis. *Curr Opin Neurobiol*, 11(1):118–26.
- [Cohen et al., 2013] Cohen, L. D., Zuchman, R., Sorokina, O., Müller, A., Dieterich, D. C., Armstrong, J. D., Ziv, T., and Ziv, N. E. (2013). Metabolic turnover of synaptic proteins: kinetics, interdependencies and implications for synaptic maintenance. *PLoS One*, 8(5):e63191.
- [Condello and Stöehr, 2018] Condello, C. and Stöehr, J. (2018). A propagation and strains: Implications for the phenotypic diversity in alzheimer’s disease. *Neurobiol Dis*, 109(Pt B):191–200.
- [Cook et al., 2009] Cook, C., Gass, J., Dunmore, J., Tong, J., Taylor, J., Eriksen, J., McGowan, E., Lewis, J., Johnston, J., and Petrucelli, L. (2009). Aging is not associated with proteasome impairment in ups reporter mice. *PLoS One*, 4(6):e5888.
- [Coste et al., 2010] Coste, B., Mathur, J., Schmidt, M., Earley, T. J., Ranade, S., Petrus, M. J., Dubin, A. E., and Patapoutian, A. (2010). Piezo1 and piezo2 are essential components of distinct mechanically activated cation channels. *Science*, 330(6000):55–60.
- [Coste et al., 2012] Coste, B., Xiao, B., Santos, J. S., Syeda, R., Grandl, J., Spencer, K. S., Kim, S. E., Schmidt, M., Mathur, J., Dubin, A. E., Montal, M., and Patapoutian, A. (2012). Piezo proteins are pore-forming subunits of mechanically activated channels. *Nature*, 483(7388):176–81.
- [Cox et al., 2016] Cox, C. D., Bae, C., Ziegler, L., Hartley, S., Nikolova-Krstevski, V., Rohde, P. R., Ng, C.-A., Sachs, F., Gottlieb, P. A., and Martinac, B. (2016). Removal of the mechanoprotective influence of the cytoskeleton reveals piezo1 is gated by bilayer tension. *Nat Commun*, 7:10366.
- [Craig et al., 2006] Craig, A. M., Graf, E. R., and Linhoff, M. W. (2006). How to build a central synapse: clues from cell culture. *Trends Neurosci*, 29(1):8–20.
- [Craig and Beavis, 2004] Craig, R. and Beavis, R. C. (2004). Tandem: matching proteins with tandem mass spectra. *Bioinformatics*, 20(9):1466–7.
- [Csicsvari et al., 1998] Csicsvari, J., Hirase, H., Czurko, A., and Buzsáki, G. (1998). Reliability and state dependence of pyramidal cell-interneuron synapses in the hippocampus: an ensemble approach in the behaving rat. *Neuron*, 21(1):179–89.
- [Cullen et al., 2010] Cullen, D. K., Gilroy, M. E., Irons, H. R., and Laplaca, M. C. (2010). Synapse-to-neuron ratio is inversely related to neuronal density in mature neuronal cultures. *Brain Res*, 1359:44–55.

- [Cutler and Mattson, 2006] Cutler, R. G. and Mattson, M. P. (2006). The adversities of aging. *Ageing Res Rev*, 5(3):221–38.
- [Dalby et al., 2014] Dalby, M. J., Gadegaard, N., and Oreffo, R. O. C. (2014). Harnessing nanotopography and integrin-matrix interactions to influence stem cell fate. *Nat Mater*, 13(6):558–69.
- [de Cabo et al., 2014] de Cabo, R., Carmona-Gutierrez, D., Bernier, M., Hall, M. N., and Madeo, F. (2014). The search for antiaging interventions: from elixirs to fasting regimens. *Cell*, 157(7):1515–26.
- [de Magalhães and Toussaint, 2004] de Magalhães, J. P. and Toussaint, O. (2004). Telomeres and telomerase: a modern fountain of youth? *Rejuvenation Res*, 7(2):126–33.
- [del Rio et al., 2009] del Rio, A., Perez-Jimenez, R., Liu, R., Roca-Cusachs, P., Fernandez, J. M., and Sheetz, M. P. (2009). Stretching single talin rod molecules activates vinculin binding. *Science*, 323(5914):638–41.
- [Dennerll et al., 1989] Dennerll, T. J., Lamoureux, P., Buxbaum, R. E., and Heidemann, S. R. (1989). The cytomechanics of axonal elongation and retraction. *J Cell Biol*, 109(6 Pt 1):3073–83.
- [Dieterich et al., 2010] Dieterich, D. C., Hodas, J. J. L., Gouzer, G., Shadrin, I. Y., Ngo, J. T., Triller, A., Tirrell, D. A., and Schuman, E. M. (2010). In situ visualization and dynamics of newly synthesized proteins in rat hippocampal neurons. *Nat Neurosci*, 13(7):897–905.
- [Dieterich et al., 2007] Dieterich, D. C., Lee, J. J., Link, A. J., Graumann, J., Tirrell, D. A., and Schuman, E. M. (2007). Labeling, detection and identification of newly synthesized proteomes with bioorthogonal non-canonical amino-acid tagging. *Nat Protoc*, 2(3):532–40.
- [Dieterich et al., 2006] Dieterich, D. C., Link, A. J., Graumann, J., Tirrell, D. A., and Schuman, E. M. (2006). Selective identification of newly synthesized proteins in mammalian cells using bioorthogonal noncanonical amino acid tagging (boncat). *Proc Natl Acad Sci U S A*, 103(25):9482–7.
- [Dong et al., 2017] Dong, C.-M., Wang, X.-L., Wang, G.-M., Zhang, W.-J., Zhu, L., Gao, S., Yang, D.-J., Qin, Y., Liang, Q.-J., Chen, Y.-L., Deng, H.-T., Ning, K., Liang, A.-B., Gao, Z.-L., and Xu, J. (2017). A stress-induced cellular aging model with postnatal neural stem cells. *Cell Death Dis*, 8(9):e3041.
- [Dong et al., 2011] Dong, W., Cheng, S., Huang, F., Fan, W., Chen, Y., Shi, H., and He, H. (2011). Mitochondrial dysfunction in long-term neuronal cultures mimics changes with aging. *Med Sci Monit*, 17(4):BR91–6.

- [Dowling et al., 2010] Dowling, R. J. O., Topisirovic, I., Alain, T., Bidinosti, M., Fonseca, B. D., Petroulakis, E., Wang, X., Larsson, O., Selvaraj, A., Liu, Y., Kozma, S. C., Thomas, G., and Sonenberg, N. (2010). mtorc1-mediated cell proliferation, but not cell growth, controlled by the 4e-bps. *Science*, 328(5982):1172–6.
- [Dufner and Thomas, 1999] Dufner, A. and Thomas, G. (1999). Ribosomal s6 kinase signalling and the control of translation. *Exp Cell Res*, 253(1):100–9.
- [DuFort et al., 2011] DuFort, C. C., Paszek, M. J., and Weaver, V. M. (2011). Balancing forces: architectural control of mechanotransduction. *Nat Rev Mol Cell Biol*, 12(5):308–19.
- [Dumitriu et al., 2010] Dumitriu, D., Hao, J., Hara, Y., Kaufmann, J., Janssen, W. G. M., Lou, W., Rapp, P. R., and Morrison, J. H. (2010). Selective changes in thin spine density and morphology in monkey prefrontal cortex correlate with aging-related cognitive impairment. *J Neurosci*, 30(22):7507–15.
- [Eaton et al., 2013] Eaton, S. L., Roche, S. L., Llavero Hurtado, M., Oldknow, K. J., Farquharson, C., Gillingwater, T. H., and Wishart, T. M. (2013). Total protein analysis as a reliable loading control for quantitative fluorescent western blotting. *PLoS One*, 8(8):e72457.
- [Eisenberg et al., 2009] Eisenberg, T., Knauer, H., Schauer, A., Büttner, S., Ruckenstein, C., Carmona-Gutierrez, D., Ring, J., Schroeder, S., Magnes, C., Antonacci, L., Fussi, H., Deszcz, L., Hartl, R., Schraml, E., Criollo, A., Megalou, E., Weiskopf, D., Laun, P., Heeren, G., Breitenbach, M., Grubeck-Loebenstein, B., Herker, E., Fahrenkrog, B., Fröhlich, K.-U., Sinner, F., Tavernarakis, N., Minois, N., Kroemer, G., and Madeo, F. (2009). Induction of autophagy by spermidine promotes longevity. *Nat Cell Biol*, 11(11):1305–14.
- [Elkin et al., 2010] Elkin, B. S., Ilankovan, A., and Morrison, 3rd, B. (2010). Age-dependent regional mechanical properties of the rat hippocampus and cortex. *J Biomech Eng*, 132(1):011010.
- [Engler et al., 2006] Engler, A. J., Sen, S., Sweeney, H. L., and Discher, D. E. (2006). Matrix elasticity directs stem cell lineage specification. *Cell*, 126(4):677–89.
- [Faden et al., 2016] Faden, F., Eschen-Lippold, L., and Dissmeyer, N. (2016). Normalized quantitative western blotting based on standardized fluorescent labeling. *Methods Mol Biol*, 1450:247–58.
- [Finch and Austad, 2001] Finch, C. E. and Austad, S. N. (2001). History and prospects: symposium on organisms with slow aging. *Exp Gerontol*, 36(4-6):593–7.
- [Fischer et al., 2012] Fischer, R. S., Myers, K. A., Gardel, M. L., and Waterman, C. M. (2012). Stiffness-controlled three-dimensional extracellular matrices for high-resolution imaging of cell behavior. *Nat Protoc*, 7(11):2056–66.

- [Flanagan et al., 2002] Flanagan, L. A., Ju, Y.-E., Marg, B., Osterfield, M., and Janmey, P. A. (2002). Neurite branching on deformable substrates. *Neuroreport*, 13(18):2411–5.
- [Folke et al., 2018] Folke, J., Pakkenberg, B., and Brudek, T. (2018). Impaired wnt signaling in the prefrontal cortex of alzheimer’s disease. *Mol Neurobiol*.
- [Freund et al., 2012] Freund, A., Laberge, R.-M., Demaria, M., and Campisi, J. (2012). Lamin b1 loss is a senescence-associated biomarker. *Mol Biol Cell*, 23(11):2066–75.
- [Gafni et al., 1997] Gafni, J., Munsch, J. A., Lam, T. H., Catlin, M. C., Costa, L. G., Molinski, T. F., and Pessah, I. N. (1997). Xestospongins: potent membrane permeable blockers of the inositol 1,4,5-trisphosphate receptor. *Neuron*, 19(3):723–33.
- [Garzón-Muvdi and Quiñones-Hinojosa, 2009] Garzón-Muvdi, T. and Quiñones-Hinojosa, A. (2009). Neural stem cell niches and homing: recruitment and integration into functional tissues. *ILAR J*, 51(1):3–23.
- [Ge et al., 2015] Ge, J., Li, W., Zhao, Q., Li, N., Chen, M., Zhi, P., Li, R., Gao, N., Xiao, B., and Yang, M. (2015). Architecture of the mammalian mechanosensitive piezo1 channel. *Nature*, 527(7576):64–9.
- [Gefen et al., 2003] Gefen, A., Gefen, N., Zhu, Q., Raghupathi, R., and Margulies, S. S. (2003). Age-dependent changes in material properties of the brain and braincase of the rat. *J Neurotrauma*, 20(11):1163–77.
- [Geissler et al., 2013] Geissler, M., Gottschling, C., Aguado, A., Rauch, U., Wetzel, C. H., Hatt, H., and Faissner, A. (2013). Primary hippocampal neurons, which lack four crucial extracellular matrix molecules, display abnormalities of synaptic structure and function and severe deficits in perineuronal net formation. *J Neurosci*, 33(18):7742–55.
- [Georges et al., 2006] Georges, P. C., Miller, W. J., Meaney, D. F., Sawyer, E. S., and Janmey, P. A. (2006). Matrices with compliance comparable to that of brain tissue select neuronal over glial growth in mixed cortical cultures. *Biophys J*, 90(8):3012–8.
- [Gilkes et al., 2014] Gilkes, D. M., Semenza, G. L., and Wirtz, D. (2014). Hypoxia and the extracellular matrix: drivers of tumour metastasis. *Nat Rev Cancer*, 14(6):430–9.
- [Glogauer et al., 1997] Glogauer, M., Arora, P., Yao, G., Sokholov, I., Ferrier, J., and McCulloch, C. A. (1997). Calcium ions and tyrosine phosphorylation interact coordinately with actin to regulate cytoprotective responses to stretching. *J Cell Sci*, 110 (Pt 1):11–21.
- [Gnanasambandam et al., 2017] Gnanasambandam, R., Ghatak, C., Yasmann, A., Nishizawa, K., Sachs, F., Ladokhin, A. S., Sukharev, S. I., and Suchyna, T. M. (2017). Gsmtx4: Mechanism of inhibiting mechanosensitive ion channels. *Biophys J*, 112(1):31–45.

- [Goodman and Hornberger, 2013] Goodman, C. A. and Hornberger, T. A. (2013). Measuring protein synthesis with sunset: a valid alternative to traditional techniques? *Exerc Sport Sci Rev*, 41(2):107–15.
- [Grillo et al., 2013] Grillo, F. W., Song, S., Teles-Grilo Ruivo, L. M., Huang, L., Gao, G., Knott, G. W., Maco, B., Ferretti, V., Thompson, D., Little, G. E., and De Paola, V. (2013). Increased axonal bouton dynamics in the aging mouse cortex. *Proc Natl Acad Sci U S A*, 110(16):E1514–23.
- [Guerra et al., 2016] Guerra, G. P., Rubin, M. A., and Mello, C. F. (2016). Modulation of learning and memory by natural polyamines. *Pharmacol Res*, 112:99–118.
- [Guizzetti and Costa, 1996] Guizzetti, M. and Costa, L. G. (1996). Inhibition of muscarinic receptor-stimulated glial cell proliferation by ethanol. *J Neurochem*, 67(6):2236–45.
- [Guo and Dipietro, 2010] Guo, S. and Dipietro, L. A. (2010). Factors affecting wound healing. *J Dent Res*, 89(3):219–29.
- [Gupta et al., 2016] Gupta, M., Doss, B., Lim, C. T., Voituriez, R., and Ladoux, B. (2016). Single cell rigidity sensing: A complex relationship between focal adhesion dynamics and large-scale actin cytoskeleton remodeling. *Cell Adh Migr*, 10(5):554–567.
- [Gupta et al., 2013] Gupta, V. K., Scheunemann, L., Eisenberg, T., Mertel, S., Bhukel, A., Koemans, T. S., Kramer, J. M., Liu, K. S. Y., Schroeder, S., Stunnenberg, H. G., Sinner, F., Magnes, C., Pieber, T. R., Dipt, S., Fiala, A., Schenck, A., Schwaerzel, M., Madeo, F., and Sigrist, S. J. (2013). Restoring polyamines protects from age-induced memory impairment in an autophagy-dependent manner. *Nat Neurosci*, 16(10):1453–60.
- [Gutierrez et al., 2013] Gutierrez, E., Shin, B.-S., Woolstenhulme, C. J., Kim, J.-R., Saini, P., Buskirk, A. R., and Dever, T. E. (2013). eif5a promotes translation of polyproline motifs. *Mol Cell*, 51(1):35–45.
- [Gygi et al., 1999] Gygi, S. P., Rist, B., Gerber, S. A., Turecek, F., Gelb, M. H., and Aebersold, R. (1999). Quantitative analysis of complex protein mixtures using isotope-coded affinity tags. *Nat Biotechnol*, 17(10):994–9.
- [Haas et al., 2007] Haas, M. A., Vickers, J. C., and Dickson, T. C. (2007). Rho kinase activates ezrin-radixin-moesin (erm) proteins and mediates their function in cortical neuron growth, morphology and motility in vitro. *J Neurosci Res*, 85(1):34–46.
- [Hands et al., 2009] Hands, S. L., Proud, C. G., and Wyttenbach, A. (2009). mtor's role in ageing: protein synthesis or autophagy? *Aging (Albany NY)*, 1(7):586–97.
- [Hanebuth et al., 2016] Hanebuth, M. A., Kityk, R., Fries, S. J., Jain, A., Kriel, A., Albanese, V., Frickey, T., Peter, C., Mayer, M. P., Frydman, J., and Deuerling, E. (2016). Multivalent

contacts of the hsp70 ssb contribute to its architecture on ribosomes and nascent chain interaction. *Nat Commun*, 7:13695.

[Harrison et al., 2009] Harrison, D. E., Strong, R., Sharp, Z. D., Nelson, J. F., Astle, C. M., Flurkey, K., Nadon, N. L., Wilkinson, J. E., Frenkel, K., Carter, C. S., Pahor, M., Javors, M. A., Fernandez, E., and Miller, R. A. (2009). Rapamycin fed late in life extends lifespan in genetically heterogeneous mice. *Nature*, 460(7253):392–5.

[Hartwig et al., 1992] Hartwig, J. H., Thelen, M., Rosen, A., Janmey, P. A., Nairn, A. C., and Aderem, A. (1992). Marcks is an actin filament crosslinking protein regulated by protein kinase c and calcium-calmodulin. *Nature*, 356(6370):618–22.

[Hayflick and Moorhead, 1961] Hayflick, L. and Moorhead, P. S. (1961). The serial cultivation of human diploid cell strains. *Exp Cell Res*, 25:585–621.

[Heinrich and Sackmann, 2006] Heinrich, D. and Sackmann, E. (2006). Active mechanical stabilization of the viscoplastic intracellular space of dictyostelia cells by microtubule-actin crosstalk. *Acta Biomater*, 2(6):619–31.

[Henderson and Hershey, 2011] Henderson, A. and Hershey, J. W. (2011). Eukaryotic translation initiation factor (eif) 5a stimulates protein synthesis in saccharomyces cerevisiae. *Proc Natl Acad Sci U S A*, 108(16):6415–9.

[Hendrickson et al., 2011] Hendrickson, M. L., Rao, A. J., Demerdash, O. N. A., and Kalil, R. E. (2011). Expression of nestin by neural cells in the adult rat and human brain. *PLoS One*, 6(4):e18535.

[Hernández et al., 2004] Hernández, G., Vázquez-Pianzola, P., Zurbriggen, A., Altmann, M., Sierra, J. M., and Rivera-Pomar, R. (2004). Two functionally redundant isoforms of drosophila melanogaster eukaryotic initiation factor 4b are involved in cap-dependent translation, cell survival, and proliferation. *Eur J Biochem*, 271(14):2923–36.

[Herndon et al., 1997] Herndon, J. G., Moss, M. B., Rosene, D. L., and Killiany, R. J. (1997). Patterns of cognitive decline in aged rhesus monkeys. *Behav Brain Res*, 87(1):25–34.

[Hinz et al., 2013] Hinz, F. I., Dieterich, D. C., and Schuman, E. M. (2013). Teaching old ncats new tricks: using non-canonical amino acid tagging to study neuronal plasticity. *Curr Opin Chem Biol*, 17(5):738–46.

[Ho et al., 2002] Ho, Y., Gruhler, A., Heilbut, A., Bader, G. D., Moore, L., Adams, S.-L., Millar, A., Taylor, P., Bennett, K., Boutilier, K., Yang, L., Wolting, C., Donaldson, I., Schandorff, S., Shewnarane, J., Vo, M., Taggart, J., Goudreault, M., Muskat, B., Alfarano, C., Dewar, D., Lin, Z., Michalickova, K., Willems, A. R., Sassi, H., Nielsen, P. A.,

- Rasmussen, K. J., Andersen, J. R., Johansen, L. E., Hansen, L. H., Jespersen, H., Podtelejnikov, A., Nielsen, E., Crawford, J., Poulsen, V., Sørensen, B. D., Matthiesen, J., Hendrickson, R. C., Gleeson, F., Pawson, T., Moran, M. F., Durocher, D., Mann, M., Hogue, C. W. V., Figgeys, D., and Tyers, M. (2002). Systematic identification of protein complexes in *Saccharomyces cerevisiae* by mass spectrometry. *Nature*, 415(6868):180–3.
- [Hollenbeck and Bamburg, 2003] Hollenbeck, P. J. and Bamburg, J. R. (2003). Comparing the properties of neuronal culture systems: a shopping guide for the cell biologist. *Methods Cell Biol*, 71:1–16.
- [Hong et al., 2010] Hong, J. H., Min, C. H., Jeong, B., Kojiya, T., Morioka, E., Nagai, T., Ikeda, M., and Lee, K. J. (2010). Intracellular calcium spikes in rat suprachiasmatic nucleus neurons induced by bapta-based calcium dyes. *PLoS One*, 5(3):e9634.
- [Hoogenraad et al., 2010] Hoogenraad, C. C., Popa, I., Futai, K., Martinez-Sanchez, E., Sanchez-Martinez, E., Wulf, P. S., van Vlijmen, T., Dortland, B. R., Oorschot, V., Govers, R., Monti, M., Heck, A. J. R., Sheng, M., Klumperman, J., Rehmann, H., Jaarsma, D., Kapitein, L. C., and van der Sluijs, P. (2010). Neuron specific rab4 effector grasp-1 coordinates membrane specialization and maturation of recycling endosomes. *PLoS Biol*, 8(1):e1000283.
- [Hoogenraad and van der Sluijs, 2010] Hoogenraad, C. C. and van der Sluijs, P. (2010). Grasp-1 regulates endocytic receptor recycling and synaptic plasticity. *Commun Integr Biol*, 3(5):433–5.
- [Horii et al., 2017] Horii, T., Morita, S., Kimura, M., Terawaki, N., Shibutani, M., and Hatada, I. (2017). Efficient generation of conditional knockout mice via sequential introduction of lox sites. *Sci Rep*, 7(1):7891.
- [Huang et al., 2007] Huang, Y., Higginson, D. S., Hester, L., Park, M. H., and Snyder, S. H. (2007). Neuronal growth and survival mediated by eif5a, a polyamine-modified translation initiation factor. *Proc Natl Acad Sci U S A*, 104(10):4194–9.
- [Humpel, 2015] Humpel, C. (2015). Organotypic brain slice cultures: A review. *Neuroscience*, 305:86–98.
- [Hussain and Ramaiah, 2007] Hussain, S. G. and Ramaiah, K. V. A. (2007). Reduced eif2alpha phosphorylation and increased proapoptotic proteins in aging. *Biochem Biophys Res Commun*, 355(2):365–70.
- [Hwang et al., 2007] Hwang, J. S., Hwang, J. S., Chang, I., and Kim, S. (2007). Age-associated decrease in proteasome content and activities in human dermal fibroblasts: restoration of normal level of proteasome subunits reduces aging markers in fibroblasts from elderly persons. *J Gerontol A Biol Sci Med Sci*, 62(5):490–9.

- [Ingber, 2003] Ingber, D. E. (2003). Mechanobiology and diseases of mechanotransduction. *Ann Med*, 35(8):564–77.
- [Ippolito and Eroglu, 2010] Ippolito, D. M. and Eroglu, C. (2010). Quantifying synapses: an immunocytochemistry-based assay to quantify synapse number. *J Vis Exp*, (45).
- [Iwasaki and Ingolia, 2017] Iwasaki, S. and Ingolia, N. T. (2017). The growing toolbox for protein synthesis studies. *Trends Biochem Sci*, 42(8):612–624.
- [Iwashita et al., 2014] Iwashita, M., Kataoka, N., Toida, K., and Kosodo, Y. (2014). Systematic profiling of spatiotemporal tissue and cellular stiffness in the developing brain. *Development*, 141(19):3793–8.
- [Jacot et al., 2010] Jacot, J. G., Martin, J. C., and Hunt, D. L. (2010). Mechanobiology of cardiomyocyte development. *J Biomech*, 43(1):93–8.
- [Jacot et al., 2008] Jacot, J. G., McCulloch, A. D., and Omens, J. H. (2008). Substrate stiffness affects the functional maturation of neonatal rat ventricular myocytes. *Biophys J*, 95(7):3479–87.
- [Jäkel and Dimou, 2017] Jäkel, S. and Dimou, L. (2017). Glial cells and their function in the adult brain: A journey through the history of their ablation. *Front Cell Neurosci*, 11:24.
- [Jang et al., 2018] Jang, S., Kim, H., Kim, H.-J., Lee, S. K., Kim, E. W., Namkoong, K., and Kim, E. (2018). Long-term culture of organotypic hippocampal slice from old 3xtg-ad mouse: An ex vivo model of alzheimer’s disease. *Psychiatry Investigig*, 15(2):205–213.
- [Jarsch et al., 2016] Jarsch, I. K., Daste, F., and Gallop, J. L. (2016). Membrane curvature in cell biology: An integration of molecular mechanisms. *J Cell Biol*, 214(4):375–87.
- [Johnson et al., 2007] Johnson, C. P., Tang, H.-Y., Carag, C., Speicher, D. W., and Discher, D. E. (2007). Forced unfolding of proteins within cells. *Science*, 317(5838):663–6.
- [Jurk et al., 2012] Jurk, D., Wang, C., Miwa, S., Maddick, M., Korolchuk, V., Tsolou, A., Gonos, E. S., Thrasivoulou, C., Saffrey, M. J., Cameron, K., and von Zglinicki, T. (2012). Postmitotic neurons develop a p21-dependent senescence-like phenotype driven by a dna damage response. *Aging Cell*, 11(6):996–1004.
- [Kaech and Bunker, 2006] Kaech, S. and Bunker, G. (2006). Culturing hippocampal neurons. *Nat Protoc*, 1(5):2406–15.
- [Kapahi et al., 2010] Kapahi, P., Chen, D., Rogers, A. N., Katewa, S. D., Li, P. W.-L., Thomas, E. L., and Kockel, L. (2010). With tor, less is more: a key role for the conserved nutrient-sensing tor pathway in aging. *Cell Metab*, 11(6):453–65.

- [Kavalali, 2015] Kavalali, E. T. (2015). The mechanisms and functions of spontaneous neurotransmitter release. *Nat Rev Neurosci*, 16(1):5–16.
- [Kennedy and Lamming, 2016] Kennedy, B. K. and Lamming, D. W. (2016). The mechanistic target of rapamycin: The grand conductor of metabolism and aging. *Cell Metab*, 23(6):990–1003.
- [Kenyon, 2005] Kenyon, C. (2005). The plasticity of aging: insights from long-lived mutants. *Cell*, 120(4):449–60.
- [Kibe et al., 2014] Kibe, R., Kurihara, S., Sakai, Y., Suzuki, H., Ooga, T., Sawaki, E., Murofushi, K., Nakamura, A., Yamashita, A., Kitada, Y., Kakeyama, M., Benno, Y., and Matsumoto, M. (2014). Upregulation of colonic luminal polyamines produced by intestinal microbiota delays senescence in mice. *Sci Rep*, 4:4548.
- [Kim et al., 2010] Kim, H.-S., Bae, C.-D., and Park, J. (2010). Glutamate receptor-mediated phosphorylation of ezrin/radixin/moesin proteins is implicated in filopodial protrusion of primary cultured hippocampal neuronal cells. *J Neurochem*, 113(6):1565–76.
- [Kim et al., 2014] Kim, S. N., Jeibmann, A., Halama, K., Witte, H. T., Wälte, M., Matzat, T., Schillers, H., Faber, C., Senner, V., Paulus, W., and Klämbt, C. (2014). Ecm stiffness regulates glial migration in drosophila and mammalian glioma models. *Development*, 141(16):3233–42.
- [Kim et al., 2009] Kim, T.-J., Seong, J., Ouyang, M., Sun, J., Lu, S., Hong, J. P., Wang, N., and Wang, Y. (2009). Substrate rigidity regulates ca²⁺ oscillation via rhoa pathway in stem cells. *J Cell Physiol*, 218(2):285–93.
- [King and Gerber, 2016] King, H. A. and Gerber, A. P. (2016). Translatome profiling: methods for genome-scale analysis of mrna translation. *Brief Funct Genomics*, 15(1):22–31.
- [Kirmizis and Logothetidis, 2010] Kirmizis, D. and Logothetidis, S. (2010). Atomic force microscopy probing in the measurement of cell mechanics. *Int J Nanomedicine*, 5:137–45.
- [Kirstein-Miles et al., 2013] Kirstein-Miles, J., Scior, A., Deuerling, E., and Morimoto, R. I. (2013). The nascent polypeptide-associated complex is a key regulator of proteostasis. *EMBO J*, 32(10):1451–68.
- [Klaas et al., 2016] Klaas, M., Kangur, T., Viil, J., Määmets-Allas, K., Minajeva, A., Vadi, K., Antsov, M., Lapidus, N., Järvekülg, M., and Jaks, V. (2016). The alterations in the extracellular matrix composition guide the repair of damaged liver tissue. *Sci Rep*, 6:27398.
- [Klein et al., 2014] Klein, C., Hain, E. G., Braun, J., Riek, K., Mueller, S., Steiner, B., and Sack, I. (2014). Enhanced adult neurogenesis increases brain stiffness: in vivo magnetic resonance elastography in a mouse model of dopamine depletion. *PLoS One*, 9(3):e92582.

- [Knaevelsrud and Simonsen, 2010] Knaevelsrud, H. and Simonsen, A. (2010). Fighting disease by selective autophagy of aggregate-prone proteins. *FEBS Lett.*, 584(12):2635–45.
- [Knowles et al., 2007] Knowles, T. P., Fitzpatrick, A. W., Meehan, S., Mott, H. R., Vendruscolo, M., Dobson, C. M., and Welland, M. E. (2007). Role of intermolecular forces in defining material properties of protein nanofibrils. *Science*, 318(5858):1900–3.
- [Koga et al., 2011] Koga, H., Kaushik, S., and Cuervo, A. M. (2011). Protein homeostasis and aging: The importance of exquisite quality control. *Ageing Res Rev*, 10(2):205–15.
- [Kōks et al., 2016] Kōks, S., Dogan, S., Tuna, B. G., González-Navarro, H., Potter, P., and Vandenbroucke, R. E. (2016). Mouse models of ageing and their relevance to disease. *Mech Ageing Dev*, 160:41–53.
- [Komatsu et al., 2007] Komatsu, M., Waguri, S., Koike, M., Sou, Y.-S., Ueno, T., Hara, T., Mizushima, N., Iwata, J.-I., Ezaki, J., Murata, S., Hamazaki, J., Nishito, Y., Iemura, S.-I., Natsume, T., Yanagawa, T., Uwayama, J., Warabi, E., Yoshida, H., Ishii, T., Kobayashi, A., Yamamoto, M., Yue, Z., Uchiyama, Y., Kominami, E., and Tanaka, K. (2007). Homeostatic levels of p62 control cytoplasmic inclusion body formation in autophagy-deficient mice. *Cell*, 131(6):1149–63.
- [Kononenko, 2017] Kononenko, N. L. (2017). Lysosomes convene to keep the synapse clean. *J Cell Biol.*
- [Kontis et al., 2017] Kontis, V., Bennett, J. E., Mathers, C. D., Li, G., Foreman, K., and Ezzati, M. (2017). Future life expectancy in 35 industrialised countries: projections with a bayesian model ensemble. *Lancet*.
- [Koser et al., 2016] Koser, D. E., Thompson, A. J., Foster, S. K., Dwivedy, A., Pillai, E. K., Sheridan, G. K., Svoboda, H., Viana, M., Costa, L. d. F., Guck, J., Holt, C. E., and Franze, K. (2016). Mechanosensing is critical for axon growth in the developing brain. *Nat Neurosci*, 19(12):1592–1598.
- [Krammer et al., 1999] Krammer, A., Lu, H., Isralewitz, B., Schulten, K., and Vogel, V. (1999). Forced unfolding of the fibronectin type iii module reveals a tensile molecular recognition switch. *Proc Natl Acad Sci U S A*, 96(4):1351–6.
- [Kuboki et al., 2012] Kuboki, T., Kantawong, F., Burchmore, R., Dalby, M. J., and Kidoaki, S. (2012). 2d-dige proteomic analysis of mesenchymal stem cell cultured on the elasticity-tunable hydrogels. *Cell Struct Funct*, 37(2):127–39.
- [Kulkarni et al., 2018] Kulkarni, A., Chen, J., and Maday, S. (2018). Neuronal autophagy and intercellular regulation of homeostasis in the brain. *Curr Opin Neurobiol*, 51:29–36.

- [Kuo and Yang, 2008] Kuo, L. J. and Yang, L.-X. (2008). Gamma-h2ax - a novel biomarker for dna double-strand breaks. *In Vivo*, 22(3):305–9.
- [Kwiatkowski et al., 2007] Kwiatkowski, A. V., Rubinson, D. A., Dent, E. W., Edward van Veen, J., Leslie, J. D., Zhang, J., Mebane, L. M., Philippar, U., Pinheiro, E. M., Burds, A. A., Bronson, R. T., Mori, S., Fässler, R., and Gertler, F. B. (2007). Ena/vasp is required for neuritogenesis in the developing cortex. *Neuron*, 56(3):441–55.
- [Laemmli, 1970] Laemmli, U. K. (1970). Cleavage of structural proteins during the assembly of the head of bacteriophage t4. *Nature*, 227(5259):680–5.
- [Lamoureux et al., 2010] Lamoureux, P. L., O'Toole, M. R., Heidemann, S. R., and Miller, K. E. (2010). Slowing of axonal regeneration is correlated with increased axonal viscosity during aging. *BMC Neurosci*, 11:140.
- [Landgraf et al., 2015] Landgraf, P., Antileo, E. R., Schuman, E. M., and Dieterich, D. C. (2015). Boncat: metabolic labeling, click chemistry, and affinity purification of newly synthesized proteomes. *Methods Mol Biol*, 1266:199–215.
- [Lansman et al., 1987] Lansman, J. B., Hallam, T. J., and Rink, T. J. (1987). Single stretch-activated ion channels in vascular endothelial cells as mechanotransducers? *Nature*, 325(6107):811–3.
- [Laßek et al., 2015] Laßek, M., Weingarten, J., and Volknandt, W. (2015). The synaptic proteome. *Cell Tissue Res*, 359(1):255–65.
- [Leach et al., 2007] Leach, J. B., Brown, X. Q., Jacot, J. G., Dimilla, P. A., and Wong, J. Y. (2007). Neurite outgrowth and branching of pc12 cells on very soft substrates sharply decreases below a threshold of substrate rigidity. *J Neural Eng*, 4(2):26–34.
- [Lebel and Monnat, 2018] Lebel, M. and Monnat, Jr., R. J. (2018). Werner syndrome (wrn) gene variants and their association with altered function and age-associated diseases. *Ageing Res Rev*, 41:82–97.
- [Lee et al., 2003] Lee, Y. M., Park, S. H., Chung, K. C., and Oh, Y. J. (2003). Proteomic analysis reveals upregulation of calreticulin in murine dopaminergic neuronal cells after treatment with 6-hydroxydopamine. *Neurosci Lett*, 352(1):17–20.
- [Li et al., 2010] Li, C. H., Ohn, T., Ivanov, P., Tisdale, S., and Anderson, P. (2010). eif5a promotes translation elongation, polysome disassembly and stress granule assembly. *PLoS One*, 5(4):e9942.
- [Li et al., 2014] Li, J., Hou, B., Tumova, S., Muraki, K., Bruns, A., Ludlow, M. J., Sedo, A., Hyman, A. J., McKeown, L., Young, R. S., Yuldasheva, N. Y., Majeed, Y., Wilson,

- L. A., Rode, B., Bailey, M. A., Kim, H. R., Fu, Z., Carter, D. A. L., Bilton, J., Imrie, H., Ajuh, P., Dear, T. N., Cubbon, R. M., Kearney, M. T., Prasad, K. R., Evans, P. C., Ainscough, J. F. X., and Beech, D. J. (2014). Piezo1 integration of vascular architecture with physiological force. *Nature*, 515(7526):279–82.
- [Li et al., 2005] Li, X., Alafuzoff, I., Soininen, H., Winblad, B., and Pei, J.-J. (2005). Levels of mtor and its downstream targets 4e-bp1, eef2, and eef2 kinase in relationships with tau in alzheimer's disease brain. *FEBS J*, 272(16):4211–20.
- [Lieber et al., 2004] Lieber, S. C., Aubry, N., Pain, J., Diaz, G., Kim, S.-J., and Vatner, S. F. (2004). Aging increases stiffness of cardiac myocytes measured by atomic force microscopy nanoindentation. *Am J Physiol Heart Circ Physiol*, 287(2):H645–51.
- [Lim et al., 2015] Lim, J., Lachenmayer, M. L., Wu, S., Liu, W., Kundu, M., Wang, R., Komatsu, M., Oh, Y. J., Zhao, Y., and Yue, Z. (2015). Proteotoxic stress induces phosphorylation of p62/sqstm1 by ulk1 to regulate selective autophagic clearance of protein aggregates. *PLoS Genet*, 11(2):e1004987.
- [Lim and Yue, 2015] Lim, J. and Yue, Z. (2015). Neuronal aggregates: formation, clearance, and spreading. *Dev Cell*, 32(4):491–501.
- [Lin et al., 2007] Lin, Y.-L., Lei, Y.-T., Hong, C.-J., and Hsueh, Y.-P. (2007). Syndecan-2 induces filopodia and dendritic spine formation via the neurofibromin-pka-ena/vasp pathway. *J Cell Biol*, 177(5):829–41.
- [Lindqvist et al., 2017] Lindqvist, L. M., Tandoc, K., Topisirovic, I., and Furic, L. (2017). Cross-talk between protein synthesis, energy metabolism and autophagy in cancer. *Curr Opin Genet Dev*, 48:104–111.
- [Link et al., 2003] Link, A. J., Mock, M. L., and Tirrell, D. A. (2003). Non-canonical amino acids in protein engineering. *Curr Opin Biotechnol*, 14(6):603–9.
- [Link et al., 2007] Link, A. J., Vink, M. K. S., and Tirrell, D. A. (2007). Preparation of the functionalizable methionine surrogate azidohomoalanine via copper-catalyzed diazo transfer. *Nat Protoc*, 2(8):1879–83.
- [Liu et al., 2010] Liu, J., Sun, Y., Oster, G. F., and Drubin, D. G. (2010). Mechanochemical crosstalk during endocytic vesicle formation. *Curr Opin Cell Biol*, 22(1):36–43.
- [Loebrich et al., 2016] Loebrich, S., Benoit, M. R., Konopka, J. A., Cottrell, J. R., Gibson, J., and Nedivi, E. (2016). Cpg2 recruits endophilin b2 to the cytoskeleton for activity-dependent endocytosis of synaptic glutamate receptors. *Curr Biol*, 26(3):296–308.

- [Lohmann and Bonhoeffer, 2008] Lohmann, C. and Bonhoeffer, T. (2008). A role for local calcium signaling in rapid synaptic partner selection by dendritic filopodia. *Neuron*, 59(2):253–60.
- [Longo et al., 2015] Longo, V. D., Antebi, A., Bartke, A., Barzilai, N., Brown-Borg, H. M., Caruso, C., Curiel, T. J., de Cabo, R., Franceschi, C., Gems, D., Ingram, D. K., Johnson, T. E., Kennedy, B. K., Kenyon, C., Klein, S., Kopchick, J. J., Lepperdinger, G., Madeo, F., Mirisola, M. G., Mitchell, J. R., Passarino, G., Rudolph, K. L., Sedivy, J. M., Shadel, G. S., Sinclair, D. A., Spindler, S. R., Suh, Y., Vijg, J., Vinciguerra, M., and Fontana, L. (2015). Interventions to slow aging in humans: Are we ready? *Aging Cell*, 14(4):497–510.
- [Lopes et al., 2017] Lopes, F. M., Bristot, I. J., da Motta, L. L., Parsons, R. B., and Klamt, F. (2017). Mimicking parkinson’s disease in a dish: Merits and pitfalls of the most commonly used dopaminergic in vitro models. *Neuromolecular Med*, 19(2-3):241–255.
- [López-Otín et al., 2013] López-Otín, C., Blasco, M. A., Partridge, L., Serrano, M., and Kroemer, G. (2013). The hallmarks of aging. *Cell*, 153(6):1194–217.
- [Lourenço et al., 2016] Lourenço, T., Paes de Faria, J., Bippes, C. A., Maia, J., Lopes-da Silva, J. A., Relvas, J. B., and Gräos, M. (2016). Modulation of oligodendrocyte differentiation and maturation by combined biochemical and mechanical cues. *Sci Rep*, 6:21563.
- [Lovinger, 2008] Lovinger, D. M. (2008). Communication networks in the brain: neurons, receptors, neurotransmitters, and alcohol. *Alcohol Res Health*, 31(3):196–214.
- [Lu et al., 2006] Lu, Y.-B., Franze, K., Seifert, G., Steinhäuser, C., Kirchhoff, F., Wolburg, H., Guck, J., Janmey, P., Wei, E.-Q., Käs, J., and Reichenbach, A. (2006). Viscoelastic properties of individual glial cells and neurons in the cns. *Proc Natl Acad Sci U S A*, 103(47):17759–64.
- [Luchessi et al., 2008] Luchessi, A. D., Cambiaghi, T. D., Alves, A. S., Parreiras-E-Silva, L. T., Britto, L. R. G., Costa-Neto, C. M., and Curi, R. (2008). Insights on eukaryotic translation initiation factor 5a (eif5a) in the brain and aging. *Brain Res*, 1228:6–13.
- [Lyons-Warren et al., 2004] Lyons-Warren, A., Lillie, R., and Hershey, T. (2004). Short- and long-term spatial delayed response performance across the lifespan. *Dev Neuropsychol*, 26(3):661–78.
- [Madeo et al., 2018] Madeo, F., Eisenberg, T., Pietrocola, F., and Kroemer, G. (2018). Spermidine in health and disease. *Science*, 359(6374).
- [Maffioli et al., 2017] Maffioli, E., Schulte, C., Nonnis, S., Grassi Scalvini, F., Piazzoni, C., Lenardi, C., Negri, A., Milani, P., and Tedeschi, G. (2017). Proteomic dissection of nanotopography-sensitive mechanotransductive signaling hubs that foster neuronal differentiation in pc12 cells. *Front Cell Neurosci*, 11:417.

- [Mamatova and Kang, 2013] Mamatova, K. N. and Kang, T. M. (2013). Activation of rat transient receptor potential cation channel subfamily v member 1 channels by 2-aminoethoxydiphenyl borate. *Integr Med Res*, 2(3):112–123.
- [Martinez-Rocha et al., 2016] Martinez-Rocha, A. L., Woriedh, M., Chemnitz, J., Willingmann, P., Kröger, C., Hadeler, B., Hauber, J., and Schäfer, W. (2016). Posttranslational hypusination of the eukaryotic translation initiation factor-5a regulates fusarium graminarum virulence. *Sci Rep*, 6:24698.
- [Maruyama et al., 1997] Maruyama, T., Kanaji, T., Nakade, S., Kanno, T., and Mikoshiba, K. (1997). 2apb, 2-aminoethoxydiphenyl borate, a membrane-penetrable modulator of ins(1,4,5)p3-induced ca²⁺ release. *J Biochem*, 122(3):498–505.
- [Marvizón and Baudry, 1993] Marvizón, J. C. and Baudry, M. (1993). Nmda receptor activation by spermine requires glutamate but not glycine. *Eur J Pharmacol*, 244(1):103–4.
- [McAllister, 2000] McAllister, A. K. (2000). Cellular and molecular mechanisms of dendrite growth. *Cereb Cortex*, 10(10):963–73.
- [McGurk et al., 1990] McGurk, J. F., Bennett, M. V., and Zukin, R. S. (1990). Polyamines potentiate responses of n-methyl-d-aspartate receptors expressed in xenopus oocytes. *Proc Natl Acad Sci U S A*, 87(24):9971–4.
- [McKellar and Shatz, 2009] McKellar, C. E. and Shatz, C. J. (2009). Synaptogenesis in purified cortical subplate neurons. *Cereb Cortex*, 19(8):1723–37.
- [McLean and Nakane, 1974] McLean, I. W. and Nakane, P. K. (1974). Periodate-lysine-paraformaldehyde fixative. a new fixation for immunoelectron microscopy. *J Histochem Cytochem*, 22(12):1077–83.
- [Meléndez et al., 2003] Meléndez, A., Tallóczy, Z., Seaman, M., Eskelinen, E.-L., Hall, D. H., and Levine, B. (2003). Autophagy genes are essential for dauer development and life-span extension in *c. elegans*. *Science*, 301(5638):1387–91.
- [Melnikov et al., 2016] Melnikov, S., Mailliot, J., Shin, B.-S., Rigger, L., Yusupova, G., Micura, R., Dever, T. E., and Yusupov, M. (2016). Crystal structure of hypusine-containing translation factor eif5a bound to a rotated eukaryotic ribosome. *J Mol Biol*, 428(18):3570–3576.
- [Minois et al., 2014] Minois, N., Rockenfeller, P., Smith, T. K., and Carmona-Gutierrez, D. (2014). Spermidine feeding decreases age-related locomotor activity loss and induces changes in lipid composition. *PLoS One*, 9(7):e102435.
- [Mitra et al., 2009] Mitra, S., Tsvetkov, A. S., and Finkbeiner, S. (2009). Protein turnover and inclusion body formation. *Autophagy*, 5(7):1037–8.

- [Miura et al., 2018] Miura, H., Quadros, R. M., Gurumurthy, C. B., and Ohtsuka, M. (2018). Easi-crispr for creating knock-in and conditional knockout mouse models using long ssDNA donors. *Nat Protoc*, 13(1):195–215.
- [Moeendarbary et al., 2017] Moeendarbary, E., Weber, I. P., Sheridan, G. K., Koser, D. E., Soleman, S., Haenzi, B., Bradbury, E. J., Fawcett, J., and Franze, K. (2017). The soft mechanical signature of glial scars in the central nervous system. *Nat Commun*, 8:14787.
- [Moore et al., 2006] Moore, T. L., Killiany, R. J., Herndon, J. G., Rosene, D. L., and Moss, M. B. (2006). Executive system dysfunction occurs as early as middle-age in the rhesus monkey. *Neurobiol Aging*, 27(10):1484–93.
- [Moser et al., 1997] Moser, B. A., Dennis, P. B., Pullen, N., Pearson, R. B., Williamson, N. A., Wettenhall, R. E., Kozma, S. C., and Thomas, G. (1997). Dual requirement for a newly identified phosphorylation site in p70s6k. *Mol Cell Biol*, 17(9):5648–55.
- [Moshayedi et al., 2010] Moshayedi, P., Costa, L. d. F., Christ, A., Lacour, S. P., Fawcett, J., Guck, J., and Franze, K. (2010). Mechanosensitivity of astrocytes on optimized polyacrylamide gels analyzed by quantitative morphometry. *J Phys Condens Matter*, 22(19):194114.
- [Moshayedi et al., 2014] Moshayedi, P., Ng, G., Kwok, J. C. F., Yeo, G. S. H., Bryant, C. E., Fawcett, J. W., Franze, K., and Guck, J. (2014). The relationship between glial cell mechanosensitivity and foreign body reactions in the central nervous system. *Biomaterials*, 35(13):3919–25.
- [Mousavi and Doweidar, 2015] Mousavi, S. J. and Doweidar, M. H. (2015). Role of mechanical cues in cell differentiation and proliferation: A 3d numerical model. *PLoS One*, 10(5):e0124529.
- [Müller et al., 2015] Müller, A., Stellmacher, A., Freitag, C. E., Landgraf, P., and Dieterich, D. C. (2015). Monitoring astrocytic proteome dynamics by cell type-specific protein labeling. *PLoS One*, 10(12):e0145451.
- [Muñoz-Espín and Serrano, 2014] Muñoz-Espín, D. and Serrano, M. (2014). Cellular senescence: from physiology to pathology. *Nat Rev Mol Cell Biol*, 15(7):482–96.
- [Murchison et al., 2004] Murchison, D., Zawieja, D. C., and Griffith, W. H. (2004). Reduced mitochondrial buffering of voltage-gated calcium influx in aged rat basal forebrain neurons. *Cell Calcium*, 36(1):61–75.
- [Murphrey and Gerner, 1987] Murphrey, R. J. and Gerner, E. W. (1987). Hypusine formation in protein by a two-step process in cell lysates. *J Biol Chem*, 262(31):15033–6.
- [Murphy et al., 2012] Murphy, M. C., Curran, G. L., Glaser, K. J., Rossman, P. J., Huston, 3rd, J., Poduslo, J. F., Jack, Jr, C. R., Felmlee, J. P., and Ehman, R. L. (2012). Magnetic

- resonance elastography of the brain in a mouse model of alzheimer's disease: initial results. *Magn Reson Imaging*, 30(4):535–9.
- [Murphy et al., 2011] Murphy, M. C., Huston, 3rd, J., Jack, Jr, C. R., Glaser, K. J., Manduca, A., Felmlee, J. P., and Ehman, R. L. (2011). Decreased brain stiffness in alzheimer's disease determined by magnetic resonance elastography. *J Magn Reson Imaging*, 34(3):494–8.
- [Nakamura and Yoshimori, 2018] Nakamura, S. and Yoshimori, T. (2018). Autophagy and longevity. *Mol Cells*, 41(1):65–72.
- [Narayan et al., 2016] Narayan, V., Ly, T., Pourkarimi, E., Murillo, A. B., Gartner, A., Lamond, A. I., and Kenyon, C. (2016). Deep proteome analysis identifies age-related processes in *c. elegans*. *Cell Syst*, 3(2):144–159.
- [Nathans, 1964] Nathans, D. (1964). Inhibition of protein synthesis by puromycin. *Fed Proc*, 23:984–9.
- [Nemir and West, 2010] Nemir, S. and West, J. L. (2010). Synthetic materials in the study of cell response to substrate rigidity. *Ann Biomed Eng*, 38(1):2–20.
- [Ní Fhlathartaigh et al., 2013] Ní Fhlathartaigh, M., McMahon, J., Reynolds, R., Connolly, D., Higgins, E., Counihan, T., and Fitzgerald, U. (2013). Calreticulin and other components of endoplasmic reticulum stress in rat and human inflammatory demyelination. *Acta Neuropathol Commun*, 1:37.
- [Nie et al., 2017] Nie, X., Li, C., Hu, S., Xue, F., Kang, Y. J., and Zhang, W. (2017). An appropriate loading control for western blot analysis in animal models of myocardial ischemic infarction. *Biochem Biophys Rep*, 12:108–113.
- [Nwe and Brechbiel, 2009] Nwe, K. and Brechbiel, M. W. (2009). Growing applications of "click chemistry" for bioconjugation in contemporary biomedical research. *Cancer Biother Radiopharm*, 24(3):289–302.
- [Oberpichler-Schwenk and Kriegstein, 1994] Oberpichler-Schwenk, H. and Kriegstein, J. (1994). Primary cultures of neurons for testing neuroprotective drug effects. *J Neural Transm Suppl*, 44:1–20.
- [O'Leary et al., 2013] O'Leary, T., Williams, A. H., Caplan, J. S., and Marder, E. (2013). Correlations in ion channel expression emerge from homeostatic tuning rules. *Proc Natl Acad Sci U S A*, 110(28):E2645–54.
- [Oliverio et al., 2014] Oliverio, S., Corazzari, M., Sestito, C., Piredda, L., Ippolito, G., and Piacentini, M. (2014). The spermidine analogue gc7 (n1-guanyl-1,7-diamineoheptane) in-

- duces autophagy through a mechanism not involving the hypusination of eif5a. *Amino Acids*, 46(12):2767–76.
- [Ostrow et al., 2003] Ostrow, K. L., Mammoser, A., Suchyna, T., Sachs, F., Oswald, R., Kubo, S., Chino, N., and Gottlieb, P. A. (2003). cdna sequence and in vitro folding of gsmtx4, a specific peptide inhibitor of mechanosensitive channels. *Toxicon*, 42(3):263–74.
- [Ozcan et al., 2008] Ozcan, U., Ozcan, L., Yilmaz, E., Düvel, K., Sahin, M., Manning, B. D., and Hotamisligil, G. S. (2008). Loss of the tuberous sclerosis complex tumor suppressors triggers the unfolded protein response to regulate insulin signaling and apoptosis. *Mol Cell*, 29(5):541–51.
- [Pacifici and Peruzzi, 2012] Pacifici, M. and Peruzzi, F. (2012). Isolation and culture of rat embryonic neural cells: a quick protocol. *J Vis Exp*, (63):e3965.
- [Pandey et al., 2000] Pandey, A., Andersen, J. S., and Mann, M. (2000). Use of mass spectrometry to study signaling pathways. *Sci STKE*, 2000(37):pl1.
- [Pankiv et al., 2007] Pankiv, S., Clausen, T. H., Lamark, T., Brech, A., Bruun, J.-A., Outzen, H., Øvervatn, A., Bjørkøy, G., and Johansen, T. (2007). p62/sqstm1 binds directly to atg8/lc3 to facilitate degradation of ubiquitinated protein aggregates by autophagy. *J Biol Chem*, 282(33):24131–45.
- [Paparcone et al., 2010] Paparcone, R., Keten, S., and Buehler, M. J. (2010). Atomistic simulation of nanomechanical properties of alzheimer’s abeta(1-40) amyloid fibrils under compressive and tensile loading. *J Biomech*, 43(6):1196–201.
- [Paredes et al., 2008] Paredes, R. M., Etzler, J. C., Watts, L. T., Zheng, W., and Lechleiter, J. D. (2008). Chemical calcium indicators. *Methods*, 46(3):143–51.
- [Park et al., 1981] Park, M. H., Cooper, H. L., and Folk, J. E. (1981). Identification of hypusine, an unusual amino acid, in a protein from human lymphocytes and of spermidine as its biosynthetic precursor. *Proc Natl Acad Sci U S A*, 78(5):2869–73.
- [Pathak et al., 2014] Pathak, M. M., Nourse, J. L., Tran, T., Hwe, J., Arulmoli, J., Le, D. T. T., Bernardis, E., Flanagan, L. A., and Tombola, F. (2014). Stretch-activated ion channel piezo1 directs lineage choice in human neural stem cells. *Proc Natl Acad Sci U S A*, 111(45):16148–53.
- [Pelham and Wang, 1997] Pelham, Jr, R. J. and Wang, Y. I. (1997). Cell locomotion and focal adhesions are regulated by substrate flexibility. *Proc Natl Acad Sci U S A*, 94(25):13661–5.
- [Perry and Fainzilber, 2014] Perry, R. B. and Fainzilber, M. (2014). Local translation in neuronal processes—in vivo tests of a "heretical hypothesis". *Dev Neurobiol*, 74(3):210–7.

- [Peters et al., 2008] Peters, A., Sethares, C., and Luebke, J. I. (2008). Synapses are lost during aging in the primate prefrontal cortex. *Neuroscience*, 152(4):970–81.
- [Pfisterer and Khodosevich, 2017] Pfisterer, U. and Khodosevich, K. (2017). Neuronal survival in the brain: neuron type-specific mechanisms. *Cell Death Dis*, 8(3):e2643.
- [Piper and Partridge, 2016] Piper, M. D. W. and Partridge, L. (2016). Protocols to study aging in drosophila. *Methods Mol Biol*, 1478:291–302.
- [Piret et al., 2015] Piret, G., Perez, M.-T., and Prinz, C. N. (2015). Support of neuronal growth over glial growth and guidance of optic nerve axons by vertical nanowire arrays. *ACS Appl Mater Interfaces*, 7(34):18944–8.
- [Potier et al., 2006] Potier, B., Jouvenceau, A., Epelbaum, J., and Dutar, P. (2006). Age-related alterations of gabaergic input to ca1 pyramidal neurons and its control by nicotinic acetylcholine receptors in rat hippocampus. *Neuroscience*, 142(1):187–201.
- [Pravincumar et al., 2012] Pravincumar, P., Bader, D. L., and Knight, M. M. (2012). Viscoelastic cell mechanics and actin remodelling are dependent on the rate of applied pressure. *PLoS One*, 7(9):e43938.
- [Press et al., 2018] Press, M., Jung, T., König, J., Grune, T., and Höhn, A. (2018). Protein aggregates and proteostasis in aging: Amylin and -cell function. *Mech Ageing Dev*.
- [Promislow, 1994] Promislow, D. E. (1994). Dna repair and the evolution of longevity: a critical analysis. *J Theor Biol*, 170(3):291–300.
- [Pullen and Thomas, 1997] Pullen, N. and Thomas, G. (1997). The modular phosphorylation and activation of p70s6k. *FEBS Lett*, 410(1):78–82.
- [Raab et al., 2010] Raab, M., Boeckers, T. M., and Neuhaber, W. L. (2010). Proline-rich synapse-associated protein-1 and 2 (prosap1/shank2 and prosap2/shank3)-scaffolding proteins are also present in postsynaptic specializations of the peripheral nervous system. *Neuroscience*, 171(2):421–33.
- [Ranade et al., 2014a] Ranade, S. S., Qiu, Z., Woo, S.-H., Hur, S. S., Murthy, S. E., Cahalan, S. M., Xu, J., Mathur, J., Bandell, M., Coste, B., Li, Y.-S. J., Chien, S., and Patapoutian, A. (2014a). Piezo1, a mechanically activated ion channel, is required for vascular development in mice. *Proc Natl Acad Sci U S A*, 111(28):10347–52.
- [Ranade et al., 2015] Ranade, S. S., Syeda, R., and Patapoutian, A. (2015). Mechanically activated ion channels. *Neuron*, 87(6):1162–1179.
- [Ranade et al., 2014b] Ranade, S. S., Woo, S.-H., Dubin, A. E., Moshourab, R. A., Wetzel, C., Petrus, M., Mathur, J., Bégay, V., Coste, B., Mainquist, J., Wilson, A. J., Francisco,

- A. G., Reddy, K., Qiu, Z., Wood, J. N., Lewin, G. R., and Patapoutian, A. (2014b). Piezo2 is the major transducer of mechanical forces for touch sensation in mice. *Nature*, 516(7529):121–5.
- [Rangamani et al., 2014] Rangamani, P., Mandadap, K. K., and Oster, G. (2014). Protein-induced membrane curvature alters local membrane tension. *Biophys J*, 107(3):751–762.
- [Rattan, 1996] Rattan, S. I. (1996). Synthesis, modifications, and turnover of proteins during aging. *Exp Gerontol*, 31(1-2):33–47.
- [Redpath et al., 1996] Redpath, N. T., Foulstone, E. J., and Proud, C. G. (1996). Regulation of translation elongation factor-2 by insulin via a rapamycin-sensitive signalling pathway. *EMBO J*, 15(9):2291–7.
- [Reiling and Sabatini, 2008] Reiling, J. H. and Sabatini, D. M. (2008). Increased mtorc1 signaling upregulates stress. *Mol Cell*, 29(5):533–5.
- [Rex et al., 2005] Rex, C. S., Kramár, E. A., Colgin, L. L., Lin, B., Gall, C. M., and Lynch, G. (2005). Long-term potentiation is impaired in middle-aged rats: regional specificity and reversal by adenosine receptor antagonists. *J Neurosci*, 25(25):5956–66.
- [Richardson et al., 2004] Richardson, C. J., Bröenstrup, M., Fingar, D. C., Jülich, K., Ballif, B. A., Gygi, S., and Blenis, J. (2004). Skar is a specific target of s6 kinase 1 in cell growth control. *Curr Biol*, 14(17):1540–9.
- [Riis et al., 1990] Riis, B., Rattan, S. I., Derventzi, A., and Clark, B. F. (1990). Reduced levels of adp-ribosylatable elongation factor-2 in aged and sv40-transformed human cell cultures. *FEBS Lett*, 266(1-2):45–7.
- [Riou et al., 2012] Riou, M., Stroebel, D., Edwardson, J. M., and Paoletti, P. (2012). An alternating glun1-2-1-2 subunit arrangement in mature nmda receptors. *PLoS One*, 7(4):e35134.
- [Ris and Godaux, 2007] Ris, L. and Godaux, E. (2007). Synapse specificity of long-term potentiation breaks down with aging. *Learn Mem*, 14(3):185–9.
- [Robinson et al., 2018] Robinson, A. A., Abraham, C. R., and Rosene, D. L. (2018). Candidate molecular pathways of white matter vulnerability in the brain of normal aging rhesus monkeys. *Geroscience*, 40(1):31–47.
- [Robinson et al., 2017] Robinson, M. M., Dasari, S., Konopka, A. R., Johnson, M. L., Manjunatha, S., Esponda, R. R., Carter, R. E., Lanza, I. R., and Nair, K. S. (2017). Enhanced protein translation underlies improved metabolic and physical adaptations to different exercise training modes in young and old humans. *Cell Metab*, 25(3):581–592.

- [Rock and MacDonald, 1992] Rock, D. M. and MacDonald, R. L. (1992). Spermine and related polyamines produce a voltage-dependent reduction of n-methyl-d-aspartate receptor single-channel conductance. *Mol Pharmacol*, 42(1):157–64.
- [Rodin et al., 2014] Rodin, S., Antonsson, L., Niaudet, C., Simonson, O. E., Salmela, E., Hansson, E. M., Domogatskaya, A., Xiao, Z., Damdimopoulou, P., Sheikhi, M., Inzunza, J., Nilsson, A.-S., Baker, D., Kuiper, R., Sun, Y., Blennow, E., Nordenskjöld, M., Grinnemo, K.-H., Kere, J., Betsholtz, C., Hovatta, O., and Tryggvason, K. (2014). Clonal culturing of human embryonic stem cells on laminin-521/e-cadherin matrix in defined and xeno-free environment. *Nat Commun*, 5:3195.
- [Rogakou et al., 2000] Rogakou, E. P., Nieves-Neira, W., Boon, C., Pommier, Y., and Bonner, W. M. (2000). Initiation of dna fragmentation during apoptosis induces phosphorylation of h2ax histone at serine 139. *J Biol Chem*, 275(13):9390–5.
- [Romero-Sandoval et al., 2008] Romero-Sandoval, A., Chai, N., Nutile-McMenemy, N., and Deleo, J. A. (2008). A comparison of spinal iba1 and gfap expression in rodent models of acute and chronic pain. *Brain Res*, 1219:116–26.
- [Rosenmund et al., 2003] Rosenmund, C., Rettig, J., and Brose, N. (2003). Molecular mechanisms of active zone function. *Curr Opin Neurobiol*, 13(5):509–19.
- [Ross et al., 2012] Ross, A. M., Jiang, Z., Bastmeyer, M., and Lahann, J. (2012). Physical aspects of cell culture substrates: topography, roughness, and elasticity. *Small*, 8(3):336–55.
- [Ross et al., 2004] Ross, P. L., Huang, Y. N., Marchese, J. N., Williamson, B., Parker, K., Hattan, S., Khainovski, N., Pillai, S., Dey, S., Daniels, S., Purkayastha, S., Juhasz, P., Martin, S., Bartlet-Jones, M., He, F., Jacobson, A., and Pappin, D. J. (2004). Multiplexed protein quantitation in saccharomyces cerevisiae using amine-reactive isobaric tagging reagents. *Mol Cell Proteomics*, 3(12):1154–69.
- [Rossi et al., 2016] Rossi, D., Barbosa, N. M., Galvão, F. C., Boldrin, P. E. G., Hershey, J. W. B., Zanelli, C. F., Fraser, C. S., and Valentini, S. R. (2016). Evidence for a negative cooperativity between eif5a and eef2 on binding to the ribosome. *PLoS One*, 11(4):e0154205.
- [Rowe and Kahn, 1998] Rowe, J. W. and Kahn, R. L. (1998). Successful aging. *Aging (Milano)*, 10(2):142–4.
- [Sack et al., 2009] Sack, I., Beierbach, B., Wuerfel, J., Klatt, D., Hamhaber, U., Papazoglou, S., Martus, P., and Braun, J. (2009). The impact of aging and gender on brain viscoelasticity. *Neuroimage*, 46(3):652–7.
- [Sackmann, 1994] Sackmann, E. (1994). The seventh datta lecture. membrane bending energy concept of vesicle- and cell-shapes and shape-transitions. *FEBS Lett*, 346(1):3–16.

- [Saini et al., 2009] Saini, P., Eyler, D. E., Green, R., and Dever, T. E. (2009). Hypusine-containing protein eif5a promotes translation elongation. *Nature*, 459(7243):118–21.
- [Sakuma et al., 2015] Sakuma, K., Aoi, W., and Yamaguchi, A. (2015). Current understanding of sarcopenia: possible candidates modulating muscle mass. *Pflugers Arch*, 467(2):213–29.
- [Salussolia et al., 2011] Salussolia, C. L., Prodromou, M. L., Borker, P., and Wollmuth, L. P. (2011). Arrangement of subunits in functional nmda receptors. *J Neurosci*, 31(31):11295–304.
- [Sarbassov et al., 2005] Sarbassov, D. D., Ali, S. M., and Sabatini, D. M. (2005). Growing roles for the mtor pathway. *Curr Opin Cell Biol*, 17(6):596–603.
- [Sato et al., 2007] Sato, T. R., Gray, N. W., Mainen, Z. F., and Svoboda, K. (2007). The functional microarchitecture of the mouse barrel cortex. *PLoS Biol*, 5(7):e189.
- [Sawada et al., 2006] Sawada, Y., Tamada, M., Dubin-Thaler, B. J., Cherniavskaya, O., Sakai, R., Tanaka, S., and Sheetz, M. P. (2006). Force sensing by mechanical extension of the src family kinase substrate p130cas. *Cell*, 127(5):1015–26.
- [Scheibel et al., 1976] Scheibel, M. E., Lindsay, R. D., Tomiyasu, U., and Scheibel, A. B. (1976). Progressive dendritic changes in the aging human limbic system. *Exp Neurol*, 53(2):420–30.
- [Schmidt et al., 2009] Schmidt, E. K., Clavarino, G., Ceppi, M., and Pierre, P. (2009). Sunset, a nonradioactive method to monitor protein synthesis. *Nat Methods*, 6(4):275–7.
- [Schneider et al., 2014] Schneider, L. S., Mangialasche, F., Andreasen, N., Feldman, H., Giacobini, E., Jones, R., Mantua, V., Mecocci, P., Pani, L., Winblad, B., and Kivipelto, M. (2014). Clinical trials and late-stage drug development for alzheimer’s disease: an appraisal from 1984 to 2014. *J Intern Med*, 275(3):251–83.
- [Schoonen, 1982] Schoonen, J. (1982). The dendritic organization of the human spinal cord: the dorsal horn. *Neuroscience*, 7(9):2057–87.
- [Schuller et al., 2017] Schuller, A. P., Wu, C. C.-C., Dever, T. E., Buskirk, A. R., and Green, R. (2017). eif5a functions globally in translation elongation and termination. *Mol Cell*, 66(2):194–205.e5.
- [Schulte et al., 2017] Schulte, C., Podestà, A., Lenardi, C., Tedeschi, G., and Milani, P. (2017). Quantitative control of protein and cell interaction with nanostructured surfaces by cluster assembling. *Acc Chem Res*, 50(2):231–239.

- [Schulze et al., 2010] Schulze, C., Wetzel, F., Kueper, T., Malsen, A., Muhr, G., Jaspers, S., Blatt, T., Wittern, K.-P., Wenck, H., and Käs, J. A. (2010). Stiffening of human skin fibroblasts with age. *Biophys J*, 99(8):2434–42.
- [Sciarretta and Minichiello, 2010] Sciarretta, C. and Minichiello, L. (2010). The preparation of primary cortical neuron cultures and a practical application using immunofluorescent cytochemistry. *Methods Mol Biol*, 633:221–31.
- [Scudellari, 2017] Scudellari, M. (2017). To stay young, kill zombie cells. *Nature*, 550(7677):448–450.
- [Sebben et al., 1990] Sebben, M., Gabrion, J., Manzoni, O., Sladeczek, F., Gril, C., Bockaert, J., and Dumuis, A. (1990). Establishment of a long-term primary culture of striatal neurons. *Brain Res Dev Brain Res*, 52(1-2):229–39.
- [Sechi and Wehland, 2004] Sechi, A. S. and Wehland, J. (2004). Ena/vasp proteins: multi-functional regulators of actin cytoskeleton dynamics. *Front Biosci*, 9:1294–310.
- [Serfass et al., 2017] Serfass, J. M., Takahashi, Y., Zhou, Z., Kawasawa, Y. I., Liu, Y., Tsotakos, N., Young, M. M., Tang, Z., Yang, L., Atkinson, J. M., Chroneos, Z. C., and Wang, H.-G. (2017). Endophilin b2 facilitates endosome maturation in response to growth factor stimulation, autophagy induction, and influenza a virus infection. *J Biol Chem*, 292(24):10097–10111.
- [Sharif and Prevot, 2017] Sharif, A. and Prevot, V. (2017). When size matters: How astrocytic processes shape metabolism. *Cell Metab*, 25(5):995–996.
- [Sharpless and Sherr, 2015] Sharpless, N. E. and Sherr, C. J. (2015). Forging a signature of in vivo senescence. *Nat Rev Cancer*, 15(7):397–408.
- [Shinozaki et al., 2017] Shinozaki, Y., Shibata, K., Yoshida, K., Shigetomi, E., Gachet, C., Ikenaka, K., Tanaka, K. F., and Koizumi, S. (2017). Transformation of astrocytes to a neuroprotective phenotype by microglia via p2y1 receptor downregulation. *Cell Rep*, 19(6):1151–1164.
- [SHOLL, 1953] SHOLL, D. A. (1953). Dendritic organization in the neurons of the visual and motor cortices of the cat. *J Anat*, 87(4):387–406.
- [Siechen et al., 2009] Siechen, S., Yang, S., Chiba, A., and Saif, T. (2009). Mechanical tension contributes to clustering of neurotransmitter vesicles at presynaptic terminals. *Proc Natl Acad Sci U S A*, 106(31):12611–6.
- [Smith et al., 2007] Smith, B. A., Roy, H., De Koninck, P., Grütter, P., and De Koninck, Y. (2007). Dendritic spine viscoelasticity and soft-glassy nature: balancing dynamic remodeling with structural stability. *Biophys J*, 92(4):1419–30.

- [Soda et al., 2009] Soda, K., Dobashi, Y., Kano, Y., Tsujinaka, S., and Konishi, F. (2009). Polyamine-rich food decreases age-associated pathology and mortality in aged mice. *Exp Gerontol*, 44(11):727–32.
- [Sotelo-Silveira et al., 2006] Sotelo-Silveira, J. R., Calliari, A., Kun, A., Koenig, E., and Sotelo, J. R. (2006). RNA trafficking in axons. *Traffic*, 7(5):508–15.
- [Soto-Gamez and Demaria, 2017] Soto-Gamez, A. and Demaria, M. (2017). Therapeutic interventions for aging: the case of cellular senescence. *Drug Discov Today*, 22(5):786–795.
- [Spedden et al., 2012] Spedden, E., White, J. D., Naumova, E. N., Kaplan, D. L., and Staii, C. (2012). Elasticity maps of living neurons measured by combined fluorescence and atomic force microscopy. *Biophys J*, 103(5):868–77.
- [Steiner et al., 2007] Steiner, J., Bernstein, H.-G., Bielau, H., Berndt, A., Brisch, R., Mawrin, C., Keilhoff, G., and Bogerts, B. (2007). Evidence for a wide extra-astrocytic distribution of s100b in human brain. *BMC Neurosci*, 8:2.
- [Stenesen et al., 2013] Stenesen, D., Suh, J. M., Seo, J., Yu, K., Lee, K.-S., Kim, J.-S., Min, K.-J., and Graff, J. M. (2013). Adenosine nucleotide biosynthesis and AMPK regulate adult life span and mediate the longevity benefit of caloric restriction in flies. *Cell Metab*, 17(1):101–12.
- [Streitberger et al., 2012] Streitberger, K.-J., Sack, I., Krefting, D., Pfüller, C., Braun, J., Paul, F., and Wuerfel, J. (2012). Brain viscoelasticity alteration in chronic-progressive multiple sclerosis. *PLoS One*, 7(1):e29888.
- [Stumpo et al., 1995] Stumpo, D. J., Bock, C. B., Tuttle, J. S., and Blackshear, P. J. (1995). Marcks deficiency in mice leads to abnormal brain development and perinatal death. *Proc Natl Acad Sci U S A*, 92(4):944–8.
- [Südhof, 2012] Südhof, T. C. (2012). Calcium control of neurotransmitter release. *Cold Spring Harb Perspect Biol*, 4(1):a011353.
- [Südhof, 2013] Südhof, T. C. (2013). Neurotransmitter release: the last millisecond in the life of a synaptic vesicle. *Neuron*, 80(3):675–90.
- [Sweers et al., 2011] Sweers, K., van der Werf, K., Bennink, M., and Subramaniam, V. (2011). Nanomechanical properties of alpha-synuclein amyloid fibrils: a comparative study by nanoindentation, harmonic force microscopy, and peakforce QNM. *Nanoscale Res Lett*, 6(1):270.
- [Syeda et al., 2015] Syeda, R., Xu, J., Dubin, A. E., Coste, B., Mathur, J., Huynh, T., Matzen, J., Lao, J., Tully, D. C., Engels, I. H., Petrassi, H. M., Schumacher, A. M.,

- Montal, M., Bandell, M., and Patapoutian, A. (2015). Chemical activation of the mechanotransduction channel piezo1. *Elife*, 4.
- [Syntichaki et al., 2007] Syntichaki, P., Troulinaki, K., and Tavernarakis, N. (2007). eif4e function in somatic cells modulates ageing in *caenorhabditis elegans*. *Nature*, 445(7130):922–6.
- [Szychowski et al., 2010] Szychowski, J., Mahdavi, A., Hodas, J. J. L., Bagert, J. D., Ngo, J. T., Landgraf, P., Dieterich, D. C., Schuman, E. M., and Tirrell, D. A. (2010). Cleavable biotin probes for labeling of biomolecules via azide-alkyne cycloaddition. *J Am Chem Soc*, 132(51):18351–60.
- [Taha et al., 2013] Taha, E., Gildish, I., Gal-Ben-Ari, S., and Rosenblum, K. (2013). The role of eef2 pathway in learning and synaptic plasticity. *Neurobiol Learn Mem*, 105:100–6.
- [Takahashi and Ono, 2003] Takahashi, M. and Ono, Y. (2003). Pulse-chase analysis of protein kinase c. *Methods Mol Biol*, 233:163–70.
- [Takahashi et al., 1985] Takahashi, R., Mori, N., and Goto, S. (1985). Accumulation of heat-labile elongation factor 2 in the liver of mice and rats. *Exp Gerontol*, 20(6):325–31.
- [Talboom et al., 2015] Talboom, J. S., Velazquez, R., and Oddo, S. (2015). The mammalian target of rapamycin at the crossroad between cognitive aging and alzheimer’s disease. *NPJ Aging Mech Dis*, 1:15008.
- [Tilghman et al., 2012] Tilghman, R. W., Blais, E. M., Cowan, C. R., Sherman, N. E., Grigera, P. R., Jeffery, E. D., Fox, J. W., Blackman, B. R., Tschumperlin, D. J., Papin, J. A., and Parsons, J. T. (2012). Matrix rigidity regulates cancer cell growth by modulating cellular metabolism and protein synthesis. *PLoS One*, 7(5):e37231.
- [Togashi et al., 2008] Togashi, K., Inada, H., and Tominaga, M. (2008). Inhibition of the transient receptor potential cation channel trpm2 by 2-aminoethoxydiphenyl borate (2-apb). *Br J Pharmacol*, 153(6):1324–30.
- [Tosato et al., 2007] Tosato, M., Zamboni, V., Ferrini, A., and Cesari, M. (2007). The aging process and potential interventions to extend life expectancy. *Clin Interv Aging*, 2(3):401–12.
- [Tóth et al., 2008] Tóth, M. L., Sigmund, T., Borsos, E., Barna, J., Erdélyi, P., Takács-Vellai, K., Orosz, L., Kovács, A. L., Csikós, G., Sass, M., and Vellai, T. (2008). Longevity pathways converge on autophagy genes to regulate life span in *caenorhabditis elegans*. *Autophagy*, 4(3):330–8.
- [Toyama and Hetzer, 2013] Toyama, B. H. and Hetzer, M. W. (2013). Protein homeostasis: live long, won’t prosper. *Nat Rev Mol Cell Biol*, 14(1):55–61.

- [Tyedmers et al., 2010] Tyedmers, J., Mogk, A., and Bukau, B. (2010). Cellular strategies for controlling protein aggregation. *Nat Rev Mol Cell Biol*, 11(11):777–88.
- [Uemura and Gerner, 2011] Uemura, T. and Gerner, E. W. (2011). Polyamine transport systems in mammalian cells and tissues. *Methods Mol Biol*, 720:339–48.
- [Ulgherait et al., 2014] Ulgherait, M., Rana, A., Rera, M., Graniel, J., and Walker, D. W. (2014). Ampk modulates tissue and organismal aging in a non-cell-autonomous manner. *Cell Rep*, 8(6):1767–1780.
- [Ullrich et al., 2014] Ullrich, M., Liang, V., Chew, Y. L., Banister, S., Song, X., Zaw, T., Lam, H., Berber, S., Kassiou, M., Nicholas, H. R., and Götz, J. (2014). Bio-orthogonal labeling as a tool to visualize and identify newly synthesized proteins in *caenorhabditis elegans*. *Nat Protoc*, 9(9):2237–55.
- [Valiente-Gabioud et al., 2016] Valiente-Gabioud, A. A., Miotto, M. C., Chesta, M. E., Lombardo, V., Binolfi, A., and Fernández, C. O. (2016). Phthalocyanines as molecular scaffolds to block disease-associated protein aggregation. *Acc Chem Res*, 49(5):801–8.
- [vandenAkker et al., 2011] vandenAkker, C. C., Engel, M. F. M., Velikov, K. P., Bonn, M., and Koenderink, G. H. (2011). Morphology and persistence length of amyloid fibrils are correlated to peptide molecular structure. *J Am Chem Soc*, 133(45):18030–3.
- [Vaudel et al., 2011] Vaudel, M., Barsnes, H., Berven, F. S., Sickmann, A., and Martens, L. (2011). Searchgui: An open-source graphical user interface for simultaneous omssa and x!tandem searches. *Proteomics*, 11(5):996–9.
- [Vaudel et al., 2015] Vaudel, M., Burkhardt, J. M., Zahedi, R. P., Oveland, E., Berven, F. S., Sickmann, A., Martens, L., and Barsnes, H. (2015). Peptideshaker enables reanalysis of ms-derived proteomics data sets. *Nat Biotechnol*, 33(1):22–4.
- [Velloso et al., 2009] Velloso, N. A., Dalmolin, G. D., Gomes, G. M., Rubin, M. A., Canas, P. M., Cunha, R. A., and Mello, C. F. (2009). Spermine improves recognition memory deficit in a rodent model of huntington’s disease. *Neurobiol Learn Mem*, 92(4):574–80.
- [Vernace et al., 2007] Vernace, V. A., Arnaud, L., Schmidt-Glenewinkel, T., and Figueiredo-Pereira, M. E. (2007). Aging perturbs 26s proteasome assembly in *drosophila melanogaster*. *FASEB J*, 21(11):2672–82.
- [Vishavkarma et al., 2014] Vishavkarma, R., Raghavan, S., Kuyyamudi, C., Majumder, A., Dhawan, J., and Pullarkat, P. A. (2014). Role of actin filaments in correlating nuclear shape and cell spreading. *PLoS One*, 9(9):e107895.
- [Voitko, 1999] Voitko, M. L. (1999). Impairments in acquisition and reversals of two-choice discriminations by aged rhesus monkeys. *Neurobiol Aging*, 20(6):617–27.

- [Wallace, 1999] Wallace, D. C. (1999). Mitochondrial diseases in man and mouse. *Science*, 283(5407):1482–8.
- [Wang et al., 2010] Wang, L. P., Li, F., Shen, X., and Tsien, J. Z. (2010). Conditional knock-out of nmda receptors in dopamine neurons prevents nicotine-conditioned place preference. *PLoS One*, 5(1):e8616.
- [Wang et al., 1993] Wang, N., Butler, J. P., and Ingber, D. E. (1993). Mechanotransduction across the cell surface and through the cytoskeleton. *Science*, 260(5111):1124–7.
- [Wang et al., 2009] Wang, N., Tytell, J. D., and Ingber, D. E. (2009). Mechanotransduction at a distance: mechanically coupling the extracellular matrix with the nucleus. *Nat Rev Mol Cell Biol*, 10(1):75–82.
- [Wang et al., 2001] Wang, X., Li, W., Williams, M., Terada, N., Alessi, D. R., and Proud, C. G. (2001). Regulation of elongation factor 2 kinase by p90(rsk1) and p70 s6 kinase. *EMBO J*, 20(16):4370–9.
- [Wang et al., 2016] Wang, Y.-H., Wang, J.-Q., Wang, Q., Wang, Y., Guo, C., Chen, Q., Chai, T., and Tang, T.-S. (2016). Endophilin b2 promotes inner mitochondrial membrane degradation by forming heterodimers with endophilin b1 during mitophagy. *Sci Rep*, 6:25153.
- [Welinder and Ekblad, 2011] Welinder, C. and Ekblad, L. (2011). Coomassie staining as loading control in western blot analysis. *J Proteome Res*, 10(3):1416–9.
- [Weng et al., 1998] Weng, Q. P., Kozlowski, M., Belham, C., Zhang, A., Comb, M. J., and Avruch, J. (1998). Regulation of the p70 s6 kinase by phosphorylation in vivo. analysis using site-specific anti-phosphopeptide antibodies. *J Biol Chem*, 273(26):16621–9.
- [Williams et al., 1991] Williams, K., Romano, C., Dichter, M. A., and Molinoff, P. B. (1991). Modulation of the nmda receptor by polyamines. *Life Sci*, 48(6):469–98.
- [Williams et al., 1993] Williams, K., Russell, S. L., Shen, Y. M., and Molinoff, P. B. (1993). Developmental switch in the expression of nmda receptors occurs in vivo and in vitro. *Neuron*, 10(2):267–78.
- [Wong et al., 2018] Wong, Y.-N., Manola, J., Hudes, G. R., Roth, B. J., Moul, J. W., Barselick, A. M., Scher, R. M., Volk, M. J., Vaughn, D. J., Williams, S. D., Fisch, M. J., Cella, D., Carducci, M. A., and Wilding, G. (2018). Phase 2 study of weekly paclitaxel plus estramustine in metastatic hormone-refractory prostate carcinoma: Ecog-acrin cancer research group (e1898) trial. *Clin Genitourin Cancer*, 16(2):e315–e322.
- [Wu et al., 2011] Wu, M., Fannin, J., Rice, K. M., Wang, B., and Blough, E. R. (2011). Effect of aging on cellular mechanotransduction. *Ageing Res Rev*, 10(1):1–15.

- [Wullschleger et al., 2006] Wullschleger, S., Loewith, R., and Hall, M. N. (2006). Tor signalling in growth and metabolism. *Cell*, 124(3):471–84.
- [Xia et al., 2017] Xia, X., Chen, W., McDermott, J., and Han, J.-D. J. (2017). Molecular and phenotypic biomarkers of aging. *F1000Res*, 6:860.
- [Xu et al., 2005] Xu, S.-Z., Zeng, F., Boulay, G., Grimm, C., Harteneck, C., and Beech, D. J. (2005). Block of trpc5 channels by 2-aminoethoxydiphenyl borate: a differential, extracellular and voltage-dependent effect. *Br J Pharmacol*, 145(4):405–14.
- [Xu, 2016] Xu, X. Z. S. (2016). Demystifying mechanosensitive piezo ion channels. *Neurosci Bull*, 32(3):307–9.
- [Yang et al., 2017] Yang, Y., Wang, K., Gu, X., and Leong, K. W. (2017). Biophysical regulation of cell behavior-cross talk between substrate stiffness and nanotopography. *Engineering (Beijing)*, 3(1):36–54.
- [Yankner et al., 2008] Yankner, B. A., Lu, T., and Loerch, P. (2008). The aging brain. *Annu Rev Pathol*, 3:41–66.
- [Ye et al., 2000] Ye, B., Liao, D., Zhang, X., Zhang, P., Dong, H., and Huganir, R. L. (2000). Grasp-1: a neuronal rasgef associated with the ampa receptor/grip complex. *Neuron*, 26(3):603–17.
- [Yeung et al., 2005] Yeung, T., Georges, P. C., Flanagan, L. A., Marg, B., Ortiz, M., Funaki, M., Zahir, N., Ming, W., Weaver, V., and Janmey, P. A. (2005). Effects of substrate stiffness on cell morphology, cytoskeletal structure, and adhesion. *Cell Motil Cytoskeleton*, 60(1):24–34.
- [Young and Engler, 2011] Young, J. L. and Engler, A. J. (2011). Hydrogels with time-dependent material properties enhance cardiomyocyte differentiation in vitro. *Biomaterials*, 32(4):1002–9.
- [Zhang et al., 2014] Zhang, Q.-Y., Zhang, Y.-Y., Xie, J., Li, C.-X., Chen, W.-Y., Liu, B.-L., Wu, X.-a., Li, S.-N., Huo, B., Jiang, L.-H., and Zhao, H.-C. (2014). Stiff substrates enhance cultured neuronal network activity. *Sci Rep*, 4:6215.
- [Zhao et al., 2017] Zhao, Q., Wu, K., Chi, S., Geng, J., and Xiao, B. (2017). Heterologous expression of the piezo1-asic1 chimera induces mechanosensitive currents with properties distinct from piezo1. *Neuron*, 94(2):274–277.
- [Zhao et al., 2016] Zhao, Q., Wu, K., Geng, J., Chi, S., Wang, Y., Zhi, P., Zhang, M., and Xiao, B. (2016). Ion permeation and mechanotransduction mechanisms of mechanosensitive piezo channels. *Neuron*, 89(6):1248–63.

- [Zhou et al., 2008] Zhou, H.-X., Rivas, G., and Minton, A. P. (2008). Macromolecular crowding and confinement: biochemical, biophysical, and potential physiological consequences. *Annu Rev Biophys*, 37:375–97.
- [Zolessi et al., 2006] Zolessi, F. R., Poggi, L., Wilkinson, C. J., Chien, C.-B., and Harris, W. A. (2006). Polarization and orientation of retinal ganglion cells in vivo. *Neural Dev*, 1:2.

A. Appendix

A1 - State of Authorship

I, Julia Abele confirm that the work presented in this master thesis has been performed and interpreted solely by myself except where explicitly identified to the contrary. I confirm that this work submitted in partial fulfillment for the degree Master of Science in Integrative Neuroscience and has not been submitted elsewhere in any other form for the fulfillment of any other degree or qualification.

Magdeburg, June 6, 2019

Vorname Name